(12) INTERNATIONAL APPLICATION PUBLISHED UNDER THE PATENT COOPERATION TREATY (PCT)

(19) World Intellectual Property Organization
International Bureau

(43) International Publication Date
16 August 2012 (16.08.2012)

WIPO | PCT

(10) International Publication Number
WO 2012/109263 A1

(51) **International Patent Classification**:
A01N 43/04 (2006.01) *A61K 31/70* (2006.01)

(21) **International Application Number**:
PCT/US2012/024169

(22) **International Filing Date**:
7 February 2012 (07.02.2012)

(25) **Filing Language**: English

(26) **Publication Language**: English

(30) **Priority Data**:
61/440,260 7 February 2011 (07.02.2011) US
61/451,455 10 March 2011 (10.03.2011) US

(71) **Applicant** *(for all designated States except US)*: **THE WASHINGTON UNIVERSITY** [US/US]; One Brookings Drive, St. Louis, Missouri 63130 (US).

(72) **Inventors; and**

(75) **Inventors/Applicants** *(for US only)*: **JANETKA, James W.** [US/US]; One Brookings Drive, St. Louis, Missouri 63130 (US). **HAN, Zhenfu** [CN/US]; One Brookings Drive, St. Louis, Missouri 63130 (US). **HULTGREN, Scott** [US/US]; One Brookings Drive, St. Louis, Missouri 63130 (US). **PINKNER, Jerry** [US/US]; One Brookings Drive, St. Louis, Missouri 63130 (US). **CUSUMANO, Corrine** [US/US]; One Brookings Drive, St. Louis, Missouri 63130 (US).

(74) **Agents**: **RILEY-VARGAS, Rebecca** et al.; Polsinelli Shughart PC, Mark Twain Plaza III, 105 West Vandalia, Suite 400, Edwardsville, IL 62025 (US).

(81) **Designated States** *(unless otherwise indicated, for every kind of national protection available)*: AE, AG, AL, AM, AO, AT, AU, AZ, BA, BB, BG, BH, BR, BW, BY, BZ, CA, CH, CL, CN, CO, CR, CU, CZ, DE, DK, DM, DO, DZ, EC, EE, EG, ES, FI, GB, GD, GE, GH, GM, GT, HN, HR, HU, ID, IL, IN, IS, JP, KE, KG, KM, KN, KP, KR, KZ, LA, LC, LK, LR, LS, LT, LU, LY, MA, MD, ME, MG, MK, MN, MW, MX, MY, MZ, NA, NG, NI, NO, NZ, OM, PE, PG, PH, PL, PT, QA, RO, RS, RU, RW, SC, SD, SE, SG, SK, SL, SM, ST, SV, SY, TH, TJ, TM, TN, TR, TT, TZ, UA, UG, US, UZ, VC, VN, ZA, ZM, ZW.

(84) **Designated States** *(unless otherwise indicated, for every kind of regional protection available)*: ARIPO (BW, GH, GM, KE, LR, LS, MW, MZ, NA, RW, SD, SL, SZ, TZ, UG, ZM, ZW), Eurasian (AM, AZ, BY, KG, KZ, MD, RU, TJ, TM), European (AL, AT, BE, BG, CH, CY, CZ, DE, DK, EE, ES, FI, FR, GB, GR, HR, HU, IE, IS, IT, LT, LU, LV, MC, MK, MT, NL, NO, PL, PT, RO, RS, SE, SI, SK, SM, TR), OAPI (BF, BJ, CF, CG, CI, CM, GA, GN, GQ, GW, ML, MR, NE, SN, TD, TG).

Published:

— *with international search report (Art. 21(3))*

WO 2012/109263 A1

(54) **Title**: MANNOSIDE COMPOUNDS AND METHODS OF USE THEREOF

(57) **Abstract**: The present invention encompasses compounds and methods for treating urinary tract infections.

MANNOSIDE COMPOUNDS AND METHODS OF USE THEREOF

GOVERNMENTAL RIGHTS

[0001] This invention was made with government support under grants numbered 1RC1DK086378, RO1AI029549, P50DK064540 and RO1BK051406-12 each of which were awarded by the National Institutes of Health. The government has certain rights in the invention.

CROSS REFERENCE TO RELATED APPLICATIONS

[0002] This application claims the priority of US provisional application number 61/440,260, filed February 7, 2011 and US provisional application number 61/451,455, filed March 10, 2011, each of which are hereby incorporated by reference in their entirety.

FIELD OF THE INVENTION

[0003] The present invention encompasses compounds and methods for treating urinary tract infections.

BACKGROUND OF THE INVENTION

[0004] Urinary tract infection (UTI) caused by uropathogenic *Escherichia coli* (UPEC) is one of the most common infectious diseases in women. The morbidity and economic impact are enormous, with over $2.5 billion spent annually on treatment. Further, recurrent infections are a significant problem despite appropriate antibiotic therapy of the index case. The high rates of recurrence, and the large numbers of women that end up in urology clinics due to their chronic recurrent UTIs highlights the need for a better understanding of the pathogenic mechanisms involved in this disease and the development of new and better therapies.

[0005] Gram-negative bacteria are the causative agents of a wide variety of acute and chronic infectious diseases. Many of these infections are initiated by a

critical interaction between host ligands (frequently polysaccharide moieties) and bacterial adhesins (frequently expressed at the distal tip of polymeric pilus fibers assembled by the chaperone/usher pathway). The mannose binding FimH adhesin of type 1 pili is critical for the colonization and invasion into the bladder epithelium. After invasion, UPEC are able to rapidly multiply inside superficial umbrella cells of the bladder forming biofilm-like intracellular bacterial communities (IBCs). Upon maturation, bacteria disperse from the IBC, spread to neighboring cells, and form next generation IBCs. This is the mechanism by which UPEC rapidly amplify in numbers in the urinary tract and cause disease.

[0006] The X-ray crystal structure of FimH bound to mannose showed that mannose is bound in a negatively charged pocket on FimH. The mannose binding site is highly conserved as it is invariant in 300 *fimH* genes sequenced from clinical UPEC strains. Thus, FimH is the critical node of the entire UPEC pathogenic cascade.

[0007] Recurrence is a serious problem for many women. Women who present with an initial episode of acute UTI have a 25-44% chance of developing a second and a 3% chance of experiencing three episodes within six months of the initial UTI. Recurrence occurs despite appropriate antibiotic treatment and clearance of the initial infection from the urine. A large percentage of recurrent UTI are caused by the same strain of bacteria as the initial infection. One study followed 58 women and found that 68% of recurrences were caused by the same initial index strain of UPEC as determined by restriction fragment length polymorphism (RFLP) analysis. In a separate study, 50% of recurrent strains isolated from female college students appeared genotypically identical to the bacterial strain corresponding to the initial UTI. Another long-term prospective study demonstrated that the same strain of UPEC can cause a recurrent UTI up to 3 years later. The high frequency of same-strain recurrences supports the notion that a UPEC reservoir can exist in the affected individual. The inventors have shown that a quiescent intracellular reservoir (QIR) can form in the bladder tissue itself after acute infection and persist even after antibiotic therapy and urine cultures become sterile. Thus, reactivation of bacteria in QIRs may also be a contributing factor in recurrent UTIs.

[0008] Therefore, there is a need for effective treatments that can cure urinary tract infections and prevent the formation of quiescent intracellular reservoirs that are the source of so many recurrent infections.

SUMMARY OF THE INVENTION

[0009] One aspect of the invention is a compound of Formula (I):

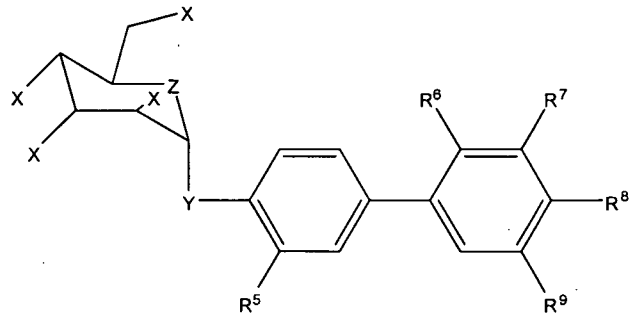

wherein

X is selected from the group consisting of hydrogen, OR^2, SR^2, NR^z;

Z is selected from the group consisting of O, S, CR^3 and NR^4;

Y is oxygen;

R^2, R^3, and R^4 are independently selected from the group consisting of hydrogen, hydrocarbyl, and substituted hydrocarbyl;

R^5 is selected from the group consisting of CF_3, halogen, CH_3, OMe, hydrocarbyl, and substituted hydrocarbyl;

R^6, R^7, R^8, and R^9 are independently selected from the group consisting of hydrogen, $-COR^{10}R^{11}$, $-CONR^{10}R^{11}$, $-COOR^{12}$, and $-NR^{12}CONR^{10}$, or R^6 and R^7 may optionally form a cycloalkyl or heterocyclo ring, R^7 and R^8 may optionally form a cycloalkyl or heterocyclo ring, and R^8 and R^9 may optionally form a cycloalkyl or heterocyclo ring; and

R^{10}, R^{11}, and R^{12} are independently selected from the group consisting of hydrogen, hydrocarbyl, substituted hydrocarbyl, aryl, and heterocycle;

R^{18} and R^{19} are independently selected from the group consisting of hydrogen, hydrocarbyl, and substituted hydrocarbyl;

R^z is independently selected from the group consisting of hydrogen hydrocarbyl, substituted hydrocarbyl, $-COR^x$, $-CONR^xR^xSO_2R^x$, and $-CO_2R^x$; and

R^x is independently selected from the group consisting of hydrogen, $-NR^{18}R^{19}$, and an optionally substituted alkyl, cycloalkyl, heterocycle, or aryl.

[0010] Another aspect of the invention is a compound of Formula (II):

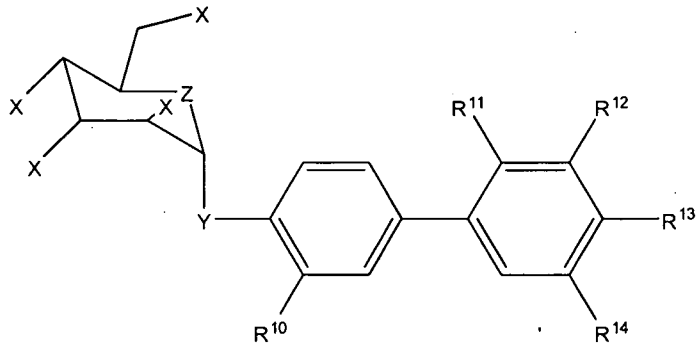

wherein

X is selected from the group consisting of hydrogen, OR^2, SR^2, NR^z;

Z is selected from the group consisting of O, S, CR^3 and NR^4;

Y is selected from the group consisting of sulfur, CR^3, NR^4, $-N(R^{18})CO-$, $-CH_2N(R^{18})-$, $-CH_2N(R^{18})CO-$, CO_2, SO_2, $-CH_2O-$, $-CH_2S-$, CO, $-CON(R^{18})-$, $-SO_2N(R^{18})-$, $-O(CH_2)_n-$, $-S(CH_2)_n-$, $-N(CH_2)_n-$, $-(CH_2)_n-$, NR^{18}, and an optionally substituted alkyl, alkene, alkyne, or heterocycle;

n is an integer from 1 to 10;

R^2, R^3, and R^4 are independently selected from the group consisting of hydrogen, hydrocarbyl, and substituted hydrocarbyl;

R^{10} is selected from the group consisting of hydrogen, CF_3, halogen, CH_3, OMe, hydrocarbyl, and substituted hydrocarbyl;

R^{11}, R^{12}, R^{13}, and R^{14} are independently selected from the group consisting of hydrogen, $-COR^{15}R^{16}$, $-CONR^{15}R^{16}$, $-COOR^{17}$, and $-NR^{17}CONR^{15}$, or R^{11} and R^{12} may optionally form a cycloalkyl or heterocyclo ring, R^{12} and R^{13} may optionally form a cycloalkyl or heterocyclo ring, and R^{13} and R^{14} may optionally form a cycloalkyl or heterocyclo ring;

R^{15}, R^{16}, and R^{17} are independently selected from the group consisting of hydrogen, hydrocarbyl, substituted hydrocarbyl, aryl, and heterocycle;

R^{18} and R^{19} are independently selected from the group consisting of hydrogen, hydrocarbyl, and substituted hydrocarbyl; and

R^z is independently selected from the group consisting of hydrogen hydrocarbyl, substituted hydrocarbyl, $-COR^x$, $-CONR^xR^xSO_2R^x$, and $-CO_2R^x$; and

R^x is independently selected from the group consisting of hydrogen, $-NR^{18}R^{19}$, and an optionally substituted alkyl, cycloalkyl, heterocycle, or aryl.

[0011] Yet another aspect of the invention is a compound of the formula (III):

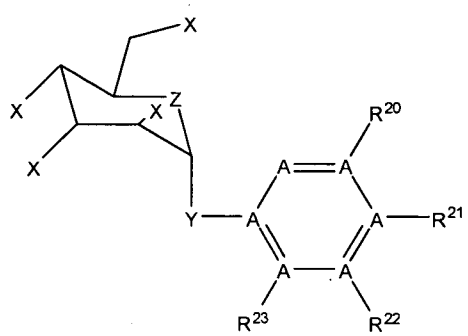

wherein

X is selected from the group consisting of hydrogen, OR^2, SR^2, NR^z;

Z is selected from the group consisting of O, S, CR^3 and NR^4;

Y is selected from the group consisting of oxygen, sulfur, CR^3, NR^4, $-N(R^5)CO-$, $-CH_2N(R^5)-$, $-CH_2N(R^5)CO-$, CO_2, SO_2, $-CH_2O-$, $-CH_2S-$, CO, $-CON(R^5)-$, $-SO_2N(R^5)-$, $-O(CH_2)_n-$, $-S(CH_2)_n-$, $-N(CH_2)_n-$, $-(CH_2)_n-$, NR^5, and an optionally substituted alkyl, alkene, alkyne, or heterocycle;

R^2, R^3, R^4, R^5 are independently selected from the group consisting of hydrogen, hydrocarbyl, and substituted hydrocarbyl;

n is an integer from 1 to 10;

A is independently selected from the group consisting of CR^6 and N;

R^6 is selected from the group consisting of hydrogen, hydrocarbyl, and substituted hydrocarbyl;

R^{20} and R^{22} are selected from the group consisting of hydrogen and $-COOR^{15}$;

R^{21} is selected from the group consisting of hydrogen, a five membered ring, and a halogen;

R^{23} is selected from the group consisting of hydrogen, halogen, hydrocarbyl, and substituted hydrocarbyl;

R^{15} is selected from the group consisting of hydrogen, hydrocarbyl, substituted hydrocarbyl, aryl, and heterocycle;

R^z is independently selected from the group consisting of hydrogen hydrocarbyl, substituted hydrocarbyl, $-COR^x$, $-CONR^xR^xSO_2R^x$, and $-CO_2R^x$; and

R^x is independently selected from the group consisting of hydrogen, $-NR^4R^5$, and an optionally substituted alkyl, cycloalkyl, heterocycle, or aryl.

[0012] Still yet another aspect of the invention encompasses a compound of formula (IV):

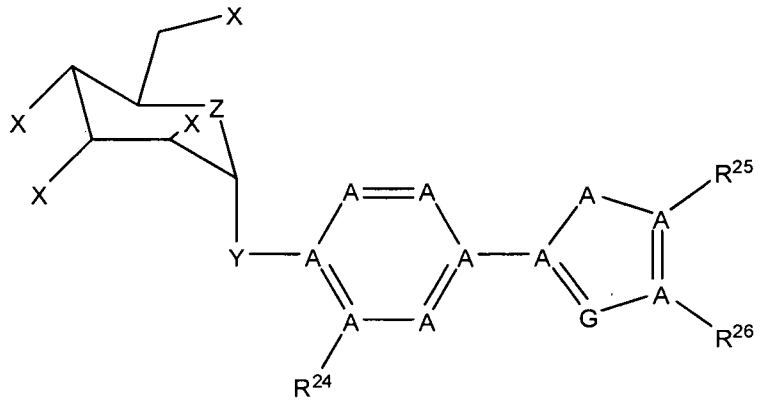

wherein

X is selected from the group consisting of hydrogen, OR^2, SR^2, and NR^z;

Z is selected from the group consisting of O, S, CR^3 and NR^4;

Y is selected from the group consisting of oxygen, sulfur, CR^3, NR^4, $-N(R^5)CO-$, $-CH_2N(R^5)-$, $-CH_2N(R^5)CO-$, CO_2, SO_2, $-CH_2O-$, $-CH_2S-$, CO, $-CON(R^5)-$, $-SO_2N(R^5)-$, $-O(CH_2)_n-$, $-S(CH_2)_n-$, $-N(CH_2)_n-$, $-(CH_2)_n-$, NR^5, and an optionally substituted alkyl, alkene, alkyne, or heterocycle;

R^2, R^3, R^4, R^5 are independently selected from the group consisting of hydrogen, hydrocarbyl, and substituted hydrocarbyl;

n is an integer from 1 to 10;

A is independently selected from the group consisting of CR^6 and N;

G is selected from the group consisting of S, O, CR^8, and NR^9;

R^6, R^8 and R^9 are independently selected from the group consisting of hydrogen, hydrocarbyl, and substituted hydrocarbyl;

R^{24} is selected from the group consisting of hydrogen, halogen, hydrocarbyl, and substituted hydrocarbyl;

R^{25} and R^{26} are selected from the group consisting of hydrogen, -$NHCONH_2$, -COOMe, and –CONHMe, and R^{25} and R^{26} can optionally form a cycloalkyl or heterocyclo ring;

R^{18} and R^{19} are independently selected from the group consisting of hydrogen, hydrocarbyl, and substituted hydrocarbyl; and

R^z is independently selected from the group consisting of hydrogen hydrocarbyl, substituted hydrocarbyl, -COR^x, -$CONR^xR^xSO_2R^x$, and -CO_2R^x; and

R^x is independently selected from the group consisting of hydrogen, -$NR^{18}R^{19}$, and an optionally substituted alkyl, cycloalkyl, heterocycle, or aryl.

[0013] A further aspect of the invention encompasses a method of treating a bacterial infection in a subject in need of treatment thereof, the method comprising administering a compound of the invention to the subject.

[0014] An alternative aspect of the invention is a medical device coated with a compound of the invention. In one embodiment, the medical device is a catheter.

[0015] Other aspects and iterations of the invention are detailed below.

REFERENCE TO COLOR FIGURES

[0016] The application file contains at least one photograph executed in color. Copies of this patent application publication with color photographs will be provided by the Office upon request and payment of the necessary fee.

BRIEF DESCRIPTION OF THE FIGURES

[0017] **Fig. 1.** depicts a graph showing that there is no defect in UTI89 invasion following implantation. Graph represents bacterial titers from homogenized bladders from non-implanted (○) or implanted (●) animals infected with UTI89 3hpi following gentamicin protection assay. Horizontal dashed lines represent the limit of detection (lod) for viable bacteria (Int=intracellular, Ext=Extracellular). Each symbol

represents a mouse from two independent experiments with n=5/condition. The horizontal bars represent the median of each dataset; *p* value by the Mann Whitney U test.

[0018] **Fig. 2** depicts microscope images and a graph showing that uropathogenic *E. coli* produce IBCs in the superficial umbrella cells of implanted bladders. (**A**) Representative images of splayed bladders of female C57Bl/6Ncr mice infected with UTI89 6hpi in the absence (non-implanted) or presence (Implanted) of implants following LacZ staining. Each black arrow indicates a purple speck, indicative of an IBC. (**B**) Quantification of IBC formation following LacZ staining at 6hpi. Each symbol represents IBC number from a single mouse from two independent experiments with n=5/group. *p* value obtained from the Mann Whitney U test. (**C**) Representative CLSM images of whole bladders from non-implanted and implanted animals infected with UTI89 ectopically expressing GFP (Green), stained with DNA dye SYTO83 (Red) and Alexa-fluor 633-conjugate of WGA (Blue) reveal the presence of IBC within umbrella cells. Scale bar =20μm.

[0019] **Fig. 3** depicts micrographs showing that IBC and filamentation occur following urinary catheterization. Representative CLSM images of whole bladders from non-implanted and implanted animals infected with UTI89 ectopically expressing GFP (Green), stained with DNA dye SYTO83 (Red) and Alexa-fluor 633-conjugate of WGA (Blue) reveal the presence of multiple IBCs within single umbrella cells (**A-C**), that unlike non-implanted bladders (**B**), the underlying epithelium is exposed following urinary catheterization (**E-F**), depict the absence of bacterial colonization of the exposed underlying epithelium in implanted animals (**E-F**), and the presence of filamenting bacteria in umbrella cells (**C-F**). Scale bar =20μm

[0020] **Fig. 4** depicts graphs showing that UPEC reservoir reactivation can lead to urinary implant and bladder colonization. Graphs represent bacterial titers in log scale recovered from implants, homogenized bladders and kidneys of non-bacteriuric animals 14days post infection with UTI89HK::GFP that were non-implanted or implanted for 3 day (**A**) or 5days (**B**). Horizontal dashed lines represent the limit of detection for viable bacteria. Each symbol represents a mouse from at least two independent

experiments with n=10-20/group/experiment. The horizontal bars represent the median of each dataset; p value by the Mann Whitney U test.

[0021] **Fig. 5** depicts two graphs showing that deletion of *fimH* reduces biofilm formation and attenuates UPEC virulence. Graphs represent crystal violet based quantification (**A**) and CFU enumeration in logarithmic scale (log scale) (**B**) of 24h old UTI89 and UTI89Δ*fimH* (Δ*fimH*) biofilms under human urine flow on silicone tubings at 37°C indicating that Δ*fimH* is defective in biofilm formation under these conditions. Bars represent mean of three independent experiments, error bars indicate standard error of the mean (SEM). *p* values from Mann Whitney U test. (**C**) Graph represents bacterial titers in log scale recovered from implants, homogenized bladders and kidneys of non-implanted (open symbols) and implanted (closed symbols) infected with either UTI89 (square) or Δ*fimH* (circle) for 24h. Horizontal dashed lines represent the limit of detection for viable bacteria. Each symbol represents a mouse from at least two independent experiments with n=5/group. The horizontal bars represent the median of each dataset; $*p<0.05$ and $***p<0.0005$ by the Mann Whitney U test.

[0022] **Fig. 6** depicts two graphs showing that S pili and curli are not critical for UPEC virulence following urinary catheterization. Graphs represent bacterial titers in log scale recovered at 24hpi from implants, homogenized bladders and kidneys of (**A**) implanted animals infected with either UTI89 (●) or UTI89 mutant strains deficient in type 1 pili, Δ*fimH* (■), S pili Δ*sfaA-H*(▲), both type 1 and S pili Δ*sfaA-H*Δ*fimB-H*(♦) and (**B**) non-implanted (open symbols) or implanted (closed symbols) animals infected with UTI89 (○,●), Δ*fimH* (□, ■) or UTI89 mutant strains deficient in curli components Δ*csgA* (Δ, ▲) and Δ*csgB*Δ*csgG* (♦,◊). Horizontal dashed lines represent the limit of detection for viable bacteria. Each symbol represents a mouse from at least two independent experiments with n=5/group. The horizontal bars represent the median of each dataset; $*p<0.05$, $***p<0.005$ $**p<0.0005$, ns corresponds to $p>0.05$ by the Mann Whitney U test.

[0023] **Fig. 7** depicts two graphs showing that methyl mannose inhibits UPEC biofilm in human urine. Graphs represent crystal violet based quantification (**A**) and CFU enumeration in logarithmic scale (log scale) (**B**) of 24h old UTI89 biofilms in

human urine with or without 1% methyl mannose under flow on silicone tubings at 37°C indicating that methyl mannose prevents UPEC biofilm formation. Bars represent mean of three independent experiments, error bars indicate standard error of the mean (SEM). *p* values from Mann Whitney U test.

[0024] **Fig. 8** depicts two graphs showing that mannoside treatment prevents IBC formation and UPEC virulence when used in combination with TMP-SMZ. (**A**) Graph represents IBC enumeration from LacZ staining of splayed bladders of female C57Bl/6Ncr mice treated i.p. with mannoside or saline prior to transurethral implantation and inoculation with UTI89 6hpi. Each symbol represents IBC number from a single mouse from two independent experiments with n=5/group. *p* value obtained from the Mann Whitney U test. (**B**) Graph represents bacterial titers in log scale recovered at 6hpi from implants, homogenized bladders and kidneys of animals treated with saline (○), mannoside (□),TMP-SMZ (●) and TMP-SMZ+Mannoside (■) prior to urinary implantation and inoculation with UTI89. Horizontal dashed lines represent the limit of detection for viable bacteria. Each symbol represents a mouse from at least two independent experiments with n=5/group. The horizontal bars represent the median of each dataset; $*p<0.05$, $**p<0.0005$, $***p<0.0005$, ns corresponds to $p>0.05$ by the Mann Whitney U test.

[0025] **Fig. 9** depicts a graph showing that treatment of chronic mice with 5 doses of Mannoside 8 eliminates UPEC from the bladder. Mannoside 8 treatment (▲), PBS treatment (●).

[0026] **Fig. 10** depcist a graph showing that Mannoside 8 is effective against the multidrug resistant UPEC isolate EC958. Mannoside 8 treatment (Δ), PBS treatment (▲).

[0027] **Fig. 11** depicts inhibition, prevention and disruption of UTI89 biofilm by mannoside. (**A**), Discovery of biphenyl mannoside lead FimH inhibitors. Cellular HAI titers ($EC_{>90}$) are shown in parentheses. (**B**) The median inhibitory concentration (IC_{50}) of mannosides **1-3** and **6** on UTI89 biofilm formation. Mannoside was added at the initiation of biofilm formation. (**C**) The IC50 of **1-3** and **6** on UTI89 biofilm prevention. Mannoside was added 24 h after biofilm growth was initiated and % biofilm was

calculated 16 h after addition of mannoside. Bars show the mean value of the experiments (n = 3). (**D, E**) **6** dispersed biofilm as measured by confocal microscopy of UTI89 biofilms grown for 24 h (**D**), then incubated for an additional 16 h in the presence of 0.3 μM 6 (**E**).

[0028] **Fig. 12** depicts mannoside effect on UTI89 colonization. (**A**) Urine PK analysis of **6** (n ≥ 3 mice) showing amounts in urine over time for each dosing regimen indicated. Horizontal dashed line is at IC_{50} (0.74 μM) as determined by the biofilm inhibition assay. (**B**) Mannoside effectively treats UTI. Chronically infected mice were treated with PBS or **6** (PO, 100 and 50 mg/kg). 6 hours post-treatment bacterial counts in the bladder were enumerated. In the mannoside-treated groups, there was a significant 3-log drop in bacterial load relative to PBS-treated mice. (**C, D**) Confocal microscopy of bladders from PBS-treated (**C**) and **6**-treated (**D**) mice. Bacteria were stained with SYTO9 (green) and the bladder luminal surface was stained with WGA (red). The image in **C** shows a normal, robust IBC whereas the arrows in **D** indicate luminal bacteria. (**E**) Total bacterial CFUs at 6 hpi from mice treated with PBS or **6** either by IP (5 mg/kg) or oral (100 mg/kg) dosing 30 min prior to inoculation of UTI89. (F) IBC quantification at 6 hpi from mice treated with PBS or **6** either by IP (5 mg/kg) or oral (100 mg/kg) dosing 30 min prior to inoculation of UTI89. (**G**) 6 hpi *ex vivo* gentamicin protection assay revealed both luminal and intracellular bacteria are significantly reduced upon IP (5 mg/kg) pretreatment of mice with **6**. Bars indicate geometric mean. Statistical significance according to Mann-Whitney is at $*P < 0.05$, $**P < 0.01$, $***P < 0.0001$. ns, not significant; LOD, limit of detection.

[0029] **Fig. 13** depicts mannoside potentiates TMP-SMZ treatment. Total bacterial CFUs were quantified 6 hpi. UTI89 colonization was reduced in mice treated with **6**, TMP-SMZ and TMP-SMZ+6. There was further decreased colonization in TMP-SMZ+6-treated mice over **6** or TMP-SMZ alone. PBC-1 colonization was reduced in mice treated with **6** and TMP-SMZ+6, but not TMP-SMZ alone. Enhanced efficacy as measured by bacterial CFUs was observed upon treatment with TMP-SMZ+**6** over **6** or TMP-SMZ treatment alone. Bars indicate geometric mean. Statistical significance

according to Mann-Whitney is at *$P < 0.05$, **$P < 0.01$, ***$P < 0.0001$. ns, not significant; LOD, limit of detection.

[0030] **Fig. 14** depicts newly designed mannosides show enhanced PK and potency at treating infection. (**A**) Optimized ortho-methyl and trifluoromethyl substituted biphenyl mannosides. Cellular HAI titers ($EC_{>90}$) are shown in parentheses. (**B**) Mannosides show improved PK. Mannosides **8** and **10** dosed at 50 mg/kg had equivalent levels of compound in the urine 6 h post-treatment relative to mannoside **6** dosed at 100 mg/kg. (**C**) Chronically infected mice were treated with PBS or mannoside **6**, **10** or **8** (PO, 50 mg/kg). 6 hours posttreatment bacterial counts in the bladder were enumerated. In the mannoside-treated groups, there was a significant 3-log drop in bacterial load relative to PBS-treated mice. The optimized mannoside **8** showed increased efficacy over **6**.

[0031] **Fig. 15** depicts structures of substituted biphenyl mannosides.

[0032] **Fig. 16** depicts a graph showing curves of HAI, Octet and DSF assay results.

[0033] **Fig. 17** depicts a proposed model of mannoside **7** bound to FimH calculated with APBS (Adaptive Poisson-Boltzmann Solver) software using PDB code: 3MCY.

[0034] **Fig. 18** depicts (**A**) Metabolic lability of the mannoside **3** glycosidic bond from hydrolysis to mannose and biphenol; (**B**) Elimination kinetics and clearance of mannoside **3** and biphenol (R) hydrolysis product in mouse urine.

[0035] **Fig. 19** depicts (**A**). Plasma pharmacokinetics of optimized ortho-substituted mannosides **5a-c, 7, 8** and mannoside **3**. (**B**) Elimination clearance kinetics of optimized ortho-substituted mannosides **5a-c, 7, 8** and mannoside **3** in urine.

[0036] **Fig. 20** depicts two graphs showing that UTI89Δ*qseC* has a defect in bladder invasion. (**A**) Bladder titers at 1 and 3 h.p.i showing decreased overall bacterial numbers recovered from bladders infected with UTI89Δ*qseC* compared to those infected with wt UTI89. (**B**) Bacterial titers recovered from gentamicin-treated bladders (intracellular population) after washing 3 times with PBS to remove the extracellular, adherent bacteria (luminal population). Fewer UTI89Δ*qseC* bacteria are

internalized, indicating that the *qseC* mutant is less efficient in invading the host bladder compared to wt UTI89. The average of 3 independent experiments is shown (*, P<0.02; **, P<0.003, by two-tailed Mann-Whitney).

[0037] **Fig. 21** depicts a diagram detailing and data showing that restoring production of type 1 pili in UTI89Δ*qseC* does not influence other Δ*qseC*-mediated defects. (**A**) Schematic showing the strategy used to lock the phase-variable *fim* promoter in the ON orientation. (**B**) Hemagglutination assays and (**C**)western blot analyses depicting restoration of type 1 pili expression in UTI89Δ*qseC* locked ON strain (Δ*qseC*_LON). (**D**) Assessment of curli production on YESCA-CR agar verifies that, similarly to UTI89Δ*qseC*, UTI89Δ*qseC*_LON remains defective for curli expression, exhibiting a white and smooth morphotype. In contrast, wt UTI89 and UTI89_LON appear red, dry and rough a phenotype indicative of curli expression.

[0038] **Fig. 22** depicts a graph showing co-inhibition of type 1 pili and QseC as a prophylactic measure for UTIs. Chart depicting the bladder cfu obtained at 2 wks post infection from mice pre-treated with mannoside and subsequently infected with either wt UTI89, or UTI89Δ*qseC* (used as a proxy for a QseC inhibitor). Significantly fewer cfu (1.5-log reduction) were obtained from pre-treated mice infected with UTI89Δ*qseC*. The average of 3 independent experiments is shown (**, P<0.01; ***, P<0.001, by two-tailed Mann-Whitney). UTI89_MAN, mice pre-treated with mannoside and challenged with wt UTI89; Δ*qseC*_MAN, mice pre-treated with mannoside and challenged with UTI89Δ*qseC*; UTI89, mice pre-treated with PBS and challenged with wt UTI89; Δ*qseC*, mice pre-treated with PBS and challenged with UTI89Δ*qseC*.

DETAILED DESCRIPTION

[0039] Compounds that inhibit the function of type I pili of bacteria have been developed. The compounds may be useful for the treatment of urinary tract infections. Significantly, the compounds may prevent bacterial colonization and invasion of the bladder tissue to prevent infection and the establishment of reservoirs that can serve as a source of recurrent infections. The invention also encompasses methods of use of a compound of the invention.

I. Compounds

[0040] One aspect of the invention is a compound of Formula (I):

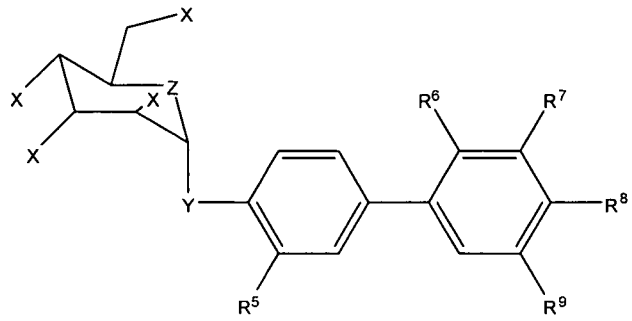

wherein

X is selected from the group consisting of hydrogen, OR^2, SR^2, NR^z;

Z is selected from the group consisting of O, S, CR^3 and NR^4;

Y is oxygen;

R^2, R^3, and R^4 are independently selected from the group consisting of hydrogen, hydrocarbyl, and substituted hydrocarbyl;

R^5 is selected from the group consisting of CF_3, halogen, CH_3, OMe, hydrocarbyl, and substituted hydrocarbyl;

R^6, R^7, R^8, and R^9 are independently selected from the group consisting of hydrogen, $-COR^{10}R^{11}$, $-CONR^{10}R^{11}$, $-COOR^{12}$, and $-NR^{12}CONR^{10}$, or R^6 and R^7 may optionally form a cycloalkyl or heterocyclo ring, R^7 and R^8 may optionally form a cycloalkyl or heterocyclo ring, and R^8 and R^9 may optionally form a cycloalkyl or heterocyclo ring; and

R^{10}, R^{11}, and R^{12} are independently selected from the group consisting of hydrogen, hydrocarbyl, substituted hydrocarbyl, aryl, and heterocycle;

R^{18} and R^{19} are independently selected from the group consisting of hydrogen, hydrocarbyl, and substituted hydrocarbyl;

R^z is independently selected from the group consisting of hydrogen hydrocarbyl, substituted hydrocarbyl, $-COR^x$, $-CONR^xR^xSO_2R^x$, and $-CO_2R^x$; and

R^x is independently selected from the group consisting of hydrogen, $-NR^{18}R^{19}$, and an optionally substituted alkyl, cycloalkyl, heterocycle, or aryl.

[0041] In one embodiment, a compound of the invention comprises Formula (I), wherein

X is selected from the group consisting of OR^2;

Z is selected from the group consisting of O, S, CR^3 and NR^4;

Y is oxygen;

R^2, R^3, and R^4 are independently selected from the group consisting of hydrogen, hydrocarbyl, and substituted hydrocarbyl;

R^5 is selected from the group consisting of CF_3, halogen, CH_3, and OMe;

R^6, R^7, R^8, and R^9 are independently selected from the group consisting of hydrogen, $-COR^{10}R^{11}$, $-CONR^{10}R^{11}$, $-COOR^{12}$, and $-NR^{12}CONR^{10}$, or R^6 and R^7 may optionally form a cycloalkyl or heterocyclo ring, R^7 and R^8 may optionally form a cycloalkyl or heterocyclo ring, and R^8 and R^9 may optionally form a cycloalkyl or heterocyclo ring; and

R^{10}, R^{11}, and R^{12} are independently selected from the group consisting of hydrogen, hydrocarbyl, substituted hydrocarbyl, aryl, and heterocycle.

[0042] In another embodiment, a compound of the invention comprises Formula (I), wherein

X is selected from the group consisting of OR^2;

Z is selected from the group consisting of O, S, CR^3 and NR^4;

Y is oxygen;

R^2, R^3, and R^4 are independently selected from the group consisting of hydrogen, hydrocarbyl, and substituted hydrocarbyl;

R^5 is selected from the group consisting of CF_3, halogen, CH_3, and OMe;

R^6 and R^8 are hydrogen;

R^7 and R^9 are independently selected from the group consisting of hydrogen, $-COR^{10}R^{11}$, $-CONR^{10}R^{11}$, $-COOR^{12}$, and $-NR^{12}CONR^{10}$; and

R^{10}, R^{11}, and R^{12} are independently selected from the group consisting of hydrogen, hydrocarbyl, substituted hydrocarbyl, aryl, and heterocycle.

[0043] In yet another embodiment, a compound of the invention comprises Formula (I), wherein

X is OH;

Z is O;

Y is oxygen;

R^2, R^3, and R^4 are independently selected from the group consisting of hydrogen, hydrocarbyl, and substituted hydrocarbyl;

R^5 is selected from the group consisting of CF_3, halogen, CH_3, and OMe;

R^6 and R^8 are hydrogen;

R^7 and R^9 are independently selected from the group consisting of hydrogen, $-CONHCH_3$, $-COOCH_3$, and $-NHCONH_2$.

[0044] Another aspect of the invention is a compound of Formula (II):

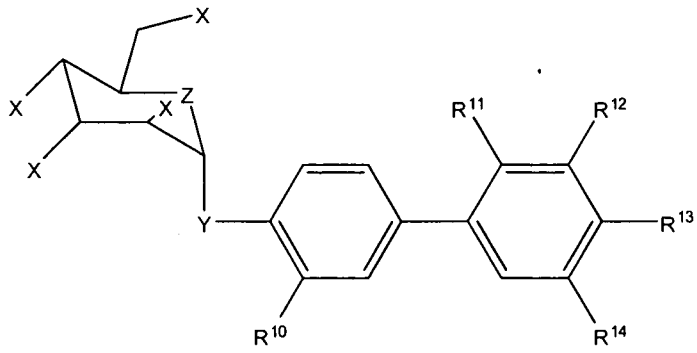

wherein

X is selected from the group consisting of hydrogen, OR^2, SR^2, NR^z;

Z is selected from the group consisting of O, S, CR^3 and NR^4;

Y is selected from the group consisting of sulfur, CR^3, NR^4, $-N(R^{18})CO-$, $-CH_2N(R^{18})-$, $-CH_2N(R^{18})CO-$, CO_2, SO_2, $-CH_2O-$, $-CH_2S-$, CO, $-CON(R^{18})-$, $-SO_2N(R^{18})-$, $-O(CH_2)_n-$, $-S(CH_2)_n-$, $-N(CH_2)_n-$, $-(CH_2)_n-$, NR^{18}, and an optionally substituted alkyl, alkene, alkyne, or heterocycle;

n is an integer from 1 to 10;

R^2, R^3, and R^4 are independently selected from the group consisting of hydrogen, hydrocarbyl, and substituted hydrocarbyl;

R^{10} is selected from the group consisting of hydrogen, CF_3, halogen, CH_3, OMe, hydrocarbyl, and substituted hydrocarbyl;

R^{11}, R^{12}, R^{13}, and R^{14} are independently selected from the group consisting of hydrogen, $-COR^{15}R^{16}$, $-CONR^{15}R^{16}$, $-COOR^{17}$, and $-NR^{17}CONR^{15}$, or R^{11} and R^{12} may optionally form a cycloalkyl or heterocyclo ring, R^{12} and R^{13} may optionally form a cycloalkyl or heterocyclo ring, and R^{13} and R^{14} may optionally form a cycloalkyl or heterocyclo ring;

R^{15}, R^{16}, and R^{17} are independently selected from the group consisting of hydrogen, hydrocarbyl, substituted hydrocarbyl, aryl, and heterocycle;

R^{18} and R^{19} are independently selected from the group consisting of hydrogen, hydrocarbyl, and substituted hydrocarbyl; and

R^z is independently selected from the group consisting of hydrogen hydrocarbyl, substituted hydrocarbyl, $-COR^x$, $-CONR^xR^xSO_2R^x$, and $-CO_2R^x$; and

R^x is independently selected from the group consisting of hydrogen, $-NR^{18}R^{19}$, and an optionally substituted alkyl, cycloalkyl, heterocycle, or aryl.

[0045] In one embodiment, a compound of the invention comprises Formula (II), wherein

X is OR^2;

Z is selected from the group consisting of O, S, CR^3 and NR^4;

Y is selected from the group consisting of sulfur, CR^3, NR^4, $-N(R^{18})CO-$, $-CH_2N(R^{18})-$, $-CH_2N(R^{18})CO-$, CO_2, SO_2, $-CH_2O-$, $-CH_2S-$, CO, $-CON(R^{18})-$, $-SO_2N(R^{18})-$, $-O(CH_2)_n-$, $-S(CH_2)_n-$, $-N(CH_2)_n-$, $-(CH_2)_n-$, NR^{18}, and an optionally substituted alkyl, alkene, alkyne, or heterocycle;

n is an integer from 1 to 10;

R^2, R^3, R^4 and R^{18} are independently selected from the group consisting of hydrogen, hydrocarbyl, and substituted hydrocarbyl;

R^{10} is selected from the group consisting of hydrogen, CF_3, halogen, CH_3, and OMe;

R^{11}, R^{12}, R^{13}, and R^{14} are independently selected from the group consisting of hydrogen, $-COR^{15}R^{16}$, $-CONR^{15}R^{16}$, $-COOR^{17}$, and $-NR^{17}CONR^{15}$, or R^{11} and R^{12} may optionally form a cycloalkyl or heterocyclo ring, R^{12} and R^{13} may optionally form a cycloalkyl

or heterocyclo ring, and R^{13} and R^{14} may optionally form a cycloalkyl or heterocyclo ring; and

R^{15}, R^{16}, and R^{17} are independently selected from the group consisting of hydrogen, hydrocarbyl, substituted hydrocarbyl, aryl, and heterocycle.

[0046] In another embodiment, a compound of the invention comprises Formula (II), wherein

X is OR^2;

Z is selected from the group consisting of O, S, CR^3 and NR^4;

Y is selected from the group consisting of sulfur, CR^3, NR^4, $-N(R^{18})CO-$, $-CH_2N(R^{18})-$, $-CH_2N(R^{18})CO-$, CO_2, SO_2, $-CH_2O-$, $-CH_2S-$, CO, $-CON(R^{18})-$, $-SO_2N(R^{18})-$, $-O(CH_2)_n-$, $-S(CH_2)_n-$, $-N(CH_2)_n-$, $-(CH_2)_n-$, and NR^{18};

n is an integer from 1 to 10;

R^2, R^3, R^4 and R^{18} are independently selected from the group consisting of hydrogen, hydrocarbyl, and substituted hydrocarbyl;

R^{10} is selected from the group consisting of hydrogen, CF_3, halogen, CH_3, and OMe;

R^{11}, R^{12}, R^{13}, and R^{14} are independently selected from the group consisting of hydrogen, $-COR^{15}R^{16}$, $-CONR^{15}R^{16}$, $-COOR^{17}$, $-NR^{17}CONR^{15}$; and

R^{15}, R^{16}, and R^{17} are independently selected from the group consisting of hydrogen, hydrocarbyl, substituted hydrocarbyl, aryl, and heterocycle.

[0047] In yet another embodiment, a compound of the invention comprises Formula (II), wherein

X is OH;

Z is selected from the group consisting of O, S, CR^3 and NR^4;

Y is selected from the group consisting of sulfur, CR^3, NR^4,

-N(R^{18})CO-, and -CH_2N(R^{18}) ;

R^3, R^4 and R^{18} are independently selected from the group consisting of hydrogen, hydrocarbyl, and substituted hydrocarbyl;

R^{10} is selected from the group consisting of hydrogen, CF_3, halogen, CH_3, and OMe;

R^{11} and R^{13} are hydrogen; and

R^{12} and R^{14} are independently selected from the group consisting of hydrogen, -$CONHCH_3$, -$COOCH_3$, and -$NHCONH_2$.

[0048] In still yet another embodiment, a compound of the invention comprises Formula (II), wherein

X is OH;

Z is selected from the group consisting of O, S, CR^3 and NR^4;

Y is selected from the group consisting of CR^3 and -CH_2N(R^{18});

R^3, R^4 and R^{18} are independently selected from the group consisting of hydrogen, hydrocarbyl, and substituted hydrocarbyl;

R^{10} is selected from the group consisting of hydrogen, CF_3, halogen, CH_3, and OMe;

R^{11} and $R^{13}$are hydrogen; and

R^{12} and R^{14} are independently selected from the group consisting of hydrogen, -$CONHCH_3$, -$COOCH_3$, and -$NHCONH_2$.

[0049] Yet another aspect of the invention is a compound of the formula (III):

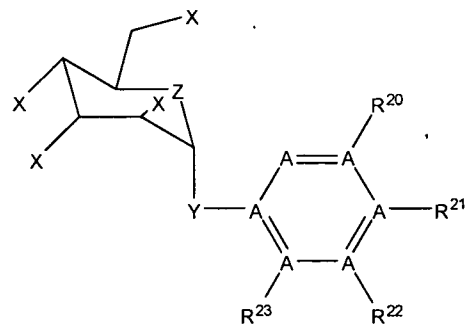

wherein

X is selected from the group consisting of hydrogen, OR^2, SR^2, NR^z;

Z is selected from the group consisting of O, S, CR^3 and NR^4;

Y is selected from the group consisting of oxygen, sulfur, CR^3, NR^4, $-N(R^5)CO-$, $-CH_2N(R^5)-$, $-CH_2N(R^5)CO-$, CO_2, SO_2, $-CH_2O-$, $-CH_2S-$, CO, $-CON(R^5)-$, $-SO_2N(R^5)-$, $-O(CH_2)_n-$, $-S(CH_2)_n-$, $-N(CH_2)_n-$, $-(CH_2)_n-$, NR^5, and an optionally substituted alkyl, alkene, alkyne, or heterocycle;

R^2, R^3, R^4, R^5 are independently selected from the group consisting of hydrogen, hydrocarbyl, and substituted hydrocarbyl;

n is an integer from 1 to 10;

A is independently selected from the group consisting of CR^6 and N;

R^6 is selected from the group consisting of hydrogen, hydrocarbyl, and substituted hydrocarbyl;

R^{20} and R^{22} are selected from the group consisting of hydrogen and $-COOR^{15}$;

R^{21} is selected from the group consisting of hydrogen, a five membered cycloalkyl or heterocyclo ring, and a halogen;

R^{23} is selected from the group consisting of hydrogen, halogen, hydrocarbyl, and substituted hydrocarbyl;

R^{15} is selected from the group consisting of hydrogen, hydrocarbyl, substituted hydrocarbyl, aryl, and heterocycle;

R^z is independently selected from the group consisting of hydrogen hydrocarbyl, substituted hydrocarbyl, $-COR^x$, $-CONR^xR^xSO_2R^x$, and $-CO_2R^x$; and

R^x is independently selected from the group consisting of hydrogen, $-NR^4R^5$, and an optionally substituted alkyl, cycloalkyl, heterocycle, or aryl.

[0050] In one embodiment, a compound of the invention comprises Formula (III), wherein

X is OR^2;

Z is selected from the group consisting of O, S, CR^3 and NR^4;

Y is selected from the group consisting of oxygen, CR^3, -$CH_2N(R^5)CO$-;

R^2, R^3, R^4, R^5 are independently selected from the group consisting of hydrogen, hydrocarbyl, and substituted hydrocarbyl;

A is CR^6;

R^6 is selected from the group consisting of hydrogen, hydrocarbyl, and substituted hydrocarbyl;

R^{20} and R^{22} are selected from the group consisting of hydrogen and $-COOR^{15}$;

R^{21} is selected from the group consisting of hydrogen, halogen, and a five membered cycloalkyl or heterocyclo ring;

R^{23} is selected from the group consisting of hydrogen, halogen, hydrocarbyl, and substituted hydrocarbyl; and

R^{15} is selected from the group consisting of hydrogen, hydrocarbyl, substituted hydrocarbyl, aryl, and heterocycle.

[0051] In another embodiment, a compound of the invention comprises Formula (III), wherein

X is OH;

Z is selected from the group consisting of O, S, CR^3 and NR^4;

Y is selected from the group consisting of oxygen, CR^3, -$CH_2N(R^5)CO$-;

R^3, R^4, and R^5 are independently selected from the group consisting of hydrogen, hydrocarbyl, and substituted hydrocarbyl;

A is CR^6;

R^6 is selected from the group consisting of hydrogen, hydrocarbyl, and substituted hydrocarbyl;

R^{20} and R^{22} are selected from the group consisting of hydrogen and $-COOR^{15}$;

R^{21} is selected from the group consisting of hydrogen, halogen, a five membered cycloalkyl or heterocyclo ring;

R^{23} is selected from the group consisting of hydrogen, halogen, hydrocarbyl, and substituted hydrocarbyl; and

R^{15} is selected from the group consisting of hydrogen, hydrocarbyl, substituted hydrocarbyl, aryl, and heterocycle.

[0052] In yet another embodiment, a compound of the invention comprises Formula (III), wherein

X is OH;

Z is selected from the group consisting of O, S, CR^3 and NR^4;

Y is selected from the group consisting of oxygen, CR^3, -$CH_2N(R^5)CO$-;

R^3, R^4, and R^5 are independently selected from the group consisting of hydrogen, hydrocarbyl, and substituted hydrocarbyl;

A is CR^6;

R^6 is selected from the group consisting of hydrogen, hydrocarbyl, and substituted hydrocarbyl;

R^{20} and R^{22} are $-COOR^{15}$;

R^{21} and R^{23} and hydrogen; and

R^{15} is selected from the group consisting of hydrogen, hydrocarbyl, substituted hydrocarbyl, aryl, and heterocycle.

[0053] In still yet another embodiment, a compound of the invention comprises Formula (III), wherein

X is OH;

Z is selected from the group consisting of O, S, CR^3 and NR^4;

Y is selected from the group consisting of oxygen, CR^3, -$CH_2N(R^5)CO$-;

R^3, R^4, R^5, R^8, and R^9 are independently selected from the group consisting of hydrogen, hydrocarbyl, and substituted hydrocarbyl;

A is CR^6;

R^6 is selected from the group consisting of hydrogen, hydrocarbyl, and substituted hydrocarbyl;

R^{20} and R^{22} are hydrogen;

R^{21} is selected from the group consisting of hydrogen, halogen,

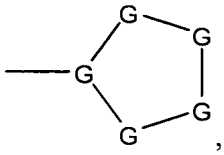

, and

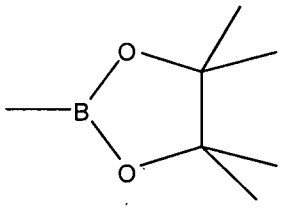

, wherein G is selected from the group consisting of S, O, CR^8, and NR^9; and

R^{23} is selected from the group consisting of hydrogen, halogen, hydrocarbyl, and substituted hydrocarbyl.

[0054] Still yet another aspect of the invention encompasses a compound of formula (IV):

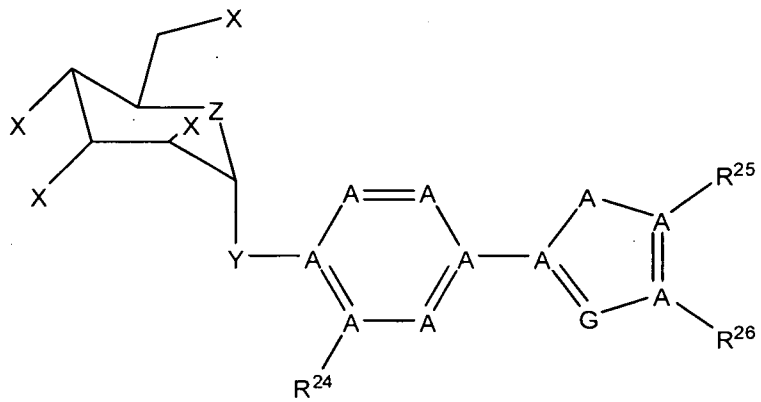

wherein

X is selected from the group consisting of hydrogen, OR^2, SR^2, and NR^z;

Z is selected from the group consisting of O, S, CR^3 and NR^4;

Y is selected from the group consisting of oxygen, sulfur, CR^3, NR^4, $-N(R^5)CO-$, $-CH_2N(R^5)-$, $-CH_2N(R^5)CO-$, CO_2, SO_2, $-CH_2O-$, $-CH_2S-$, CO, $-CON(R^5)-$, $-SO_2N(R^5)-$, $-O(CH_2)_n-$, $-S(CH_2)_n-$, $-N(CH_2)_n-$, $-(CH_2)_n-$, NR^5, and an optionally substituted alkyl, alkene, alkyne, or heterocycle;

R^2, R^3, R^4, R^5 are independently selected from the group consisting of hydrogen, hydrocarbyl, and substituted hydrocarbyl;

n is an integer from 1 to 10;

A is independently selected from the group consisting of CR^6 and N;

G is selected from the group consisting of S, O, CR^8, and NR^9;

R^6, R^8 and R^9 are independently selected from the group consisting of hydrogen, hydrocarbyl, and substituted hydrocarbyl;

R^{24} is selected from the group consisting of hydrogen, halogen, hydrocarbyl, and substituted hydrocarbyl;

R^{25} and R^{26} is selected from the group consisting of hydrogen, $-NHCONH_2$, -COOMe, and –CONHMe, and R^{25} and R^{26} can optionally form a cycloalkyl or heterocyclo ring;

R^z is independently selected from the group consisting of hydrogen hydrocarbyl, substituted hydrocarbyl, $-COR^x$, $-CONR^xR^xSO_2R^x$, and $-CO_2R^x$; and

R^x is independently selected from the group consisting of hydrogen, $-NR^4R^5$, or an optionally substituted alkyl, cycloalkyl, heterocycle, or aryl.

[0055] In one embodiment, a compound of the invention encompasses formula (IV) wherein:

X is selected from the group consisting of hydrogen, OR^2, and SR^2;

Z is selected from the group consisting of O, S, CR^3 and NR^4;

Y is selected from the group consisting of oxygen, sulfur, CR^3, NR^4,

$-N(R^5)CO-$, $-CH_2N(R^5)-$, $-CH_2N(R^5)CO-$, CO_2, SO_2, $-CH_2O-$, $-CH_2S-$, CO, $-CON(R^5)-$, $-SO_2N(R^5)-$, $-O(CH_2)_n-$, $-S(CH_2)_n-$, $-N(CH_2)_n-$, $-(CH_2)_n-$, NR^5, and an optionally substituted alkyl, alkene, alkyne, or heterocycle;

R^2, R^3, R^4, R^5 are independently selected from the group consisting of hydrogen, hydrocarbyl, and substituted hydrocarbyl;

n is an integer from 1 to 10;

A is independently selected from the group consisting of CR^6 and N;

G is selected from the group consisting of S, O, CR^8, and NR^9;

R^6, R^8 and R^9 are independently selected from the group consisting of hydrogen, hydrocarbyl, and substituted hydrocarbyl;

R^{24} is selected from the group consisting of hydrogen, halogen, hydrocarbyl, and substituted hydrocarbyl;

R^{25} and R^{26} is selected from the group consisting of hydrogen, $-NHCONH_2$, -COOMe, and –CONHMe, or R^{25} and R^{26} can optionally form a cycloalkyl or heterocyclo ring.

[0056] In another embodiment, a compound of the invention encompasses formula (IV) wherein:

X is OR^2;

Z is selected from the group consisting of O, S, CR^3 and NR^4;

Y is selected from the group consisting of oxygen, sulfur, CR^3, NR^4, $-N(R^5)CO-$, $-CH_2N(R^5)-$, $-CH_2N(R^5)CO-$, CO_2, SO_2, $-CH_2O-$, $-CH_2S-$, CO, $-CON(R^5)-$, $-SO_2N(R^5)-$, $-O(CH_2)_n-$, $-S(CH_2)_n-$, $-N(CH_2)_n-$, $-(CH_2)_n-$, and NR^5;

R^2, R^3, R^4, R^5 are independently selected from the group consisting of hydrogen, hydrocarbyl, and substituted hydrocarbyl;

n is an integer from 1 to 10;

A is independently selected from the group consisting of CR^6 and N;

G is selected from the group consisting of S, O, CR^8, and NR^9;

R^6, R^8 and R^9 are independently selected from the group consisting of hydrogen, hydrocarbyl, and substituted hydrocarbyl;

R^{24} is selected from the group consisting of hydrogen, halogen, hydrocarbyl, and substituted hydrocarbyl;

R^{25} and R^{26} are selected from the group consisting of hydrogen, -$NHCONH_2$, -COOMe, and –CONHMe, or R^{25} and R^{26} can optionally form the structure:

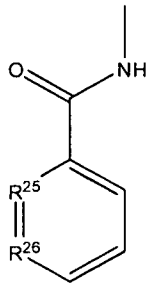

[0057] In yet another embodiment, a compound of the invention encompasses a compound of formula (IV) wherein:

X is OR^2;

Z is selected from the group consisting of O, S, CR^3 and NR^4;

Y is selected from the group consisting of oxygen, CR^3, NR^4, and -$CH_2N(R^5)$- ;

R^2, R^3, R^4, R^5 are independently selected from the group consisting of hydrogen, hydrocarbyl, and substituted hydrocarbyl;

A is independently selected from the group consisting of CR^6 and N;

G is selected from the group consisting of S, O, CR^8, and NR^9;

R^6, R^8 and R^9 are independently selected from the group consisting of hydrogen, hydrocarbyl, and substituted hydrocarbyl;

R^{24} is selected from the group consisting of hydrogen, halogen, CH_3, CF_3, and OMe;

R^{25} and R^{26} are selected from the group consisting of hydrogen, -$NHCONH_2$, -COOMe, and –CONHMe, or R^{25} and R^{26} can optionally form the structure

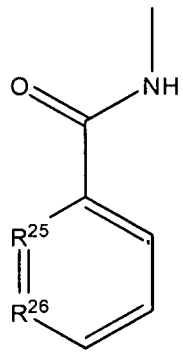

[0058] In an exemplary alternative of each of the foregoing embodiments, a compound comprising formula (I) is a compound comprising any of the Formulas in **Table 7 or 8**.

[0059] In a further exemplary alternative of each of the foregoing embodiments, a compound of the invention is 4ZFH284 or 4ZFH269 from **Table 8**.

[0060] In certain embodiments, the sugar residue of the above compounds may encompass any stereoisomer of mannose. In other embodiments, the sugar residue of the above compounds may encompass any stereoisomer of mannose other than glucose. In an exemplary embodiment, the sugar residue of the above compounds is alpha D mannose.

[0061] Exemplary methods of synthesizing a compound of the invention are detailed in the Examples.

[0062] A compound of the invention may also be an intermediate in the synthesis of a compound of the invention. For instance, in one embodiment, a compound of the invention may be an ester intermediate in the synthesis of a compound of the invention. In another embodiment, a compound of the invention may be a boronate ester of a mannoside or a boronic acid ester of a mannoside. In yet another embodiment, a compound of the invention may have the formula (XX), wherein R' is selected from H, alkyl, or both R' groups may together form a ring.

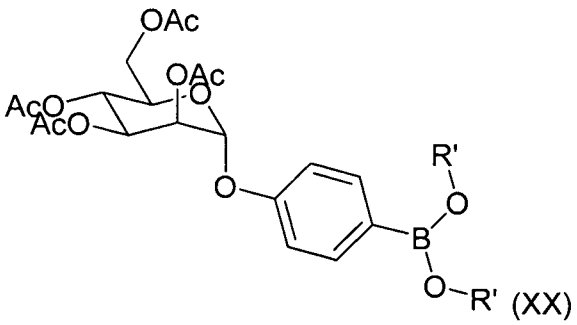

(XX)

[0063] A compound of the invention may also comprise an imaging agent, such as a fluorescent moiety. In an exemplary embodiment, the imaging agent is bound to the sugar portion of a compound of the invention, either directly, or via a linker.

[0064] Compounds of the invention may block the function of FimH of the type I pili of pathogenic bacteria and prevent bacterial adherence and invasion and thus prevent bacterial amplification in the IBC and subsequent spreading and repeated rounds of amplification via new generation IBCs.

[0065] FimH functional assays used to measure activity of the compounds are known to individuals skilled in the art. Non-limiting examples of functional assays include hemmagglutination titer using guinea pig red blood cells, affinity of binding to FimH, and the ability of the compounds to prevent biofilm formation.

[0066] In some embodiments, activity of the compound is measured using hemmagglutination titer of guinea pig red blood cells. Hemagglutination of guinea pig red blood cells by type1 piliated UPEC is dependent upon FimH mannose binding ability and serial dilutions allow a quantitative analysis. Hemagglutination titer may generally be defined as the amount of compound required for decreasing hemagglutination by 75%. In some embodiments, the hemmagglutiantion titer of the compound of the invention may be less than about 14, 13, 12, 11, 10, 9, 8, 7, 6, 5, 4, 3, 2, or 1μM. In a preferred alternative of the embodiments, the hemmagglutiantion titer of the compound of the invention may be less than about 9μM. In another preferred alternative of the embodiments, the hemmagglutiantion titer of the compound of the invention may be less than about 7μM. In yet another preferred alternative of the embodiments, the hemmagglutiantion titer of the compound of the invention may be less than about 1μM.

[0067] In other embodiments, activity of the compound may be measured using affinity of binding of the compound of the invention to FimH. In some embodiments of the invention, the Kd value for a compound of the invention and FimH may be less than about 5μM. For instance, the Kd value may be about 0.2, 0.3, 0.5, 0.6, 0.7, or 3.5μM.

[0068] In yet other embodiments, activity of the compound may be measured using the ability of the compound to prevent or disrupt biofilm formation. In general, titration curves measuring the ability of a compound inhibit biofilm formation may be performed to determine the IC_{50}. In some embodiments, the IC_{50} of the compound may be less than about 700, 600, 500, 400, 300, 200 or 100μM. In other embodiments, the IC_{50} of the compound may be less than about 500, 400, 300, 200, 100, 50, 40, 30, 20 10, 9, 8, 7, 6, or 5μM. In preferred embodiments, the IC_{50} of the compound may be less than about 20μM.

II. Combinations

[0069] Another aspect of the present invention encompasses a combination of a compound of the invention (described in Section I above) with one or more bactericidal compounds. In some embodiments, a compound of the invention may comprise a combination with 1, 2, 3, 4, or 5 bactericidal compounds. In one embodiment, the bactericidal compound is an antibiotic. Suitable antibiotics are known in the art, and may include Amikacin, Gentamicin, Kanamycin, Neomycin, Netilmicin, Tobramycin, Paromomycin, Geldanamycin, Herbimycin, Carbacephem, Loracarbef, Ertapenem, Doripenem, Imipenem/Cilastatin, Meropenem, Cefadroxil, Cefazolin, Cefalotin, Cefalexin, Cephalosporins, Cefaclor, Cefamandole, Cefoxitin, Cefprozil, Cefuroxime, Cefixime, Cefdinir, Cefditoren, Cefoperazone, Cefotaxime, Cefpodoxime, Ceftazidime, Ceftibuten, Ceftizoxime, Ceftriaxone, Cefepime, Ceftobiprole, Teicoplanin, Vancomycin, Telavancin, Clindamycin, Lincomycin, Azithromycin, Clarithromycin, Dirithromycin, Erythromycin, Roxithromycin, Troleandomycin, Telithromycin, Spectinomycin, Aztreonam, Furazolidone, Nitrofurantoin, Amoxicillin, Ampicillin, Azlocillin, Carbenicillin, Cloxacillin, Dicloxacillin, Flucloxacillin, Mezlocillin, Methicillin,

Nafcillin, Oxacillin, Penicillin G, Penicillin V, Piperacillin, Temocillin, Ticarcillin, Bacitracin, Colistin, Polymyxin B, Ciprofloxacin, Enoxacin, Gatifloxacin, Levofloxacin, Lomefloxacin, Moxifloxacin, Nalidixic acid, Norfloxacin, Ofloxacin, Trovafloxacin, Grepafloxacin, Sparfloxacin, Temafloxacin, Mafenide, Sulfonamidochrysoidine, Sulfacetamide, Sulfadiazine, Silver sulfadiazine, Sulfamethizole, Sulfamethoxazole (SMZ), Sulfanilimide, Sulfasalazine, Sulfisoxazole, Trimethoprim (TMP), Trimethoprim-Sulfamethoxazole (such as Bactrim, Septra), Demeclocycline, Doxycycline, Minocycline, Oxytetracycline, Tetracycline, Clofazimine, Dapsone, Capreomycin, Cycloserine, Ethambutol, Ethionamide, Isoniazid, Pyrazinamide, Rifampicin, Rifabutin, Rifapentine, Streptomycin, Arsphenamine, Chloramphenicol, Fosfomycin, Fusidic acid, Linezolid, Metronidazole, Mupirocin, Platensimycin, Quinupristin/Dalfopristin, Rifaximin, Thiamphenicol, or Tinidazole. In an exemplary embodiment, the antibiotic is TMP, SMZ, or a combination thereof.

[0070] In another embodiment, a compound of the invention may be combined with a QseC inhibitor. In a preferred embodiment, a compound of the invention may be combined with a QseC phosphatase inhibitor.

III. Pharmaceutical compositions

[0071] Yet another aspect of the invention encompasses a pharmaceutical composition. A compound of the invention described in section I above may exist in tautomeric, geometric or stereoisomeric forms. The present invention contemplates all such compounds, including cis- and trans-geometric isomers, E- and Z-geometric isomers, R- and S-enantiomers, diastereomers, d-isomers, l-isomers, the racemic mixtures thereof and other mixtures thereof. Pharmaceutically acceptable salts of such tautomeric, geometric or stereoisomeric forms are also included within the invention. The terms "cis" and "trans", as used herein, denote a form of geometric isomerism in which two carbon atoms connected by a double bond will each have a hydrogen atom on the same side of the double bond ("cis") or on opposite sides of the double bond ("trans"). Some of the compounds described contain alkenyl groups, and are meant to include both cis and trans or "E" and "Z" geometric forms. Furthermore, some of the

compounds described contain one or more stereocenters and are meant to include R, S, and mixtures of R and S forms for each stereocenter present.

[0072] In a further embodiment, the inhibitors of the present invention may be in the form of free bases or pharmaceutically acceptable acid addition salts thereof. The term "pharmaceutically-acceptable salts" are salts commonly used to form alkali metal salts and to form addition salts of free acids or free bases. The nature of the salt may vary, provided that it is pharmaceutically acceptable. Suitable pharmaceutically acceptable acid addition salts of compounds for use in the present methods may be prepared from an inorganic acid or from an organic acid. Examples of such inorganic acids are hydrochloric, hydrobromic, hydroiodic, nitric, carbonic, sulfuric and phosphoric acid. Appropriate organic acids may be selected from aliphatic, cycloaliphatic, aromatic, araliphatic, heterocyclic, carboxylic and sulfonic classes of organic acids, examples of which are formic, acetic, propionic, succinic, glycolic, gluconic, lactic, malic, tartaric, citric, ascorbic, glucuronic, maleic, fumaric, pyruvic, aspartic, glutamic, benzoic, anthranilic, mesylic, 4-hydroxybenzoic, phenylacetic, mandelic, embonic (pamoic), methanesulfonic, ethanesulfonic, benzenesulfonic, pantothenic, 2-hydroxyethanesulfonic, toluenesulfonic, sulfanilic, cyclohexylaminosulfonic, stearic, algenic, hydroxybutyric, salicylic, galactaric and galacturonic acid. Suitable pharmaceutically-acceptable base addition salts of compounds of use in the present methods include metallic salts made from aluminum, calcium, lithium, magnesium, potassium, sodium and zinc or organic salts made from N, N'-dibenzylethylenediamine, chloroprocaine, choline, diethanolamine, ethylenediamine, meglumine- (N-methylglucamine) and procaine. All of these salts may be prepared by conventional means from the corresponding compound by reacting, for example, the appropriate acid or base with any of the compounds of the invention.

[0073] Injectable preparations, for example, sterile injectable aqueous or oleaginous suspensions, may be formulated according to the known art using suitable dispersing or wetting agents and suspending agents. The sterile injectable preparation may also be a sterile injectable solution or suspension in a nontoxic parenterally acceptable diluent or solvent. Among the acceptable vehicles and solvents that may be

employed are water, Ringer's solution, and isotonic sodium chloride solution. In addition, sterile, fixed oils are conventionally employed as a solvent or suspending medium. For this purpose, any bland fixed oil may be employed, including synthetic mono- or diglycerides. In addition, fatty acids such as oleic acid are useful in the preparation of injectables. Dimethyl acetamide, surfactants including ionic and non-ionic detergents, and polyethylene glycols can be used. Mixtures of solvents and wetting agents such as those discussed above are also useful.

[0074] Solid dosage forms for oral administration may include capsules, tablets, pills, powders, and granules. In such solid dosage forms, the compound is ordinarily combined with one or more adjuvants appropriate to the indicated route of administration. If administered per os, the compound can be admixed with lactose, sucrose, starch powder, cellulose esters of alkanoic acids, cellulose alkyl esters, talc, stearic acid, magnesium stearate, magnesium oxide, sodium and calcium salts of phosphoric and sulfuric acids, gelatin, acacia gum, sodium alginate, polyvinylpyrrolidone, and/or polyvinyl alcohol, and then tableted or encapsulated for convenient administration. Such capsules or tablets can contain a controlled-release formulation as can be provided in a dispersion of active compound in hydroxypropylmethyl cellulose. In the case of capsules, tablets, and pills, the dosage forms can also comprise buffering agents such as sodium citrate, or magnesium or calcium carbonate or bicarbonate. Tablets and pills can additionally be prepared with enteric coatings.

[0075] For therapeutic purposes, formulations for parenteral administration may be in the form of aqueous or non-aqueous isotonic sterile injection solutions or suspensions. These solutions and suspensions may be prepared from sterile powders or granules having one or more of the carriers or diluents mentioned for use in the formulations for oral administration. The compounds may be dissolved in water, polyethylene glycol, propylene glycol, ethanol, corn oil, cottonseed oil, peanut oil, sesame oil, benzyl alcohol, sodium chloride, and/or various buffers. Other adjuvants and modes of administration are well and widely known in the pharmaceutical art. For

instance, a compound of the invention may be administered with a carrier. Non-limiting examples of such a carrier include protein carriers and lipid carriers.

[0076] Liquid dosage forms for oral administration may include pharmaceutically acceptable emulsions, solutions, suspensions, syrups, and elixirs containing inert diluents commonly used in the art, such as water. Such compositions may also comprise adjuvants, such as wetting agents, emulsifying and suspending agents, and sweetening, flavoring, and perfuming agents.

[0077] The amount of the compound of the invention that may be combined with the carrier materials to produce a single dosage of the composition will vary depending upon the subject and the particular mode of administration. Those skilled in the art will appreciate that dosages may also be determined with guidance from Goodman & Goldman's The Pharmacological Basis of Therapeutics, Ninth Edition (1996), Appendix II, pp. 1707-1711 and from Goodman & Goldman's The Pharmacological Basis of Therapeutics, Tenth Edition (2001), Appendix II, pp. 475-493.

[0078] A compound of the invention may also be formulated as a prodrug. Such a prodrug formulation may increase the bioavailability of a compound of the invention. In one embodiment, the sugar portion of a compound of the invention may encompass a prodrug. In another embodiment R^1 may comprise a prodrug. Non-limiting examples of a compound of the invention formulated as a prodrug include the compounds below:

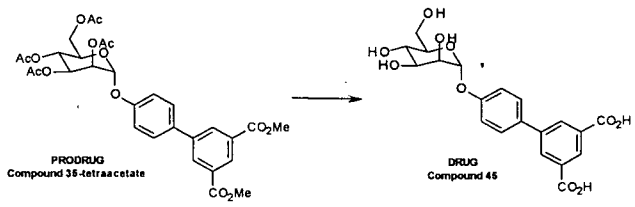

IV. Methods of the invention

[0079] Compounds of the invention may be used in methods of treating a bacterial infection, methods of reducing resistance to a bactericidal compound in a bacterium, and methods of treating a catheter-associated urintary tract infection.

(a) methods of treating a bacterial infection

[0080] One embodiment of the invention encompasses a method for treating bacterial infections. As used herein, "treating" refers to preventing infection in a subject not currently infected, and reducing or eliminating infection in a subject that is currently infected. Generally, such a method comprises administering a pharmaceutical composition comprising a compound of the invention to a subject. An infection may be "treated" by preventing bacterial adherence. Alternatively, an infection may be "treated" by preventing bacterial invasion.

[0081] In one embodiment, a bacterial infection may be a urinary tract infection. In another embodiment, a bacterial infection may be chronic cystitis or interstitial cystitis. In yet another embodiment, a bacterial infection may be pyelonephritis. In still another embodiment, a bacterial infection may refer to the formation of quiescent intracellular reservoirs (QIRs). In an alternative embodiment, a bacterial infection may be an infection mediated by type 1 pili.

[0082] As used herein, "subject" includes any mammal prone to urinary tract infections by E. coli. In one embodiment, a subject is prone to recurring UTIs. In some embodiments, a subject may not have clinical symptoms of a UTI. In such embodiments, the subject may have a latent infection. In other embodiments, a subject may have clinical symptoms of a UTI.

[0083] In some embodiments, a compound of the invention may be administered to a subject in combination with a bactericidal compound as described in Section II above. When administered in a combination, a compound of the invention may be administered before, simultaneously, or after administration of a bactericidal compound. When administered before or after a bactericidal compound, the time between administration of a compound of the invention and a bactericidal compound may be about 1, 2, 3, 4, 5, 6, 7, 8, 9, 10, 11, 12, 13, 14, 15, 16, 17, 18, 19, 20, 21, 22, 23, 24, 25, 26, 27, 28, 29, 30, 31, 32, 33, 34, 35, 36, 37, 38, 39, 40, 41, 42, 43, 44, 45, 46, 47, 48, 49, 50, 51, 52, 53, 54, 55, 56, 57, 58, 59, or 60 min. In another embodiment, the time between administration of a compound of the invention and a bactericidal compound may be about 1, 2, 3, 4, 5, 6, 7, 8, 9, 10, 11, 12, 13, 14, 15, 16, 17, 18, 19,

20, 21, 22, 23, 24, 25, 26, 27, 28, 29, 30, 31, 32, 33, 34, 35, 36, 37, 38, 39, 40, 41, 42, 43, 44, 45, 46, 47, 48, 49, 50, 51, 52, 53, 54, 55, 56, 57, 58, 59, 60, 61, 62, 63, 64, 65, 66, 67, 68, 69, 70, 71, or 72 hours.

[0084] A compound or pharmaceutical composition of the invention may be administered by several different means that will deliver a therapeutically effective dose. Such compositions may be administered orally, parenterally, by inhalation spray, rectally, intradermally, intracisternally, intraperitoneally, transdermally, bucally, as an oral or nasal spray, topically (i.e. powders, ointments or drops), or via a urinary catheter in dosage unit formulations containing conventional nontoxic pharmaceutically acceptable carriers, adjuvants, and vehicles as desired. Topical administration may also involve the use of transdermal administration such as transdermal patches or iontophoresis devices. The term parenteral as used herein includes subcutaneous, intravenous, intramuscular, or intrasternal injection, or infusion techniques. In an exemplary embodiment, the pharmaceutical composition will be administered in an oral dosage form. Formulation of drugs is discussed in, for example, Hoover, John E., Remington's Pharmaceutical Sciences, Mack Publishing Co., Easton, Pa. (1975), and Liberman, H. A. and Lachman, L., Eds., Pharmaceutical Dosage Forms, Marcel Decker, New York, N.Y. (1980).

[0085] The amount of a compound of the invention that constitutes an "effective amount" can and will vary. The amount will depend upon a variety of factors, including whether the administration is in single or multiple doses, and individual subject parameters including age, physical condition, size, and weight. Those skilled in the art will appreciate that dosages may also be determined with guidance from Goodman & Goldman's The Pharmacological Basis of Therapeutics, Ninth Edition (1996), Appendix II, pp. 1707-1711 and from Goodman & Goldman's The Pharmacological Basis of Therapeutics, Tenth Edition (2001), Appendix II, pp. 475-493.

[0086] In order to selectively control the release of an inhibitor to a particular region of the gastrointestinal tract for release, the pharmaceutical compositions of the invention may be manufactured into one or several dosage forms for the controlled, sustained or timed release of one or more of the ingredients. In this

context, typically one or more of the ingredients forming the pharmaceutical composition is microencapsulated or dry coated prior to being formulated into one of the above forms. By varying the amount and type of coating and its thickness, the timing and location of release of a given ingredient or several ingredients (in either the same dosage form, such as a multi-layered capsule, or different dosage forms) may be varied.

[0087] In an exemplary embodiment, the coating may be an enteric coating. The enteric coating generally will provide for controlled release of the ingredient, such that drug release can be accomplished at some generally predictable location in the lower intestinal tract below the point at which drug release would occur without the enteric coating. In certain embodiments, multiple enteric coatings may be utilized. Multiple enteric coatings, in certain embodiments, may be selected to release the ingredient or combination of ingredients at various regions in the lower gastrointestinal tract and at various times.

[0088] As will be appreciated by a skilled artisan, the encapsulation or coating method can and will vary depending upon the ingredients used to form the pharmaceutical composition and coating, and the desired physical characteristics of the microcapsules themselves. Additionally, more than one encapsulation method may be employed so as to create a multi-layered microcapsule, or the same encapsulation method may be employed sequentially so as to create a multi-layered microcapsule. Suitable methods of microencapsulation may include spray drying, spinning disk encapsulation (also known as rotational suspension separation encapsulation), supercritical fluid encapsulation, air suspension microencapsulation, fluidized bed encapsulation, spray cooling/chilling (including matrix encapsulation), extrusion encapsulation, centrifugal extrusion, coacervation, alginate beads, liposome encapsulation, inclusion encapsulation, colloidosome encapsulation, sol-gel microencapsulation, and other methods of microencapsulation known in the art. Detailed information concerning materials, equipment and processes for preparing coated dosage forms may be found in Pharmaceutical Dosage Forms: Tablets, eds. Lieberman et al. (New York: Marcel Dekker, Inc., 1989), and in Ansel et al.,

Pharmaceutical Dosage Forms and Drug Delivery Systems, 6th Ed. (Media, Pa.: Williams & Wilkins, 1995).

[0089] A bacterium may be contacted with a compound of the invention in vivo, in vitro, in situ, or ex vivo. In some embodiments, a bacterium may be directly contacted with the compound of the invention. In other embodiments, an intracellular bacterium may be contacted with a compound of the invention. Suitable cells comprising one or more bacteria may be grown, sub-cultured, stored and manipulated using standard techniques known to individuals skilled in the art. Cell culture and microbiological techniques for growing, culturing, storing, and manipulating cells comprising one or more bacteria are commonly known in the art.

(b) methods of reducing bactericidal resistance

[0090] Another method of the invention comprises reducing the resistance of a bacterium to a bactericidal compound. Such a method comprises contacting a bacterium resistant to a bactericidal compound with a compound of the invention. For instance, a subject infected with a bacterium resistant to a bactericidal compound may be administered a compound of the invention, as described in section IV(a) above. In an exemplary embodiment, a method comprises contacting a bacterium resistant to an antibiotic with a compound of the invention. In a further exemplary embodiment, a method comprises contacting a bacterium resistant to TMP or SMZ with a compound of the invention.

[0091] Methods of measuring resistance of a bacterium to an antibiotic are known in the art. For more details, see the examples.

(c) methods of treating catheter-associated urinary tract infections

[0092] In a further embodiment, a method of the invention encompasses a method for treating catheter-associated urinary tract infections. As used herein, "treating" refers to preventing infection in a subject not currently infected, and reducing or eliminating infection in a subject that is currently infected. Generally, such a method comprises administering a pharmaceutical composition comprising a compound of the

invention to a subject. For this embodiment, "subject" refers to any mammal with an indwelling urinary catheter. In one embodiment, a subject with a urinary catheter is prone to recurring UTIs. In some embodiments, a subject with a urinary catheter may not have clinical symptoms of a UTI. In such embodiments, the subject may have a latent infection. In other embodiments, a subject with a urinary catheter may have clinical symptoms of a UTI.

[0093] In some embodiments, a compound of the invention may be administered to a subject in combination with a bactericidal compound as described in Section II and IV(a) above.

V. Coatings

[0094] An additional aspect of the present invention encompasses coatings comprising a compound of the invention. Such a coating may be used on a medical device to prevent bacterial adherence or infection of the host. Suitable means of coating medical devices are known in the art. In one embodiment, a catheter may be coated with a compound of the invention. In another embodiment, a urinary catheter may be coated with a compound of the invention.

VI. Nutritional Supplement

[0095] An alternative aspect of the present invention encompasses a nutritional supplement that comprises a compound of the invention. Such a supplement may be used to treat a bacterial infection as described in section IV above.

DEFINITIONS

[0096] The term "acyl," as used herein alone or as part of another group, denotes the moiety formed by removal of the hydroxyl group from the group --COOH of an organic carboxylic acid, e.g., RC(O)--, wherein R is R', R_1O--, $R'R_2$ N--, or R_1S--, R_1 is hydrocarbyl, heterosubstituted hydrocarbyl, or heterocyclo and R_2 is hydrogen, hydrocarbyl or substituted hydrocarbyl.

[0097] The term "acyloxy," as used herein alone or as part of another group, denotes an acyl group as described above bonded through an oxygen linkage (--O--), e.g., RC(O)O-- wherein R is as defined in connection with the term "acyl."

[0098] Unless otherwise indicated, the alkyl groups described herein are preferably lower alkyl containing from one to eight carbon atoms in the principal chain and up to 20 carbon atoms. They may be straight or branched chain or cyclic and include methyl, ethyl, propyl, isopropyl, butyl, hexyl and the like.

[0099] Unless otherwise indicated, the alkenyl groups described herein are preferably lower alkenyl containing from two to eight carbon atoms in the principal chain and up to 20 carbon atoms. They may be straight or branched chain or cyclic and include ethenyl, propenyl, isopropenyl, butenyl, isobutenyl, hexenyl, and the like.

[0100] Unless otherwise indicated, the alkynyl groups described herein are preferably lower alkynyl containing from two to eight carbon atoms in the principal chain and up to 20 carbon atoms. They may be straight or branched chain and include ethynyl, propynyl, butynyl, isobutynyl, hexynyl, and the like.

[0101] The terms "aryl" or "ar" as used herein alone or as part of another group denote optionally substituted homocyclic aromatic groups, preferably monocyclic or bicyclic groups containing from 6 to 12 carbons in the ring portion, such as phenyl, biphenyl, naphthyl, substituted phenyl, substituted biphenyl or substituted naphthyl. Phenyl and substituted phenyl are the more preferred aryl.

[0102] As used herein, the term “functional group” includes a group of atoms within a molecule that is responsible for certain properties of the molecule and/or reactions in which it takes part. Non-limiting examples of functional groups include, alkyl, carboxyl, hydroxyl, amino, sulfonate, phosphate, phosphonate, thiol, alkyne, azide, halogen, and the like.

[0103] The terms "halogen" or "halo" as used herein alone or as part of another group refer to chlorine, bromine, fluorine, and iodine.

[0104] The terms "heterocyclo" or "heterocyclic" as used herein alone or as part of another group denote optionally substituted, fully saturated or unsaturated, monocyclic or bicyclic, aromatic or nonaromatic groups having at least one heteroatom

in at least one ring, and preferably 5 or 6 atoms in each ring. The heterocyclo group preferably has 1 or 2 oxygen atoms, 1 or 2 sulfur atoms, and/or 1 to 4 nitrogen atoms in the ring, and may be bonded to the remainder of the molecule through a carbon or heteroatom. Exemplary heterocyclo include heteroaromatics such as furyl, thienyl, pyridyl, oxazolyl, pyrrolyl, indolyl, quinolinyl, or isoquinolinyl and the like. Exemplary substituents include one or more of the following groups: hydrocarbyl, substituted hydrocarbyl, keto, hydroxy, protected hydroxy, acyl, acyloxy, alkoxy, alkenoxy, alkynoxy, aryloxy, halogen, amido, amino, nitro, cyano, thiol, ketals, acetals, esters and ethers.

[0105] The term "heteroaromatic" as used herein alone or as part of another group denote optionally substituted aromatic groups having at least one heteroatom in at least one ring, and preferably 5 or 6 atoms in each ring. The heteroaromatic group preferably has 1 or 2 oxygen atoms; 1 or 2 sulfur atoms, and/or 1 to 4 nitrogen atoms in the ring, and may be bonded to the remainder of the molecule through a carbon or heteroatom. Exemplary heteroaromatics include furyl, thienyl, pyridyl, oxazolyl, pyrrolyl, indolyl, quinolinyl, or isoquinolinyl and the like. Exemplary substituents include one or more of the following groups: hydrocarbyl, substituted hydrocarbyl, keto, hydroxy, protected hydroxy, acyl, acyloxy, alkoxy, alkenoxy, alkynoxy, aryloxy, halogen, amido, amino, nitro, cyano, thiol, ketals, acetals, esters and ethers.

[0106] The terms "hydrocarbon" and "hydrocarbyl" as used herein describe organic compounds or radicals consisting exclusively of the elements carbon and hydrogen. These moieties include alkyl, alkenyl, alkynyl, and aryl moieties. These moieties also include alkyl, alkenyl, alkynyl, and aryl moieties substituted with other aliphatic or cyclic hydrocarbon groups, such as alkaryl, alkenaryl and alkynaryl. Unless otherwise indicated, these moieties preferably comprise 1 to 20 carbon atoms.

[0107] The "substituted hydrocarbyl" moieties described herein are hydrocarbyl moieties which are substituted with at least one atom other than carbon, including moieties in which a carbon chain atom is substituted with a hetero atom such as nitrogen, oxygen, silicon, phosphorous, boron, sulfur, or a halogen atom. These

substituents include halogen, carbocycle, aryl, heterocyclo, alkoxy, alkenoxy, alkynoxy, aryloxy, hydroxy, protected hydroxy, keto, acyl, acyloxy, nitro, amino, amido, nitro, cyano, thiol, ketals, acetals, esters and ethers.

[0108] The following examples are included to demonstrate preferred embodiments of the invention. It should be appreciated by those of skill in the art that the techniques disclosed in the examples that follow represent techniques discovered by the inventors to function well in the practice of the invention. Those of skill in the art should, however, in light of the present disclosure, appreciate that many changes can be made in the specific embodiments that are disclosed and still obtain a like or similar result without departing from the spirit and scope of the invention, therefore all matter set forth or shown in the accompanying drawings is to be interpreted as illustrative and not in a limiting sense.

EXAMPLES

[0109] The following examples illustrate various iterations of the invention.

Introduction for Examples 1-5.

[0110] Catheter-associated urinary tract infections (CAUTIs) often arise from multidrug resistant Gram-positive and Gram-negative bacterial colonization and biofilm aggregation on the surface of indwelling urologic devices such as urinary catheters, rendering treatment very difficult. Uropathogenic Escherichia coli (UPEC), the primary cause of community-acquired UTI, account for 50% of nosocomial UTIs, including CAUTIs. Yet, very little is known about its pathogenesis following urinary catheterization, which results in the disruption of the normal mechanical and antimicrobial defenses of the bladder. Previous reports using human biopsies and rodent models of infections have shown that the catheterized bladder is edematous and highly inflamed with immune cell infiltration and pro-inflammatory cytokine production, an environment quite different from that which UPEC encounters in a non-catheterized bladder. We hypothesized that these profound catheter-related changes may affect UPEC pathogenesis.

[0111] The UPEC pathogenic cascade has been extensively characterized in a non-catheterized murine model of cystitis. UPEC elaborate on their surface adhesive type 1 pili which mediate binding to and invasion of superficial umbrella cells lining the bladder epithelium. Once intracellular UPEC can escape into the cytoplasm, replicate rapidly and undergo morphological differentiation within bladder epithelial cells to produce mature intracellular bacterial communities (IBCs) of ~10^4-10^5 bacteria with biofilm-like properties. UPEC then flux out from infected cells and can reinvade neighboring cells and start the process de novo. This acute phase of UPEC infection can lead to the development of chronic cystitis, pyelonephritis, and the formation of quiescent intracellular reservoirs (QIRs) with absence of bacteriuria. Detailed understanding of the critical steps of this pathogenic cascade has led to the development of small molecule inhibitors called mannosides. Mannosides specifically target the bacterial type 1 pili tip adhesin, FimH, which binds to mannosylated residues present on the surface of the bladder epithelium. Rationally designed to interfere and prevent FimH interaction with these residues, mannosides inhibit UPEC binding and invasion of the superficial umbrella cells during urinary tract infections (UTIs). Mannosides, in combination with existing antibiotic-based UTI therapy, have recently been shown to be effective in preventing and treating UPEC infections in non-catheterized infection models. The present study investigates whether this therapeutic approach could be beneficial in the prevention and treatment of CAUTIs.

[0112] In **Examples 1-5**, the optimized murine model of foreign body-associated UTI that closely mimics CAUTI was used to investigate the consequences of urinary catheterization on the pathophysiology of UPEC infection. For these studies, several UPEC virulence parameters, including the contribution of type 1 pili, IBC formation, and QIR reactivation, were assessed. The results obtained indicate that urinary catheterization provides UPEC with the opportunity to exploit the extracellular milieu of the bladder via type 1 pili-mediated biofilm formation on the surface of the foreign body, which results in a shift in the niche population. Administration of mannosides in combination with trimethoprim/sulfamethoxazole prior to urinary catheterization prevents UPEC colonization of the urinary tract. These Examples

provide important insights into the mechanisms underlying UPEC-mediated CAUTI, and informs efforts to design better therapeutic approaches to prevent and potentially treat these infections.

Materials and methods for Examples 1-5

Bacterial strains and growth conditions.

[0113] All strains used in this study and their characteristics are listed in **Table 1**. Unless otherwise specified, a single colony of *E. coli* grown on Luria Bertani (LB, Becton Dickinson) agar plate supplemented with appropriate antibiotics was inoculated into LB broth and grown statically at 37°C for 18 h.

Table 1: Strains used in this study

Species and Strains	**Relevant Antibiotic resistance**	**Characteristics**
UTI89		Parental UPEC UTI89 strain, cystitis isolate
UTI89Δ*fimH*		UTI89 with an in-frame deletion of *fimH*, type 1 pili defective
UTI89Δ*sfaA-H*		UTI89 with an in-frame deletion of *sfa* operon, S pili defective
UTI89Δ*sfaA-H*Δ*fimB-H*	Kan^R Cm^R	UTI89 with in-frame deletion of the *sfa* operon and the fim operon from *fimB* to *fimH*, S and type1 pili defective
UTI89Δ*csgA*		UTI89 with an in-frame deletion of *csgA*, curli deficient
UTI89Δ*csgB*Δ*csgG*		UTI89 with in-frame deletions of *csgB* and *csgG*, curli deficient
UTI89HK::GFP	Kan^R	UTI89 with an

		insertion of kanamycin cassette and GFP at the HK site
UTI89pCOMGFP	Kan^R	UTI89 ectopically expressing GFP from pCOM plasmid

In vitro cultivation and quantification of biofilms.

[0114] Biofilms were grown as described by Ferrieres et al. (2007; FEMS Immun. Med. Micro 51:212) on All Silicone Foley catheters (Bard Medical, GA) or silicone tubing (Thermo Fisher Scientific Inc., PA) and modified as follows. All tubing and connectors in the system were autoclaved and ethanol sterilized prior to use. The system was assembled similar to the previously described flow-chamber system. Priming of the catheter or the silicone tubing occurred at 37°C for 20min by flowing pre-warmed pooled human urine. Urine was collected from healthy volunteers as approved by the Institutional Review Board of Washington University in St. Louis. Pooled samples were spun at 10000xg for 15min, filtered through 33μM filters, and, if necessary, stored at 4°C for no more than 3 days. Three milliliters of stationary-phase *E. coli* from overnight cultures were diluted to 1-2x10^6 CFU/ml in human urine and injected into the catheter or silicone tubing using a 30 cc gauge needle. The bacteria were allowed to attach to the substratum for 1 h before urine flow via Watson-Marlow peristaltic pump 205S was resumed at 0.5 ml min^{-1}. When indicated, urine was supplemented with 1% methyl mannose (Sigma, MO) prior to the experiment. After 24 hours, the remaining medium was exchanged for sterile ddH_2O that was allowed to flow at 0.5 ml min^{-1} to remove residual urine and non-adherent bacteria in the system. The liquid from catheter or silicone tubing was then removed by capillary action onto absorbent paper. The tubing was cut into pieces for CFU enumeration or crystal violet staining, respectively. For CFU enumeration, at least three pieces (1cm in length) of incubated tubing were separately further cut into smaller pieces and placed into 1ml PBS. Adherent cells were detached by sonication (10min) and vigorous vortexing (3min). Viable bacterial counts were assessed by serial dilution on LB plate with appropriate antibiotics. Crystal violet

staining was used to determine biofilm biomass. At least 3 pieces of incubated tubing (3cm in length) were filled with 0.5% crystal violet at room temperature for 10 min. Excess dye was removed by washing three times with ddH_2O and dried by capillary action on absorbent paper. The bound crystal violet was then dissolved in 200 µl of 33% acetic acid and absorbance measured at 595nm. The amount of biofilm was expressed as CFU/ml per cm^2 and $A595/cm^2$. The experiment was repeated at least three times with different urine samples.

Animal implantation and infections.

[0115] Six to seven week-old female wild-type C57BL/6Ncr mice purchased from the National Cancer Institute (NCI) were used in this study. Experiments were performed following one week adaptation in the animal facility after arrival from NCI. Animals were implanted and infected with the indicated bacterial strain as previously described. Briefly, seven to eight week-old female mice were anesthetized by inhalation of isoflurane and implanted with platinum-cured silicone tubing (4-5 mm in length) (Implanted). Immediately following implantation, 50µl of ~1-2x10^7 CFU bacteria in 1xPBS were introduced in the bladder lumen by transurethral inoculation. Non-implanted animals were inoculated in the same manner. Animals were sacrificed at indicated time points by cervical dislocation under anesthesia inhalation. Bladders and kidneys were aseptically harvested. Subsequently, the silicone implant was retrieved from the bladder when present, placed in PBS, sonicated for 10 min and then vortexed at maximum speed for 3 min. Bladder and kidneys from each mouse were homogenized in PBS. Samples were serially diluted and plated on LB agar plates supplemented with appropriate antibiotics. CFU were enumerated after 24h incubation at 37°C. In all cases, experiments were performed at least twice with n=5 mice/strain/condition. All studies and procedures were approved by the Animal Studies Committee at Washington University School of Medicine.

Mannoside and antibiotic treatment.

[0116] For pretreatment experiments, 50µl mannoside (mannoside 2ZFH56; 5 mg/kg mouse body weight) or PBS was administered intraperitoneally 30min prior to implantation as previously described. As indicated for pre-infection treatment, trimethoprim/sulfamethoxazole (TMP-SMZ) was added to the drinking water for three days prior to infection at 54 and 270 µg/ml, respectively. The drinking water was changed every 24h. To assess the effects of mannoside and/or TMP-SMZ on established infections, animals were implanted and infected for 24h. At 24hpi, TMP-SMZ was added to the drinking at the concentrations indicated above and mannoside 2ZFH56 or PBS was administered i.p. 6h prior to sacrifice. Animals were sacrificed 48hpi.

UPEC reservoir reactivation.

[0117] Non-implanted animals were infected with UTI89HK::GFP as described above. At fourteen days post infection, urine was collected, serially diluted and plated for CFU and a subset of animals implanted as described above. Animals determined to be bacteriuric (bacterial loads greater than or equal to 10^4 CFU/ml in urine) as counted on titer plates the next day were eliminated from further study. QIR reactivation post-implantation was assessed by CFU enumeration of bacteria on implants and in the organs 3 or 5 days post-implantation (17 or 19 dpi). UTI89HK::GFP titers greater than 10^4 CFU/ml on implants or bladders were considered reactivation events. Measures of reactivation events of animals, which were non-bacteruric at 14 dpi but non-implanted served as controls.

[0118] IBC enumeration and visualization. Implanted and non-implanted animals were infected with UTI89 for 6h. When indicated, mannoside 2ZFH56 (5mg/kg) or PBS was administered i.p. at 30 min prior to implantation. At 6hpi, bladders were harvested, bisected, splayed on silicone plates and fixed in 2% paraformaldehyde. LacZ staining of whole bladders was performed as previously described. Punctate violet spots characteristic of IBCs were enumerated by light microscopy.

[0119] For IBC visualization, animals were infected with UTI89 constitutively expressing GFP (UTI89pCom-GFP). At the indicated time point, bladders were removed, bisected, splayed, and fixed as described above. The splayed bladders were then incubated for 20 min at room temperature with Alexa Fluor 633-conjugated wheat germ agglutinin (WGA; 1:1000 in PBS; Molecular Probes) for staining of the bladder surface and, when indicated, SYTO83 (1:1000 in PBS; Molecular Probes) to stain bacteria. Bladders were rinsed with PBS, mounted using Prolong Gold antifade reagent (Invitrogen) and examined with a Zeiss LSM510 confocal laser scanning microscope under a 63X objective. SYTO83 and WGA were excited at 543 and 633 nm, respectively.

Gentamicin protection assay.

[0120] To quantify intracellular and extracellular bacteria, bladders were aseptically harvested at 3 and 6 hpi. Bladders were cut in 4 parts and washed three times in 500 µl PBS. The wash fractions were pooled, centrifuged at 500 rpm for 5 min to pellet exfoliated bladder cells. The supernatants were then serially diluted and plated on LB agar supplemented with appropriate antibiotics, which were incubated at 37°C for 24 hrs to obtain extracellular bacterial CFU counts. Rinsed bladders were then treated with 100 µg/ml gentamicin for 90 min at 37°C. Following gentamicin treatment, the bladder tissue was washed twice with PBS to eliminate residual antibiotics, homogenized in 1 ml PBS, and bacterial CFU counts of determined as above to determine the levels of intracellular bacteria (protected from gentamicin killing).

Statistical methods.

[0121] Comparisons between groups were conducted by nonparametric Mann-Whitney U test using GraphPad Prism (GraphPad software, version 5). Values below the limit of detection for *in vivo* experiments (20 CFU for organs, 40 CFU for implants) were assigned the appropriate LOD value for statistical analyses. All tests were two tailed, and a *p*-value less than 0.05 was considered significant. Colonization

and infection was defined as organs/implants with bacterial titers above the limit of detection.

Example 1: UPEC adherence, invasion, and IBC morphology are unaltered in catheterized bladders.

[0122] IBC formation occurs in the pathogenesis of UPEC in non-catheterized patients and has been shown in mouse models to be critical for infection. To assess the effects of urinary catheterization on IBC formation, 4-5mm platinum-cured silicone tubing sections were implanted in the bladders of C57Bl/6Ncr female mice, which were then immediately infected with 1-2x10^7 CFU of the well-studied virulent UPEC strain UTI89 by transurethral catheterization. Gentamicin protection assays performed at 3hpi revealed no statistical difference in either the extracellular or intracellular UPEC populations in the presence or absence of implants (**Fig. 1**), indicating no gross defect in bacterial invasion in implanted animals. IBC formation within both implanted and non-implanted bladders was assessed by LacZ staining and confocal scanning laser microscopy (CSLM) at 6hpi (**Fig 2A**). Inoculation of UPEC into implanted animals resulted in significantly fewer IBCs with a median of 8 IBCs/bladder (p=0.0044; **Fig 2B**) compared to non-implanted animals in which IBC numbers ranged up to >250 IBCs/bladder with a median of 55 IBCs/bladder. However, bacterial CFU in implanted bladders were similar to those in non-implanted animals (data not shown). To account for this observation, we postulated that IBC morphology might be different in implanted animals. However, IBCs formed in implanted animals were observed to be overall similar in size and shape as those produced in non-implanted bladders (**Fig 2C**). UPEC were also seen to produce multiple IBCs within one umbrella cell and filamentous bacterial clumps in both catheter implanted and non-implanted bladders at 6hpi (**Fig. 3**). UPEC colonization at 6hpi was selectively localized in the remaining umbrella cells and not observed in the exposed underlying epithelium in implanted bladders (**Fig. 3**). Together, these findings indicate that urinary catheterization negatively impacts IBC formation by UPEC, possibly due to a correlated increase in exfoliation.

Example 2: Bacteria originating from existing UPEC reservoirs can seed urinary implant colonization.

[0123] One troubling possible outcome of the UPEC pathogenic cascade is the establishment of quiescent intracellular reservoirs (QIR) in the underlying epithelial layers, which have been shown can be a source of recurrent UTIs (rUTIs). QIRs were shown to be reactivated following treatment with protamine sulfate, a chemical that leads to exfoliation of the superficial umbrella cells of the uroepithelium. Like protamine sulfate, we have previously shown that urinary catheterization causes severe damage to the protective uroepithelial layer. Thus, we hypothesized that urinary catheterization might also reactivate existing UPEC reservoirs; resulting in bacteruria, catheter colonization and further dissemination. To test this hypothesis, mice were infected with 1-2x10^7 CFU UTI89HK::GFP and infection allowed to resolve over the course of 2 weeks. On day 14 post-infection, urine was collected from each animal to assess infection state prior to urinary implantation of a subset of these animals. Those animals in which titering of urines 14 dpi indicating bacteriuria (≥10^4 CFU/ml) were considered to have active (non-resolved and or recurrent) infection and were removed from further analysis. The remaining mice were presumed to either have completely cleared the infection or to have established QIRs with bacteria loads between 10^1 and 10^4 CFU/ml. 3 or 5 days post implantation, reservoir reactivation was assessed by bacterial colonization of implants and bladder. On day 3 post implantation, UPEC UTI89HK::GFP was recovered from implants in 3 of 26 implanted mice (~11.5%). One mouse with implant had bladder colonization greater than 10^4 CFU/ml compared to none of the 22 similarly infected but non-implanted animals (**Fig. 4A**). There was no significant difference between groups at 3dpi. For mice assessed at 5 days post-implantation, UTI89HK::GFP was recovered from implants of 4 out of 32 animals (~13%) with two of them having bladder titers greater than 10^4 CFU/ml (**Fig. 4B**) compared to 0 out of 23 in non-implanted animals. Interestingly, there were overall significantly fewer bacteria recovered from the bladders of implanted animals compared to non-implanted animals at 5 dpi ($p=0.0010$), suggesting that either reactivated reservoirs are cleared by the immune response prior to day 5 following implantation or

increased exfoliation prevents establishment of persistent infections. Together, these data indicate that urinary catheter colonization can occur from previous urinary infections even if those infections appear by bacteriuria counts to have been resolved.

Example 3: FimH is required for biofilm formation and UPEC colonization of the urinary tract following catheter implantation.

[0124] Biofilm formation is a critical component of CAUTI pathophysiology. We have previously shown that UPEC is able to produce biofilms on the surface of the foreign body and is recovered for the catheterized murine bladder at very high titers. Type 1 pili are major UPEC virulence factors that have been shown to be critical for biofilm aggregation, IBC formation, and other aspects of UPEC uropathogenesis. Thus, we assessed the contribution of these extracellular pili as well as other UPEC fibers, including curli which contribute to biofilm formation or S pili associated with *E. coli* clinical isolates producing strong biofilms, to biofilm formation in filtered human urine under flow conditions and UPEC-mediated CAUTI *in vivo*. Deletion of the gene for the tip adhesin of type 1 pili, FimH, in UTI89 resulted in significantly ($p<0.0001$) lower biomass (**Fig. 5A**) and an approximate 2-fold reduction in adherent viable bacteria (**Fig. 5B**) in biofilms formed in human urine *in vitro*. These data indicate that type 1 pili are a major contributor to UPEC biofilm formation in urine. The biofilm defect was specifically associated with the *fimH* mutant under these conditions, and was not observed following deletions of the *sfa* operon to prevent S pili formation, *csgA* required for curli fiber formation, or a component of the flagellar system *fliC* (data not shown).

[0125] *In vivo*, similar to findings in a murine model of cystitis, UTI89Δ*fimH* is severely attenuated in the murine model of foreign body-associated UTI (**Fig. 5C**). UTI89Δ*fimH* displayed >3 log fewer CFU in the bladder and was unable to ascend to the kidneys at 24hpi. Further, deletion of *fimH* resulted in significant reduction in implant colonization ($p<0.0001$). Similar to in vitro experiments, S-pili are not required for CAUTI since UTI89Δ*sfaA-H* is as virulent as wildtype UTI89 and a double deletion of both *sfaA-H* and *fimB-H* recapitulated the UTI89Δ*fimH* phenotype (**Fig. 6A**). Furthermore, components of the curli system important for biofilm formation in vitro under certain

conditions, but not in human urine (**Fig. 5A-B**), were also dispensable during CAUTI (**Fig. 6B**). The residual binding to implants and bladders in implanted animals could therefore be attributed to other pili or biofilm determinants. Together, these data strongly suggest that the tip adhesin FimH of type I pili is a critical determinant of UPEC virulence in mediating biofilm formation and virulence during CAUTI.

Example 4: Mannoside treatment reduces IBC formation.

[0126] Having established that FimH is required for UPEC virulence in implanted bladders, we investigated this as a potential therapeutic target for CAUTI using small molecules inhibitors designed to interfere with FimH binding to mannosylated residues. This family of small molecules, called mannosides, has recently been shown to prevent acute and chronic UPEC infections and potentiated the effectiveness of antibiotics in combinatorial treatment.

[0127] To investigate the potential therapeutic effects of mannosides on CAUTI, we first assessed the inhibitory effects of methyl-α-D-mannopyranoside (methyl mannose), on UTI89 biofilm formation in urine under flow. Similar to the deletion of *fimH* (**Fig. 5A**), UTI89 biofilms grown in presence of 1% methyl mannose had significantly reduced biomass (p=0.0022) and biofilm-adherent cells (p=0.0012), compared to untreated controls (**Fig. 7**). Since methyl mannose is a FimH antagonist, these data confirm the critical role of type 1 pili to biofilm formation in urine as was previously described for biofilms formed in LB media.

[0128] The effects of mannoside treatment were then assessed *in vivo* by using IBC formation as well as implant and urinary tract colonization as benchmarks of disease progression. Mice were treated intraperitoneally (i.p.) with saline or 5mg/kg of mannoside 2ZFH56, which is more potent than methyl mannose *in vitro* and *in vivo*, in PBS 30 min prior to urinary implantation. Catheter implantation was immediately followed by transurethral inoculation of UTI89. IBC formation and bacterial colonization were assayed by LacZ staining and CFU enumeration of implants, bladders, and kidneys at 6hpi and 24hpi, respectively. As shown in **Fig. 8A** and **8B**, mannoside treatment further reduced IBC formation (p=0.0051) and bladder colonization

(p=0.0114) in implanted animals at 6hpi, suggesting that this treatment prevents intracellular infection. While eliminated from their intracellular niche, data further indicated that UPEC were able to persist in the extracellular milieu where they can colonize the surface of the implants to relatively similar levels as saline-treated animals (p=0.0547) (**Fig. 8B**). No statistical difference was observed in kidney colonization in the presence or absence of mannosides (**Fig. 8B**). By 24hpi, a time point at which the mannosides have been eliminated from the bladder, similar bacterial loads were recovered from implants, bladders, and kidneys in implanted animals in the presence or absence of mannoside treatment (data not shown).

Example 5: Mannoside treatment increases the efficiency of TMP-SMZ in preventing UPEC colonization.

[0129] In order to examine whether mannosides could prevent establishment of CAUTI when used in combination with antibiotics, animals were treated with 54 and 270μg/ml of TMP-SMZ, respectively, in their drinking water for three days and then treated with saline or mannoside (5mg/kg) i.p. 30 min prior to implantation and bacterial inoculation. At 6hpi, UPEC colonized the implants and bladders at significantly lower levels in animals that only received antibiotics compared to those who received water or were only administered mannoside (**Fig. 8B**). Interestingly, mannoside treatment in addition to TMP-SMZ further decreased UPEC colonization of implants, bladders, and kidneys compared to treatment with antibiotic alone (p<0.0005 in all cases). Furthermore, treatment with mannosides alone did not reduce bacterial titers from a 24h old UPEC infection and in combination with TMP-SMZ showed no additive effects on established UPEC CAUTI 24hpi (data not shown). Together, these findings indicate that virulence-targeted therapies in combination with established antibiotic treatment can help prevent or delay the onset of CAUTI and that further research is warranted for enhancing mannosides potential as therapeutics against CAUTIs.

Discussion for Examples 1-5

[0130] UPEC is the major etiological agents of CAUTI. Yet, the molecular mechanisms of urinary catheter and bladder colonization following urinary catheterization have not been elucidated. Studies in an optimized murine model of foreign body-associated UTI10 show that urinary catheterization favors UPEC exploitation of the bladder extracellular milieu. This occurs via type 1 pili-dependent biofilm formation on the surface of silicone implants in the murine bladder. The data further indicate that of the biofilm determinants tested, type 1 pili are necessary for implant, bladder, and kidney colonization during CAUTI; providing definitive experimental evidence for previous reports postulating that type 1 pili may be required for UPEC persistence during CAUTIs. Interestingly, *fimH*-deficient UPEC strains have the ability to adhere to some extent to the surface of the foreign body, probably using other biofilm determinants such as other chaperone-usher pili systems, curli, or surface adhesins.

[0131] In addition to colonizing the foreign body in the bladder lumen, UPEC is able to exploit intracellular niches in implanted animals, albeit to a lesser degree than in non-implanted animals, by invading and producing IBCs in the early stages of infection. Reduced IBC formation in implanted animals may be a result of loss of the host superficial facet cells in which IBCs form due to increased exfoliation or damage to the uroepithelium following urinary catheterization. Nonetheless, this finding is of particular interest for treatment strategies against UPEC-mediated CAUTI. In humans, removal of the contaminated urinary catheter is the preferred method for treatment of these infections; however, the presence of bacteria in an intracellular compartment protected from host immune defenses and antibiotic treatment requires more comprehensive approaches as intracellular UPEC can lead to re-infection of a novel catheter or serve as a nidus for future UTI.

[0132] Quiescent intracellular reservoirs are an important outcome of UPEC pathogenic cascade because they are proposed to be a mechanism of recurrent UTI following damage to the uroepithelium. Findings from the current study indicate that

urinary implantation of animals with a history of UTI can lead to bladder infection and implant colonization with the UPEC causing the first infection. This finding suggests that in addition to introduction of extracellular and periurethral bacteria, urinary catheter colonization can occur from bacteria originating from pre-existing reservoirs or other niches within the urinary tract not appreciated by assessment of bacteriuria. Interestingly, by day 5 following implantation in animals with a history of UTI, there is overall a significant reduction in the number of QIRs compared to that in non-implanted animals as assessed by bladder CFU. This reduction in bacterial load could be a result of enhanced immune-mediated clearance of infected cells or to exfoliation of infected cells in implanted animals. These hypotheses are currently being evaluated.

[0133] The identification of FimH as a critical virulence factor during UPEC CAUTI provides an interesting avenue for the development of novel preventative measures against these infections. In fact, there has recently been an upsurge in recommendations and guidelines for management of CAUTIs and rUTIs in catheterized patients, with a particular focus on preventative measures including the limited use of catheters and even the prophylatic use of antibiotics prior and following catheter removal. However, the inappropriate use of antibiotics can worsen the problems of increasing antibiotic resistance. Accordingly, the present study suggests that the use of small molecules inhibitors, such as mannosides, in combination with existing UTI treatment regimes, can lead to prevention or delay of UPEC colonization. Mannosides, were rationally designed to interfere with FimH-mediated binding to mannosylated proteins on the surface of the uroepithelium. Recent studies show that the use of mannosides in combination with antibiotics is highly effective in preventing IBC formation and acute stages of UPEC infection as well as treating chronic cystitis. Similarly, pretreatment with mannosides further prevents IBC formation following UPEC infection of implanted bladders and reduces UPEC binding to the uroepithelium. However, the presence of the abiotic implant surface provided a favorable environment for adherence of extracellular bacteria. The inability of mannoside treatment to eliminate UPEC from the implant, given that the experimental evidence that mannose inhibits UPEC biofilm on catheter material in urine in vitro, may be due to the lack of urine flow

in this implanted murine model. It is possible that if it were possible to truly catheterize mice in a manner analogous to clinical catheterization of humans in which urine flows through the catheter that mannoside may have a more efficacious effect on implant clearance. Nonetheless, by preventing invasion and shifting UPEC's niche to the extracellular milieu, mannosides enhanced the bacteriocidal efficacy of antibiotics, such as TMP-SMZ, which does not cross host cell membranes. Mannosides could also be used in combination with bacterial interference strategy being offered as alternatives in the prevention of CAUTI. Previous reports have shown that pre-colonization of urinary catheters with an avirulent *E. coli* strain 83972 delays the onset of CAUTI in catheterized patients. Thus, it is quite possible that if used in combination with mannosides, UPEC will be kept from the intracellular niche as well as from binding to the catheter during bacterial interference with the avirulent strain. An attractive avirulent strain should be able to colonize the catheter in a type 1-independent manner to prevent invasion into urothelial cell, however *E. coli* strain 83972 enhanced binding to silicone catheter requires ectopic expression of *fim*. However, the therapeutic effects of mannoside 2ZFH56 could not be recapitulated in our model of CAUTI (data not shown), possibly because the small molecules are ineffective at disrupting established biofilms in vivo or that UPEC may employ additional type 1 pili-independent mechanisms for maintaining biofilms. It is a well-established fact that the extracellular matrix of bacterial biofilms is impermeable to antimicrobial and antibiotics, providing a safe haven for the microbes within. Further research is thus needed for better therapeutics against CAUTIs. Nonetheless, the prophylatic use of mannosides prior to urinary catheterization can help reduce the rate of recurrent UTIs from intracellular bacterial reservoirs following the removal of contaminated catheters.

[0134] Urinary catheterization is a necessary medical procedure that causes major damage to the urinary tract. Pathogens, such as UPEC, take advantage of this compromised environment to exploit new and existing niches and establish severe infections. This report uncovers important molecular mechanisms underlying UPEC pathogenesis following urinary catheterization. It raises important questions regarding the deleterious consequences of urinary catheterization and the origins of

urinary catheter colonization. These novel aspects of CAUTI pathophysiology, especially the presence of intracellular bacterial niches even in presence of urinary catheters, should thus be taken into consideration for better diagnosis and the development of anti-virulence based preventative and therapeutic approaches against these infections.

Example 6. Treatment of chronic mice with 5 doses of 4ZFH284 eliminates UPEC from the bladder.

[0135] Mice were infected with the uropathogenic *E. coli* (UPEC) strain UTI89. Animals that established chronic infection were treated at day 12 post infection with 5 doses of 50mg/kg of Mannoside 4ZFH284 administered 8h apart (mice treated with PBS in the same way were included as controls). Mice were sacrificed 48h post initial dose and bladder titers were enumerated.

[0136] The results clearly show a greatly reduced titer of UPEC in mice treated with Mannoside 4ZFH284 versus control mice treated with PBS (**Fig. 9**).

Example 7. Mannoside 4ZFH284 is effective against the multidrug resistant UPEC isolate EC958.

[0137] Mice were infected with the multidrug resistant (MDR) UPEC strain EC958. Animals that established chronic infection were treated at day 12 post infection with 1 dose of 50mg/kg of Mannoside 4ZFH284 (mice treated with PBS in the same way were included as controls). Mice were sacrificed 6h post initial dose and bladder titers were enumerated.

[0138] The results show that titers of MDR UPEC in mice treated with Mannoside 8 had significantly lower titers of the MDR UPEC compared to MDR UPEC titers in control mice treated with PBS (**Fig. 10**).

Introduction for Examples 8-12

[0139] The development of antibiotics to broadly treat infections has led to significant advances in human health. Increasing bacterial resistance to traditional

antibiotics and the dearth of programs to develop innovative antibiotics threatens to reverse these advances. This has been described as an impending "public health crisis". For example, over 15 million women suffer from urinary tract infections (UTI) annually in the U.S. with an estimated cost exceeding $2.5 billion. Uropathogenic *E. coli* (UPEC) account for up to 85% of all UTIs, which are exacerbated by increasing antimicrobial resistance. Resistance of UPEC to the antibiotic cocktail, trimethoprim-sulfamethoxazole (TMP-SMZ) has increased significantly in the past decade and thus therapy has increasingly required the use of last-line antibiotics such as fluoroquinolones, leading to increased treatment costs and an associated rise in multidrug resistance. These developments make UTI one of the most visible manifestations of increasing gram-negative antibiotic resistance. Recurrent UTI in healthy women is a major problem despite the fact that standard antibiotic treatment typically results in clearance of bacteriuria.

[0140] The two relevant niches during acute UTI are tissue and urine. The ability of bacteria to associate within the tissue niche is critical for establishing infection. Extracellular adhesive fibers known as pili are promising targets of anti-virulence therapeutics as they are critical factors for colonizing and invading host tissues and forming biofilms. UPEC use the chaperone/usher pathway to assemble type 1 pili tipped with the FimH adhesin. FimH mediates binding to mannosylated receptors present on the luminal surface of mammalian bladder epithelial cells, which facilitates bacterial invasion into these cells. Subversion of innate expulsion mechanisms requires entry into the cytoplasm where a single UPEC can replicate rapidly into 10^4-10^5 bacteria, which aggregate in a type 1 dependent manner into a biofilm-like intracellular bacterial community (IBC) that protects UPEC from host defenses and antibiotics. Bacteria later disperse from the IBC to spread to neighboring cells. FimH-dependent IBCs and the filaments that emerge from them commonly exist in women with recurrent cystitis as revealed in a clinical study of 100 women as IBC formation is thought to represent a mechanism that allows UPEC to rapidly expand in numbers. Virulence factors that increase the fitness of UPEC in the urinary tract are predicted to be under positive selection and the *fimH* gene is under positive selection in clinical isolates of UPEC,

consistent with its role in human disease. FimH is found in virtually all UPEC, the mannose binding pocket is invariant and mutations which disrupt mannose binding are attenuated. Previous studies support the utility of mannosides, to disrupt FimH function, as an effective therapeutic strategy to treat UTI our refs. The rational X-ray structure based design and synthesis of novel biphenyl mannosides FimH inhibitors were recently described, starting from phenyl mannoside 1 (**Fig. 11A**). In the following examples, it is shown that lead compound 6 (2ZFH56) and newly developed orally bioavailable mannosides are potent and fast acting antibacterial compounds. It is demonstrated that these mannosides are effective at treating and preventing UTI in mice as well as potentiating the antimicrobial effects of TMP-SMZ.

Example 8. Mannosides disrupt and inhibit the formation of biofilms.

[0141] Functional activity of mannoside FimH inhibitors **1-6** (**Fig. 11A**) was first assessed *in vitro* using a hemagglutination and UPEC biofilm assays. The relative ability of compounds to block biofilm formation and disrupt preformed biofilms was used to prioritize and select compounds for further *in vivo* evaluation. Biofilm formation is complex and the multiple determinants that contribute to their development and maintenance may vary depending on growth conditions, medium and substrates. *E. coli* biofilm formation in LB at room temperature on polyvinyl chloride (PVC) is dependent on type 1 pili and therefore these conditions were used to determine the efficacy of the mannosides. The median inhibitory concentration (IC_{50}) values for compounds **1-3** and **6** were all low micromolar but compound **6** showed the best activity with an IC_{50} of 0.74 μM (**Fig. 11B**). In addition to preventing the formation of biofilms, it was also found that the mannosides inhibited the buildup up of preformed biofilms (**Fig. 11C**). Confocal microscopy of preformed biofilms treated with mannoside **6** showed effective disruption of a preformed biofilm, likely explaining in part, the activity seen in **Fig 11C**. Furthermore, preformed biofilms treated with **6** lacked continuity as seen by gaping holes and lack of the tall mushroom-like structures observed in untreated biofilms (**Fig. 11D, E**). The propensity of *E. coli* to form biofilms contributes to antibiotic treatment

failures since antibiotics are unable to penetrate the dense biofilm matrix providing compelling evidence that biofilm inhibitors can potentiate the effects of antibiotics.

Example 9. Mannoside is efficacious at clearing severe infection.

[0142] From the *in vitro* studies in **Example 8**, mannosides **4** and **6** showed similar activity in the hemagglutination inhibition (HAI) assay which is predictive of relative activity in biofilm inhibition. However, the ester group in compound **4** was unstable for oral dosing and it was found that its hydrolysis product **5** was 13-fold less potent. Mannoside **6** which contains an amide in place of the ester, was not only equipotent to **4** but was also more stable plus had increased solubility and thus was selected as our lead compound for initial in vivo evaluation. Pharmacokinetic (PK) studies with lead compound 6 in mice was performed using intraperitoneal (IP) injection and oral (PO) gavage. Following IP dosing, 6 concentrations in the urine were quantified at several time points using HPLC and mass spectrometry (MS). Doses of 5 mg/kg and 10 mg/kg resulted in concentrations of 1 mM in the urine 30 min after treatment (**Fig. 12A**). Eight hours after administration, 6 levels remained near the IC_{50} (0.74 μM) of biofilm inhibition. The mouse PK of **6** dosed orally was next evaluated at several concentrations up to 200 mg/kg. A 100 mg/kg dose of 6 resulted in 3-fold higher concentrations relative to IP (10 mg/kg) eight hours post-dosing demonstrating some oral bioavailability of **6**. It is also noteworthy that >95% of drug was excreted in the urine unchanged and no apparent toxicity was observed up to a 200 mg/kg dose as measured by survival and weight gain/loss.

[0143] In order to determine the therapeutic potential of **6** for treating chronic UTIs, a unique preclinical murine model was adopted. In humans, the ultimate outcome of UPEC infection of the urinary tract ranges from asymptomatic bacteriuria to acute self-limiting infection to chronic/recurrent UTI. Similarly, the outcome of UTI in C3H/HeN mice ranges from self-limiting to long-lasting, chronic cystitis characterized by persistent, high titer bacteriuria (>10^4 colony forming units (CFU)/ml), high titer bacterial bladder burdens at sacrifice >2 weeks post-infection (wpi), chronic inflammation, and urothelial necrosis. The acute host response, within the first 24 hours, to tissue-

associated UPEC has been shown to determine disease outcome including predisposition to chronic/recurrent UTI. Thus, C3H/HeN mice were infected with 1 x 10^7 CFU of UTI89 and mice developing chronic cystitis, as determined by persistent urine titers of >10^6 through 2 weeks post infection (wpi), were PO treated at 2 wpi with **6** at a single dose of 100 or 50 mg/kg to evaluate the ability of mannoside to treat UTI. 6 hours post-treatment bacterial counts in the bladder were enumerated. A dramatic 3-log drop in bacterial titers was observed suggesting mannoside is efficacious at clearing severe infection within 6 hours of oral delivery of a chronic long lasting infection (**Fig. 12B**).

Example 10. Prophylactic use of mannoside

[0144] Since **6** successfully treated chronic cystitis, it was of interest to elucidate if mannosides could also prevent a UTI as a prospective prophylactic therapy. To mimic this clinical scenario, the efficacy of **6** in *in vivo* treatment was evaluated by dosing mice either IP or PO 30 min prior to infecting with UTI89. At 6 hours post infection (hpi), bladders were removed and total bacterial CFUs were quantified. In both the IP and PO treated cohorts a significant drop in bacterial counts was observed, demonstrating the efficacy of **6** in reducing overall UPEC colonization of the bladder (**Fig. 12E**). Furthermore, there was also a significant reduction of IBCs in the mice that were pretreated with mannoside (**Fig. 12F**). To demonstrate **6** reduced IBC formation by blocking UPEC invasion into the bladder tissue, gentamicin treatment assays were performed. Gentamicin kills extracellular UPEC but is unable to penetrate tissue and thus intracellular bacteria survive treatment. It was found that in the **6**-treated mice, gentamicin treatment of the bladders eliminated all CFUs (**Fig. 12G**). In bladders from untreated mice, 10^3 – 10^4 CFUs remained after gentamicin treatment, reflecting the bacteria present that had invaded the bladder epithelium and thus circumvented the treatment. Confocal microscopy of bladders in the untreated cohort showed normal, robust IBC formation (**Fig. 12C**) whereas IBCs were rarely seen in the mannoside treated mouse bladders however bacteria were observed in the bladder luminal compartment (**Fig. 12D**). These results demonstrate that a mannoside FimH inhibitor prevents bacterial invasion into the bladder tissue and significantly reduces infection in

the bladder. This novel class of orally active biphenyl mannosides has potential utility for the treatment of women suffering from chronic/recurrent UTIs as an alternative to prophylactic antibiotic treatment and would significantly benefit women with increased incidence of UTI due to sexual intercourse.

Example 11. Mannosides inhibit the invasion of UPEC into the bladder tissue and potentiate the efficacy of TMP-SMZ.

[0145] The first-line treatment of choice for UTI has traditionally been a 3-day course of TMP-SMZ. Women suffering from chronic/recurrent UTIs are often given TMP-SMZ prophylactically to prevent recurrence. However, resistance to this TMP-SMZ regimen is rapidly expanding. It was hypothesized that by preventing bacterial invasion into the bladder tissue, a FimH inhibitor may result in anti-virulence synergism with TMP-SMZ and may curtail or circumvent the problem of TMP-SMZ resistance. This theory was evaluated in a preclinical animal model where mice given TMP-SMZ for 3 days were infected with either UTI89 or the TMP-SMZR strain, PBC-1. Mice were IP treated with 6 30 min prior to inoculation with bacteria and compared to a control group of untreated animals. After inoculation with UTI89 or PBC-1, bacterial CFUs were quantified at 6 hpi. As expected, treatment with TMP-SMZ alone resulted in a significant drop in bacterial load in the UTI89-infected mice but had no effect on PBC-1, since it is resistant to TMP-SMZ. Upon treatment with **6** alone there was a significant drop in bacterial load of both strains in the bladder. In the dual treatment group there was also a significant drop in bacterial CFUs compared to mannoside alone or TMP-SMZ alone for both strains which was most pronounced for PBC-1 (**Fig. 13**). It was determined that the presence of mannoside had no effect on growth or killing efficiency of either strain during growth in vitro in the presence or absence of TMP-SMZ. Therefore, the observation that in combination with **6**, the TMP-SMZR strain PBC-1 succumbed to antibiotic treatment suggested that the mannoside potentiates the efficacy of TMP-SMZ by a unique mechanism. Based on growth curves in TMP-SMZ, PBC-1 was calculated to have a Minimum Inhibition Concentration (MIC) of 256 and 1280 μg/ml for TMP and SMZ, respectively and UTI89 was calculated to have an MIC of 0.05 μg/ml TMP and

0.25 μg/ml SMZ. The presence of mannoside had no effect on growth or killing efficiency of either strain. It is well established that TMP concentrates in the urine and this serendipitous feature is a major reason TMP-SMZ has been the preferred antibiotic for UTI over the last several decades. Using quantitative HPLC-MS, the concentration of TMP-SMZ was measured in the urine of mice after 3 days of treatment with 54 μg/ml and 270 μg/ml TMP and SMZ, respectively. TMP concentrations were determined to be 9.95 +/- 4.36 mg/ml and SMZ at 67.17 +/- 32.51 μg/ml. These results indicate that by preventing bacterial invasion, **6** compartmentalizes the microbes to the bladder lumen thus exposing them to TMP-SMZ concentrations above the MIC of PBC-1, resulting in augmentation of bacterial cell killing. Presumably TMP-SMZ concentrations reach tissue concentrations above the MIC needed for UTI89 killing but fail to reach tissue levels needed for killing PBC-1. These results clearly highlight the importance of the intracellular pathway in bacterial persistence. In addition to escaping the immune system in their intracellular niche, bacteria are also able to evade exposure to antibiotics as highlighted by the clinically TMP-SMZ resistant strain. In summary, mannosides could benefit those women on suppressive antibiotic therapy by inhibiting the invasion of UPEC into the bladder tissue and potentiating the efficacy of TMP-SMZ creating a cost-effective treatment, which is predicted to lower the rate of treatment failures.

Example 12. Mannoside optimization.

[0146] While **6** shows good efficacy *in vivo*, it was sought to identify optimized mannosides with further improved pharmacokinetics in particular those encompassing increased cell permeability and thus better oral bioavailability and bladder tissue penetration. The inherent polarity of mannosides and other sugar-derived compounds often limits their cellular permeability and increasing their hydrophobicity (LogP/LogD) is predicted to improve the latter. Computational modeling of mannosides bound to FimH suggested that the ortho-position of the biphenyl ring attached to mannose is aimed at Tyr137 and improved hydrophobic contact could be achieved by substitution. The increased hydrophobicity was not only predicted to improve FimH binding affinity but also the oral bioavailability and bladder tissue penetration relative to

starting mannoside **6**. Furthermore, these derivatives will likely display increased metabolic stability through protection of the glycosidic bond from hydrolysis both in the gut and by α-mannosidases. Thus, a matched pair analysis was performed of monoamide 3 compared to ortho-substituted analogs bearing methyl, trifluoromethyl, and chloro groups. The compounds were evaluated for their potency in the hemagglutination inhibition (HAI) assay and it was discovered that all biphenyl ring substitutions yielded more potent inhibitors (**Fig. 14A**). Ortho-chloro mannoside **7** inhibited hemagglutination with a potency of 125 nM which is 10-fold better than matched pair 3 while the ortho-methyl analog **8** was even 2-fold more active (HAI=62 nM). Substitution with trifluoromethyl gave the most potent analog **9** with an HAI=32 nM. This data suggests that our prediction for increased hydrophobic contact with Tyr137 might explain this enhanced potency since the trifluoromethyl analog **9** has the largest hydrophobic surface area and also shows the highest activity. However, it is also possible that the orientation of the phenyl rings are altered slightly and conformationally restricted in a more productive form conducive to improved FimH binding. In any case, the outcome of this preliminary study directed us to develop ortho-trifluoromethyl diamide **10** which is exponentially more potent than any previously reported mannoside FimH inhibitor with an HAI=8 nM. This unprecedented level of potency corresponds to a 15,000-fold improvement over butyl-α-D-mannoside (125 μM) and is 50-fold better than lead **6**. Based on their improved in vitro properties, we tested the optimized mannosides for mouse oral PK (**Fig 14B**) and found at 50 mg/kg compounds **8** and **10** yielded the highest concentrations in urine at 6 hours post dosing with 8 displaying equivalent concentrations to 100 mg/kg of mannoside **6**. Due to their enhanced potency and optimal PK, mannosides **8** and **10** were selected for further testing in our chronic infection mouse model. C3H/HeN mice having chronic cystitis at 2 weeks post infection were treated with **6**, **8** or **10**. Treatment with **8** and **10** resulted in a significant and dramatic 4 log reduction in bacterial counts in the bladder 6 hours posttreatment (Fig 4c). Although ortho-trifluoromethyl diamide **10** is 8-fold more potent in vitro than ortho-methyl monoamide **8**, it was found that when dosed orally at 50 mg/kg **8** showed better efficacy in vivo. **8** reduced bacterial CFUs in the bladder almost 2 Log units better than

6 at the identical 50 mg/kg dose and was still more efficacious than a 100 mg/kg dose of **6**. These results can be explained by increased FimH inhibition combined with improved PK of the ortho-substituted mannosides relative to **6**. Mannoside 8 represents a very promising lead preclinical candidate for the oral treatment and prevention of recurrent urinary tract infections.

Discussion for examples 8-12.

[0147] The efficacy of anti-virulence compounds in vivo has not been extensively characterized. Herein, the most potent orally active small molecule FimH antagonists described are reported to date. This is also the first demonstration that a mannoside FimH inhibitor shows therapeutic potential for treating an established chronic urinary tract infection *in vivo*. These innovative compounds also show excellent efficacy *in vivo* when used prophylactically. Furthermore, the mechanism of action displayed by FimH inhibitors keeps bacteria extracellular and sensitizes a TMP-SMZ resistant strain by prolonging exposure to antibiotic levels above its MIC. This enhanced susceptibility may help overcome the rising problem of TMP-SMZ resistance amongst E. coli. Not only are these anti-virulence FimH antagonists effective as a treatment against UTI, but their oral availability represents a major step toward effective preclinical optimization and drug development. Alternative management strategies are needed for patients suffering from chronic/recurrent UTIs. Prophylactic administration of mannoside alone or in combination with TMP-SMZ could potentially reduce the incidence of treatment failure and shorten the time span of currently administered suppressive therapy. A shift to reduce the use of fluoroquinolones would provide both a more cost-effective treatment option as well as slow the spread of resistance to this class of antibiotics. Given that resistance to antibiotic therapy is rapidly increasing, it is time to reconsider standard UTI therapy in order to preserve the effectiveness of current antibiotics. The use of FimH inhibitors as a targeted therapeutic strategy benefits from the fact that it is not broad spectrum and will specifically target those bacteria expressing type 1 pili, ubiquitous amongst UPEC. Given the unique welldefined clinical population of patients with UTI, of which nearly 85% of the cases are caused by UPEC,

the narrow spectrum afforded by mannosides provides an advantage over alternative therapies and other broad spectrum anti-virulence drugs currently in clinical trials. It is predicted that mannosides either dosed alone or in combination with commonly used antibiotics can treat almost all initial and chronic UTIs.

[0148] Outside of UTI, cell-cell adherence to host tissues is the first step in most infectious diseases. Thus, due to the commonality of adhesion mechanisms in bacterial and viral pathogenesis, similar but unique anti-virulence compounds can be tailored to treat a multitude of infectious diseases. The results in **Examples 8-12** validate the utility of employing a rational approach to study the molecular mechanisms of pathogenesis and resulted in the discovery and development of potential anti-virulence therapeutics, which specifically target mechanisms essential in UPEC pathogenesis. In conclusion, these studies have the potential to revolutionize current approaches to both antimicrobial and anti-viral treatment and provides not only new opportunities for effectively treating a broad range of infectious diseases, but also the potential to curtail the ever expanding medical crisis of pathogen resistance to traditional antibiotics.

Methods for Example 8-12.

[0149] UTI89 biofilm was grown in LB +/- mannoside for 24 h at 22°C in PVC plates and quantified using crystal violet. UTI89 biofilm for confocal microscopy was grown in LB for 24 h at 22°C on PVC coverslips followed by mannoside treatment for 16 h. For all animal experiments UTI89 or PBC-1 was grown 2x24 h statically in LB at 37°C and inoculated at a dose of $1x10^7$ bacteria in 50 µl. All mice used were female C3H/HeN (Harlan). For the chronic UTI model, mice were infected for 2 weeks prior to treatment with mannoside. For IP dosing, 50 µl of 2 mg/ml (5 mg/kg) or 4 mg/ml (10 mg/kg) **6** in PBS was injected into the mouse 30 min prior to inoculation of bacteria. For oral dosing, 100 µl of 10 mg/ml (50 mg/kg) or 20 mg/ml (100 mg/kg) mannoside in 8% DMSO was inoculated with a gavage needle 30 min prior to inoculation of bacteria. Mass spectrometry was used to quantify urinary mannoside or TMP-SMZ concentrations. For CFU counts, bladders were harvested at 6 hpi and placed in 1 mL

PBS. Bladders were then homogenized, diluted and plated on LB. After growth at 37°C overnight, bacterial counts were determined. LacZ staining and gentamicin protection assays were performed at 6 hpi. For antibiotic experiments, mice were given TMP-SMZ in the drinking water at a concentration of 54 μg/ml and 270 μg/ml, respectively. Water was changed daily with fresh antibiotics. Standard growth curve and hemagglutination assays were performed. All statistical analysis performed was a two-tailed Mann-Whitney U test. Compounds **1-6** were prepared as outlined in Han et. al. (2010; J. Med Chem. 53:4779). Compounds 7-10 were prepared using slightly modified procedures. All compounds are >95% pure as determined by HPLC/MS and ^{1}H NMR.

Bacterial strains.

[0150] UTI89 is a prototypical cystitis isolate of serotype O18:K1:H7. PBC-1 is a TMP-SMZ^R strain of serotype OX13:K1:H10 isolated from a 59 year old asymptomatic female with a history of recurrent UTI and diagnosis of primary biliary cirrhosis.

Synthesis of mannosides.

[0151] 1. General synthesis, purification, and analytical chemistry procedures.

[0152] Starting materials, reagents, and solvents were purchased from commercial vendors unless otherwise noted. ^{1}H NMR spectra were measured on a Varian 300 MHz NMR instrument. The chemical shifts were reported as δ ppm relative to TMS using residual solvent peak as the reference unless otherwise noted. The following abbreviations were used to express the multiplicities: s = singlet; d = doublet; t = triplet; q = quartet; m = multiplet; br = broad. High-performed liquid chromatography (HPLC) was carried out on GILSON GX-281 using Waters C18 5μM, 4.6*50mm and Waters Prep C18 5μM, 19*150mm reverse phase columns, eluted with a gradient system of 5:95 to 95:5 acetonitrile:water with a buffer consisting of 0.05% TFA. Mass spectra (MS) were performed on HPLC/MSD using electrospray ionization (ESI) for

detection. All reactions were monitored by thin layer chromatography (TLC) carried out on Merck silica gel plates (0.25 mm thick, 60F254), visualized by using UV (254 nm) or dyes such as $KMnO_4$, *p*-Anisaldehyde and CAM. Silica gel chromatography was carried out on a Teledyne ISCO CombiFlash purification system using pre-packed silica gel columns (12g~330g sizes). All compounds used for biological assays are greater than 95% purity based on NMR and HPLC by absorbance at 220 nm and 254 nm wavelengths.

2. Experimental procedure for the preparation of mannoside 8

2.1 **[(2R,3S,4S,5R,6R)-4,5-diacetoxy-6-(acetoxymethyl)-2-(4-bromo-2-methyl-phenoxy)tetrahydropyran-3-yl] acetate**.

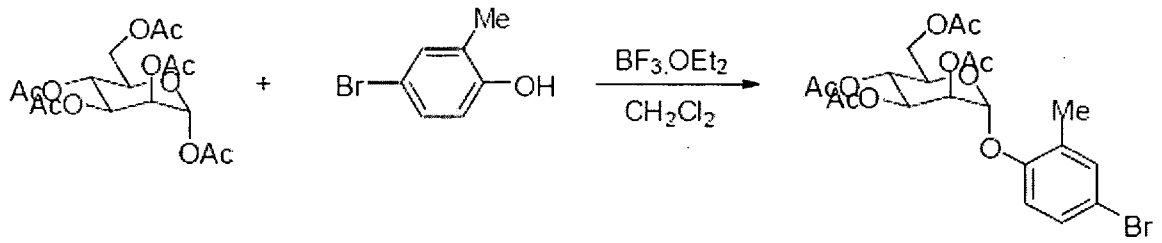

[0153] Under nitrogen atmosphere and at room temperature, boron trifluoride diethyl etherate (3.41 g, 24 mmol) was added dropwise into the solution of α-D-mannose pentaacetate (3.12 g, 8 mmol) and 4-bromo-2-methylphenol (2.99 g, 16 mmol) in 100 ml of anhydrous CH_2Cl_2. After a few mins the mixture was heated to reflux and kept stirring for 45 hrs. The reaction was then quenched with water and extracted with CH_2Cl_2. The CH_2Cl_2 layer was collected dried with Na_2SO_4, concentrated. The resulting residue was purified by silica gel chromatography with hexane/ethyl acetate combinations as eluent, giving the title compound (3.22 g) in 77% yield. ^1H NMR (300 MHz, CHLOROFORM-d) δ 7.18 - 7.38 (m, 2H), 6.97 (d, J = 8.79 Hz, 1H), 5.50 - 5.59 (m, 1H), 5.43 - 5.50 (m, 2H), 5.32 - 5.42 (m, 1H), 4.28 (dd, J = 5.63, 12.50 Hz, 1H), 3.99

- 4.15 (m, 2H), 2.27 (s, 3H), 2.20 (s, 3H), 2.02 - 2.11 (three singlets, 9H); MS (ESI): found: [M + Na]+, 539.0.

2.2 **N-methyl-3-[3-methyl-4-[(2R,3S,4S,5S,6R)-3,4,5-trihydroxy-6-(hydroxymethyl)tetrahydropyran-2-yl]oxy-phenyl]benzamide (8).**

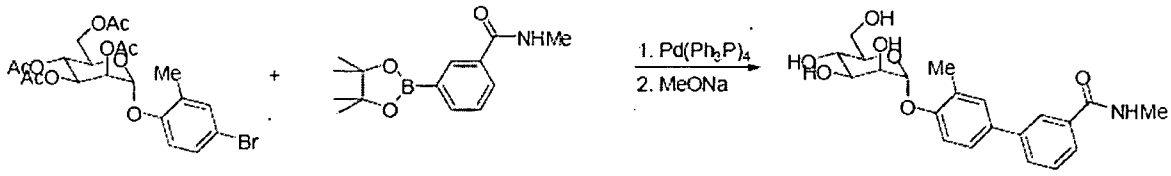

[0154] Under nitrogen atmosphere, the mixture of [(2R,3S,4S,5R,6R)-4,5-diacetoxy-6-(acetoxymethyl)-2-(4-bromo-2-methyl-phenoxy)tetrahydropyran-3-yl] acetate (0.517 g, 1 mmol), 3-(N-Methylaminocarbonyl)phenylboronic acid pinacol ester (0.392g, 1.5 mmol), cesium carbonate (0.977 g, 3 mmol) and tetrakis(triphenylphosphine)palladium (0.116 g, 0.1 mmol) in dioxane/water (15 mL/3 mL) was heated at 80°C with stirring for 1 h under a nitrogen atmosphere. After cooling to RT, the mixture was filtered through silica gel column to remove the metal catalyst and salts with hexane/ethyl acetate combinations as eluent. The filtrate was concentrated, and then dried in vacuo. The residue was diluted with 15 mL of methanol containing a catalytic amount of sodium methoxide (0.02 M) and the mixture was stirred at RT overnight. H+ exchange resin (DOWEX 50WX4-100) was added to neutralize the mixture. The resin was filtered off and the filtrate was concentrated. The resulting residue was purified by silica gel chromatography with CH_2Cl_2/MeOH combinations as eluent, giving the title compound (0.260 g) in 64% yield for two steps. ^{1}H NMR (300 MHz, METHANOL-d4) δ 7.94 (t, J = 1.65 Hz, 1H), 7.57 - 7.72 (m, 2H), 7.33 - 7.50 (m, 3H), 7.23 (d, J = 8.52 Hz, 1H), 5.48 (d, J = 1.92 Hz, 1H), 4.00 (dd, J = 1.79, 3.43 Hz, 1H), 3.83 - 3.94 (m, 1H), 3.60 - 3.76 (m, 3H), 3.46 - 3.58 (m, 1H), 2.87 (s, 3H), 2.24 (s, 3H). MS (ESI): found: [M + H]+, 404.2.

[0155] Mannosides **7** and **9** were prepared following a similar procedure to the synthesis of **8**.

3. Experimental procedure for the preparation of mannoside **10**

3.1 **[(2R,3S,4S,5R,6R)-4,5-diacetoxy-6-(acetoxymethyl)-2-(4-bromo-2-trifluoromethylphenoxy) tetrahydropyran-3-yl] acetate**:

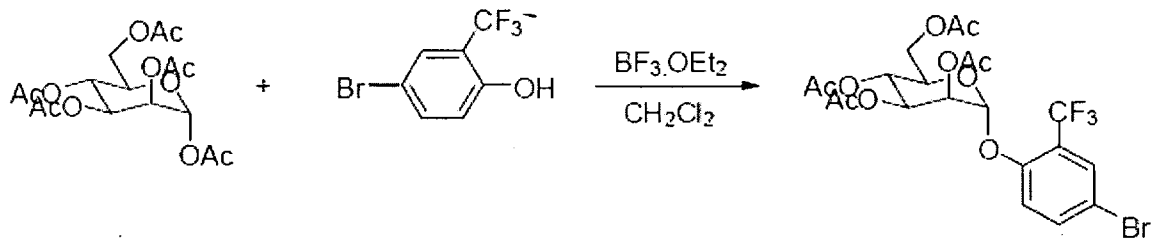

[0156] Using the procedure outlined in 2.1 using 4-bromo-2-trifluoromethylphenol, the title compound was obtained (2.5 g) in 54% yield. ^{1}H NMR (300 MHz, CHLOROFORM-d) δ 7.75 (d, J = 2.20 Hz, 1H), 7.61 (dd, J = 2.47, 8.79 Hz, 1H), 7.15 (d, J = 8.79 Hz, 1H), 5.61 (d, J = 1.65 Hz, 1H), 5.32 - 5.58 (m, 3H), 4.28 (dd, J = 5.22, 12.36 Hz, 1H), 3.95 - 4.22 (m, 2H), 2.21 (s, 3H), 2.07 (s, 3H), 2.06 (s, 3H), 2.04 (s, 3H) ; MS (ESI): found: [M + Na]+, 593.0.

3.2 **N1,N3**-dimethyl-**5-(4,4,5,5-tetramethyl-1,3,2-dioxaborolan-2-yl)benzene-1,3-dicarboxamide**.

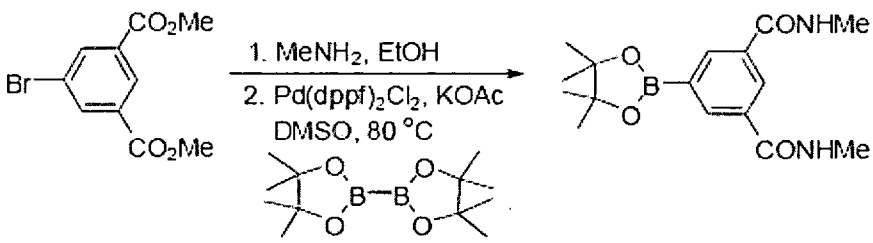

[0157] Dimethyl 5-bromobenzene-1,3-dicarboxylate (10.6 g, 36.8 mmol) was dissolved in a 33 wt% solution of methylamine in EtOH (30 mL) and stirred for 6h at RT. The precipitate that formed during the reaction was filtered to give 5.3 g (53%) of the intermediate 5-bromo-N1,N3-dimethyl-benzene-1,3-dicarboxamide as a white solid. Concentration of the remaining filtrate yielded an additional 4.6 g (46%) of product. 5-bromo-N1,N3- dimethyl-benzene-1,3-dicarboxamide (5.3 g, 19.5 mmol), $Pd(dppf)_2Cl_2$ (0.87 g, 1.2 mmol), di-pinacolborane (6.1 g, 24 mmol), and potassium acetate (7.8 g, 80 mmol) were dissolved in DMSO (100 mL). The solution was stirred under vacuum and then repressurized with nitrogen. This process was repeated 3 times and then the resultant mixture was stirred at 80 °C for 5h under a nitrogen atmosphere. After removal of the solvent under high vacuum, the crude material was purified by silica gel chromatography to give the title compound as a light tan solid (2.2 g, 35%). ^{1}H NMR (300 MHz, DMSO-d6 δ 8.63 (m, 2H), 8.41 (t, J = 1.51 Hz, 1H), 8.23 (d, J = 1.65 Hz, 2H), 2.80 (s, 3H), 2.78 (s, 3H), 1.33 (s, 12H). MS (ESI): found: [M + H]+, 319.2.

3.3 **N1,N3-dimethyl-5-[3-(trifluoromethyl)-4-[(2R,3S,4S,5S,6R)-3,4,5-trihydroxy-6-(hydroxymethyl)tetrahydropyran-2-yl]oxy-phenyl]benzene-1,3-dicarboxamide (10)**.

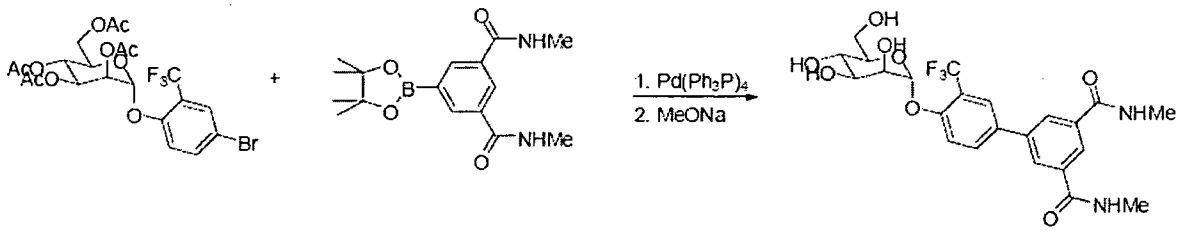

[0158] Using the procedure outlined in 2.2 with [(2R,3S,4S,5R,6R)-4,5-diacetoxy-6-(acetoxymethyl)-2-(4-bromo-2-trifluoromethyl-phenoxy)tetrahydropyran-3-yl] acetate (0.57 g) and N1,N3-dimethyl-5-(4,4,5,5-tetramethyl-1,3,2-dioxaborolan-2-yl)benzene-1,3-dicarboxamide (0.48 g), the title compound was obtained (0.340 g) in 69% yield for the two steps. ^{1}H NMR (300 MHz, METHANOL-d4) δ 8.17 - 8.24 (m, 1H),

8.14 (d, J = 1.65 Hz, 2H), 7.92 (d, J = 1.92 Hz, 1H), 7.87 (dd, J = 2.20, 8.79 Hz, 1H), 7.57 (d, J = 8.79 Hz, 1H), 5.64 (d, J = 1.65 Hz, 1H), 4.04 (dd, J = 1.65, 3.30 Hz, 1H), 3.87 - 3.96 (dd, 1H), 3.64 - 3.83 (m, 3H), 3.48 - 3.63 (m, 1H), 2.93 (s, 6H). MS (ESI): found: [M + H]+, 515.1.

Biofilm assay.

[0159] UTI89 was grown in LB broth in wells of PVC microtiter plates at 23°C in the presence of individual mannosides at varying concentrations. After 48 h of growth, wells were rinsed with water and stained with crystal violet for quantification as described. For biofilm disruption activity in PVC plates, UTI89 was grown in LB broth in wells of PVC microtiter plates at 23°C. After 24 h of growth, mannoside was added and biofilms were grown for an additional 16 h. Wells were then rinsed, stained with crystal violet and quantified. For biofilm disruption activity on PVC coverslips, UTI89 was grown in LB broth in 50 mL conicals containing PBC coverslips at 23°C. After 24 h of growth, 0.3 μM ZFH-2056 was added and biofilm was grown for an additional 16 h. Coverslips were then rinsed, fixed with 2% paraformaldehyde (v/v), stained with SYTO9 (1:1000 in PBS; Molecular Probes) and observed with a Zeiss LSM410 confocal laser scanning microscope under a 63X objective.

Animal infections.

[0160] Bacteria were grown under type 1 pili-inducing conditions (2x24 h at 37°C statically in LB). The bacteria were harvested and resuspended to an OD_{600} of 0.5 in PBS. Eight-week-old C3H/HeN (Harlan) female mice were anesthetized by inhalation of isoflurane and infected via transurethral catheterization with 50 μl of the bacterial suspension, resulting in 1-2 x 10^7 inoculum. At 6 hpi, mice were sacrificed by cervical dislocation under anesthesia and the bladders were immediately harvested and processed as described below. All animal studies using mice were approved by the Animal Studies Committee of Washington University (Animal Protocol Number 20100002).

Chronic infection.

[0161] Mice were infected with UTI89 and the infection was allowed to continue for 2 weeks. At 12 days post-infection, urine was collected and titered to determine mice chronically infected (urine titers $>10^6$). At 2 wpi, chronically infected mice were treated PO with 50 mg/kg or 100 mg/kg of mannoside. 6 h posttreatment, mice were sacrificed and bladders were aseptically removed and homogenized to determine tissue titers.

Enumeration of bladder IBCs.

[0162] For animal pretreatment experiments, mannoside ZFH-2056 was administered either IP (5 mg/kg) or orally (100 mg/kg) 30 min prior to inoculation with UTI89. To accurately count the number of IBCs, mice were sacrificed 6 hpi and bladders were aseptically removed, bisected, splayed on silicone plates and fixed in 2% paraformaldehyde (v/v). IBCs, readily discernable as punctate violet spots, were quantified by LacZ staining of whole bladders.

Pharamacokinetic analysis.

[0163] For intraperitoneal dosing, 50 µl of a 2 mg/ml (5 mg/kg) or 4 mg/ml (10 mg/kg) solution of **6** in PBS was injected into the peritoneal cavity of the mouse. For oral dosing, 100 µl of a 20 mg/ml (100 mg/kg) solution of ZFH-2056 in 8% DMSO was inoculated with a gavage needle into the mouse stomach. Urine was collected at 30 min, 1, 2, 3, 4, 6, and 8 h post-treatment. An equal volume of 10 µM internal standard (ZFH-2050) was added to the urine. Mannosides were extracted from the urine by loading on C18 columns (100 mg, Waters), washing with 30% methanol, and eluting with 60% methanol. Vacuum-concentrated eluates were analyzed using liquid chromatography-mass spectrometry system with a lower heated capillary temperature of 190°C and a gradient as follows: Solvent B (80% acetonitrile in 0.1% formic acid) was held constant at 5% for 5 minutes, increased to 44% B by 45 minutes, and then to a 95% B by 65 minutes. SRM mode quantification was performed with collision gas energy of 30% for the following MS/MS transitions (precursor m/z/product m/z):

compound **6**, 447/285; compound **3**, 390/228. Absolute quantification was achieved by comparison to a calibration curve.

Bladder tissue bacterial titer determination.

[0164] Mannoside ZFH-2056 was administered either IP (5 mg/kg) or orally (100 mg/kg) 30 min prior to inoculation with UTI89. To enumerate the bacteria present, mice were sacrificed at 6 hpi and bladders were aseptically removed and homogenized in 1 ml PBS, serially diluted and plated onto LB agar plates. CFU was enumerated after 16 h of growth at 37°C.

Confocal microscopy.

[0165] Mannoside **6** was administered IP (5 mg/kg) 30 min prior to inoculation with UTI89. To visualize bacterial behavior within the bladder, mice were sacrificed at 6 hpi and bladders were aseptically removed, bisected, splayed on silicone plates revealing the luminal surface and fixed in 2% paraformaldehyde (v/v). The splayed bladders were then incubated for 20 min at room temperature with (i) SYTO9 (1:1000 in PBS; Molecular Probes) to stain bacteria and (ii) Alexa Fluor 594-conjugated wheat germ agglutinin (WGA; 1:1000 in PBS; Molecular Probes) to stain the bladder luminal surface. Bladders were rinsed with PBS, mounted using Prolong Gold antifade reagent (Invitrogen) and examined with a Zeiss LSM510 confocal laser scanning microscope under a 63X objective. SYTO9 and WGA were excited at 488 and 594 nm, respectively.

Gentamicin protection assay.

[0166] To enumerate bacteria present in the intracellular versus extracellular compartments, bladders were aseptically harvested at 6 hpi. The bladders were then bisected twice and washed three times in 500 µl of PBS each. The wash fractions were pooled, lightly spun at 500 rpm for 5 min to pellet exfoliated bladder cells, serially diluted, and plated onto LB agar to obtain the luminal fraction. The bladders were treated with 100 µg of gentamicin/ml for 90 min at 37°C. After treatment, the

bladders were washed twice with PBS to eliminate residual gentamicin, homogenized in 1 ml of PBS, serially diluted, and plated onto LB agar to enumberate the CFUs in the intracellular fraction.

Antibiotic treatment.

[0167] Mice were given TMP-SMZ in the drinking water at a concentration of 54 μg/ml and 270 μg/ml, respectively. Water was changed daily for 3 days prior to inoculation with UTI89. Mice remained on TMP-SMZ during the infection. To determine TMP-SMZ concentration in the urine, urine was collected after 3 days of TMP-SMZ treatment and quantified by LC-MS following addition of sulfisoxazole as an internal standard.

Growth curve.

[0168] An overnight culture of PBC-1 was diluted 1:1000 in LB in the absence or presence of TMP-SMZ and/or mannoside **6**. The highest concentration of TMP-SMZ used was 512 μg/ml and 2560 μg/ml, respectively. Two-fold dilutions of TMP-SMZ were performed. Mannoside **6** was added at 100 μM. Growth curves were performed in a 96-well plate at 37°C with A_{600} readings taken every 30 min for 8 h. Minimum inhibitory concentration (MIC) was calculated as the lowest concentration of antibiotic that prevented growth of the bacterial strain.

Statistical analysis.

[0169] Observed differences in bacterial titers and IBC numbers were analyzed for significance using the nonparametric Mann-Whitney U test (Prizm; GraphPad Software)

Introduction for Examples 13-18.

[0170] FimH is a mannose-specific bacterial lectin located at the tip of type 1 pili, an adhesive fiber produced by uropathogenic *E. coli* (UPEC). FimH is known to bind to mannosylated human uroplakins that coat the luminal surface of the bladder and

has also been shown to be involved in invasion of human bladder cells and mast cells, triggering apoptosis and exfoliation and inducing elevated levels of cAMP. Furthermore, FimH recognizes N-linked oligosaccharides on beta1 and alpha3 integrins, which are expressed throughout the urothelium. Murine uroplakin is highly homologous to human and FimH has been shown to facilitate bacterial colonization and invasion of the bladder epithelium in murine models. Internalized UPEC are exocytosed in a TLR-4 dependent process; however, bacteria can escape into the host cell cytoplasm, where they are able to subvert expulsion and innate defenses by aggregating into biofilm-like intracellular bacterial communities (IBCs) in a FimH dependent process. Subsequently, UPEC disperse from the IBC, escape into the bladder lumen, and re-initiate the process by binding and invading naive epithelial cells where they are able to establish quiescent intracellular reservoirs that can persist in a dormant state, tolerant to antibiotic therapy and subsequently serve as seeds for recurrent infection. In humans, the severity of UTI was increased and the immunological response was greater in children with infections caused by type 1 piliated UPEC strains and type 1 pilus expression has been shown to be essential for UTI in mouse models. In addition, a recent study concluded that type 1 pili play an important role in human cystitis and it has been reported that type 1 pili fulfill "Molecular Koch's postulates of microbial pathogenesis. In agreement with these findings and in support of a role for FimH in humans, it has been shown that the fimH gene is under positive selection in human clinical isolates of UPEC. Aspects of the UPEC pathogenic cascade extensively characterized in a murine model of infection have been documented in samples from human clinical studies such as filamentation and IBC formation.Targeted inhibitors of FimH adhesion which block both *E. coli* invasion and biofilm formation thus hold promising therapeutic potential as new antibacterials for the treatment of UTI and the prevention of recurrence.

[0171] The discovery of simple D-mannose derivatives as inhibitors of bacterial adherence was first reported almost three decades ago but early mannosides showed only weak inhibition of bacterial adhesion. Consequently, the vast majority of research in this area has been focused on multivalent mannosides, which have been pursued in an effort to improve binding avidity to type 1 pili, which can be present in

large numbers on a single bacterium (up to hundreds). While substantial progress has been made with this approach, these high molecular weight structures are not suitable for in vivo evaluation or clinical development as oral drugs. The recent X-ray crystal structures of D-mannose, butyl mannoside, and mannotriose bound to FimH have enabled the rational structure-based design of tighter binding alkyl-, phenyl- and biphenyl- mannoside FimH inhibitors. The urgency for developing new orally bioavailable FimH inhibitors as a targeted strategy for the treatment of UTI alternative to broad spectrum antibiotics is reinforced by the rate of recurrence seen in these type of infections as well as increasing clinical resistance of UPEC to first line antibiotic treatments.

Example 13. Tight Binding Ortho-substituted Biphenyl Mannosides.

[0172] A matched pair analysis was performed of monoester **1** compared to ortho-substituted analogs bearing halogen and small alkyl groups shown in **Fig. 15**. The compounds were evaluated for their potency in the hemagglutination inhibition (HAI) assay and it was discovered that all biphenyl ring substitutions yielded more potent inhibitors (**Table 2**). Ortho-Cl mannoside **4b** had a HAI Titer EC_{90} of 30 nM which is more than 30-fold better than matched pair **1** while the Me analog **4c** was 8-fold more active (HAI Titer EC_{90} = 120 nM). Substitution with CF3 gave the most potent analog **4d** with an HAI Titer EC_{90} of 30 nM whereas the OMe (**4e**) and F (**4a**) analogs showed smaller improvements in activity following the trend CF3 > Cl = Me > OMe > F. This data suggests that increased hydrophobic contact with the tyrosine gate and Ile52, or with Ile13 at the opposite ridge of the mannose binding pocket could explain this enhanced potency since better activity correlates well with increased hydrophobicity as evidenced by the fact that fluoro analog **4a** shows no improvement in activity relative to unsubstituted matched pair **1** and the trifluoromethyl analog **4c** which has the largest hydrophobic surface area shows the highest activity. However, it is possible that the orientation of both phenyl rings are altered slightly and are restricted to a conformation more conducive to improved FimH binding with Tyr137, Tyr48, Ile52, Ile13 and/or Arg98 residues.

Table 2. Potency enhancement and PAMPA data from ortho-substitution of biphenyl mannosides.

Compound	HAI Titer $EC_{>90}$ (μM)	Biofilm Prevention IC_{50} (μM)	MW (g/mol)	PSA	$CLogD_{7.4}$	PAMPA $LogP_e$ (cm^2/sec)
1 (ester)	1.00	0.94	390.4	126	1.17	-5.42
4a (F)	0.75		408.4	126	1.00	
4b (Cl)	0.03	0.26	424.8	126	1.64	-4.29
4c (Me)	0.12	0.33	404.4	126	1.82	
4d (CF_3)	0.03	0.17	458.4	126	1.62	-3.91
4e (OMe)	0.19	0.89	420.4	135	0.47	
6 (*m*-CO_2Me)	1.0		448.4	152	0.93	-4.08
2 (amide)	0.50	1.35	389.4	128	0.28	
5a (Cl)	0.12	0.52	423.8	128	0.75	
5b (Me)	0.06	0.16	403.4	128	0.93	-3.89
5c (CF_3)	0.03	0.13	457.4	128	0.73	
3 (di-amide)	0.37	0.74	446.4	158	0.71	-4.51
7 (CF_3)	0.01	0.043	514.5	158	1.15	-6.27
8 (Me)	0.02	0.073	460.5	158	1.35	-8.46

[0173] The outcome of this preliminary study, directed the investigation of analogs which were more metabolically stable and soluble than esters such as amides **5a-c** (**Fig. 15 and Table 2**). A similar trend was observed (CF3 > Me > Cl) with CF3

amide **5c** having the best activity but in this case the Me analog **5b** showed better activity than Cl analog **5a**. Analogs were also explored with substitution on the meta position, exemplified by ester **6**, which retains potency relative to **1** but did not lead to any enhancement. Ortho-CF3 **7** and Me **8** diamide matched pairs to original lead compound **3** were next developed which were exponentially more potent than any previously reported mannoside FimH inhibitors with an HAI Titer EC_{90} of 8 nM and 16 nM, respectively. This unprecedented level of cellular activity corresponds to a 200,000-fold improvement over α-D-mannose and a 15,000-fold improvement over an early reported inhibitor butyl-α-D-mannoside (HAI Titer EC90 = 125 μM) and 50-fold better than previous lead compound **3**.

[0174] The biofilm inhibition assay was utilized to test these mannosides' ability to prevent bacteria from forming IBCs, a critical pathogenic process in the development of UTIs. As shown in **Table 2**, the Biofilm Prevention IC_{50}s correlate quite well with the potencies determined by the HAI assay. Introduction of an ortho-substituent (e.g. methyl) to the biphenyl mannoside improved the biofilm activity by 8-fold from mannoside 2 (IC_{50} = 1.35 μM) to mannoside 5b (IC_{50} = 0.16 μM). This data confirmed the mannoside's functional effect and activity on UPEC derived from FimH inhibition with a secondary assay. Biofilm IC_{50}s were utilized in conjunction with pharmacokinetic parameters as a key measure of the predicted lowest effective mannoside concentration in the urine required for efficacy in vivo to be discussed vide infra.

[0175] Mannosides were synthesized by traditional Lewis acid mediated glycosylation of mannose penta-acetate by reaction with 2-substituted 4-bromophenols using BF3 etherate (**Scheme 1**). Suzuki cross-coupling with commercially available 3-substituted phenyl boronic acid derivatives gave protected ortho-substituted 4'-biphenyl mannosides in excellent yields and subsequent deprotection with NaOMe gave mannosides **4-5**. **6** was prepared following the procedure previously described. Synthesis of di-amides **7-8** followed a similar procedure but required the synthesis of 3,5-di-(N-methyl aminocarbonyl)phenyl boronic acid pinacol ester **9**. Shown in **Scheme 1**, amidation of dimethyl 5-bromoisophthalate by reaction of methylamine in ethanol

proceeded in quantitative yield to give N,N-dimethyl 5-bromoisophthalamide. Installation of the boronate ester was accomplished by Pd-mediated coupling with bis(pinacolato)diboron to give **9**. Suzuki coupling and deprotection as before yielded compounds **7-8**.

Scheme 1[a]. Synthesis of ortho-substituted biphenyl mannosides

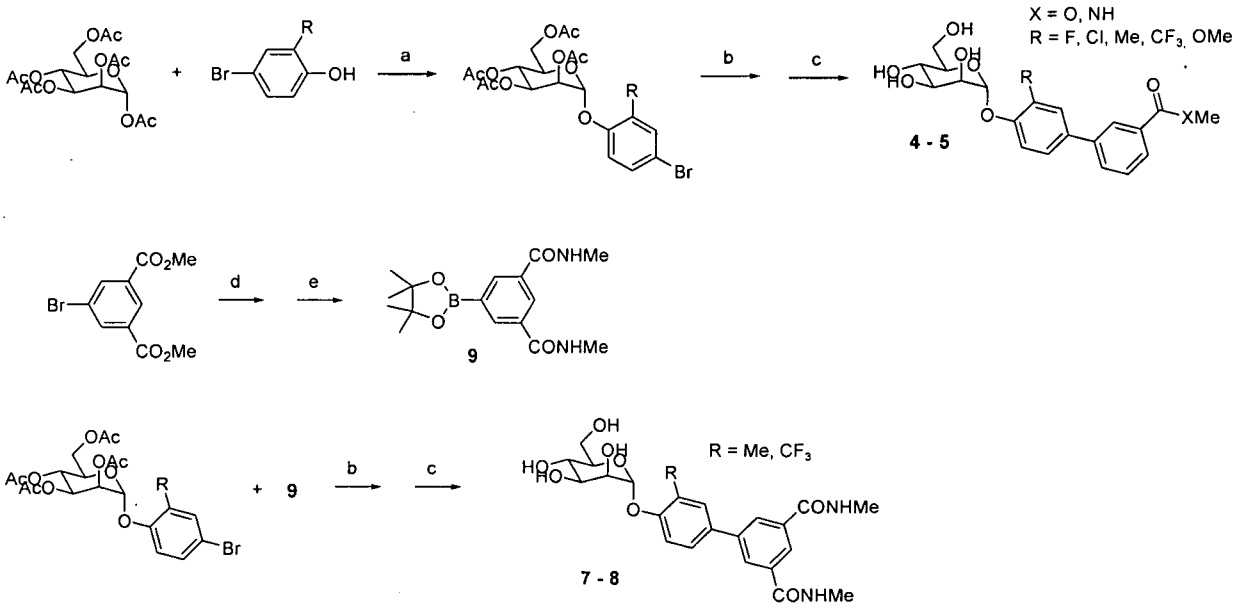

a. Reagents and conditions: (a) BF_3-Et_2O, CH_2Cl_2, reflux; (b) 3-substituted phenyl boronic acid derivatives, Cat. $Pd(PPh_3)_4$, Cs_2CO_3, dioxane/water(5/1), 80 °C; (c) Cat. MeONa, MeOH, rt; (d) $MeNH_2$/EtOH, rt; (e) bis(pinacolato)diboron, Cat. $Pd(dppf)Cl_2$, KOAc, DMSO, 80 °C..

Example 14. Mannosides with Increased pKa Functionality.

[0176] To help improve tissue penetration and exposure of mannosides in the bladder, amide derivatives were explored containing functional groups with higher pKa (**Table 3**). Higher pKa compounds containing basic moieties such as amines tend to have increased tissue penetration. Therefore, mannosides **10a-f** were prepared via standard HATU-mediated coupling reaction of 4'-(α-D-mannopyranosyloxy)biphenyl-3-carboxylic acid with various amines. Unexpectedly, aminoethyl amide **10b** showed a disappointing 6-fold drop in activity relative to methyl amide **2**. However, hydroxyethyl

amide **10a** was equipotent to **2**. It was also found that more hydrophobic tertiary amide piperazine analogs **10c** and **10d** had largely decreased potency (HAI EC_{90} = 4 μM). Interestingly, pyridyl amides **10e** and **10f** showed slightly improved activity most pronounced with 4-pyridyl derivative **10e**. While it is unclear to the reason for decreased potency of higher pKa substituents it is plausible that this effect could originate from charge-charge repulsion with Arg98 side chain at the edge of FimH binding pocket.

Table 3. Exploration of amide substitution with increased pKa

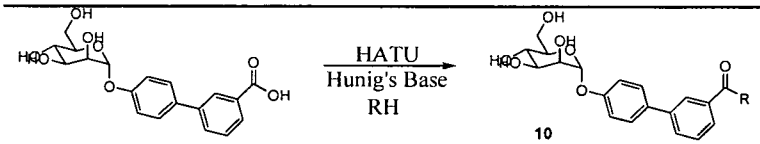

Compound	R	HAI Titer $EC_{>90}$ (μM)
10a	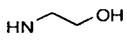	0.50
10b	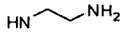	3.0
10c		4.0
10d		4.0
10e	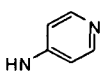	0.25
10f	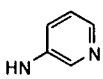	0.37

Example 15a. Mannosides with Heterocyclic Replacements.

[0177] Heterocyclic replacements of the terminal biphenyl ring were then persued as an alternate approach to improve the drug-like properties of lead mannosides. In target compounds the key H-bond donor to Arg98 of FimH was retained so we could directly compare the effects of heterocyclic ring replacement. In order to synthesize a library of heterocycles in a divergent fashion, a new Suzuki synthesis was developed using a 4-mannopyranosyloxyphenyl boronate intermediate **11** in place of 4-bromophenyl-α-D-mannoside. Only a limited number of heteroaryl boronates are commercially available and this new methodology allows for the use of more readily obtainable heteroaryl bromides as coupling partners. All heteroaryl bromides used in **Table 4** were commercially available with reasonable prices except bromothiophene derivatives **16** and **17** (**Scheme 2**). **16** was prepared via Curtius reaction by first treatment of 5-bromothiophene-3-carboxylic acid with diphenylphosphoryl azide (DPPA) to form isocyanate intermediate, then quenching with ammonia. **17** was synthesized according to previous method. As shown in **Scheme 2**, Starting from 4-bromophenyl-α-D-mannoside, bis(pinacolato)diboron and $Pd(dppf)Cl_2$ in DMSO, intermediate **11** was prepared in good yield. Suzuki cross coupling of **11** with various aryl bromides, followed by acetyl deprotection gave target compounds. Compounds synthesized, shown in **Table 4**, include pyridyl esters **12a** and **12b** which showed excellent activity in the HAI titer with improvement over phenyl ester **1**. Furthermore, ring replacement with a thiophene urea carboxylate led to dramatic advancements in FimH activity as exemplified by compound **13a** which has an HAI EC_{90} = 16 nM. In order to ascertain whether the carboxylate ester group or urea were responsible for this large increase in potency, ester **13b** and urea **13c** were synthesized to discover that the enhancement results from a combined effect of both functional since **13b** or **13c** have much decreased activity. It is unknown why there is a synergistic effect from the compound with both urea and carboxylate but from previous work on thiophene carboxamide ureas it was shown that an intramolecular H-bond exists between the internal NH of the urea and the carbonyl of the ester. This conformational restriction might enhance binding entropically to FimH likely from the urea carbonyl. Several fused rings were also

persued such as isoquinoline derivatives **14** and **15** to examine the effects of isosteric replacement for the aryl carbonyl H-bond acceptor where the heterocyclic ring nitrogen is designed to accept a H-bond from the FimH Arg98 side chain. The promising HAI assay results for **14a-b** to **15a-b** clearly provides much evidence that the orientation of the C=N in **15a** or C=O in **15b** is likely the same as the conformation of C=O of mannoside **1** in crystal structure of FimH- mannoside **1**[25] bringing the potency up by as much as 10-fold over mannoside **1**.

Scheme 2[a]. Synthesis of heterocyclic mannosides

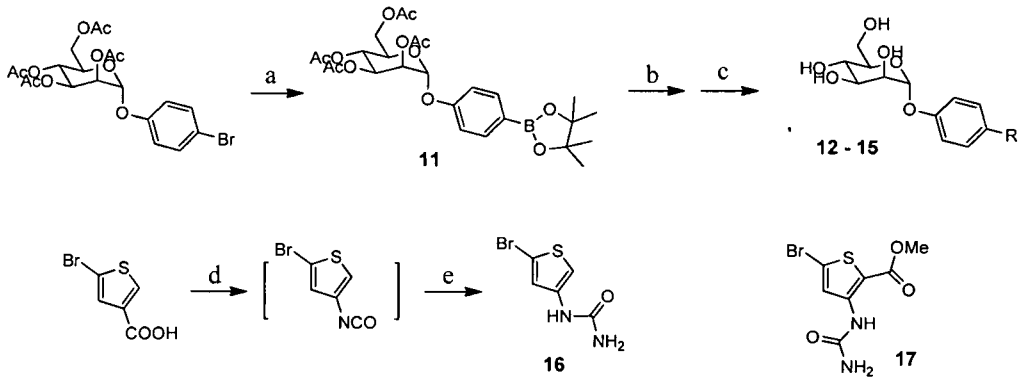

a. Reagents and conditions: (a) bis(pinacolato)diboron, Cat. $Pd(dppf)Cl_2$, KOAc, DMSO, 80 °C; (b) heteroaryl bromide derivatives, Cat. $Pd(PPh_3)_4$, Cs_2CO_3, dioxane/water(5/1), 80 °C; (c) Cat. MeONa, MeOH, rt; (d) DPPA, $^iPr_2NEt$, dioxane, 85 °C; (e) NH_3/dioxane (0.5 M), rt.

Table 4. Heterocyclic modifications to biphenyl ring for improving drug-like properties

Compound	R	HAI Titer $EC_{>90}$ (μM)
12a	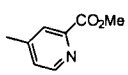	0.50

12b	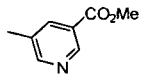	0.19
13a	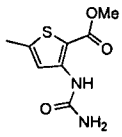	0.02
13b	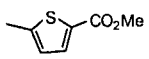	1.0
13c	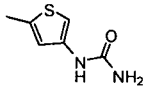	1.0
13d	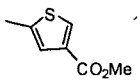	2.0
14a	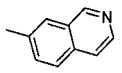	0.75
14b	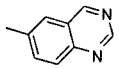	0.38
15a	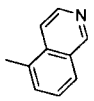	0.25
15b	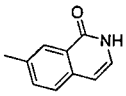	0.10

Example 15b. Direct Binding of FimH-Mannoside.

[0178] In order to better understand how the excellent potency in cell-based HAI and biofilm assays is correlated with FimH binding by biaryl mannosides and to more precisely select the best lead compounds for in vivo pharmacokinetic (PK) studies, a biolayer interferometry method was developed to directly measure the binding affinities (K_d) of FimH inhibitors. As shown in **Table 5**, earlier mannosides **19 ~ 33**

showing moderate potency in the HAI assay had K_d values as low as 1~10 nM. Strikingly, for compounds **1** and **2**, K_d values were in the picomolar range. For mannosides **5**, **7**, and **8**, however, K_d could not be calculated because the off-rates were too low to measure. In order to overcome this obstacle, differential scanning fluorimetry (DSF) was utilized to rank the high-affinity mannosides. DSF measures the melting temperature change of protein when binding to small molecules. Melting temperature shifts are proportional to the free energy of binding, and melting temperatures increase even as ligand concentration exceeds the K_d. As illustrated in **Table 5** (and **Table 7**) and **Fig. 16**, the melting temperature of FimH without mannoside was about 60°C and rose to between 68°C and 74°C when binding to mannosides **19** ~ **33** of moderate potency. With tight binding mannosides **5b**, **7**, **8** the melting temperature of FimH ranged from 74°C to 76°C, suggesting that improved mannosides likely bind FimH with low picomolar affinity. **Fig. 16** illustrates that DSF ranks mannosides in a similar fashion to the HAI assay except for **5c** and **25**, demonstrating that this is a general and reliable method to qualitatively rank FimH-mannoside binding when K_ds span many orders of magnitude. Thus, these direct FimH binding studies solidified that the high potencies stemming from mannosides **5b**, **7**, **8** derives directly from extremely tight binding to the FimH lectin and not other non-specific effects from the cell assays.

Table 5. Results of Octet assay and DSF assay

Compound	Structure of 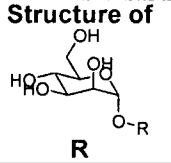 R	HAI Titer $EC_{>90}$ (μM)	Octet K_d (nM)	DSF Melting Temp. (°C)
7	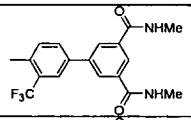	0.008	N.D.*	76.15
8	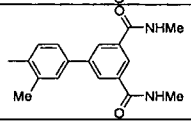	0.016	N.D.*	75.76

Table 5. Results of Octet assay and DSF assay

Compound	Structure of 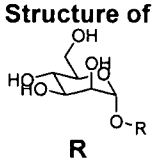 R	HAI Titer $EC_{>90}$ (μM)	Octet K_d (nM)	DSF Melting Temp. (°C)
5c	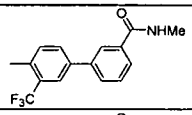	0.032	N.D.*	72.29
5b	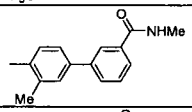	0.060	N.D.*	74.46
18	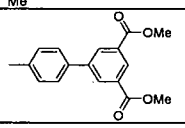	0.150	N.D.*	72.53
10f	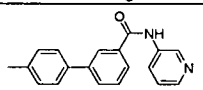	0.375	N.D.*	72.53
3	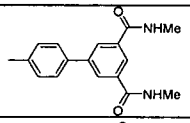	0.375	0.14	74.39
12a	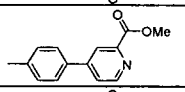	0.500	N.D.*	73.68
2	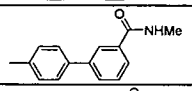	0.500	0.01	73.38
19	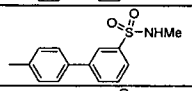	1.000	0.49	72.05
1	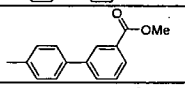	1.000	0.08	73.39
20	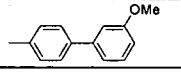	1.500	1.25	71.77
21	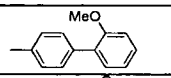	2.000	N.D.*	70.72
22	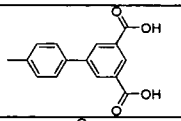	2.000	14.5	72.39
23	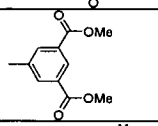	2.000	3.45	73.25
24	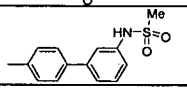	2.000	2.00	70.90

Table 5. Results of Octet assay and DSF assay

Compound	Structure of 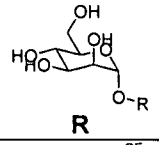 R	HAI Titer $EC_{>90}$ (μM)	Octet K_d (nM)	DSF Melting Temp. (°C)
25	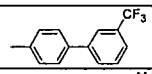	2.000	1.56	68.32
26	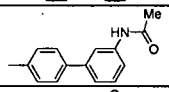	2.000	1.14	72.30
27	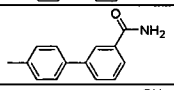	2.000	1.00	71.69
28	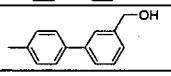	3.000	2.61	71.16
29	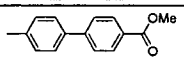	4.000	3.99	68.69
30	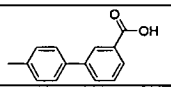	4.000	2.21	70.93
31	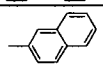	6.000	2.72	70.75
32	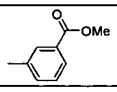	6.000	2.72	70.75
33	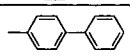	8.000	3.00	71.17
Phenyl-α-D-mannoside		30.000	N.D.*	68.93
34		60.000	43.66	68.11

*N.D. = not determined

[0179] An electrostatic surface was generated with the most potent mannoside **7** docked to FimH shown in **Fig. 17**. The large boost in binding affinity to FimH can be attributed to the fact that in the model the ortho trifluorometyl group orients directly at Ile13 resulting in a very strong hydrophobic interaction with FimH. The added hydrophobicity encompassed by the fluorine atoms in mannoside **7** results in further augmented binding to FimH relative to ortho methyl mannoside **8**.

Example 16. Stability and Elimination Kinetics of Mannoside.

[0180] Mannoside **3** shows efficacy *in vivo* in the treatment and prevention of established UTIs in mice when dosed orally but the compound displayed some metabolic instability from hydrolysis of the glycosidic bond (**Fig. 18A**) and very rapid elimination kinetics to the urine partly due to its low CLogD value. While renal clearance is an attractive feature for UTI therapy, improved mannosides were desirable encompassing lower clearance rates as well as increased oral bioavailability and bladder tissue permeability. In order to have a general idea of the elimination rate of mannoside **3**, pharmacokinetic (PK) studies of its urinary clearance were conducted in mice (**Fig. 18B**). These experiments demonstrated that the lower oral dosing of 20 mg/kg was unlikely to maintain effective concentrations (as determined by Biofilm IC_{50}) due to rapid clearance. Maintenance of mannoside **3** levels above the minimal effective level of 0.74 μM during in an eight-hour period required a larger, 100 mg/kg dose. During the PK study, a small amount of a phenolic biphenyl metabolite (**R**) (**Fig. 18A**) was detected in the urine indicating some glycoside bond hydrolysis takes place upon oral dosing. Urine levels of the R group were unchanged from the 100 and 200 mg/kg doses, suggesting that metabolism by glycoside bond hydrolysis is saturated between the 20 and 100 mg/kg doses (**Fig. 18B**).

Example 17. Parallel Artificial Membrane Permeability Assay (PAMPA).

[0181] The low LogD of polyhydroxylated sugar-based mannosides and other carbohydrate-derived compounds can limit their ability to cross cell membranes in the absence of active transport mechanisms and so increasing their hydrophobicity is one strategy to help improve cell permeability and oral bioavailability of this class of molecules. The ortho-substituted mannosides described above were designed for increased hydrophobic contact with FimH but also in part to increase the LogD and were predicted to improve the solubility, oral bioavailability and bladder tissue penetration relative to starting mannosides **1-3**. It was anticipated that the newly designed inhibitors would also have increased metabolic stability *via* protection of the glycosidic bond from acidic hydrolysis in the gut and enzymatic hydrolysis by α-

mannosidases in blood and tissues. In order to test these hypotheses experimentally, the Parallel Artificial Membrane Permeability Assay (PAMPA) was used. PAMPA is commonly used as an *in vitro* model of passive, transcellular permeability to predict oral bioavailability for drug candidates. The most potent biphenyl mannosides was tested in this model for prioritizing compounds to evaluate further in animal PK and efficacy studies. Shown in **Table 2** (and **Table 7**), Compound **5b** with $LogP_e$ of -3.89 cm^2/sec proved to have the highest oral absorption, while the most potent mannosides (determined by HAI assay) **7** and **8** with $LogP_e$ of -6.27 and -8.46 cm^2/sec exhibited significantly lower oral bioavailability.

Example 18. Pharmacokinetic Studies for Selected Mannoside Inhibitors.

[0182] Based on these results, oral PK studies were performed in mice to assess any improvements in the PK of these ortho-substituted mannosides. Compounds were dosed at 50 mg/kg and plasma and urine samples were taken at 30 min and 1, 2, 3, 4, 6 hours after dosing. As demonstrated in **Fig. 19**, a generally 10-fold higher mannoside concentration was observed in urine (**Fig. 19B**) compared to plasma (**Fig. 19A**), indicating a high clearance rate for these mannosides, which in this case aids in clearing uropathogens on the bladder surface. It was found that compounds **8** and **5b** consistently maintain a high level of concentration in both urine and plasma, which is well above the predicted minimum effective concentration within a 6-hour period. While 100 mg/kg dosing of mannoside **3** was required to achieve effective mannoside concentrations, only 50 mg/kg dosing of mannoside **5b** was required, permitting a much larger therapeutic window for treatment. Taken together with PAMPA results, high oral bioavailability and *in vivo* efficacy in recently reported animal studies support mannoside **5b** as the most promising therapeutic candidate for UTI treatment/prevention.

Conclusions for examples 13-18

[0183] Using a combination of traditional ligand-based and X-ray structure-guided approaches with structure-activity relationship (SAR) driven by cell-based

hemagglutination and biofilm assays in combination with direct FimH binding assays, a diverse array of biaryl mannoside FimH inhibitors that exhibit affinities into the picomolar range were identified. While it was found the most potent mannoside **7** with respect to FimH binding affinity and activity in cell assays contains an ortho-trifluoromethyl group off the phenyl ring adjacent to the mannose ring group, the most promising inhibitor from *in vivo* studies is the ortho-methyl analog **8** showing prolonged compound exposure in plasma and urine PK studies. A variety of heterocyclic biaryl mannosides that either retain or improve FimH binding activity were also discovered. The novel inhibitors of UPEC type 1 mediated bacterial adhesion reported herein show unprecedented activity in hemagglutination and biofilm *in vitro* assays in addition to desirable pharmacokinetic properties *in vivo*. Further optimization of lead mannosides is currently being focused on the identification of mannose modifications with reduced sugar-like character. Biaryl mannosides have high potential as innovative therapeutics for the clinical treatment and prevention of urinary tract infections. The unique mechanism of action of targeting the pilus tip adhesin, FimH, circumvents the conventional requirement for drug penetration of the outer membrane and the potential for development of resistance by porin mutations, efflux or degradative enzymes, all mechanisms that promote resistance to antibiotics. Current efforts are directed at the selection of one or more clinical candidate drugs through rigorous preclinical evaluation in several models of recurrent UTI with antibiotic resistant forms of UPEC. These preclinical models will facilitate further optimization of current lead compounds.

Experimental Section for Examples 13-18

General synthesis, purification, and analytical chemistry procedures.

[0184] Starting materials, reagents, and solvents were purchased from commercial vendors unless otherwise noted. ^{1}H NMR spectra were measured on a Varian 300 MHz NMR instrument. The chemical shifts were reported as δ ppm relative to TMS using residual solvent peak as the reference unless otherwise noted. The following abbreviations were used to express the multiplicities: s = singlet; d = doublet; t

= triplet; q = quartet; m = multiplet; br = broad. High-performed liquid chromatography (HPLC) was carried out on GILSON GX-281 using Waters C18 5μM, 4.6*50mm and Waters Prep C18 5μM, 19*150mm reverse phase columns, eluted with a gradient system of 5:95 to 95:5 acetonitrile:water with a buffer consisting of 0.05% TFA. Mass spectra (MS) were performed on HPLC/MSD using electrospray ionization (ESI) for detection. All reactions were monitored by thin layer chromatography (TLC) carried out on Merck silica gel plates (0.25 mm thick, 60F254), visualized by using UV (254 nm) or dyes such as $KMnO_4$, *p*-Anisaldehyde and CAM. Silica gel chromatography was carried out on a Teledyne ISCO CombiFlash purification system using pre-packed silica gel columns (12g~330g sizes). All compounds used for biological assays are greater than 95% purity based on NMR and HPLC by absorbance at 220 nm and 254 nm wavelengths.

Procedures for the preparation of biphenyl mannoside derivatives through Suzuki coupling reaction with bromophenyl mannoside derivatives as intermediate

[0185] **N-methyl-3-[3-methyl-4-[(2R,3S,4S,5S,6R)-3,4,5-trihydroxy-6-(hydroxymethyl)tetrahydropyran-2-yl]oxy-phenyl]benzamide (5b).** **[(2R,3S,4S,5R,6R)-4,5-diacetoxy-6-(acetoxymethyl)-2-(4-bromo-2-methyl-phenoxy)tetrahydropyran-3-yl] acetate.** Under nitrogen atmosphere and at room temperature, boron trifluoride diethyl etherate (3.41 g, 24 mmol) was added dropwise into the solution of α-D-mannose pentaacetate (3.12 g, 8 mmol) and 4-bromo-2-methylphenol (2.99 g, 16 mmol) in 100 ml of anhydrous CH_2Cl_2. After a few mins the mixture was heated to reflux and kept stirring for 45 hrs. The reaction was then quenched with water and extracted with CH_2Cl_2. The CH_2Cl_2 layer was collected dried with Na_2SO_4, concentrated. The resulting residue was purified by silica gel chromatography with hexane/ethyl acetate combinations as eluent, giving [(2R,3S,4S,5R,6R)-4,5-diacetoxy-6-(acetoxymethyl)-2-(4-bromo-2-methyl-phenoxy)tetrahydropyran-3-yl] acetate (3.22 g) in 77% yield. ^1H NMR (300 MHz, CHLOROFORM-d) δ ppm 7.18 - 7.38 (m, 2H), 6.97 (d, J = 8.79 Hz, 1H), 5.50 - 5.59 (m, 1H), 5.43 - 5.50 (m, 2H), 5.32 - 5.42 (m, 1H), 4.28 (dd, J = 5.63, 12.50 Hz, 1H), 3.99 -

4.15 (m, 2H), 2.27 (s, 3H), 2.20 (s, 3H), 2.02 - 2.11 (three singlets, 9H). MS (ESI): found: $[M + Na]^+$, 539.0.

[0186] ***N*-methyl-3-[3-methyl-4-[(*2R,3S,4S,5S,6R*)-3,4,5-trihydroxy-6-(hydroxymethyl)tetrahydropyran-2-yl]oxy-phenyl]benzamide (5b).** Under nitrogen atmosphere, the mixture of [(*2R,3S,4S,5R,6R*)-4,5-diacetoxy-6-(acetoxymethyl)-2-(4-bromo-2-methyl-phenoxy)tetrahydropyran-3-yl] acetate (0.517 g, 1 mmol), 3-(N-methylaminocarbonyl)phenylboronic acid pinacol ester (0.392g, 1.5 mmol), cesium carbonate (0.977 g, 3 mmol) and tetrakis(triphenylphosphine)palladium (0.116 g, 0.1 mmol) in dioxane/water (15 mL/3 mL) was heated at 80 °C with stirring for 1 h under a nitrogen atmosphere. After cooling to RT, the mixture was filtered through silica gel column to remove the metal catalyst and salts with hexane/ethyl acetate combinations as eluent. The filtrate was concentrated, and then dried *in vacuo*. The residue was diluted with 15 mL of methanol containing a catalytic amount of sodium methoxide (0.02 M) and the mixture was stirred at RT overnight. H^+ exchange resin (DOWEX 50WX4-100) was added to neutralize the mixture. The resin was filtered off and the filtrate was concentrated. The resulting residue was purified by silica gel chromatography with CH_2Cl_2/MeOH combinations as eluent, giving the title compound (0.260 g) in 64% yield for two steps. ^1H NMR (300 MHz, METHANOL-d_4) δ ppm 7.94 (t, *J* = 1.65 Hz, 1H), 7.57 - 7.72 (m, 2H), 7.33 - 7.50 (m, 3H), 7.23 (d, *J* = 8.52 Hz, 1H), 5.48 (d, *J* = 1.92 Hz, 1H), 4.00 (dd, *J* = 1.79, 3.43 Hz, 1H), 3.83 - 3.94 (m, 1H), 3.60 - 3.76 (m, 3H), 3.46 - 3.58 (m, 1H), 2.87 (s, 3H), 2.24 (s, 3H). MS (ESI): found: $[M + H]^+$, 404.2.

[0187] **Methyl 3-[3-fluoro-4-[(*2R,3S,4S,5S,6R*)-3,4,5-trihydroxy-6-(hydroxymethyl)tetrahydropyran-2-yl]oxy-phenyl]benzoate (4a).** **[(*2R,3S,4S,5R,6R*)-4,5-diacetoxy-6-(acetoxymethyl)-2-(4-bromo-2-fluoro-phenoxy)tetrahydropyran-3-yl] acetate:** it was prepared using the same procedure as for [(*2R,3S,4S,5R,6R*)-4,5-diacetoxy-6-(acetoxymethyl)-2-(4-bromo-2-methyl-phenoxy)tetrahydropyran-3-yl] acetate in the synthesis of 5b. Yield: 25%. ^1H NMR (300 MHz, CHLOROFORM-d) δ ppm 7.30 (dd, *J* = 2.34, 10.03 Hz, 1H), 7.21 (td, *J* = 1.79, 8.79 Hz, 1H), 7.08 (t, *J* = 8.52 Hz, 1H), 5.48 - 5.58 (m, 2H), 5.46 (d, *J* = 1.65 Hz, 1H),

5.31 - 5.41 (m, 1H), 4.23 - 4.31 (m, 1H), 4.13 - 4.22 (m, 1H), 4.05 - 4.13 (m, 1H), 2.20 (s, 3H), 2.02 - 2.08 (three singlets, 9H). MS (ESI): found: $[M + Na]^+$, 543.0.

[0188] **Methyl 3-[3-fluoro-4-[(*2R,3S,4S,5S,6R*)-3,4,5-trihydroxy-6-(hydroxymethyl)tetrahydropyran-2-yl]oxy-phenyl]benzoate (4a). 4a** was prepared using the same procedure as for 5b with [(*2R,3S,4S,5R,6R*)-4,5-diacetoxy-6-(acetoxymethyl)-2-(4-bromo-2-fluoro-phenoxy)tetrahydropyran-3-yl] acetate and 3-methoxycarbonylphenyl boronic acid as the reactants. Yield: 66%. ^{1}H NMR (300 MHz, METHANOL-d_4) δ ppm 8.21 (t, *J* = 1.65 Hz, 1H), 7.99 (td, *J* = 1.44, 7.83 Hz, 1H), 7.84 (ddd, *J* = 1.10, 1.92, 7.69 Hz, 1H), 7.35 - 7.62 (m, 4H), 5.55 (d, *J* = 1.92 Hz, 1H), 4.10 (dd, *J* = 1.79, 3.43 Hz, 1H), 3.94 (s, 3H), 3.86 - 4.00 (m, 1H), 3.59 - 3.86 (m, 4H). MS (ESI): found $[M + Na]^+$, 431.1.

[0189] **Methyl 3-[3-chloro-4-[(*2R,3S,4S,5S,6R*)-3,4,5-trihydroxy-6-(hydroxymethyl)tetrahydropyran-2-yl]oxy-phenyl]benzoate (4b). [(*2R,3S,4S,5R,6R*)-4,5-diacetoxy-6-(acetoxymethyl)-2-(4-bromo-2-chloro-phenoxy)tetrahydropyran-3-yl] acetate:** it was prepared using the same procedure as for [(*2R,3S,4S,5R,6R*)-4,5-diacetoxy-6-(acetoxymethyl)-2-(4-bromo-2-methyl-phenoxy)tetrahydropyran-3-yl] acetate in the synthesis of 5b. Yield: 46%. ^{1}H NMR (300 MHz, CHLOROFORM-d) δ ppm 7.55 (d, *J* = 2.47 Hz, 1H), 7.33 (dd, *J* = 2.47, 8.79 Hz, 1H), 7.06 (d, *J* = 8.79 Hz, 1H), 5.58 (dd, *J* = 3.02, 10.16 Hz, 1H), 5.52 (s, 1H), 5.49 - 5.54 (m, 1H), 5.33 - 5.42 (m, 1H), 4.22 - 4.32 (m, 1H), 4.04 - 4.17 (m, 2H), 2.21 (s, 3H), 2.07 (s, 3H), 2.05 (s, 3H), 2.04 (s, 3H). MS (ESI): found $[M + Na]^+$, 561.0 .

[0190] **Methyl 3-[3-chloro-4-[(*2R,3S,4S,5S,6R*)-3,4,5-trihydroxy-6-(hydroxymethyl)tetrahydropyran-2-yl]oxy-phenyl]benzoate (4b). 4b** was prepared using the same procedure as for 5b with [(*2R,3S,4S,5R,6R*)-4,5-diacetoxy-6-(acetoxymethyl)-2-(4-bromo-2-chloro-phenoxy)tetrahydropyran-3-yl] acetate and 3-methoxycarbonylphenyl boronic acid as the reactants. It was further purified by HPLC (C18, 15*150 mm column; eluent: acetonitrile/water (0.1% TFA)). Yield: 43%. ^{1}H NMR (300 MHz, METHANOL-d_4) δ ppm 3.59 - 3.71 (m, 1 H) 3.71 - 3.85 (m, 3 H) 3.94 (s, 3 H) 4.01 (dd, *J*=9.34, 3.30 Hz, 1 H) 4.12 (dd, *J*=3.30, 1.92 Hz, 1 H) 5.61 (d, *J*=1.65 Hz, 1 H) 7.40 - 7.49 (m, 1 H) 7.49 - 7.62 (m, 2 H) 7.68 (d, *J*=2.20 Hz, 1 H) 7.82 (ddd, *J*=7.76,

1.85, 1.10 Hz, 1 H) 7.98 (dt, *J*=7.83, 1.30 Hz, 1 H) 8.14 - 8.25 (m, 1 H). MS (ESI): found $[M + H]^+$, 425.1.

[0191] **Methyl 3-[3-methyl-4-[(*2R,3S,4S,5S,6R*)-3,4,5-trihydroxy-6-(hydroxymethyl)tetrahydropyran-2-yl]oxy-phenyl]benzoate (4c). 4c** was prepared using the same procedure as for **5b** with [(*2R,3S,4S,5R,6R*)-4,5-diacetoxy-6-(acetoxymethyl)-2-(4-bromo-2-methyl-phenoxy)tetrahydropyran-3-yl] acetate and 3-methoxycarbonylphenyl boronic acid as the reactants. Yield: 54%. ^{1}H NMR (300 MHz, METHANOL-d_4) δ ppm 8.20 (t, *J* = 1.51 Hz, 1H), 7.94 (td, *J* = 1.41, 7.90 Hz, 1H), 7.77 - 7.87 (m, 1H), 7.52 (t, *J* = 7.55 Hz, 1H), 7.39 - 7.48 (m, 2H), 7.27 - 7.38 (m, 1H), 5.56 (d, *J* = 1.65 Hz, 1H), 4.08 (dd, *J* = 1.92, 3.30 Hz, 1H), 3.94 - 4.01 (m, 1H), 3.90 - 3.94 (m, 3H), 3.68 - 3.83 (m, 3H), 3.55 - 3.65 (m, 1H), 2.31 (s, 3H). MS (ESI): found $[M + Na]^+$, 427.1.

[0192] **Methyl 3-[3-(trifluoromethyl)-4-[(*2R,3S,4S,5S,6R*)-3,4,5-trihydroxy-6-(hydroxymethyl)tetrahydropyran-2-yl]oxy-phenyl]benzoate (4d). [(*2R,3S,4S,5R,6R*)-4,5-diacetoxy-6-(acetoxymethyl)-2-[4-bromo-2-(trifluoromethyl)phenoxy]tetrahydropyran-3-yl] acetate:** it was prepared using the same procedure as for [(*2R,3S,4S,5R,6R*)-4,5-diacetoxy-6-(acetoxymethyl)-2-(4-bromo-2-methyl-phenoxy)tetrahydropyran-3-yl] acetate in the synthesis of 5b. Yield: 54%. ^{1}H NMR (300 MHz, CHLOROFORM-d) δ ppm 7.74 (d, *J* = 2.20 Hz, 1H), 7.61 (dd, *J* = 2.33, 8.93 Hz, 1H), 7.15 (d, *J* = 8.79 Hz, 1H), 5.61 (d, *J* = 1.92 Hz, 1H), 5.48 - 5.56 (m, 1H), 5.33 - 5.48 (m, 2H), 4.21 - 4.34 (m, 1H), 3.97 - 4.14 (m, 2H), 2.21 (s, 3H), 1.99 - 2.12 (three singlets, 9H). MS (ESI): found $[M + Na]^+$, 593.0.

[0193] **Methyl 3-[3-(trifluoromethyl)-4-[(*2R,3S,4S,5S,6R*)-3,4,5-trihydroxy-6-(hydroxymethyl)tetrahydropyran-2-yl]oxy-phenyl]benzoate (4d). 4d** was prepared using the same procedure as for 5b with [(*2R,3S,4S,5R,6R*)-4,5-diacetoxy-6-(acetoxymethyl)-2-[4-bromo-2-(trifluoromethyl)phenoxy]tetrahydropyran-3-yl] acetate and 3-methoxycarbonylphenyl boronic acid as the reactants. Yield: 53%. ^{1}H NMR (300 MHz, METHANOL-d_4) δ ppm 8.23 (t, *J* = 1.51 Hz, 1H), 8.01 (td, *J* = 1.37, 7.69 Hz, 1H), 7.80 - 7.93 (m, 3H), 7.52 - 7.67 (m, 2H), 5.66 (d, *J* = 1.65 Hz, 1H), 4.07

(dd, *J* = 1.79, 3.43 Hz, 1H), 3.95 (s, 3H), 3.90 - 4.00 (m, 1H), 3.66 - 3.87 (m, 3H), 3.52 - 3.66 (m, 1H). MS (ESI): found $[M + Na]^+$, 481.0.

[0194] **Methyl 3-[3-methoxy-4-[(*2R,3S,4S,5S,6R*)-3,4,5-trihydroxy-6-(hydroxymethyl)tetrahydropyran-2-yl]oxy-phenyl]benzoate (4e)**. **4e** was prepared using the same procedure as for **5b**. In the first step of glycosidation reaction 4-bromo-2-methoxyphenol was used as glycosidation acceptor and in the second step of Suzuki coupling reaction 3-methoxycarbonylphenyl boronic acid was used instead. All intermediates were directly taken to the next step reaction without further purification. **4e** was further purified by HPLC (C18, 15*150 mm column; eluent: acetonitrile/water (0.1% TFA)). Yield: 3%. ^{1}H NMR (300 MHz, METHANOL-d_4) δ ppm 8.21 (t, *J* = 1.51 Hz, 1H), 7.96 (td, *J* = 1.44, 7.83 Hz, 1H), 7.84 (ddd, *J* = 1.24, 1.92, 7.83 Hz, 1H), 7.49 - 7.61 (m, 1H), 7.30 (d, *J* = 8.24 Hz, 1H), 7.24 (d, *J* = 1.92 Hz, 1H), 7.13 - 7.21 (m, 1H), 5.47 (d, *J* = 1.92 Hz, 1H), 4.11 (dd, *J* = 1.79, 3.43 Hz, 1H), 3.94 (s, 3H), 3.92 (s, 3H), 3.86 - 4.03 (m, 1H), 3.67 - 3.86 (m, 4H). MS (ESI): found $[M + Na]^+$, 443.1.

[0195] **3-[3-Chloro-4-[(*2R,3S,4S,5S,6R*)-3,4,5-trihydroxy-6-(hydroxymethyl)tetrahydropyran-2-yl]oxy-phenyl]-*N*-methyl-benzamide (5a). 5a** was prepared using the same procedure as for **5b**. Yield: 59%. ^{1}H NMR (300 MHz, METHANOL-d_4) δ ppm 8.03 (t, *J* = 1.51 Hz, 1H), 7.69 - 7.83 (m, 3H), 7.32 - 7.67 (m, 3H), 5.60 (d, *J* = 1.65 Hz, 1H), 4.12 (dd, *J* = 1.79, 3.43 Hz, 1H), 4.01 (dd, *J* = 3.57, 9.34 Hz, 1H), 3.69 - 3.84 (m, 3H), 3.61 - 3.69 (m, 1H), 2.95 (s, 3H). MS (ESI): found $[M + Na]^+$, 424.1.

[0196] ***N*-Methyl-3-[3-(trifluoromethyl)-4-[(*2R,3S,4S,5S,6R*)-3,4,5-trihydroxy-6-(hydroxymethyl)tetrahydropyran-2-yl]oxy-phenyl]benzamide (5c). 5c** was prepared using the same procedure as for 5b. Yield: 65%. ^{1}H NMR (300 MHz, METHANOL-d_4) δ ppm 7.98 (t, *J* = 1.65 Hz, 1H), 7.77 - 7.87 (m, 2H), 7.65 - 7.77 (m, 2H), 7.42 - 7.60 (m, 2H), 5.58 (d, *J* = 1.65 Hz, 1H), 3.99 (dd, *J* = 1.79, 3.43 Hz, 1H), 3.81 - 3.91 (m, 1H), 3.59 - 3.80 (m, 3H), 3.45 - 3.58 (m, 1H), 2.87 (s, 3H). MS (ESI): found $[M + H]^+$, 458.1.

[0197] **Methyl 2-(3-methoxycarbonylphenyl)-5-[(*2R,3S,4S,5S,6R*)-3,4,5-trihydroxy-6-(hydroxymethyl)tetrahydropyran-2-yl]oxy-benzoate (6). Methyl 5-**

hydroxy-2-(3-methoxycarbonylphenyl)benzoate: The reactants of methyl 2-bromo-5-hydroxybenzoate (0.231 g, 1 mmol), 3-methoxycarbonylphenyl boronic acid (0.214 g, 1.2 mmol), palladium acetate (0.022g, 0.1 mmol), potassium carbonate (0.346 g, 2.5 mmol) and tetrabutylammonium bromide (0.322 g, 1 mmol) in 1.2 ml of water was heated with stirring at 70 °C for 1 h and 20 mins in a sealed vial by microwave. Then the mixture was partitioned between AcOEt and 1 N HCl aqueous solution. The organic layer was collected, dried with Na_2SO_4, then concentrated. The resulting residue was purified by silica gel chromatography with AcOEt/Hex combinations as eluent, giving the title compound (0.240 g) in 84% yield. ^{1}H NMR (300 MHz, DMSO-d_6) δ ppm 10.02 (s, 1H), 7.90 (td, *J* = 2.03, 6.66 Hz, 1H), 7.72 - 7.81 (m, 1H), 7.45 - 7.60 (m, 2H), 7.28 (d, *J* = 8.52 Hz, 1H), 7.16 (d, *J* = 2.47 Hz, 1H), 7.03 (dd, *J* = 2.61, 8.38 Hz, 1H), 3.86 (s, 3H), 3.56 (s, 3H). MS (ESI): found $[M + Na]^+$, 309.2.

[0198] **Methyl 2-(3-methoxycarbonylphenyl)-5-[(*2R,3S,4S,5S,6R*)-3,4,5-trihydroxy-6-(hydroxymethyl)tetrahydropyran-2-yl]oxy-benzoate (6). 6** was prepared via glycosidation between α-D-mannose pentaacetate and methyl 5-hydroxy-2-(3-methoxycarbonylphenyl)benzoate following the procedure previously described.[25] Yield: 73%. ^{1}H NMR (300 MHz, METHANOL-d_4) δ ppm 3.56 - 3.68 (m, 4 H) 3.68 - 3.84 (m, 3 H) 3.86 - 3.98 (m, 4 H) 4.06 (dd, *J*=3.30, 1.92 Hz, 1 H) 5.60 (d, *J*=1.92 Hz, 1 H) 7.29 - 7.43 (m, 2 H) 7.45 - 7.53 (m, 2 H) 7.56 (d, *J*=2.47 Hz, 1 H) 7.84 - 7.92 (m, 1 H) 7.93 - 8.04 (m, 1 H). MS (ESI): found $[M + H]^+$, 449.0.

[0199] ***N1,N3*-Dimethyl-5-[3-(trifluoromethyl)-4-[(*2R,3S,4S,5S,6R*)-3,4,5-trihydroxy-6-(hydroxymethyl)tetrahydropyran-2-yl]oxy-phenyl]benzene-1,3-dicarboxamide (7). *N1,N3*-dimethyl-5-(4,4,5,5-tetramethyl-1,3,2-dioxaborolan-2-yl)benzene-1,3-dicarboxamide (9)**: dimethyl 5-bromobenzene-1,3-dicarboxylate (10.6 g, 36.8 mmol) was dissolved in a 33 wt% solution of methylamine in EtOH (30 mL) and stirred for 6h at RT. The precipitate that formed during the reaction was filtered to give 5.3 g (53%) of the intermediate 5-bromo-*N1,N3*-dimethyl-benzene-1,3-dicarboxamide as a white solid. Concentration of the remaining filtrate yielded an additional 4.6 g (46%) of product. 5-bromo-*N1,N3*-dimethyl-benzene-1,3-dicarboxamide (5.3 g, 19.5 mmol), Pd(dppf)Cl_2 (0.87 g, 1.2 mmol), bis(pinacolato)diboron (6.1 g, 24 mmol), and potassium

acetate (7.8 g, 80 mmol) were dissolved in DMSO (100 mL). The solution was stirred under vacuum and then repressurized with nitrogen. This process was repeated 3 times and then the resultant mixture was stirred at 80 °C for 5h under a nitrogen atmosphere. After removal of the solvent under high vacuum, the crude material was purified by silica gel chromatography to give 9 as a light tan solid (2.2 g, 35%). ^{1}H NMR (300 MHz, DMSO-d6) δ ppm 8.63 (m, 2H), 8.41 (t, *J* = 1.51 Hz, 1H), 8.23 (d, *J* = 1.65 Hz, 2H), 2.79 (d, *J* = 4.40 Hz, 6H), 1.33 (s, 12H). MS (ESI): found: $[M + H]^+$, 319.2.

[0200] ***N1,N3*-Dimethyl-5-[3-(trifluoromethyl)-4-[(*2R,3S,4S,5S,6R*)-3,4,5-trihydroxy-6-(hydroxymethyl)tetrahydropyran-2-yl]oxy-phenyl]benzene-1,3-dicarboxamide (7).** Using the procedure outlined in the synthesis of 5b with [(*2R,3S,4S,5R,6R*)-4,5-diacetoxy-6-(acetoxymethyl)-2-(4-bromo-2-trifluoromethyl-phenoxy)tetrahydropyran-3-yl] acetate (0.57 g) and *N1,N3*-dimethyl-5-(4,4,5,5-tetramethyl-1,3,2-dioxaborolan-2-yl)benzene-1,3-dicarboxamide (9) (0.48 g), the title compound was obtained (0.340 g) in 69% yield for the two steps. ^{1}H NMR (300 MHz, METHANOL-d_4) δ ppm 8.17 - 8.24 (m, 1H), 8.14 (d, *J* = 1.65 Hz, 2H), 7.92 (d, *J* = 1.92 Hz, 1H), 7.87 (dd, *J* = 2.20, 8.79 Hz, 1H), 7.57 (d, *J* = 8.79 Hz, 1H), 5.64 (d, *J* = 1.65 Hz, 1H), 4.04 (dd, *J* = 1.65, 3.30 Hz, 1H), 3.87 - 3.96 (dd, 1H), 3.64 - 3.83 (m, 3H), 3.48 - 3.63 (m, 1H), 2.93 (s, 6H). MS (ESI): found: $[M + H]^+$, 515.1.

[0201] ***N1,N3*-Dimethyl-5-[3-methyl-4-[(*2R,3S,4S,5S,6R*)-3,4,5-trihydroxy-6-(hydroxymethyl)tetrahydropyran-2-yl]oxy-phenyl]benzene-1,3-dicarboxamide (8). 8** was prepared using the same procedure as for 5b with *N1,N3*-dimethyl-5-(4,4,5,5-tetramethyl-1,3,2-dioxaborolan-2-yl)benzene-1,3-dicarboxamide as the Suzuki coupling partner. Yield: 56%. ^{1}H NMR (300 MHz, METHANOL-d_4) δ ppm 8.09 - 8.23 (m, 3H), 7.46 - 7.59 (m, 2H), 7.33 (d, *J* = 8.52 Hz, 1H), 5.57 (d, *J* = 1.92 Hz, 1H), 4.08 (dd, *J* = 1.92, 3.30 Hz, 1H), 3.97 (dd, *J* = 3.43, 9.48 Hz, 1H), 3.67 - 3.85 (m, 3H), 3.60 (ddd, *J* = 2.47, 5.01, 7.35 Hz, 1H), 2.96 (s, 6H), 2.32 (s, 3H). MS (ESI): found: $[M + H]^+$, 461.2.

Procedure for the preparation of mannosides via amide coupling reaction:

[0202] ***N*-(2-Hydroxyethyl)-3-[4-[(*2R,3S,4S,5S,6R*)-3,4,5-trihydroxy-6-(hydroxymethyl)tetrahydropyran-2-yl]oxyphenyl]benzamide (10a).** Under nitrogen atmosphere, at 0 °C anhydrous DMF (5 mL) was added into the RB flask containing 4'-(α-D-mannopyranosyloxy)biphenyl-3-carboxylic acid[25] (0.038 g, 0.1 mmol) and HATU (0.046 g, 0.12 mmol). After stirring for 10 min, aminoethanol (0.007 g, 0.12 mmol), then *N,N*-diisopropylethylamine (0.039 g, 0.3 mmol) were added. The mixture was stirred overnight while being warmed to rt naturally. The solvent was removed and the residue was purified by HPLC (C18, 15*150 mm column; eluent: acetonitrile/water (0.1% TFA)) to give the title compound (0.032 g) in 76% yield. ^{1}H NMR (300 MHz, DEUTERIUM OXIDE) δ ppm 3.53 - 3.63 (m, 2 H) 3.68 - 3.94 (m, 6 H) 4.11 (dd, *J*=9.20, 3.43 Hz, 1 H) 4.22 (dd, *J*=3.30, 1.92 Hz, 1 H) 5.66 (d, *J*=1.65 Hz, 1 H) 7.21 (d, *J*=8.79 Hz, 2 H) 7.47 - 7.62 (m, 3 H) 7.66 - 7.78 (m, 2 H) 7.87 (t, *J*=1.65 Hz, 1 H). MS (ESI): found $[M + H]^+$, 420.1.

[0203] ***N*-(2-Aminoethyl)-3-[4-[(*2R,3S,4S,5S,6R*)-3,4,5-trihydroxy-6-(hydroxymethyl)tetrahydropyran-2-yl]oxyphenyl]benzamide (10b). 10b** was prepared using the same procedure as for 10a. Yield: 60%. ^{1}H NMR (300 MHz, METHANOL-d_4) δ ppm 3.14 - 3.26 (m, 2 H) 3.57 - 3.66 (m, 1 H) 3.66 - 3.83 (m, 5 H) 3.87 - 4.00 (m, 1 H) 4.03 (dd, *J*=3.30, 1.92 Hz, 1 H) 5.49 - 5.62 (m, 1 H) 7.19 - 7.31 (m, 2 H) 7.49 - 7.59 (m, 1 H) 7.59 - 7.72 (m, 2 H) 7.75 - 7.89 (m, 2 H) 8.03 - 8.21 (m, 1 H). MS (ESI): found $[M + H]^+$, 419.2.

[0204] **Piperazin-1-yl-[3-[4-[(*2R,3S,4S,5S,6R*)-3,4,5-trihydroxy-6-(hydroxymethyl)tetrahydropyran-2-yl]oxyphenyl]phenyl]methanone (10c). 10c** was prepared using the same procedure as for 10a. Yield: 65%. ^{1}H NMR (300 MHz, METHANOL-d_4) δ ppm 3.54 - 3.67 (m, 1 H) 3.67 - 3.85 (m, 4 H) 3.85 - 3.99 (m, 4 H) 4.03 (dd, *J*=3.30, 1.92 Hz, 1 H) 5.54 (d, *J*=1.65 Hz, 1 H) 7.19 - 7.29 (m, 2 H) 7.42 (dt, *J*=7.69, 1.24 Hz, 1 H) 7.50 - 7.64 (m, 3 H) 7.67 - 7.79 (m, 2 H). MS (ESI): found $[M + H]^+$, 445.3.

[0205] **(4-Methylpiperazin-1-yl)-[3-[4-[(*2R,3S,4S,5S,6R*)-3,4,5-trihydroxy-6-(hydroxymethyl)tetrahydropyran-2-yl]oxyphenyl]phenyl]methanone**

(10d). 10d was prepared using the same procedure as for 10a. Yield: 87%. ^{1}H NMR (300 MHz, METHANOL-d_4) δ ppm 2.96 (s, 3 H) 3.05~3.65 (m, 9 H) 3.68 - 3.85 (m, 3 H) 3.87 - 3.97 (m, 1 H) 4.03 (dd, *J*=3.30, 1.92 Hz, 1 H) 5.54 (d, *J*=1.65 Hz, 1 H) 7.17 - 7.30 (m, 2 H) 7.42 (dt, *J*=7.62, 1.27 Hz, 1 H) 7.50 - 7.66 (m, 3 H) 7.67 - 7.80 (m, 2 H). MS (ESI): found $[M + H]^+$, 459.0.

[0206] ***N*-(4-Pyridyl)-3-[4-[(*2R,3S,4S,5S,6R*)-3,4,5-trihydroxy-6-(hydroxymethyl)tetrahydropyran-2-yl]oxyphenyl]benzamide (10e). 10e** was prepared using the same procedure as for **10a**. Yield: 93%. ^{1}H NMR (300 MHz, METHANOL-d_4) δ ppm 3.57 - 3.69 (m, 1 H) 3.69 - 3.84 (m, 3 H) 3.93 (dd, *J*=9.34, 3.30 Hz, 1 H) 4.04 (dd, *J*=3.30, 1.92 Hz, 1 H) 5.56 (d, *J*=1.65 Hz, 1 H) 7.18 - 7.37 (m, 2 H) 7.57 - 7.78 (m, 3 H) 7.82 - 8.06 (m, 2 H) 8.24 (t, *J*=1.65 Hz, 1 H) 8.36 - 8.51 (m, 2 H) 8.68 (d, *J*=7.42 Hz, 2 H). MS (ESI): found $[M + H]^+$, 453.1.

[0207] ***N*-(3-Pyridyl)-3-[4-[(*2R,3S,4S,5S,6R*)-3,4,5-trihydroxy-6-(hydroxymethyl)tetrahydropyran-2-yl]oxyphenyl]benzamide (10f). 10f** was prepared using the same procedure as for **10a**. Yield: 75%. ^{1}H NMR (300 MHz, METHANOL-d_4) δ ppm 3.55 - 3.68 (m, 1 H) 3.68 - 3.85 (m, 3 H) 3.88 - 3.98 (m, 1 H) 4.04 (dd, *J*=3.43, 1.79 Hz, 1 H) 5.56 (d, *J*=1.92 Hz, 1 H) 7.20 - 7.32 (m, 2 H) 7.52 - 7.73 (m, 3 H) 7.80 - 7.91 (m, 1 H) 7.91 - 7.99 (m, 1 H) 8.04 (dd, *J*=8.65, 5.63 Hz, 1 H) 8.23 (t, *J*=1.65 Hz, 1 H) 8.59 (d, *J*=5.49 Hz, 1 H) 8.67 - 8.79 (m, 1 H) 9.55 (s, 1 H). MS (ESI): found $[M + H]^+$, 453.2.

Procedure for the *preparation of biphenyl mannoside derivatives through Suzuki coupling reaction with [(2R,3S,4S,5R,6R)-4,5-diacetoxy-6-(acetoxymethyl)-2-[4-(4,4,5,5-tetramethyl-1,3,2-dioxaborolan-2-yl)phenoxy]tetrahydropyran-3-yl] acetate (9) as intermediates:*

[0208] **Methyl 5-[4-[(*2R,3S,4S,5S,6R*)-3,4,5-trihydroxy-6-(hydroxymethyl)tetrahydropyran-2-yl]oxyphenyl]pyridine-3-carboxylate (12b). [(*2R,3S,4S,5R,6R*)-4,5-diacetoxy-6-(acetoxymethyl)-2-[4-(4,4,5,5-tetramethyl-1,3,2-dioxaborolan-2-yl)phenoxy]tetrahydropyran-3-yl] acetate (11):** Under nitrogen atmosphere, the mixture of 4-bromophenyl 2,3,4,6-tetra-*O*-acetyl-α-D-mannopyranoside

(2.791 g, 5.55 mmol), bis(pinacolato)diboron (1.690g, 6.66 mmol), potassium acetate (2.177 g, 22.18 mmol) and (1.1'-bis(diphenylphosohino)ferrocene)dichloropalladium(II) (0.244 g, 0.33 mmol) in DMSO (50 ml) was heated at 80 °C with stirring for 2.5 h. The solvent was removed and the resulting residue was purified by silica gel chromography with hexane/ethyl acetate combinations as eluent to give 11 (2.48 g) in 81% yield. ^{1}H NMR (300 MHz, CHLOROFORM-*d*) δ ppm 1.33 (s, 12 H) 1.98 - 2.12 (m, 9 H) 2.20 (s, 3 H) 3.93 - 4.19 (m, 2 H) 4.21 - 4.36 (m, 1 H) 5.32 - 5.42 (m, 1 H) 5.45 (dd, *J*=3.57, 1.92 Hz, 1 H) 5.51 - 5.62 (m, 2 H) 7.00 - 7.15 (m, 2 H) 7.67 - 7.84 (m, 2 H). MS (ESI): found: $[M + Na]^+$, 573.2.

[0209] **Methyl 5-[4-[(*2R,3S,4S,5S,6R*)-3,4,5-trihydroxy-6-(hydroxymethyl)tetrahydropyran-2-yl]oxyphenyl]pyridine-3-carboxylate (12b).** Under nitrogen atmosphere, the mixture of [(2R,3S,4S,5R,6R)-4,5-diacetoxy-6-(acetoxymethyl)-2-[4-(4,4,5,5-tetramethyl-1,3,2-dioxaborolan-2-yl)phenoxy]tetrahydropyran-3-yl] acetate (0.132 g, 0.24 mmol), methyl 5-bromonicotinate (0.043g, 0.2 mmol), cesium carbonate (0.196 g, 0.6 mmol) and tetrakis(triphenylphosphine)palladium (0.023 g, 0.02 mmol) in dioxane/water (5 mL/1 mL) was heated at 80 °C with stirring for 1 h. After cooling down, the mixture was filtered through silica gel column to remove the metal catalyst and salts with hexane/ethyl acetate (2/1) containing 2% triethylamine as eluent. The filtrate was concentrated , then dried in vacuo. Into the residue, 6 mL of methanol with catalytic amount of sodium methoxide (0.02 M) was added and the mixture was stirred at room temperature overnight. The solvent was removed. The resulting residue was purified by silica gel chromography with CH_2Cl_2/MeOH combinations containing 2% NH_3/H_2O as eluent, giving rise to 12b (0.031 g) in 40% yield. ^{1}H NMR (300 MHz, CD_3OD) δ ppm 3.53 - 3.65 (m, 1 H) 3.67 - 3.83 (m, 3 H) 3.89 - 3.96 (m, 1 H) 3.99 (s, 3 H) 4.04 (dd, J=3.43, 1.79 Hz, 1 H) 5.57 (d, J=1.92 Hz, 1 H) 7.22 - 7.37 (m, 2 H) 7.58 - 7.73 (m, 2 H) 8.54 (t, J=2.06 Hz, 1 H) 8.97 (d, J=2.20 Hz, 1 H) 9.04 (d, J=1.92 Hz, 1 H). MS (ESI): found: $[M + H]^+$, 392.1.

[0210] **Methyl 4-[4-[(*2R,3S,4S,5S,6R*)-3,4,5-trihydroxy-6-(hydroxymethyl)tetrahydropyran-2-yl]oxyphenyl]pyridine-2-carboxylate (12a). 12a**

was prepared using the same procedure as for 12b and was purified by HPLC (C18, 15*150 mm column; eluent: acetonitrile/water (0.1% TFA)). Yield: 15%. ^{1}H NMR (300 MHz, METHANOL-d_4) δ ppm 3.51 - 3.63 (m, 1 H) 3.65 - 3.84 (m, 3 H) 3.88 - 3.95 (m, 1 H) 4.00 - 4.13 (m, 4 H) 5.62 (d, *J*=1.65 Hz, 1 H) 7.28 - 7.40 (m, 2 H) 7.82 - 7.95 (m, 2 H) 8.13 (dd, *J*=5.49, 1.92 Hz, 1 H) 8.55 (d, *J*=1.65 Hz, 1 H) 8.73 (d, *J*=5.49 Hz, 1 H). MS (ESI): found $[M + H]^+$, 392.2.

[0211] **Methyl 5-[4-[(*2R,3S,4S,5S,6R*)-3,4,5-trihydroxy-6-(hydroxymethyl)tetrahydropyran-2-yl]oxyphenyl]-3-ureido-thiophene-2-carboxylate (13a). 13a** was prepared using the same procedure as for 12b and was purified by HPLC (C18, 15*150 mm column; eluent: acetonitrile/water (0.1% TFA)). Yield: 10%. ^{1}H NMR (300 MHz, METHANOL-d_4) δ ppm 3.58 (ddd, *J*=7.21, 4.88, 2.47 Hz, 1 H) 3.66 - 3.83 (m, 3 H) 3.83 - 3.96 (m, 4 H) 4.02 (dd, *J*=3.30, 1.92 Hz, 1 H) 5.54 (d, *J*=1.65 Hz, 1 H) 7.12 - 7.27 (m, 2 H) 7.56 - 7.69 (m, 2 H) 8.12 (s, 1 H). MS (ESI): found $[M + H]^+$, 455.1.

[0212] **Methyl 5-[4-[(*2R,3S,4S,5S,6R*)-3,4,5-trihydroxy-6-(hydroxymethyl)tetrahydropyran-2-yl]oxyphenyl]thiophene-2-carboxylate (13b). 13b** was prepared using the same procedure as for 12b and was purified by silica gel chromography with CH_2Cl_2/MeOH combinations. Yield: 23%. ^{1}H NMR (300 MHz, METHANOL-d_4) δ ppm 3.53 - 3.62 (m, 1 H) 3.68 - 3.81 (m, 3 H) 3.85 - 3.94 (m, 4 H) 4.02 (dd, *J*=3.60, 2.1 Hz, 1 H) 5.54 (d, *J*=1.8 Hz, 1 H) 7.19 (m, 2 H) 7.34 (d, *J*=3.9 Hz, 1 H) 7.64 (m, 2 H) 7.75 (d, *J*=3.9 Hz, 1 H). MS (ESI): found $[M + Na]^+$, 419.1.

[0213] **(5-bromo-3-thienyl)urea (16)**. Under nitrogen atmosphere *N,N*-diisopropylethylamine (0.390 g, 3 mmol) was added to the solution of 5-bromothiophene-3-carboxylic acid (0.207g, 1 mmol) and diphenylphosphoryl azide (DPPA) (0.330 g, 1.2 mmol) in dioxane (5 ml) at rt. After stirring for 30 min, the mixture was heated at 85 for 1.5 h. After the mixture cooled down to rt, 0.5 M of ammonia solution in dioxane (12 ml) was added. 30 min's later, the solvents was removed and the resulting residue was purified by silica gel chromography with CH_2Cl_2/MeOH combinations to give (5-bromo-3-thienyl)urea (0.072g) in 32% yield. ^{1}H NMR (300 MHz,

DMSO-d_6) δ ppm 8.80 (s, 1H), 7.09 (s, 2H), 5.87 (s, 2H). MS (ESI): found $[M + H]^+$, 223.0.

[0214] **[5-[4-[(*2R,3S,4S,5S,6R*)-3,4,5-Trihydroxy-6-(hydroxymethyl)tetrahydropyran-2-yl]oxyphenyl]-3-thienyl]urea (13c). 13c** was prepared using the same procedure as for **12b** and was purified by HPLC (C18, 15*150 mm column; eluent: acetonitrile/water (0.1% TFA)). Yield: 80%. ^{1}H NMR (300 MHz, METHANOL-d_4/ACETONITRILE-d_3(3/1)) δ 7.50 - 7.62 (m, 2H), 7.11 - 7.21 (m, 3H), 7.08 (d, *J* = 1.37 Hz, 1H), 5.53 (d, *J* = 1.65 Hz, 1H), 4.02 (dd, *J* = 1.92, 3.30 Hz, 1H), 3.82 - 3.95 (m, 1H), 3.66 - 3.81 (m, 3H), 3.51 - 3.64 (m, 1H). MS (ESI): found $[M + H]^+$, 397.1.

[0215] **Methyl 5-[4-[(*2R,3S,4S,5S,6R*)-3,4,5-trihydroxy-6-(hydroxymethyl)tetrahydropyran-2-yl]oxyphenyl]thiophene-3-carboxylate (13d). 13d** was prepared using the same procedure as for 12b and was purified by silica gel chromography with CH_2Cl_2/MeOH combinations. Yield: 33%. ^{1}H NMR (300 MHz, METHANOL-d_4) δ ppm 3.55 - 3.63 (m, 1 H) 3.68 - 3.81 (m, 3 H) 3.84 - 3.94 (m, 4 H) 4.02 (dd, *J*=3.30, 1.8 Hz, 1 H) 5.53 (d, *J*=1.8 Hz, 1 H) 7.18 (m, 2 H) 7.59 (m, 2 H) 7.64 (d, *J*=1.5 Hz, 1 H) 8.11 (d, *J*=1.5 Hz, 1 H). MS (ESI): found $[M + Na]^+$, 419.1.

[0216] **(*2R,3S,4S,5S,6R*)-2-(Hydroxymethyl)-6-[4-(7-isoquinolyl)phenoxy]tetrahydropyran-3,4,5-triol (14a). 14a** was prepared using the same procedure as for 12b and was purified by HPLC (C18, 15*150 mm column; eluent: acetonitrile/water (0.1% TFA)). Yield: 73%. ^{1}H NMR (300 MHz, METHANOL-d_4) δ 9.73 (s, 1H), 8.59 - 8.71 (m, 1H), 8.47 - 8.58 (m, 2H), 8.42 (d, *J* = 6.59 Hz, 1H), 8.33 (d, *J* = 8.79 Hz, 1H), 7.76 - 7.89 (m, 2H), 7.25 - 7.41 (m, 2H), 5.60 (d, *J* = 1.92 Hz, 1H), 4.06 (dd, *J* = 1.92, 3.30 Hz, 1H), 3.87 - 4.00 (m, 1H), 3.68 - 3.87 (m, 3H), 3.55 - 3.68 (m, 1H). MS (ESI): found $[M + H]^+$, 384.2.

[0217] **(*2R,3S,4S,5S,6R*)-2-(Hydroxymethyl)-6-(4-quinazolin-6-ylphenoxy)tetrahydropyran-3,4,5-triol (14b). 14b** was prepared using the same procedure as for **12b.** Yield: 28%. ^{1}H NMR (300 MHz, METHANOL-d_4) δ 9.51 (s, 1H), 9.15 (s, 1H), 8.21 - 8.35 (m, 2H), 8.02 (d, *J* = 8.52 Hz, 1H), 7.63 - 7.80 (m, *J* = 8.79 Hz, 2H), 7.14 - 7.32 (m, *J* = 8.79 Hz, 2H), 5.50 (d, *J* = 1.37 Hz, 1H), 3.94 - 4.03 (m, 1H),

3.80 - 3.94 (m, 1H), 3.62 - 3.80 (m, 3H), 3.48 - 3.62 (m, 1H). MS (ESI): found $[M + H]^+$, 385.1.

[0218] **(*2R,3S,4S,5S,6R*)-2-(Hydroxymethyl)-6-[4-(5-isoquinolyl)phenoxy]tetrahydropyran-3,4,5-triol (15a). 15a** was prepared using the same procedure as for **12b** and was purified by HPLC (C18, 15*150 mm column; eluent: acetonitrile/water (0.1% TFA)). Yield: 90%. ^{1}H NMR (300 MHz, METHANOL-d_4) δ 9.80 (s, 1H), 8.45 - 8.60 (m, 2H), 8.35 (d, *J* = 6.59 Hz, 1H), 8.01 - 8.21 (m, 2H), 7.45 - 7.55 (m, 2H), 7.31 - 7.42 (m, 2H), 5.62 (d, *J* = 1.92 Hz, 1H), 4.07 (dd, *J* = 1.92, 3.30 Hz, 1H), 3.89 - 3.99 (m, 1H), 3.70 - 3.86 (m, 3H), 3.60 - 3.69 (m, 1H). MS (ESI): found $[M + H]^+$, 384.2.

[0219] **7-[4-[(*2R,3S,4S,5S,6R*)-3,4,5-Trihydroxy-6-(hydroxymethyl)tetrahydropyran-2-yl]oxyphenyl]-2H-isoquinolin-1-one (15b). 15b** was prepared using the same procedure as for **12b** and was purified by HPLC (C18, 15*150 mm column; eluent: acetonitrile/water (0.1% TFA)). Yield: 75%. ^{1}H NMR (300 MHz, METHANOL-d_4) δ 8.51 (d, *J* = 2.20 Hz, 1H), 7.93 - 8.05 (m, 1H), 7.62 - 7.77 (m, 3H), 7.21 - 7.31 (m, 2H), 7.18 (d, *J* = 7.14 Hz, 1H), 6.71 (d, *J* = 7.14 Hz, 1H), 5.56 (d, *J* = 1.92 Hz, 1H), 4.04 (dd, *J* = 1.92, 3.57 Hz, 1H), 3.88 - 4.00 (m, 1H), 3.69 - 3.87 (m, 3H), 3.57 - 3.69 (m, 1H). MS (ESI): found $[M + H]^+$, 400.2.

Affinity Measurement by Bio-Layer Interferometry.

[0220] Samples or buffer (200 µL per well) were dispensed into 96-well microtiter plates (Greiner Bio-One, Monroe NC) and maintained at 30°C with 1000RPM shaking. Pre-manufactured pins for individual assays were made by biotinylating FimH lectin domain[25] at a 1:1 molar ratio with NHS-PEO4-Biotin (Thermo Fisher, Rockford IL), diluting it to 50µg/ml in 20mM HEPES pH 7.5, 150mM NaCl (HBS), immobilizing it on high-binding streptavidin-coated biosensor tips (Super Streptavidin, FortéBio, Inc., Menlo Park, CA) for 10 minutes at 30°C, blocking the pins with 10µg/ml biocytin for 2 minutes, washing in HBS for 1 hour, and rinsing in 15% sucrose in HBS. Pins were then air dried for 30 minutes and stored in their original packaging with a dessicant packet. Assays were performed by re-wetting premade pins with HBS for 15 minutes,

then storing them in fresh HBS until use. Individual affinity assays were performed on an Octet Red instrument (FortéBio, Inc., Menlo Park, CA) and consisted of a short baseline measurement followed by incubation of pins for 10 minutes with 7 twofold dilutions (in HBS) of compound in a concentration range experimentally determined to give well-measured association and dissociation kinetics, then a 30-minute dissociation phase in HBS. Each experimental pin was referenced to a biocytin-blocked pin to control for instrument drift and a second biocytin-blocked pin that was passed through a duplicate experiment in the same 96-well plate to control for nonspecific binding of the compound to the pin. Kinetics data and affinity constants were generated automatically by the global fitting protocol in ForteBio Data Analysis version 6.3. Typical signal for compound binding was approximately 0.2 "nm shift" units, while the noise level of the instrument is around 0.0025nm.

Differential Scanning Fluorimetry (DSF) Method.

[0221] FimH lectin domain (residues 1–158 of UPEC J96 FimH, without an affinity tag)[22] was purified as described previously. Five micrograms FimH in 5µl HBS were mixed with HBS to yield a final volume of 50µl containing compound at a final concentration of 100µM and a "5X" final concentration of SYPRO Orange (sold as a "5000X" stock in DMSO and mixed with HBS to a working stock of 50X immediately before use: Life Technologies Inc.; Grand Island, NY) . Compounds were diluted to 100µM from stocks in DMSO and compared to matched control wells with FimH alone plus 0.2% DMSO. 50µl reactions were placed in 96-well clear-bottom PCR plates and subjected to a melt curve from 20-90°C in 0.5 °C increments of 15 seconds each followed by a fluorescence read of the "HEX" channel in a Bio-Rad CFX96 thermocycler (Bio-Rad, Hercules, CA). Melt curves were fitted to the Boltzmann equation to determine the melting temperature (T_m) ($y = A2 + (A1-A2)/(1 + \exp((x-x0)/dx))$ where x0 is the T_m) using OriginPro 8 (OriginLab, Northampton MA) . Melting temperatures are represented as the mean of three replicates plus or minus 1 standard deviation in Figure 4.

Pharmacokinetic Studies.

[0222] Compound levels in mouse urine and plasma were made using an AB Sciex API-4000 QTrap (AB Sciex, Foster City, CA) as previously described.[36] Selected reaction monitoring (SRM) mode quantification was performed with using the following MS/MS transitions [precursor mass/charge ratio (*m/z*)/product *m/z*]: compound **3**, 447/285; compound **5a**, 424/262; compound **5b**, 404/242; compound **5c**, 548/296; compound **7**, 515/353; compound **8**, 461/299; compound **3 R group**, 285/254.

Parallel Artificial Membrane Permeability Assay (PAMPA).

[0223] **Materials.** The assay was carried out using Multiscreen PVDF 96-well plates (Millipore, Billerica, MA) using the company's Transporter Receiver Plate. The lipid (dioleyoylphosphotidylcholine (DOPC):Stearic Acid (80:20, wt%) in dodecane was obtained from Avanti Polar lipids (Alabaster, AL). Hank's Buffered Salt Solution (HBSS), pH 7.4 was obtained from MediaTech (Manassas, VA).

[0224] **Methods.** Each of the test compounds was diluted to 2.5 mM in DMSO (Sigma, St Louis, MO) and further diluted prior to testing to 2.5 μM in HBSS, pH 7.4. The assay was performed using a Millipore 96-well Multiscreen-IP PAMPA plate, 5 μl of the lipid suspension was directly added to the PVDF membrane of the filter plate. Immediately following the addition of the lipid to the membrane, 200 μl of HBSS solution containing the test compound was added to the donor (upper) chamber. HBSS (300 μl) is also added to the receiver plate and the filter and receiver plates assembled and incubated overnight at room temperature in a moistened sealed bag to prevent evaporation. The concentration in the receiver plate as well as an equilibrium plate, that represents a theoretical, partition-free sample, was determined by HPLC-tandem mass spectrometry. Analysis of each compound was performed in triplicate.

[0225] **Analysis.** Analysis of both the acceptor and equilibrium samples were performed using an AB 3200 triple quadripole mass spectrometer linked to a Shimadzu DGU-20A HPLC with a Prevail C18 column (3 μm, 2.1x10mm) with a flow rate of 0.35 ml/min. The mobile phase used was A: 0.1% Formic Acid in water, B: 0.1%

Formic Acid in methanol. The elation gradient method is described in the table . Data acquisition and peak height determination was performed using Analyst v.1.4.2.

Time, min	A	B
0.01	95	5
0.50	95	5
1.00	5	95
2.00	5	95
2.01	95	5
6.01	Stop	

[0226] **Calculations.** The $\log_{10}$ of the effective permeability ($LogP_e$) was calculated using the following equation

$$\log P_e = \log\left\{C \cdot -\ln\left(1 - \frac{[\text{drug}]_{\text{acceptor}}}{[\text{drug}]_{\text{equilibrium}}}\right)\right\} \text{ where } C = \left(\frac{V_D \cdot V_A}{(V_D + V_A)\text{Area} \cdot \text{Time}}\right)$$

[0227] Where the drug concentration is the peak areas for the analyte and V_D and V_A is the volume of the donor and acceptor compartment respectively. The area is the surface area of the PVDF membrane (0.11 cm^2) and time is the incubation in seconds (64,800 sec). Each value is the mean of triplicates performed on the same day.

Introduction for Examples 19-21

[0228] Type 1 pili constitute the major UPEC virulence factor, being critical for attachment to and invasion of the bladder epithelium as well as for IBC formation. Type 1 pili belong to a class of extracellular fibers assembled by the chaperone-usher pathway. They are encoded by the *fim* gene cluster, and their expression is directed by a phase-variable promoter (*fimS*), which facilitates a switch between piliated and nonpiliated bacterial states. UPEC populations are heterogeneous consisting of bacteria that are bald, low-, moderately- and highly piliated. The ratio of each piliated fraction shifts depending on the environment; studies investigating the expression of type 1 pili revealed that UPEC associated with epithelial cells are highly piliated, consistent with

the critical role of type 1 pili in urothelium colonization, while bacteria recovered from urine samples of patients have *fimS* primarily in the OFF phase and are likely non-piliated. Regulation of *fimS* phase-variation is controlled by the FimB, FimE and FimX recombinases, the expression of which is in turn influenced by numerous regulatory factors. We recently identified the QseC sensor kinase as one of the factors implicated in regulation of type 1 pili expression. In the *qseC* mutant, the *fim* promoter is found primarily in the OFF orientation, resulting in reduced type 1 pili expression, an effect that stems from uncontrolled activation of the QseB response regulator in this mutant. In addition to influencing type 1 pili expression in the absence of *qseC*, over-active QseB aberrantly regulates conserved cellular pathways and impacts several virulence-associated genes, resulting in UPEC attenuation.

[0229] Numerous investigations highlighted the importance of type 1 pili in pathogenesis and spurred the onset of research towards the development of anti-adhesion agents, known as mannosides, aimed at inhibiting FimH-host receptor interactions. Given that disruption of QseC simultaneously affects *fim* expression and a number of other cellular processes, type 1 pili were disengaged from QseC control to determine the infection stages at which other QseC-mediated defects become important. By locking the invertible *fim* promoter element in the ON orientation, type 1 pili expression was restored in the *qseC* mutant and it was shown that the resulting mutant is competent in infection initiation and IBC formation. However, even upon expression of type 1 pili the *qseC* mutant is rapidly outcompeted by the parent strain during co-infection studies and cannot survive long-term in the urinary tract in mono-infections. These findings indicate that although type 1 pili mask the *qseC* deletion phenotypes at the onset of infection, additional QseC-mediated processes are required for persistence. Therefore, the examples below explore whether co-inhibition of QseC and type 1 pili would have a synergistic effect on clearing UPEC from the urinary tract. Given the lack of available QseC inhibitors a prophylactic approach was taken, using the *qseC* mutant as a proxy to QseC-inhibition. The data showed that mice pre-treated with mannoside (to block FimH-mediated adhesion) and subsequently challenged with the *qseC* mutant were more effectively protected against chronic UTI compared to mice

challenged with the parent strain. These examples indicate that targeting of QseC can be exploited as a potential preventative strategy, alone or in combination with other anti-virulence agents.

Example 19. Deletion of QseC impairs the ability of UPEC to invade the bladder.

[0230] It was previously shown that deletion of *qseC* in UTI89 leads to reduced bladder bacterial titers during the acute stages of infection (6 and 16 h post infection) in a cystitis murine model. Given that type 1 pili are critical for bladder adherence and invasion and are significantly reduced in the absence of QseC, it was rationalized that the *in vivo* attenuation of UTI89Δ*qseC* could be, at least partly, attributed to reduced bacterial internalization. Thus, the ability of UTI89Δ*qseC* to adhere to and invade the bladder epithelium was assessed and compared to the parent strain. Female C3H/HeN mice were transurethrally inoculated with 10^7 wild-type (wt) UTI89 or UTI89Δ*qseC* and bacterial invasion was assessed at 1 and 3 h post infection (h.p.i), time-points previously shown to be sufficient for completion of the invasion events. Enumeration of colony forming units (cfu) recovered from infected bladders indicated that compared to wt UTI89, UTI89Δ*qseC* had significantly lower overall bacterial titers (intracellular and luminal) at both time-points (**Fig. 20A**). Treatment of infected bladders with gentamicin to eradicate the luminal bacterial population but leave the intracellular population unharmed revealed decreased intracellular numbers for UTI89Δ*qseC* (**Fig. 20B**). Thus, these data indicate that deletion of *qseC* affects the ability of UTI89 to initiate infection by compromising its ability to colonize and invade the host bladder.

Example 20. Expression of type 1 pili rescues the adherence properties of UTI89Δ*qseC* in vitro, but does not influence other Δ*qseC*-related defects.

[0231] Attenuation of UTI89Δ*qseC* is linked to reduced bacterial internalization due to decreased type 1 pili production. Therefore, it was investigated whether restoration of type 1 pili expression alone would be sufficient to overcome the *in vivo* defects of UTI89Δ*qseC*. It was previously reported that in the absence of QseC the phase-variable *fim* promoter driving type 1 pili expression, *fimS*, is primarily

switched to the OFF orientation. Therefore, *fimS* was locked in the ON orientation in the chromosome of wt UTI89 and UTI89Δ*qseC* to attain expression of type 1 pili independently of QseC (**Fig. 21A**). Electron microscopy revealed that the resulting strains, UTI89_LON and UTI89Δ*qseC*_LON, were not hyper-piliated, but rather a larger population of piliated versus non-piliated bacteria was observed compared to wt UTI89 (data not shown). UTI89_LON and UTI89Δ*qseC*_LON exhibited comparable mannose-sensitive hemagglutination (HA) properties, which were higher than wt UTI89 since inversion of the promoter to the OFF state can no longer occur (**Fig. 21B**). Consistently, western blot analyses probing for FimA, the major type 1 pilus subunit, verified that type 1 pili production in UTI89Δ*qseC*_LON is comparable to UTI89_LON, but again, higher than wt UTI89 (**Fig. 21B**).

Example 21. Dual inhibition of type 1 pili and QseC potentiates UPEC elimination from the bladder

[0232] Type 1 pili are sufficient for establishment of acute infection whereas QseC is a critical determinant for persistence in the bladder; thus targeting both factors could constitute an excellent means of potentiating UPEC clearance from the urinary tract by interfering with both the acute and chronic aspects of infection. Mannosides, compounds that bind with high affinity the mannose-binding pocket of the FimH adhesin at the tip of type 1 pili, are potent inhibitors of type 1 pili function. In particular, mannosides **6** and **8**, the most potent mannosides tested, drastically reduce bacterial titers within 6 hours of oral delivery when used prophylactically or as a therapeutic strategy. These studies are a significant step towards a new anti-bacterial therapeutic; however, a fraction of the bacterial population persists after mannoside treatment and could lead to relapse, suggesting that mannoside effectiveness can be further optimized. It was therefore rationalized that co-inhibition of QseC may enhance mannoside efficacy. However, no QseC inhibitors are currently available. Although previous work has identified LED209 as an inhibitor of the kinase activity of QseC, It has been established that it is the disruption of the QseC phosphatase property that is responsible for the attenuation of a *qseC* mutant. To circumvent the lack of available

QseC-specific phosphatase inhibitors, UTI89Δ*qseC* was used as a proxy to QseC inhibition and a prophylactic strategy was employed to investigate whether targeting both factors (type 1 pili and QseC) could effectively protect the host against UTI. Mice were pretreated with mannoside **6**, and infected 30 min post treatment with wt UTI89 or UTI89Δ*qseC*. Mice treated with PBS prior to infection were included as controls. Bladder bacterial titers were enumerated at 2 weeks post infection as a measure of chronic infection. Compared to non-treated mice, there was a 2-log reduction in mannoside-treated mice infected with wt UTI89 (**Fig. 22**, UTI89 vs. UTI89_MAN) that was similar to the reduction observed in non-treated mice infected with UTI89Δ*qseC* (**Fig. 22**, UTI89_MAN vs. UTI89Δ*qseC*). Notably, in mannoside-treated animals infected with UTI89Δ*qseC*, bacterial reduction was further enhanced, as indicated by an additional 1.5-log drop compared to mannoside-treated animals infected with wt UTI89 (**Fig. 22**, UTI89_MAN vs. UTI89Δ*qseC*_MAN). These data strongly indicate that dual targeting of type 1 pili and QseC could potentiate UPEC elimination from the host bladder.

Materials and Methods for Examples 19-21

Strains, constructs and growth conditions

[0233] UTI89_LON and UTI89Δ*qseC*_LON were created using λ Red Recombinase and the primers listed in **Table 6**, so as to mutate 7 out of 9 nucleotides in the left invertible repeat of the *fim* promoter in the chromosome [43]. Bacteria were incubated in Luria Bertani (LB) media at 37°C for 4h under shaking conditions, sub-cultured (1:1000) in fresh LB media and incubated statically at 37°C for 18h.

Mouse infections

[0234] Female C3H/HeN mice (Harlan), 7–9 weeks old, were used for all studies described below and in each case mice were infected with 10^7 bacteria.

[0235] Short-term infections: Mice were transurethrally infected with bacteria carrying the GFP-expressing plasmid pCom-GFP, as previously described, and sacrificed at 1 and 3 h.p.i. Bladders were aseptically removed, homogenized and plated

for total bacterial enumeration or gentamicin-treated to determine intracellular bacterial titers. Experiment was repeated 3 times.

[0236] *Ex vivo* gentamicin assay: Bladders were bisected and washed 3 times in 500 µl PBS. The washes were collected and plated for cfu enumeration, to determine luminal bacteria. Washed bladders were incubated for 90 min at 37°C with 100 µg/ml gentamicin to kill adherent extracellular bacteria. Following wash (3x) wit PBS, bladders were homogenized in 1 ml PBS and plated to determine intracellular bacterial titers. Two-tailed Mann-Whitney ($P<0.05$) was used for statistical analyses

[0237] Acute infection studies: Mice were transurethrally infected with 10^7 bacteria carrying the plasmid pCom-GFP as previously described. Experiments were repeated three times and statistically analyzed using two-tailed Mann-Whitney ($P<0.05$, considered significant).

[0238] Long-term infection studies: Mice were infected with chromosomally marked strains of wt UTI89, UTI89_LON, UTI89Δ*qseC* or UTI89Δ*qseC*_LON. Mice were sacrificed at 2 weeks post inoculation and organs were processed for cfu enumeration on LB and LB/Kanamycin agar plates. Experiment was repeated 2 times. Cumulative data from all experiments are presented.

Immunoblots, HA and phase assays

[0239] Bacteria were grown statically in LB for 18 h at 37°C. Immunoblots (using anti-type 1 pili antibody), HA and phase assays were performed on normalized cells ($OD_{600}=1$) as previously described.

qPCR analyses

[0240] RNA extraction, DNase treatment and reverse transcription were prerformed using reagents and methods as reported by Kostakioti et al.[32]. Relative transcript abundance was determined by qPCR as previously described[32] using aceB-[31] or qseB-specific[32] primers.

Table 7

Compound Name	Structure	HAI Titer $EC_{>90}$ (μM)	Biofilm Prevention IC_{50} (μM)	Biofilm Disruption IC_{50} (μM)	PAMPA (LogPe)	DSF melting Temp (C)
1JWJ149	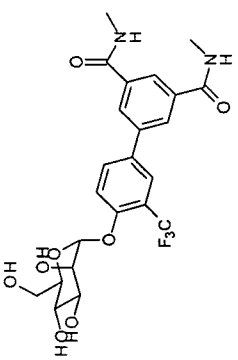	**0.008**	**0.043**		-6.27	76.15
4ZFH52	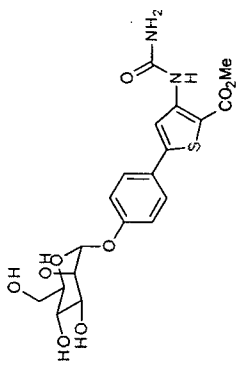	**0.016**	**0.181**			
4ZFH284	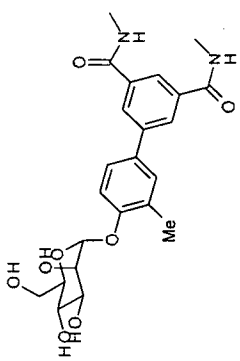	**0.016**	??			

4ZFH272	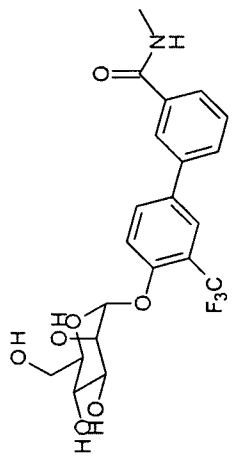	0.032	0.127		-3.91	72.29
4ZFH222	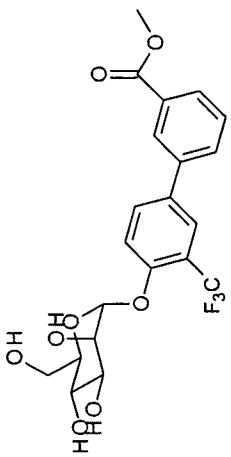	0.032	0.167		-3.91	
4ZFH269	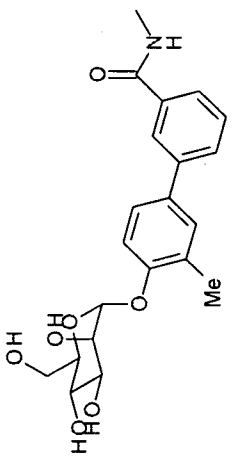	0.06	0.159		-3.89	74.46
5ZFH63	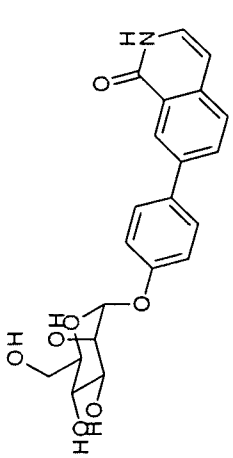	0.100				

4ZFH224	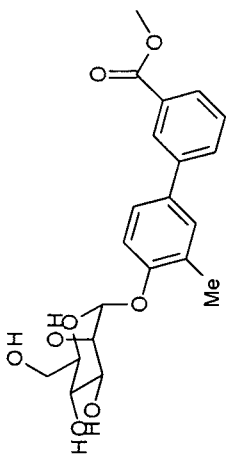	0.125	0.3329		
4ZFH170	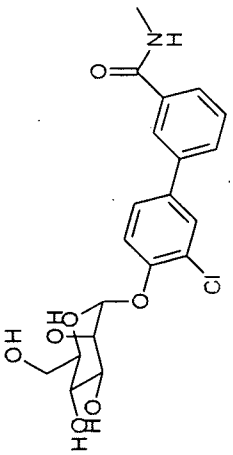	0.125	0.523		
4ZFH228	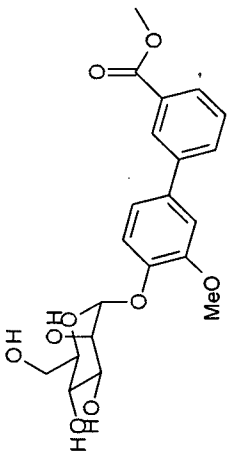	0.188	0.886		
5ZFH61	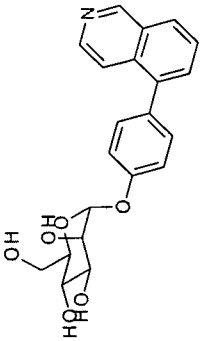	0.250			

4ZFH308	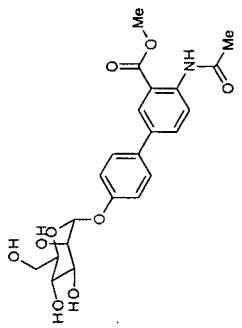	0.250		
5ZFH38	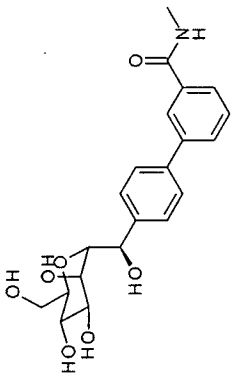	0.250		
4ZFH247	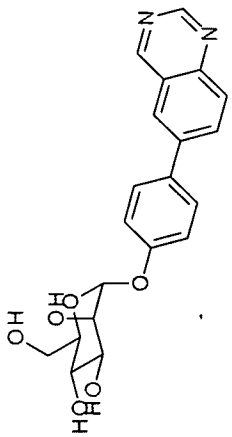	0.375		
4ZFH306	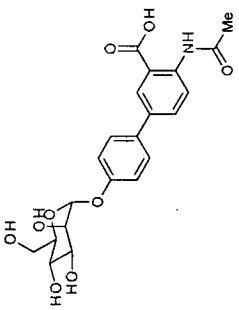	0.750		

4ZFH275	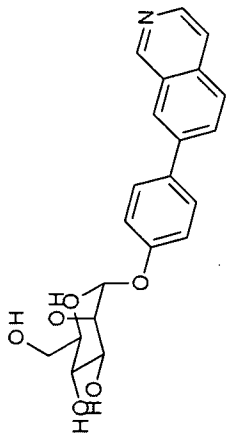	0.750			
4ZFH220	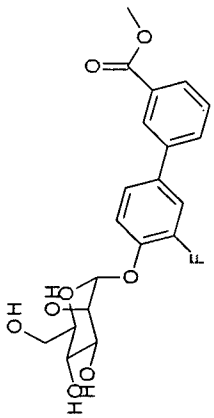	0.750			
4ZFH303	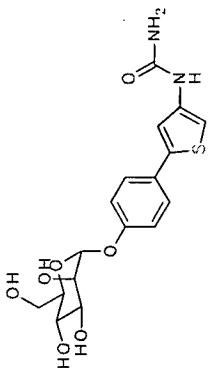	1.000			
4ZFH277	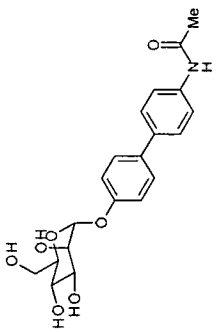	1.000			

5ZFH49	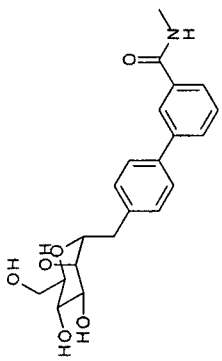	1.000			
4ZFH218	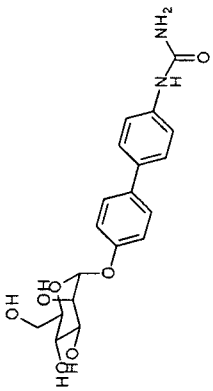	3.000		-4.35	
3ZFH26	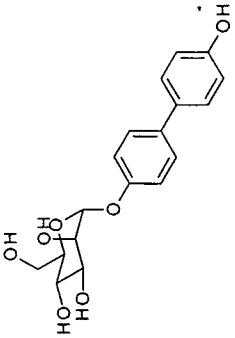	6.000		-6.890	
3ZF117	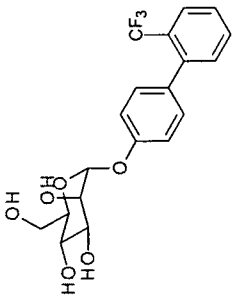	8.000			

4ZFH131	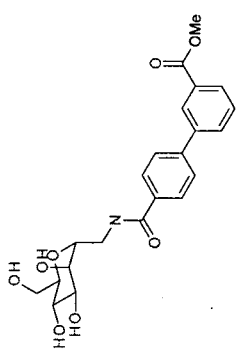	16.000			
4ZFH123	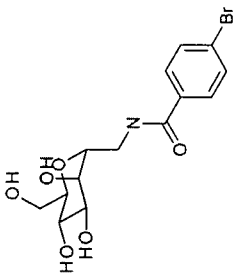	16.000			
5ZFH48	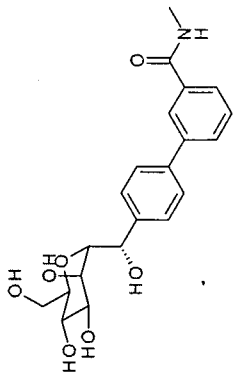	24.000			
1ZFH84	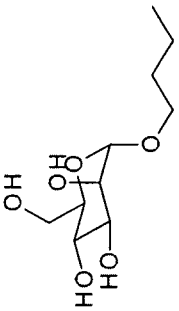	125.000	(~500)		

1ZFH74	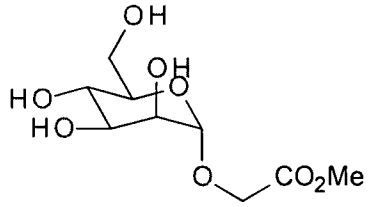	500.000				
2ZFH20	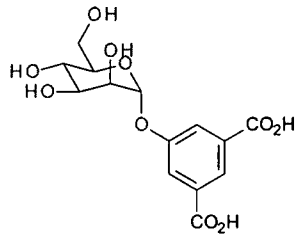					
1JWJ93	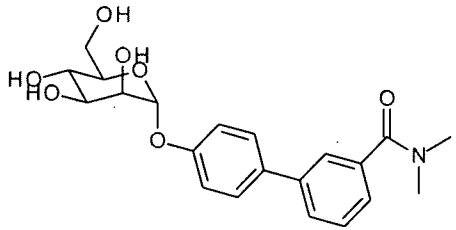					
2ZFH238	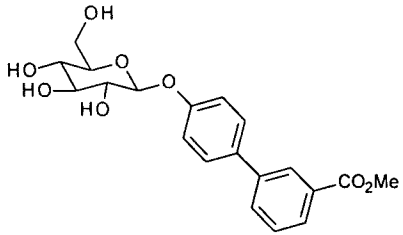	>2.5 mM				

2ZFH236	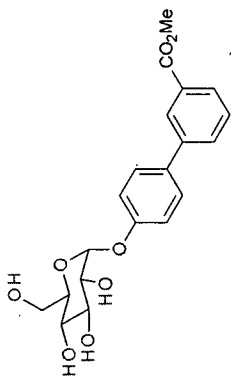	>2.5 mM			-4.250	
1ZFH134	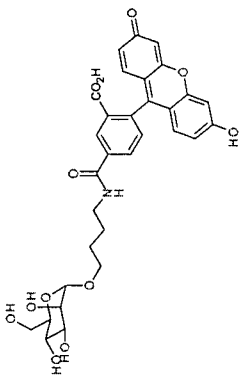	125				
α-D-mannose	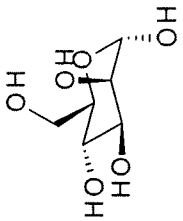					

Table 8

Compound Name	IUPAC Name	Structure	Molecular Formula	Mol. Weight (g/mol)	HAI Titer $EC_{>90}$ (μM)
1JWJ149	N1,N3-dimethyl-5-[3-(trifluoromethyl)-4-[(3R,4S,5S,6S)-3,4,5-trihydroxy-6-(hydroxymethyl)tetrahydropyran-2-yl]oxy-phenyl]benzene-1,3-dicarboxamide	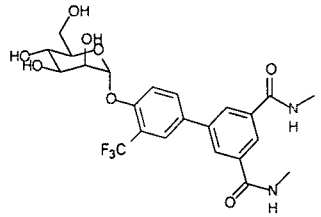	$C_{23}H_{25}F_3N_2O_8$	514.4	0.008
4ZFH284	N1,N3-dimethyl-5-[3-methyl-4-[(3R,4S,5S,6S)-3,4,5-trihydroxy-6-(hydroxymethyl)tetrahydropyran-2-yl]oxy-phenyl]benzene-1,3-dicarboxamide	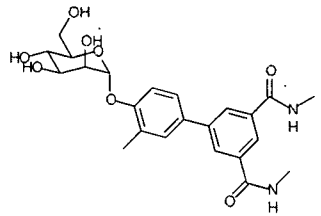	$C_{23}H_{28}N_2O_8$	460.5	0.016
4ZFH222	methyl 3-[3-(trifluoromethyl)-4-[(3R,4S,5S,6S)-3,4,5-trihydroxy-6-(hydroxymethyl)tetrahydropyran-2-yl]oxy-phenyl]benzoate	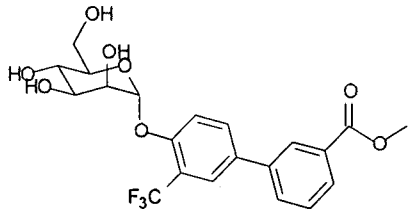	$C_{21}H_{21}F_3O_8$	458.4	0.032
4ZFH272	N-methyl-3-[3-(trifluoromethyl)-4-[(3R,4S,5S,6S)-3,4,5-trihydroxy-6-(hydroxymethyl)tetrahydropyran-2-yl]oxy-phenyl]benzamide	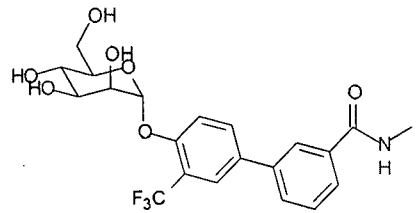	$C_{21}H_{22}F_3NO_7$	457.4	0.032

4ZFH269	N-methyl-3-[3-methyl-4-[(3R,4S,5S,6S)-3,4,5-trihydroxy-6-(hydroxymethyl)tetrahydropyran-2-yl]oxy-phenyl]benzamide		$C_{21}H_{25}NO_7$	403.4	0.062
4ZFH170	3-[3-chloro-4-[(3R,4S,5S,6S)-3,4,5-trihydroxy-6-(hydroxymethyl)tetrahydropyran-2-yl]oxy-phenyl]-N-methyl-benzamide		$C_{20}H_{22}ClNO_7$	423.8	0.125
4ZFH224	methyl 3-[3-methyl-4-[(3R,4S,5S,6S)-3,4,5-trihydroxy-6-(hydroxymethyl)tetrahydropyran-2-yl]oxy-phenyl]benzoate		$C_{21}H_{24}O_8$	404.4	0.125
4ZFH228	methyl 3-[3-methoxy-4-[(3R,4S,5S,6S)-3,4,5-trihydroxy-6-(hydroxymethyl)tetrahydropyran-2-yl]oxy-phenyl]benzoate		$C_{21}H_{24}O_9$	420.4	0.188

4ZFH247	(2S,3S,4S,5R)-2-(hydroxymethyl)-6-(4-quinazolin-6-yloxyphenoxy)tetrahydropyran-3,4,5-triol		$C_{20}H_{20}N_2O_6$	384.4	0.375
4ZFH220	methyl 3-[3-fluoro-4-[(3R,4S,5S,6S)-3,4,5-trihydroxy-6-(hydroxymethyl)tetrahydropyran-2-yl]oxy-phenyl]benzoate		$C_{20}H_{21}FO_8$	408.4	0.750
4ZFH275	(2S,3S,4S,5R)-2-(hydroxymethyl)-6-[4-(7-isoquinolyl)phenoxy]tetrahydropyran-3,4,5-triol		$C_{21}H_{21}NO_6$	383.4	0.750
4ZFH218	[4-[4-[(3R,4S,5S,6S)-3,4,5-trihydroxy-6-(hydroxymethyl)tetrahydropyran-2-yl]oxyphenyl]phenyl]urea		$C_{19}H_{22}N_2O_7$	390.4	3.000

2ZFH20	5-[(3R,4S,5S,6S)-3,4,5-trihydroxy-6-(hydroxymethyl)tetrahydropyran-2-yl]oxybenzene-1,3-dicarboxylic acid		$C_{14}H_{16}O_{10}$	344.3	?
4ZFH131	methyl 3-[4-[[(3R,4R,5S,6S)-3,4,5-trihydroxy-6-(hydroxymethyl)tetrahydropyran-2-yl]methylcarbamoyl]phenyl]benzoate		$C_{22}H_{25}NO_8$	431.44	16.000
4ZFH123	4-bromo-N-[[(3R,4R,5S,6S)-3,4,5-trihydroxy-6-(hydroxymethyl)tetrahydropyran-2-yl]methyl]benzamide		$C_{14}H_{18}BrNO_6$	376.2	16.000
			$C_{13}H_{17}BrO_6$	349.2	

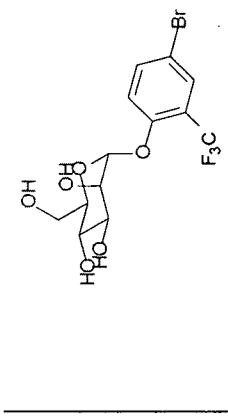	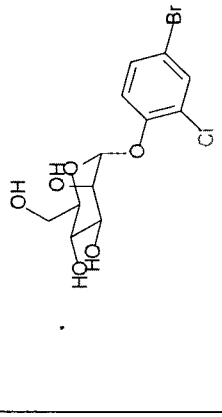	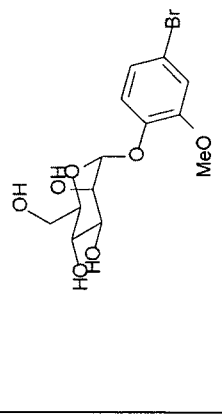	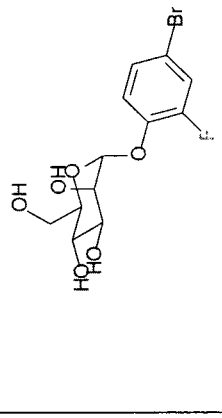
$C_{13}H_{14}BrF_3O_6$	$C_{12}H_{14}BrClO_6$	$C_{13}H_{17}BrO_7$	$C_{12}H_{14}BrFO_6$
403.1	369.6	365.2	353.14

396.2	450.2	416.7	412.2
$C_{19}H_{29}BO_8$	$C_{19}H_{26}BF_3O_8$	$C_{18}H_{26}BClO_8$	$C_{19}H_{29}BO_9$
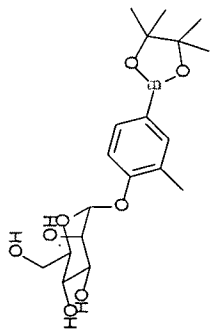	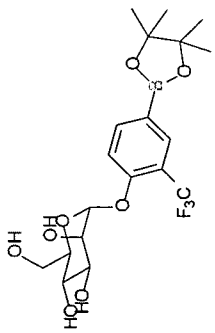	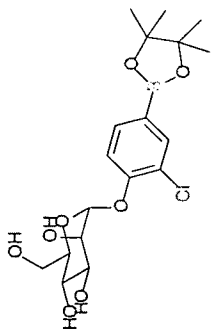	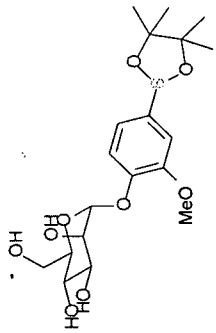

400.2	480.9	464.4	476.5
$C_{18}H_{26}BFO_8$	$C_{22}H_{25}ClN_2O_8$	$C_{22}H_{25}FN_2O_8$	$C_{23}H_{28}N_2O_9$
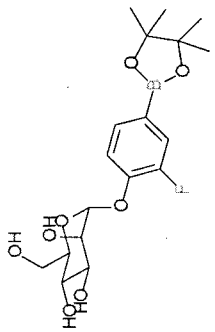	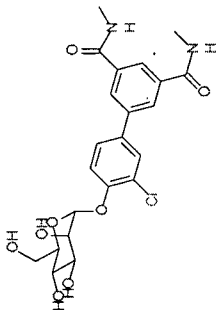	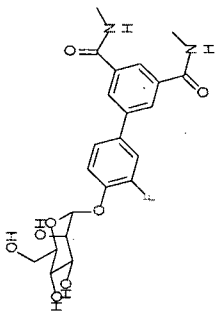	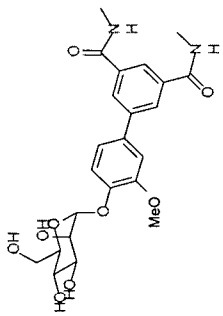

468.5	522.4	484.5	488.9
$C_{20}H_{24}N_2O_9S$	$C_{20}H_{21}F_3N_2O_9S$	$C_{20}H_{24}N_2O_{10}S$	$C_{19}H_{21}ClN_2O_9S$
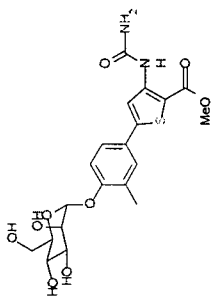	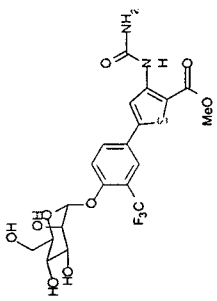	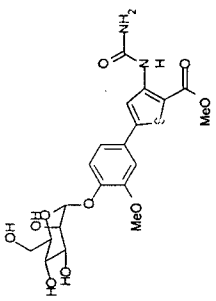	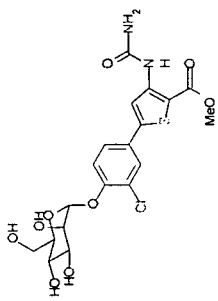

472.4	438.4	452.5	506.4
$C_{19}H_{21}FN_2O_9S$	$C_{19}H_{22}N_2O_8S$	$C_{20}H_{24}N_2O_8S$	$C_{20}H_{21}F_3N_2O_8S$
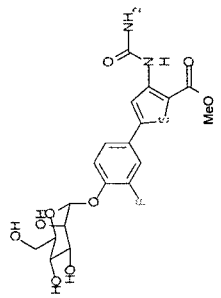	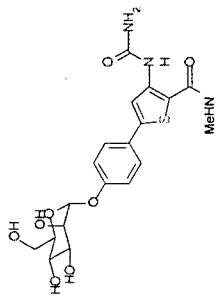	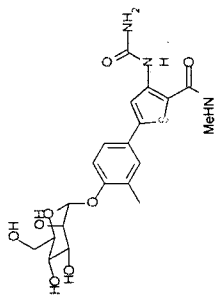	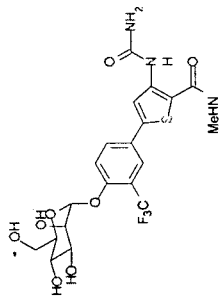				

468.5	472.9	456.4	396.4
$C_{20}H_{24}N_2O_9S$	$C_{19}H_{21}ClN_2O_8S$	$C_{19}H_{21}FN_2O_8S$	$C_{17}H_{20}N_2O_7S$
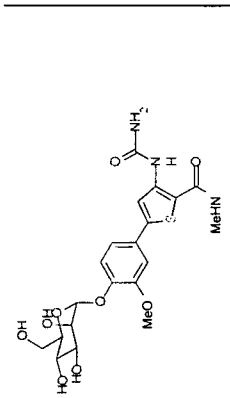	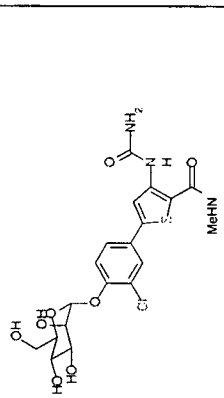	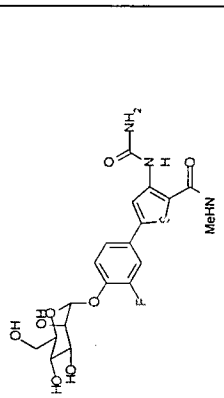	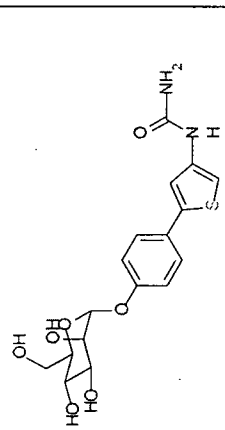

410.4	464.4	430.9	426.4
$C_{18}H_{22}N_2O_7S$	$C_{18}H_{19}F_3N_2O_7S$	$C_{17}H_{19}ClN_2O_7S$	$C_{18}H_{22}N_2O_8S$
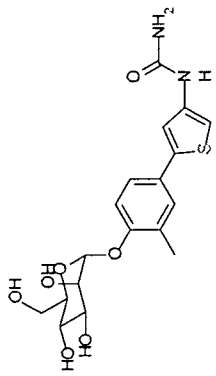	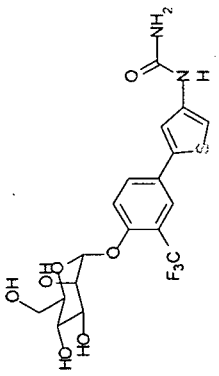	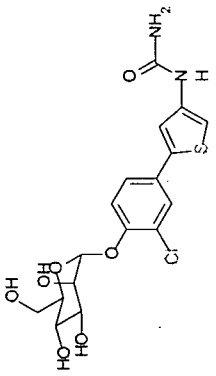	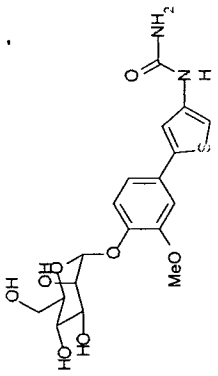

414.4	454.4	438.4	396.4
$C_{17}H_{19}FN_2O_7S$	$C_{19}H_{22}N_2O_9S$	$C_{19}H_{22}N_2O_8S$	$C_{17}H_{20}N_2O_7S$
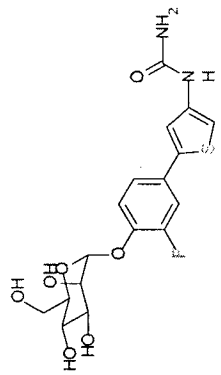	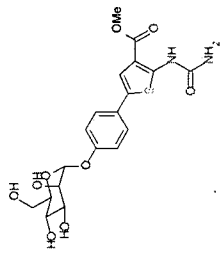	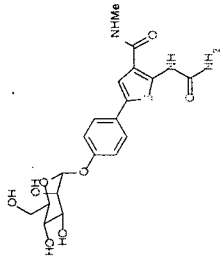	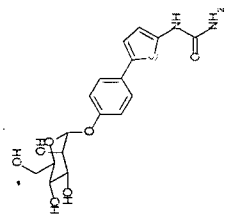

383.4	384.4	384.4	445.5
$C_{21}H_{21}NO_6$	$C_{20}H_{20}N_2O_6$	$C_{20}H_{20}N_2O_6$	$C_{22}H_{23}NO_7S$
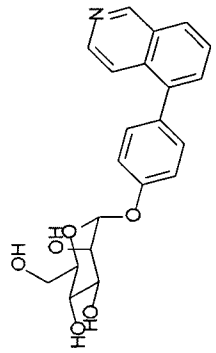	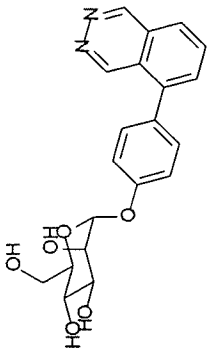	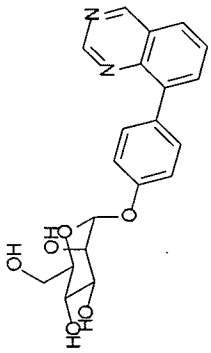	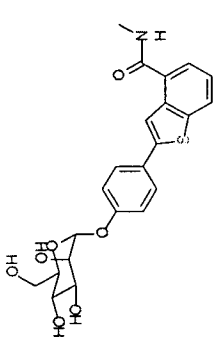

429.4	428.4	429.4	446.5
$C_{22}H_{23}NO_8$	$C_{22}H_{24}N_2O_7$	$C_{21}H_{23}N_3O_7$	$C_{21}H_{22}N_2O_7S$
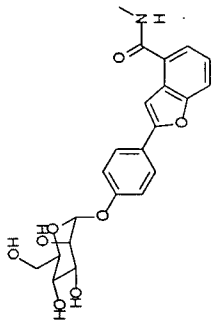	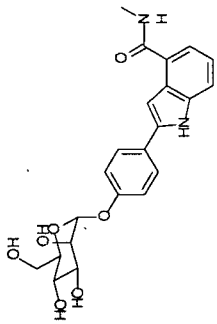	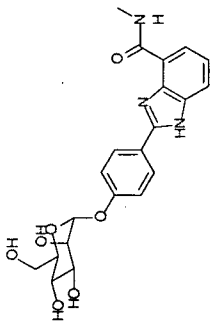	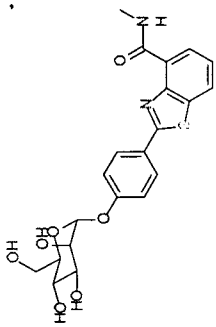

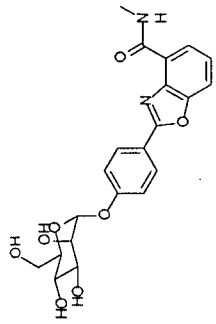	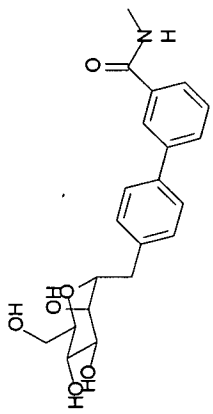	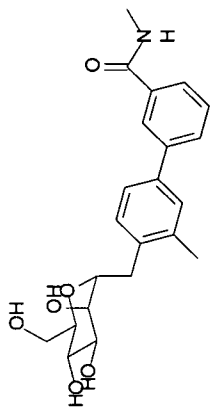	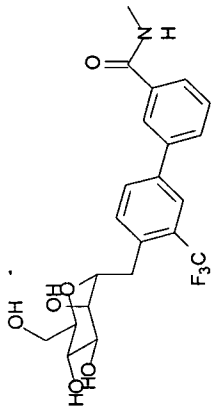
$C_{21}H_{22}N_2O_8$ 430.4	$C_{21}H_{25}NO_6$ 387.4	$C_{22}H_{27}NO_6$ 401.4	$C_{22}H_{24}F_3NO_6$ 455.4

$C_{21}H_{24}ClNO_6$ 421.9	$C_{21}H_{24}FNO_6$ 405.4	$C_{22}H_{27}NO_7$ 417.4	$C_{23}H_{28}N_2O_7$ 444.5
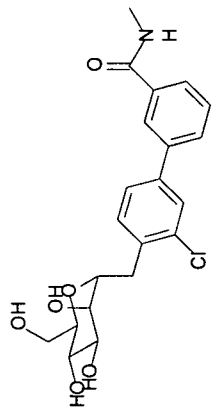	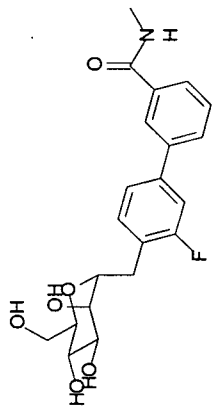	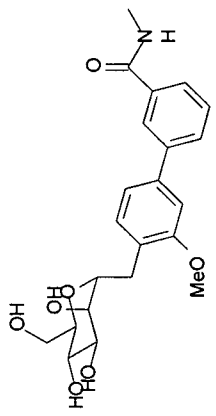	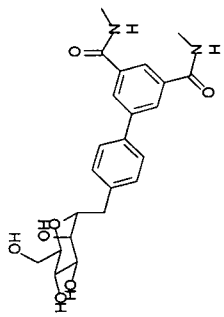

$C_{24}H_{30}N_2O_7$ 458.5	$C_{24}H_{27}F_3N_2O_7$ 512.5	$C_{23}H_{27}ClN_2O_7$ 478.9	$C_{23}H_{27}FN_2O_7$ 462.5
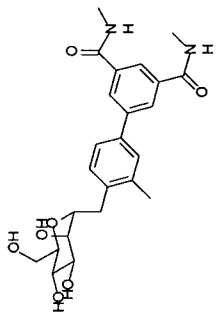	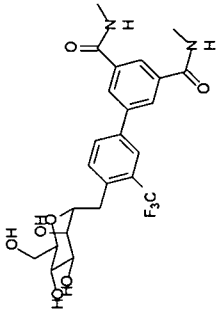	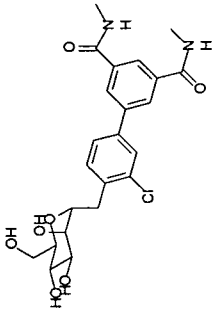	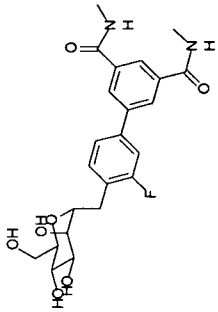

$C_{24}H_{30}N_2O_8$	474.5	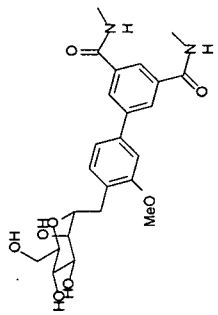

CLAIMS

What is claimed is:

1. A compound, the compound comprising Formula (I):

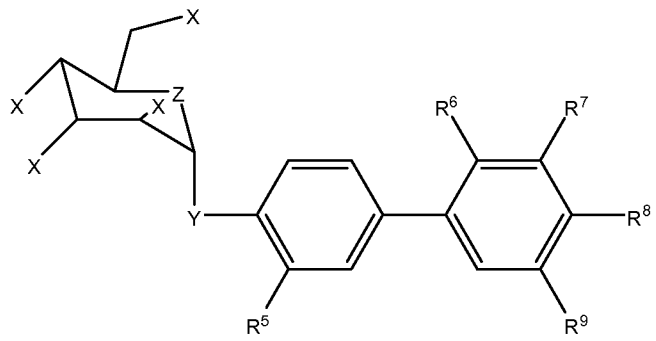

wherein

X is selected from the group consisting of hydrogen, OR^2, SR^2, NR^z;

Z is selected from the group consisting of O, S, CR^3 and NR^4;

Y is oxygen;

R^2, R^3, and R^4 are independently selected from the group consisting of hydrogen, hydrocarbyl, and substituted hydrocarbyl;

R^5 is selected from the group consisting of CF_3, halogen, CH_3, OMe, hydrocarbyl, and substituted hydrocarbyl;

R^6, R^7, R^8, and R^9 are independently selected from the group consisting of hydrogen, $-COR^{10}R^{11}$, $-CONR^{10}R^{11}$, $-COOR^{12}$, and $-NR^{12}CONR^{10}$, or R^6 and R^7 may optionally form a cycloalkyl or heterocyclo ring, R^7 and R^8 may optionally form a cycloalkyl or heterocyclo ring, and R^8 and R^9 may optionally form a cycloalkyl or heterocyclo ring; and

R^{10}, R^{11}, and R^{12} are independently selected from the group consisting of hydrogen, hydrocarbyl, substituted hydrocarbyl, aryl, and heterocycle;

R^{18} and R^{19} are independently selected from the group consisting of hydrogen, hydrocarbyl, and substituted hydrocarbyl;

R^z is independently selected from the group consisting of hydrogen hydrocarbyl, substituted hydrocarbyl, $-COR^x$, $-CONR^xR^xSO_2R^x$, and $-CO_2R^x$; and

R^x is independently selected from the group consisting of hydrogen, $-NR^{18}R^{19}$, and an optionally substituted alkyl, cycloalkyl, heterocycle, or aryl.

2. A compound, the compound comprising Formula (II):

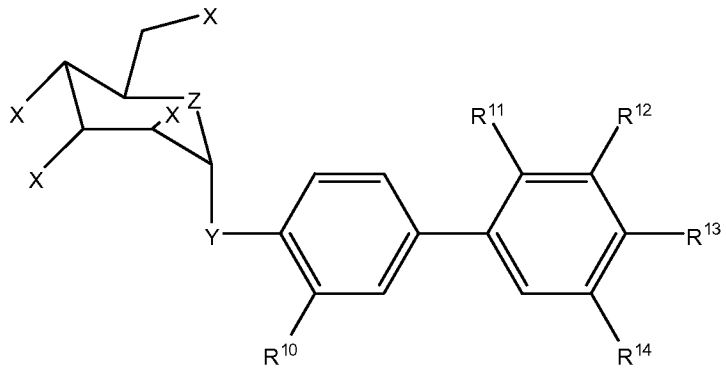

wherein

X is selected from the group consisting of hydrogen, OR^2, SR^2, NR^z;

Z is selected from the group consisting of O, S, CR^3 and NR^4;

Y is selected from the group consisting of sulfur, CR^3, NR^4, $-N(R^{18})CO-$, $-CH_2N(R^{18})-$, $-CH_2N(R^{18})CO-$, CO_2, SO_2, $-CH_2O-$, $-CH_2S-$, CO, $-CON(R^{18})-$, $-SO_2N(R^{18})-$, $-O(CH_2)_n-$, $-S(CH_2)_n-$, $-N(CH_2)_n-$, $-(CH_2)_n-$, NR^{18}, and an optionally substituted alkyl, alkene, alkyne, or heterocycle;

n is an integer from 1 to 10;

R^2, R^3, and R^4 are independently selected from the group consisting of hydrogen, hydrocarbyl, and substituted hydrocarbyl;

R^{10} is selected from the group consisting of hydrogen, CF_3, halogen, CH_3, OMe, hydrocarbyl, and substituted hydrocarbyl;

R^{11}, R^{12}, R^{13}, and R^{14} are independently selected from the group consisting of hydrogen, $-COR^{15}R^{16}$, $-CONR^{15}R^{16}$, $-COOR^{17}$, and $-NR^{17}CONR^{15}$, or R^{11} and R^{12} may optionally form a cycloalkyl or heterocyclo ring, R^{12} and R^{13} may optionally form a cycloalkyl or heterocyclo ring, and R^{13} and R^{14} may optionally form a cycloalkyl or heterocyclo ring;

R^{15}, R^{16}, and R^{17} are independently selected from the group consisting of hydrogen, hydrocarbyl, substituted hydrocarbyl, aryl, and heterocycle;

R^{18} and R^{19} are independently selected from the group consisting of hydrogen, hydrocarbyl, and substituted hydrocarbyl; and

R^z is independently selected from the group consisting of hydrogen hydrocarbyl, substituted hydrocarbyl, $-COR^x$, $-CONR^xR^xSO_2R^x$, and $-CO_2R^x$; and

R^x is independently selected from the group consisting of hydrogen, $-NR^{18}R^{19}$, and an optionally substituted alkyl, cycloalkyl, heterocycle, or aryl.

3. A compound, the compound comprising Formula (III):

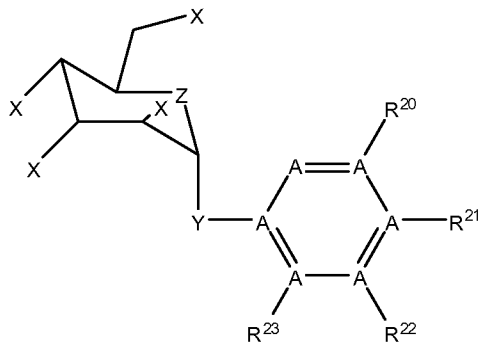

wherein

X is selected from the group consisting of hydrogen, OR^2, SR^2, NR^z;

Z is selected from the group consisting of O, S, CR^3 and NR^4;

Y is selected from the group consisting of oxygen, sulfur, CR^3, NR^4, $-N(R^5)CO-$, $-CH_2N(R^5)-$, $-CH_2N(R^5)CO-$, CO_2, SO_2, $-CH_2O-$, $-CH_2S-$, CO, $-CON(R^5)-$, $-SO_2N(R^5)-$, $-O(CH_2)_n-$, $-S(CH_2)_n-$, $-N(CH_2)_n-$, $-(CH_2)_n-$, NR^5, and an optionally substituted alkyl, alkene, alkyne, or heterocycle;

R^2, R^3, R^4, R^5 are independently selected from the group consisting of hydrogen, hydrocarbyl, and substituted hydrocarbyl;

n is an integer from 1 to 10;

A is independently selected from the group consisting of CR^6 and N;

R^6 is selected from the group consisting of hydrogen, hydrocarbyl, and substituted hydrocarbyl;

R^{20} and R^{22} are selected from the group consisting of hydrogen and $-COOR^{15}$;

R^{21} is selected from the group consisting of hydrogen, a five membered cycloalkyl or heterocyclo ring, and a halogen;

R^{23} is selected from the group consisting of hydrogen, halogen, hydrocarbyl, and substituted hydrocarbyl;

R^{15} is selected from the group consisting of hydrogen, hydrocarbyl, substituted hydrocarbyl, aryl, and heterocycle;

R^z is independently selected from the group consisting of hydrogen hydrocarbyl, substituted hydrocarbyl, $-COR^x$, $-CONR^xR^xSO_2R^x$, and $-CO_2R^x$; and

R^x is independently selected from the group consisting of hydrogen, $-NR^4R^5$, and an optionally substituted alkyl, cycloalkyl, heterocycle, or aryl.

4. Still yet another aspect of the invention encompasses a compound of formula (IV):

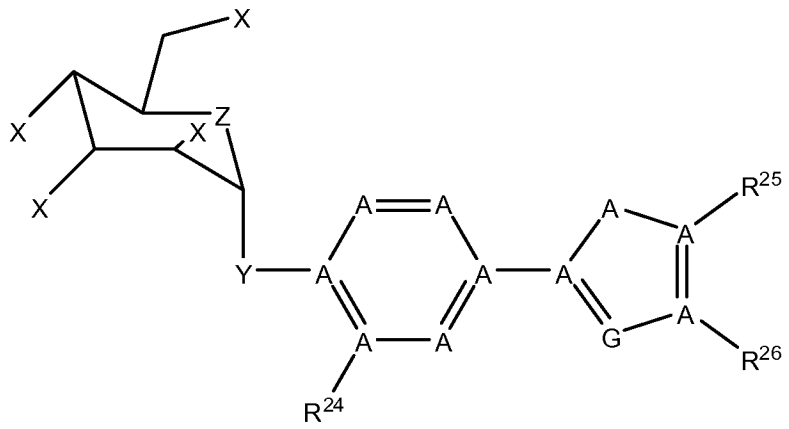

wherein

X is selected from the group consisting of hydrogen, OR^2, SR^2, and NR^z;

Z is selected from the group consisting of O, S, CR^3 and NR^4;

Y is selected from the group consisting of oxygen, sulfur, CR^3, NR^4, $-N(R^5)CO-$, $-CH_2N(R^5)-$, $-CH_2N(R^5)CO-$, CO_2, SO_2, $-CH_2O-$, $-CH_2S-$, CO, $-CON(R^5)-$, $-SO_2N(R^5)-$, $-O(CH_2)_n-$, $-S(CH_2)_n-$, $-N(CH_2)_n-$, $-(CH_2)_n-$, NR^5, and an optionally substituted alkyl, alkene, alkyne, or heterocycle;

R^2, R^3, R^4, R^5 are independently selected from the group consisting of hydrogen, hydrocarbyl, and substituted hydrocarbyl;

n is an integer from 1 to 10;

A is independently selected from the group consisting of CR^6 and N;

G is selected from the group consisting of S, O, CR^8, and NR^9;

R^6, R^8 and R^9 are independently selected from the group consisting of hydrogen, hydrocarbyl, and substituted hydrocarbyl;

R^{24} is selected from the group consisting of hydrogen, halogen, hydrocarbyl, and substituted hydrocarbyl;

R^{25} and R^{26} is selected from the group consisting of hydrogen, $-NHCONH_2$, -COOMe, and –CONHMe, and R^{25} and R^{26} can optionally form a cycloalkyl or heterocyclo ring;

R^z is independently selected from the group consisting of hydrogen hydrocarbyl, substituted hydrocarbyl, $-COR^x$, $-CONR^xR^xSO_2R^x$, and $-CO_2R^x$; and

R^x is independently selected from the group consisting of hydrogen, $-NR^4R^5$, or an optionally substituted alkyl, cycloalkyl, heterocycle, or aryl.

5. A method of treating a bacterial infection in a subject in need of treatment thereof, the method comprising administering a compound of claims 1, 2, 3, or 4 to the subject.

6. A food supplement, wherein the food supplement comprises a compound of claims 1, 2, 3, or 4.

7. A medical device, wherein the medical device comprises a coating comprising a compound of claims 1, 2, 3, or 4.

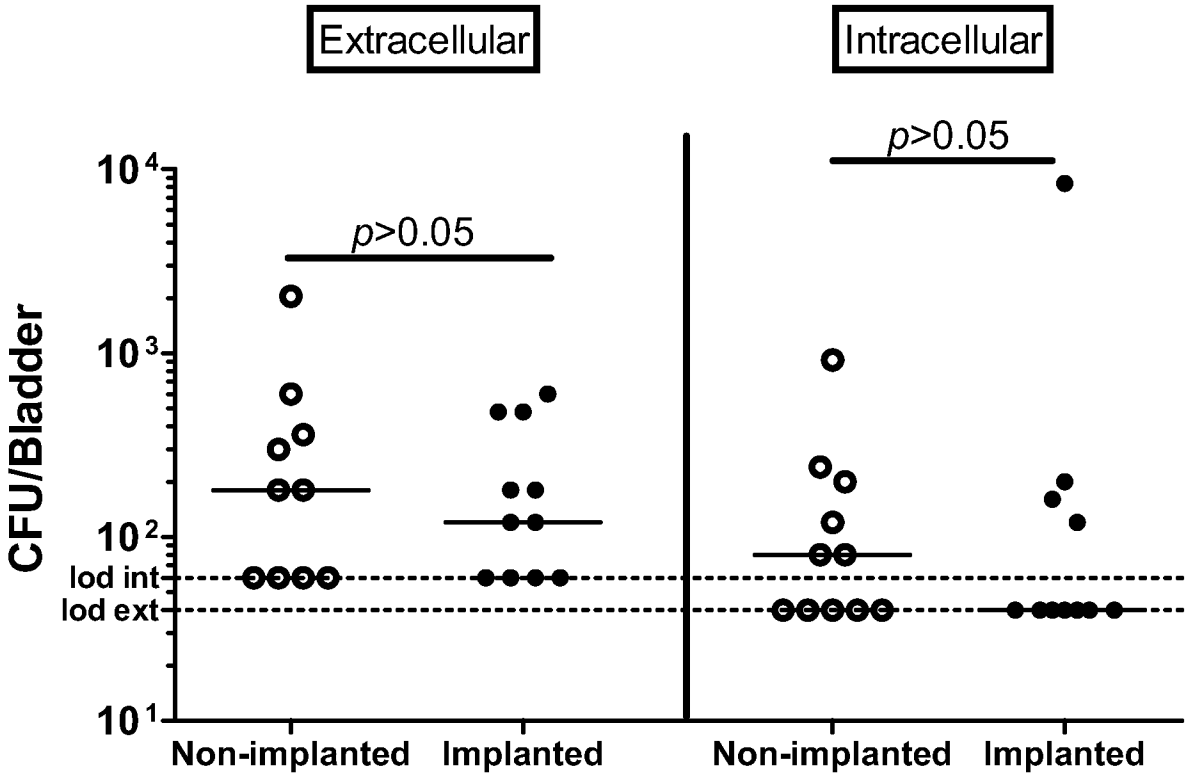
Extracellular
Intracellular
p>0.05
p>0.05
CFU/Bladder
10 4
10 3
10 2
10 1
lod int
lod ext
Non-implanted
Implanted
Non-implanted
Implanted

FIG. 1

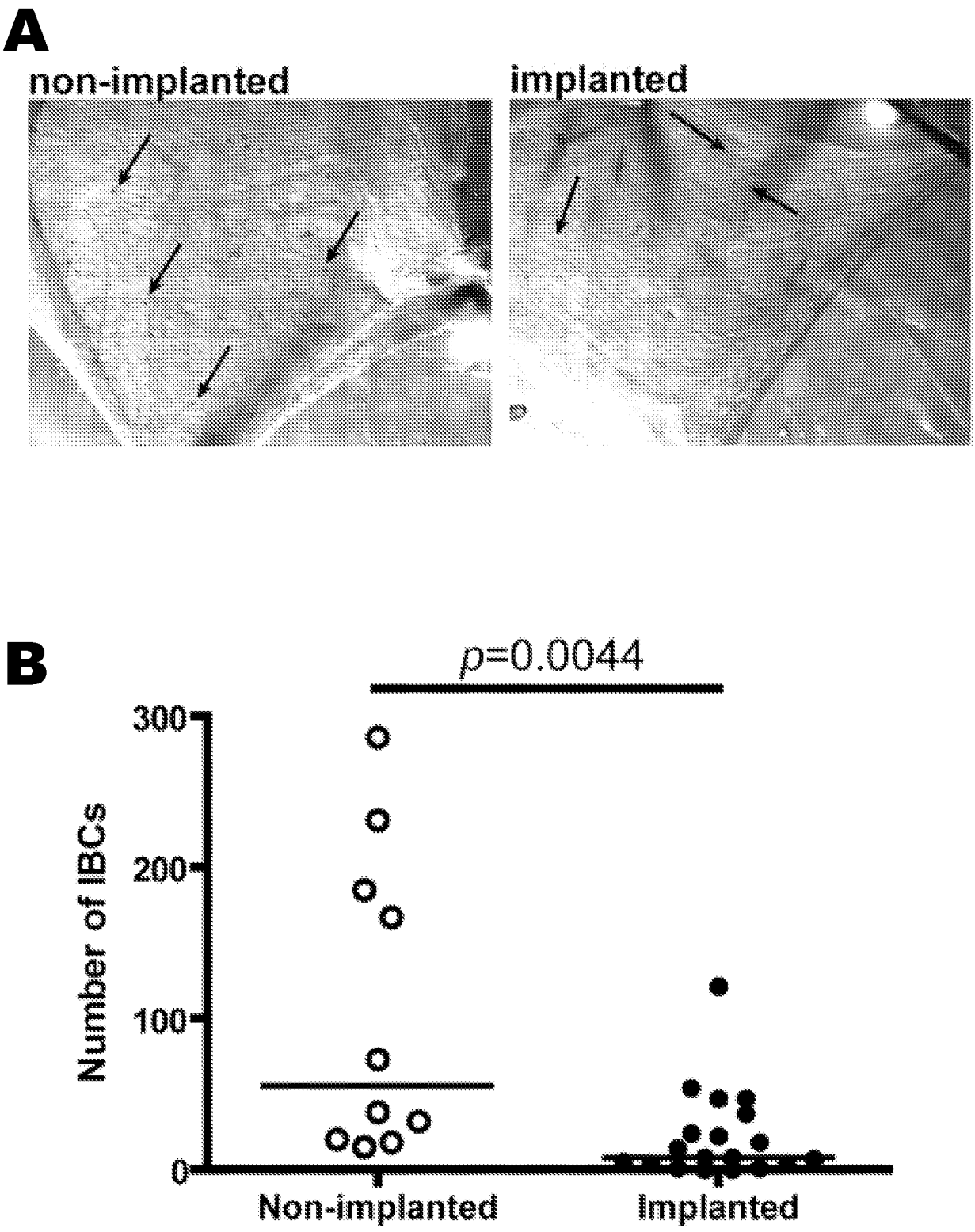
A
non-implanted
implanted
B
p=0.0044
Number of IBCs
300
200
100
0
Non-implanted
Implanted

FIG. 2

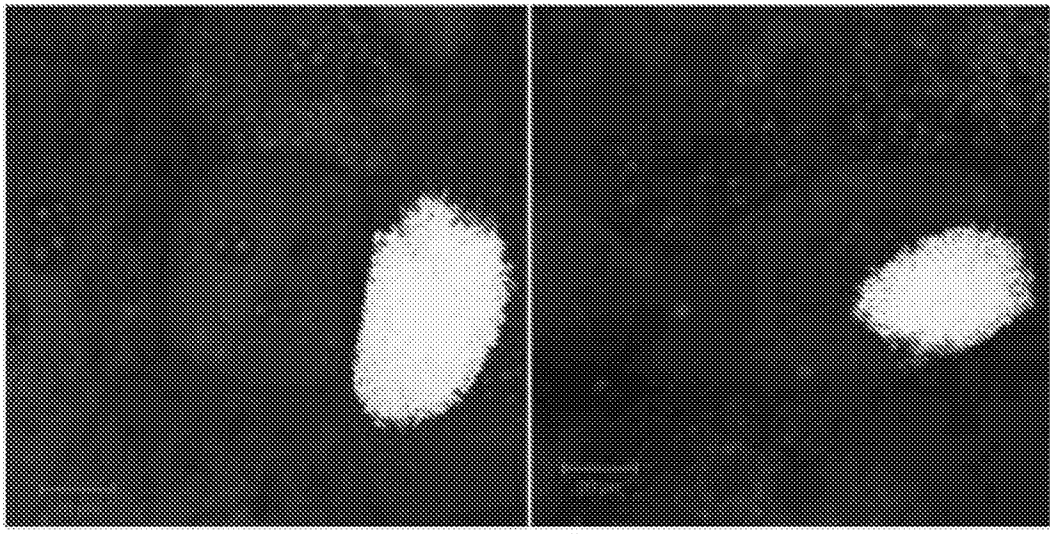

FIG. 2C

A

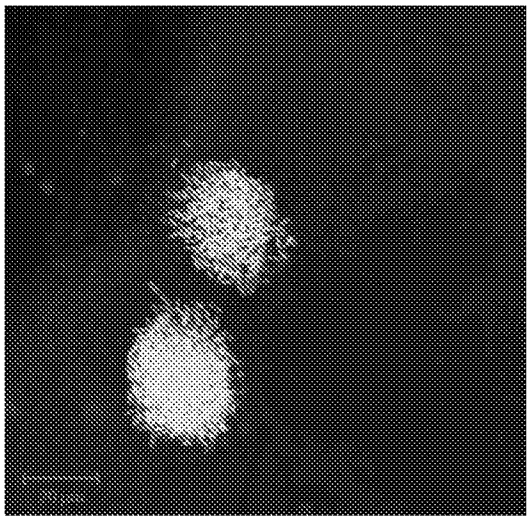

B

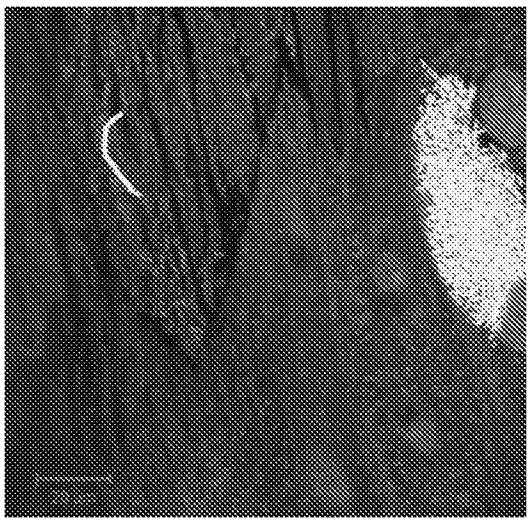

C

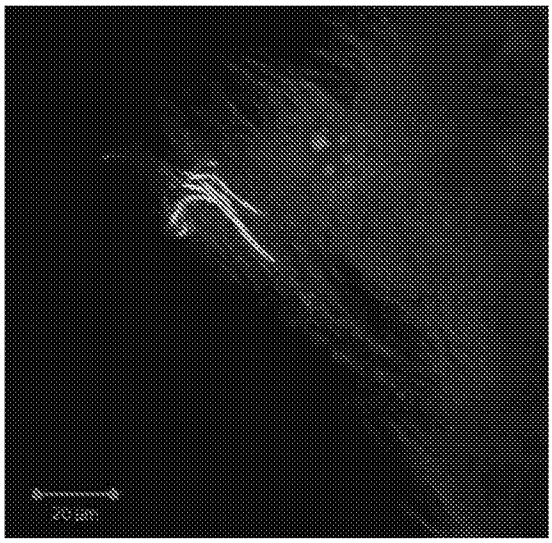

FIG. 3

D

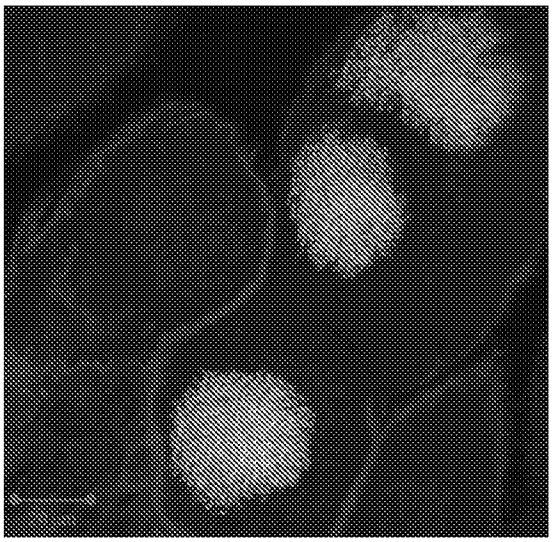

E

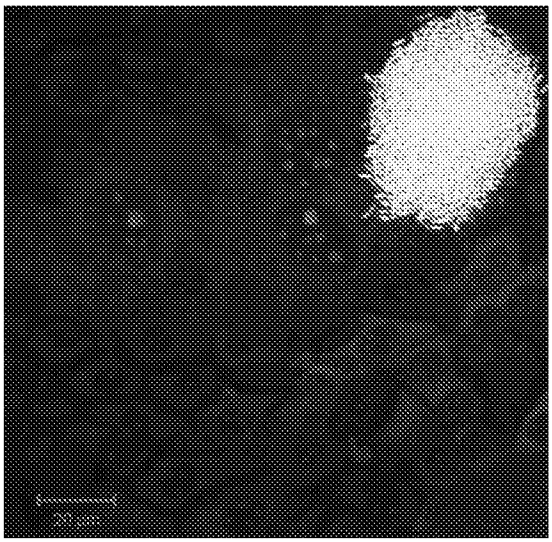

F

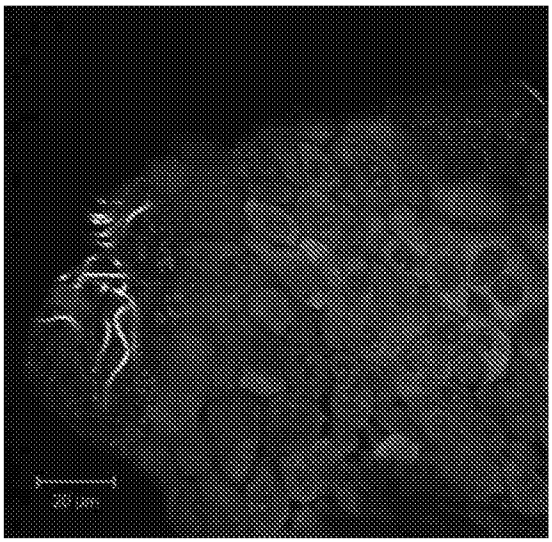

FIG. 3

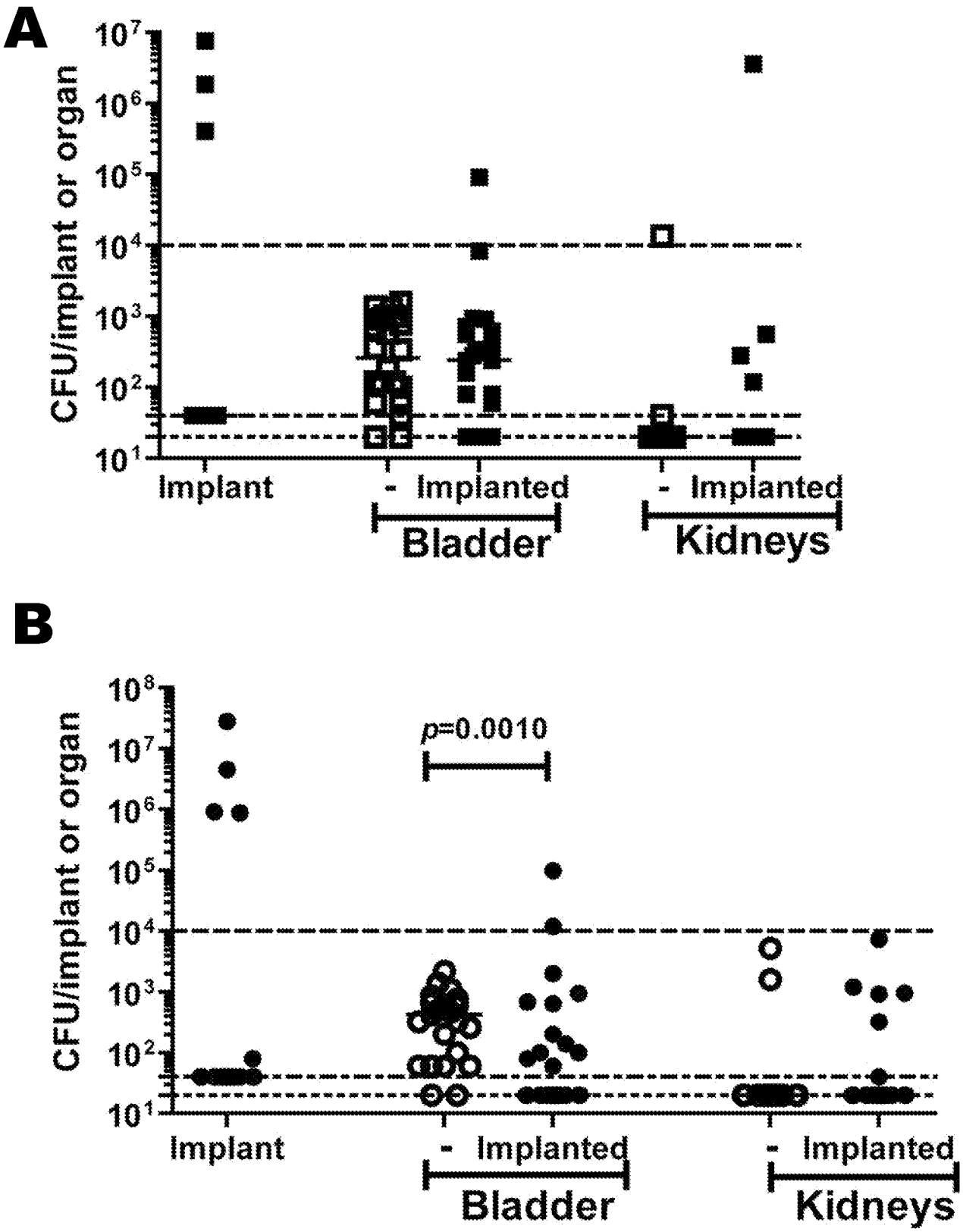
A
CFU/implant or organ
10^7
10^6
10^5
10^4
10^3
10^2
10^1
Implant
- Implanted
Bladder
- Implanted
Kidneys
B
CFU/implant or organ
10^8
10^7
10^6
10^5
10^4
10^3
10^2
10^1
p=0.0010
Implant
- Implanted
Bladder
- Implanted
Kidneys

FIG. 4

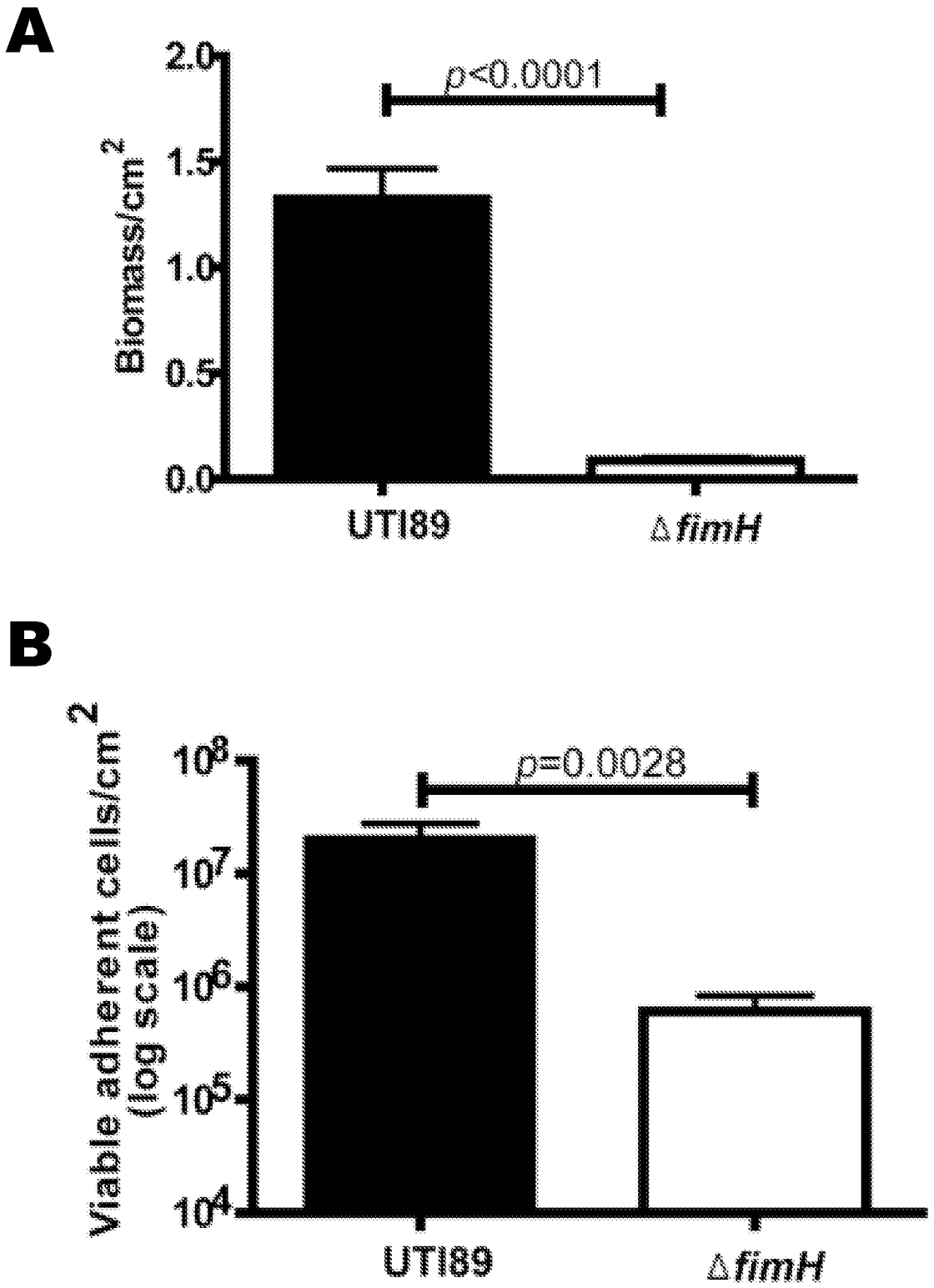
A
2.0
1.5
1.0
0.5
0.0
Biomass/cm2
p<0.0001
UTI89
ΔfimH
B
Viable adherent cells/cm2 (log scale)
10^8
10^7
10^6
10^5
10^4
p=0.0028
UTI89
ΔfimH

FIG. 5

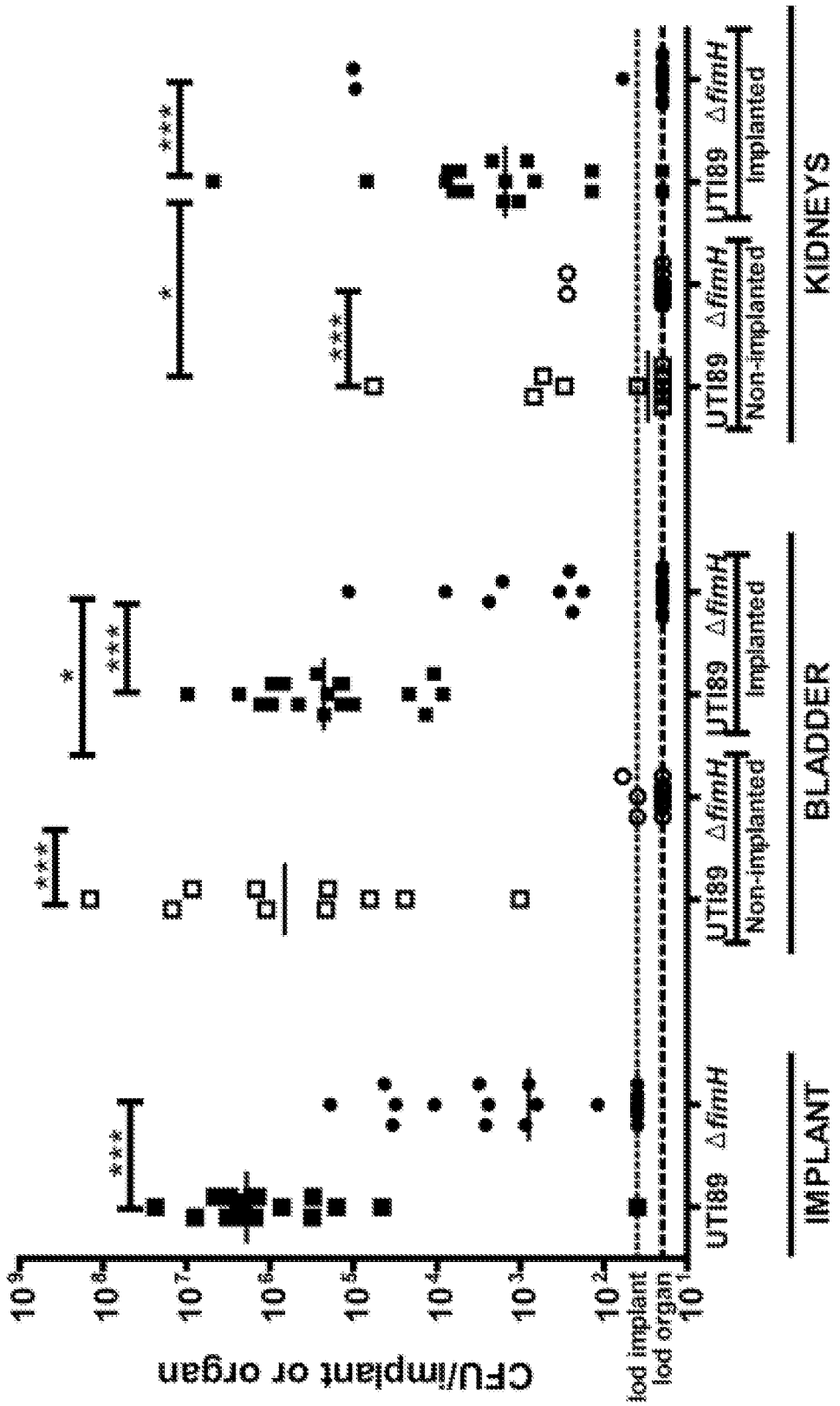
CFU/implant or organ
10^9
10^8
10^7
10^6
10^5
10^4
10^3
10^2
10^1
lod implant
lod organ
***
*
***
***
*
***
UTI89
ΔfimH
UTI89
ΔfimH
Non-implanted
UTI89
ΔfimH
Implanted
UTI89
ΔfimH
Non-implanted
UTI89
ΔfimH
Implanted
IMPLANT
BLADDER
KIDNEYS

FIG. 5C

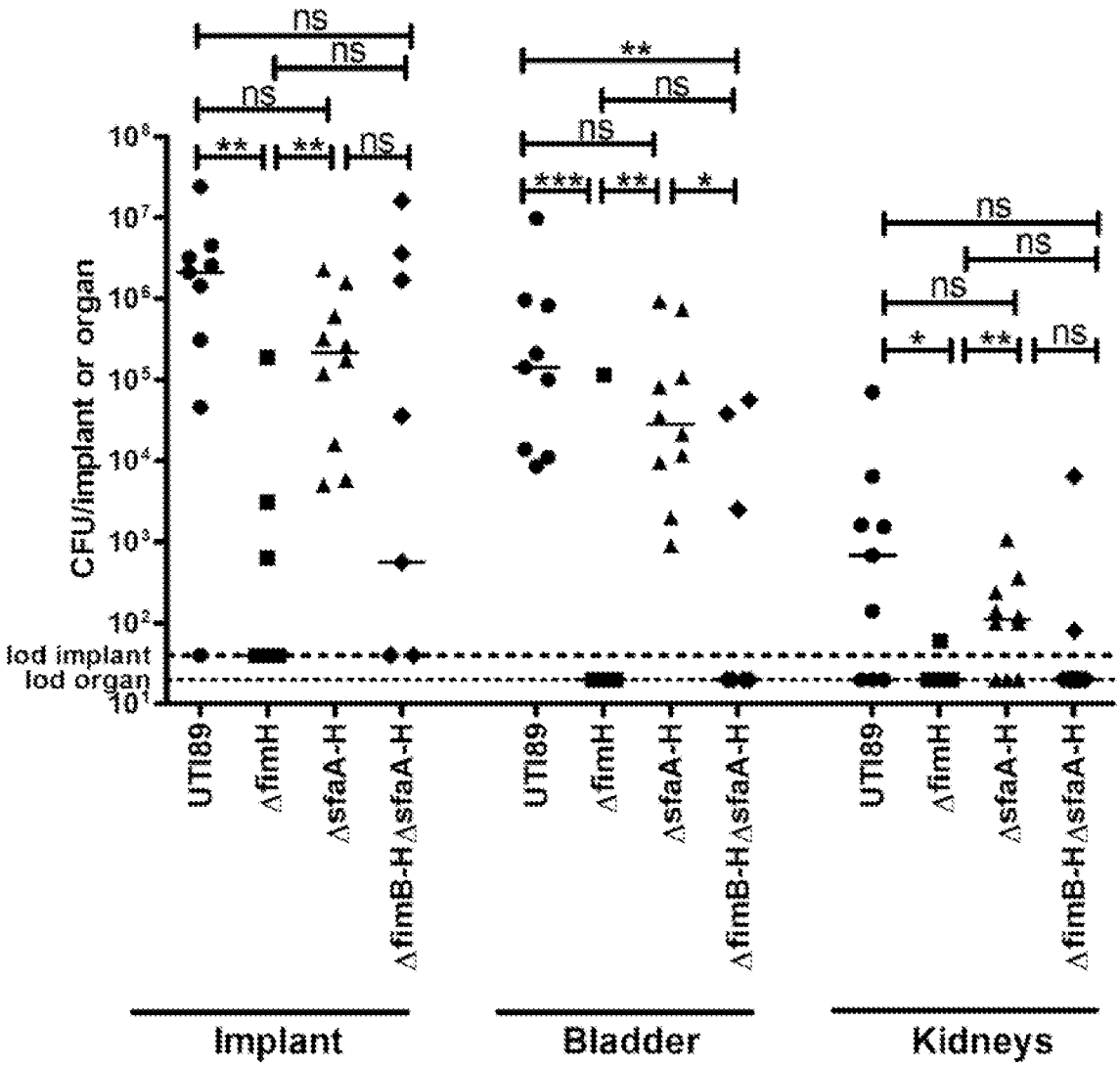
CFU/implant or organ
10^8
10^7
10^6
10^5
10^4
10^3
10^2
10^1
lod implant
lod organ
ns
ns
ns
**
**
ns
**
ns
***
**
*
ns
ns
ns
*
**
ns
UTI89
ΔfimH
ΔsfaA-H
ΔfimB-HΔsfaA-H
Implant
Bladder
Kidneys

FIG. 6A

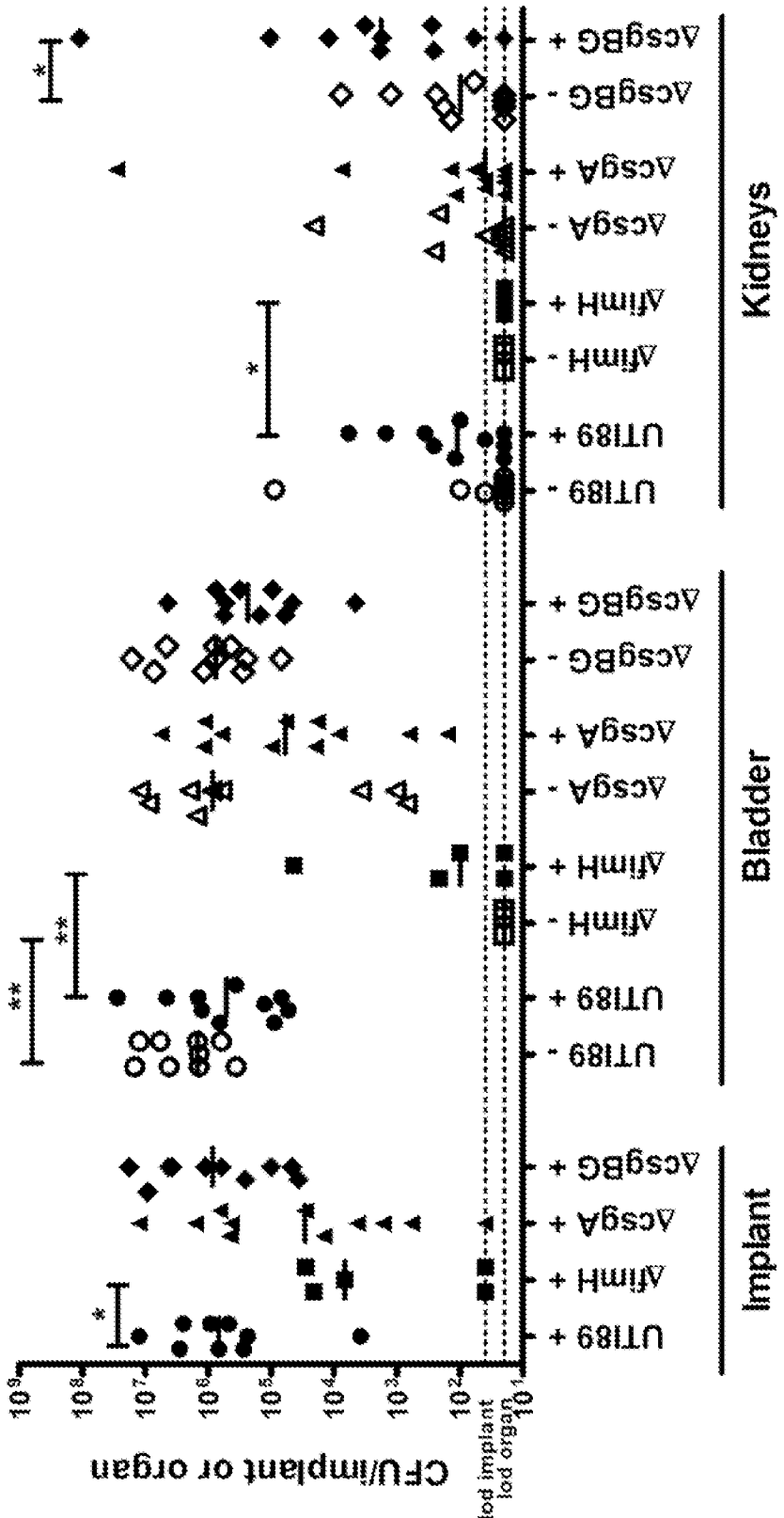
CFU/implant or organ
lod implant
lod organ
Implant
Bladder
Kidneys
UTI89 +
UTI89 -
ΔfimH +
ΔfimH -
ΔcsgA +
ΔcsgA -
ΔcsgBG +
ΔcsgBG -
*
**
**
*
*

FIG. 6B

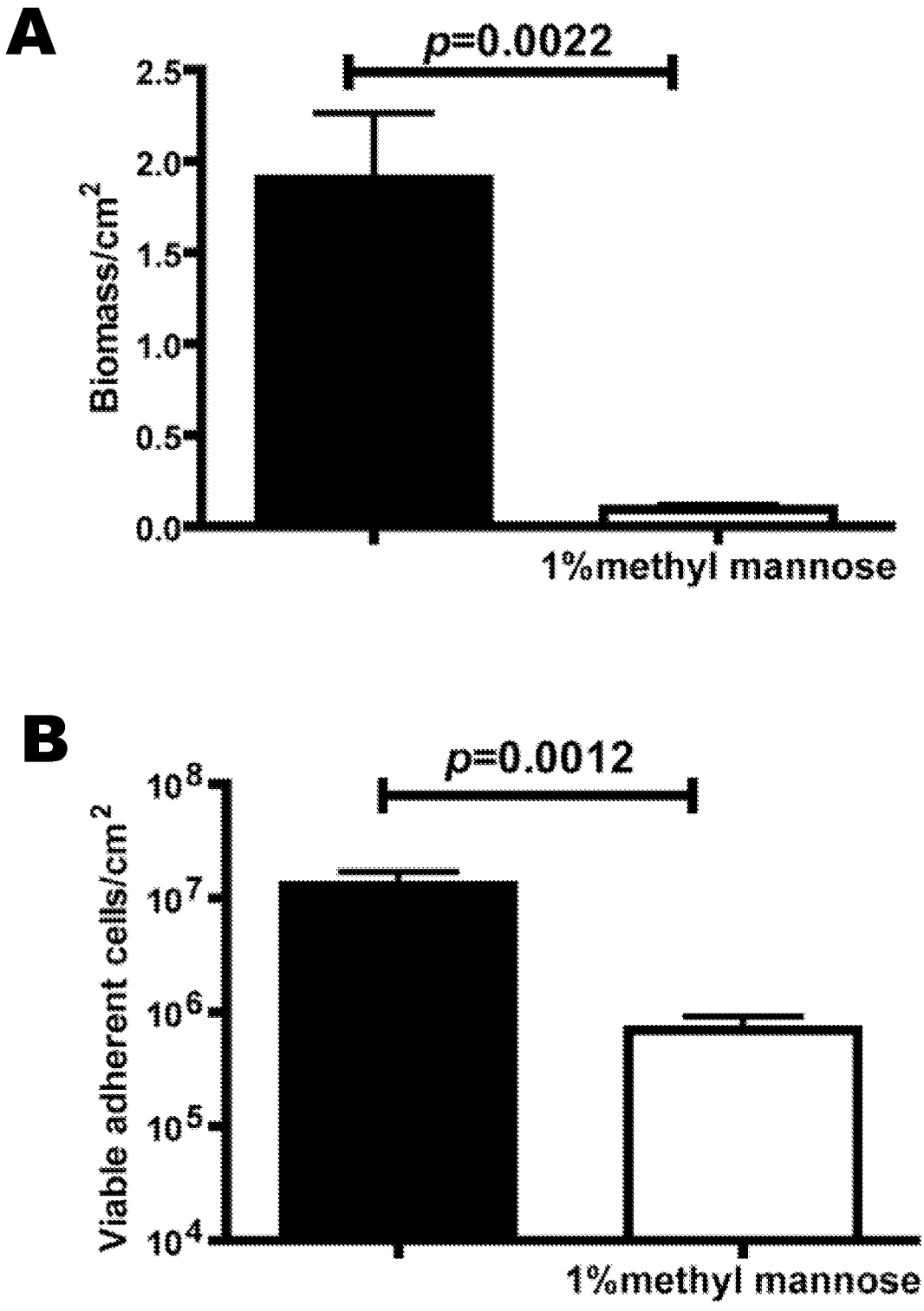
A
p=0.0022
2.5
2.0
1.5
1.0
0.5
0.0
Biomass/cm2
1%methyl mannose
B
p=0.0012
10^8
10^7
10^6
10^5
10^4
Viable adherent cells/cm2
1%methyl mannose

FIG. 7

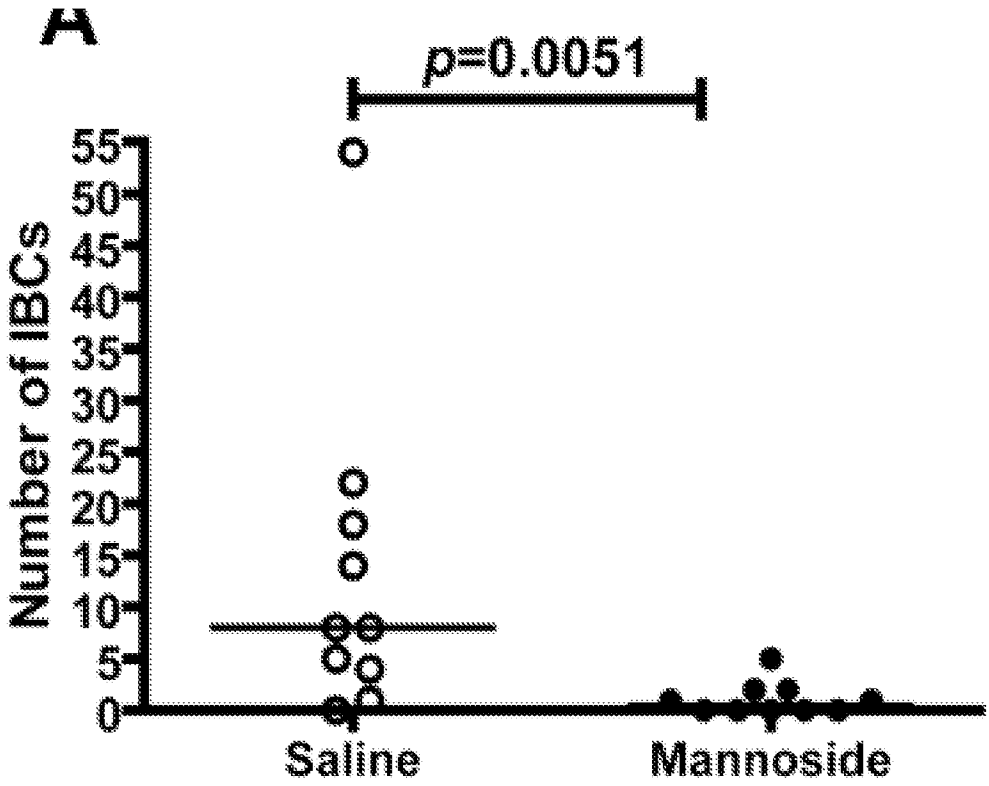
A
p=0.0051
Number of IBCs
55
50
45
40
35
30
25
20
15
10
5
0
Saline
Mannoside

FIG. 8A

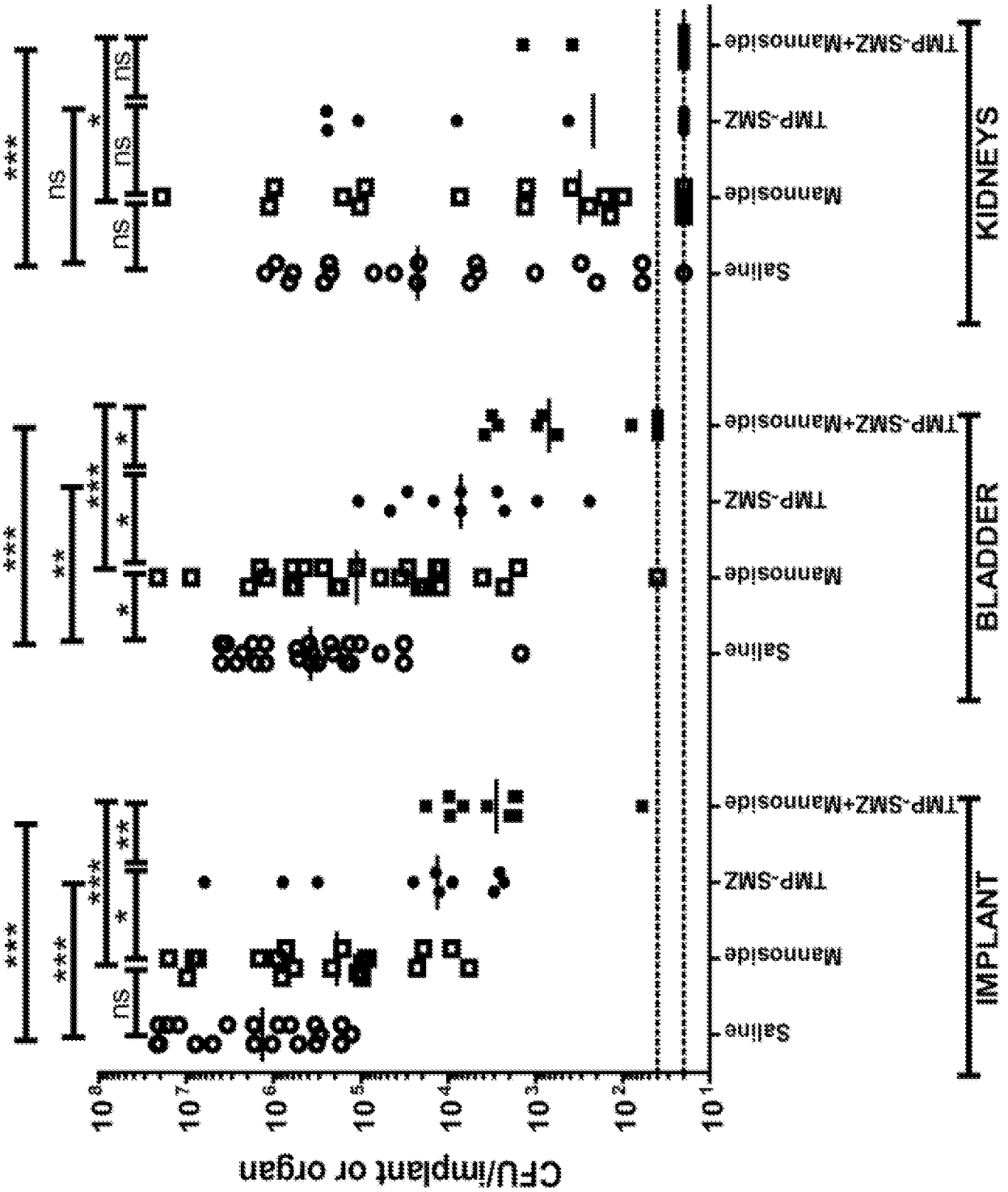
CFU/implant or organ
10^8
10^7
10^6
10^5
10^4
10^3
10^2
10^1
IMPLANT
BLADDER
KIDNEYS
Saline
Mannoside
TMP-SMZ
TMP-SMZ+Mannoside
***
**
*
ns

FIG. 8B

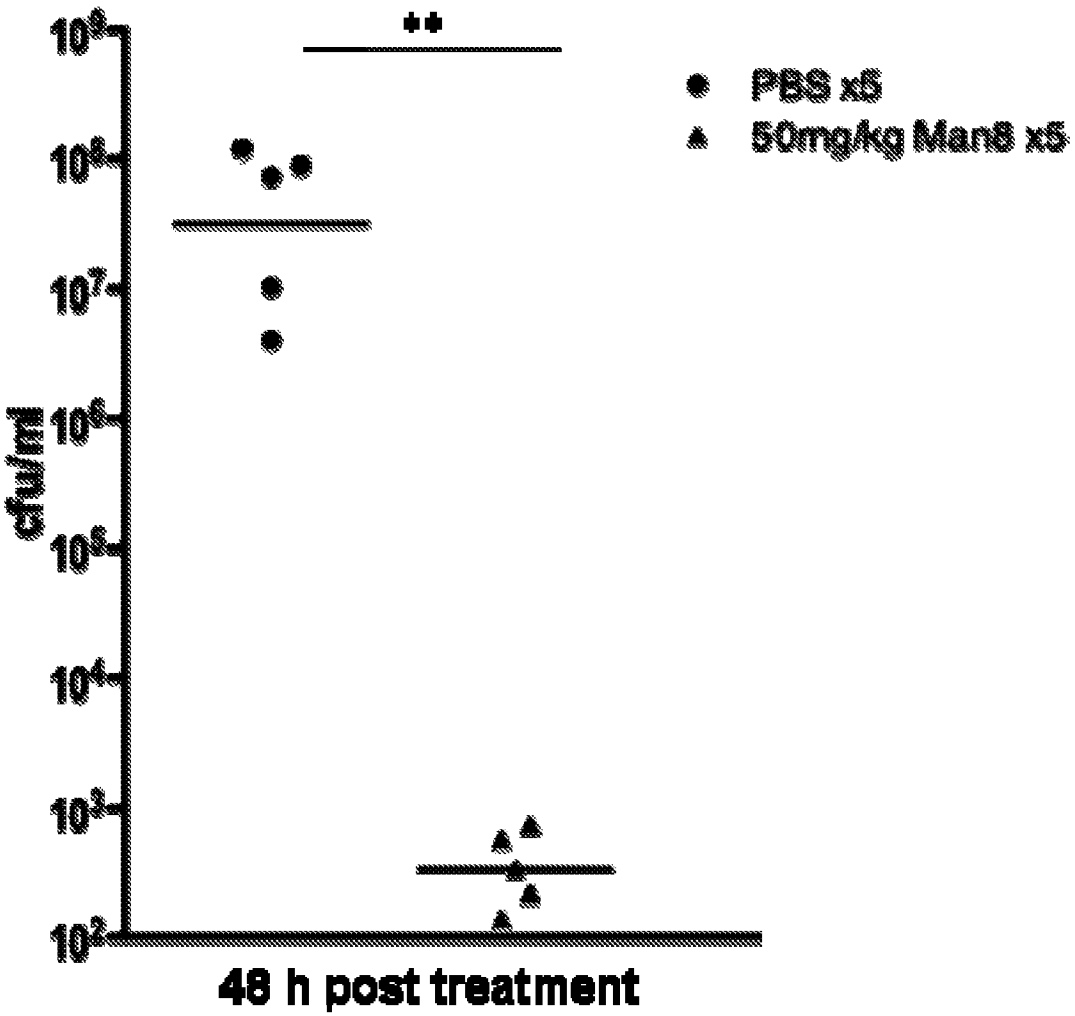

FIG. 9

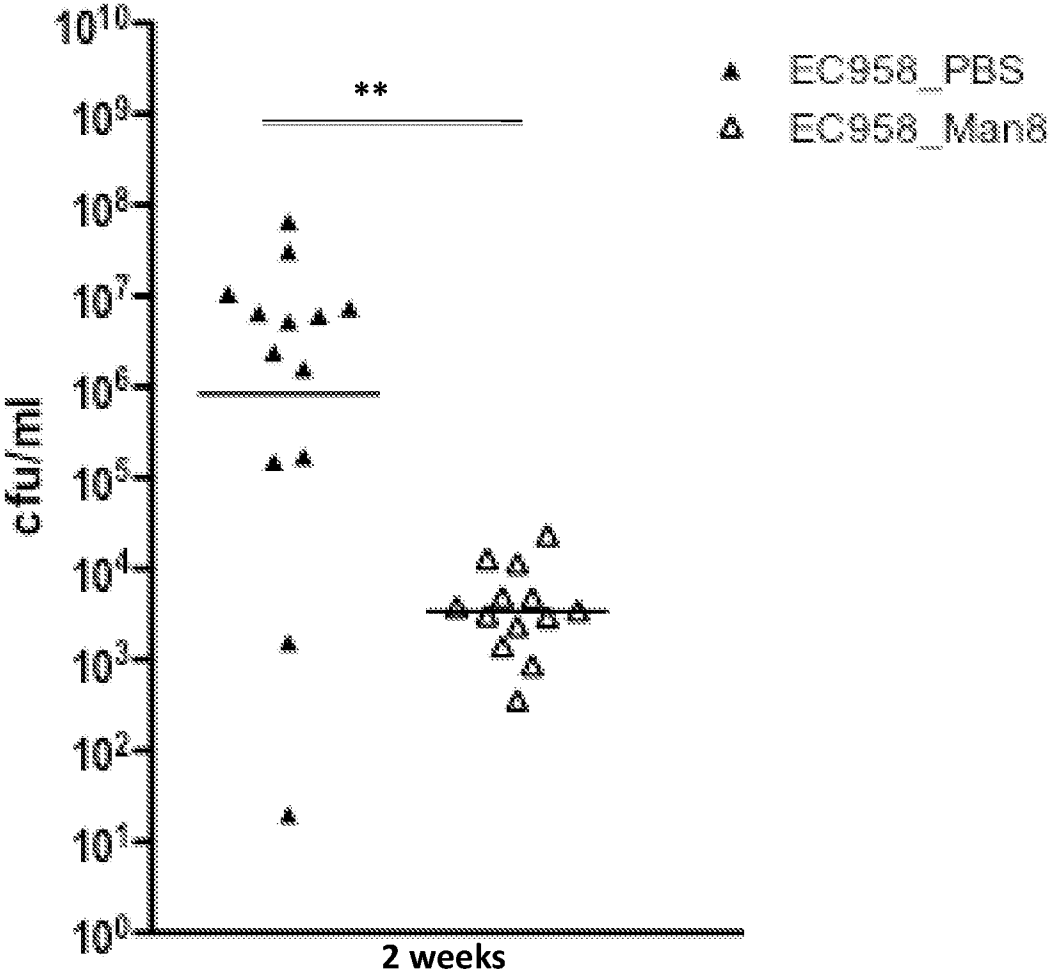
10^{10}
10^{9}
10^{8}
10^{7}
10^{6}
10^{5}
10^{4}
10^{3}
10^{2}
10^{1}
10^{0}
cfu/ml
**
EC958_PBS
EC958_Man8
2 weeks

FIG. 10

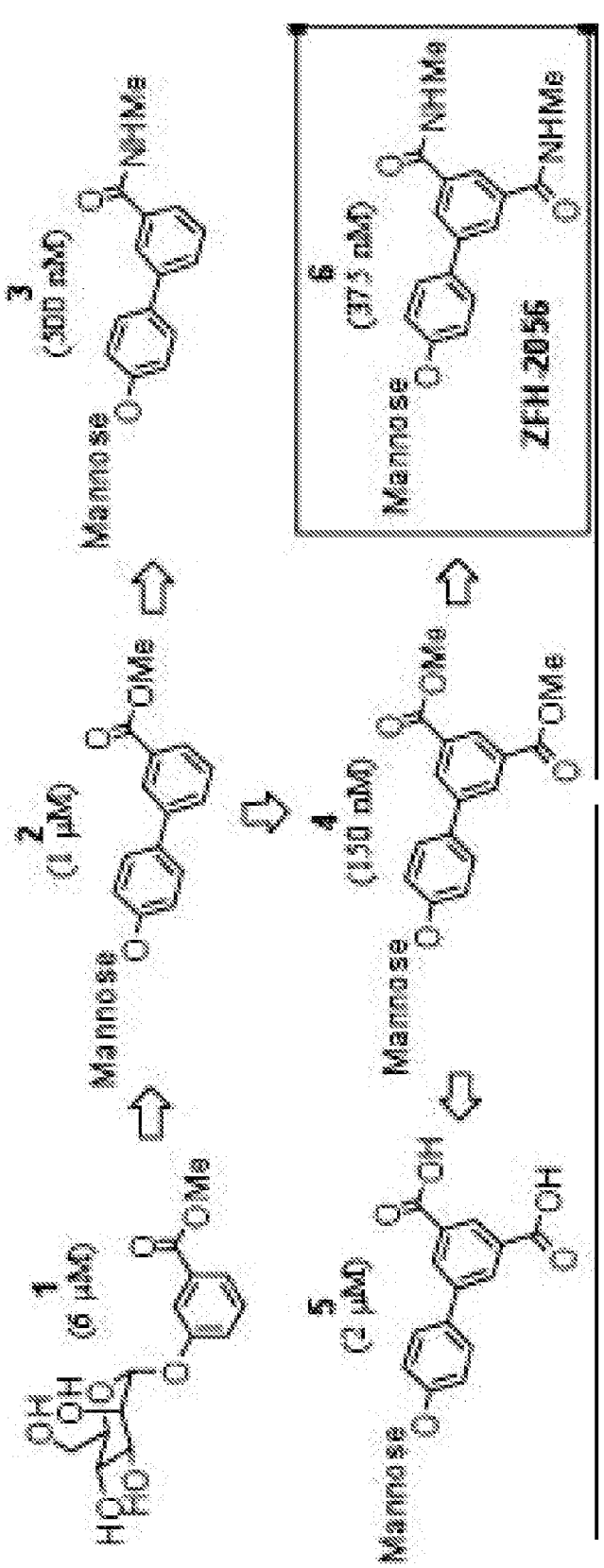
1
(6 μM)
2
(1 μM)
3
(300 nM)
4
(150 nM)
5
(2 μM)
6
(37.5 nM)
ZFH 2056
Mannose
OMe
NHMe
OH

FIG. 11A

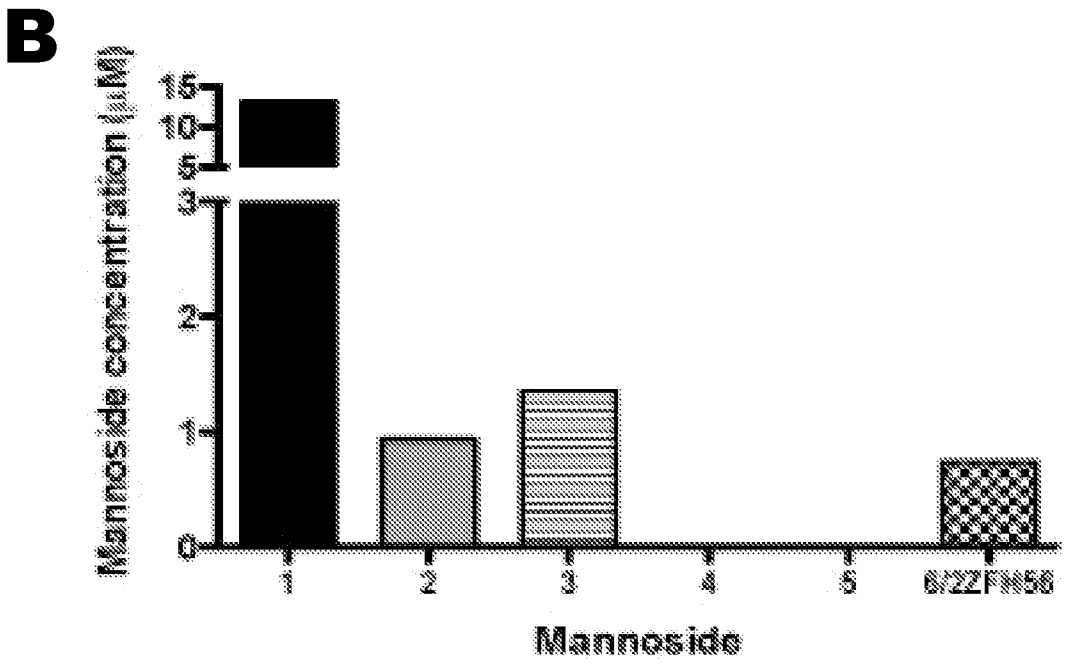
B
Mannoside concentration (μM)
15
10
5
3
2
1
0
1
2
3
4
5
6/22FH56
Mannoside

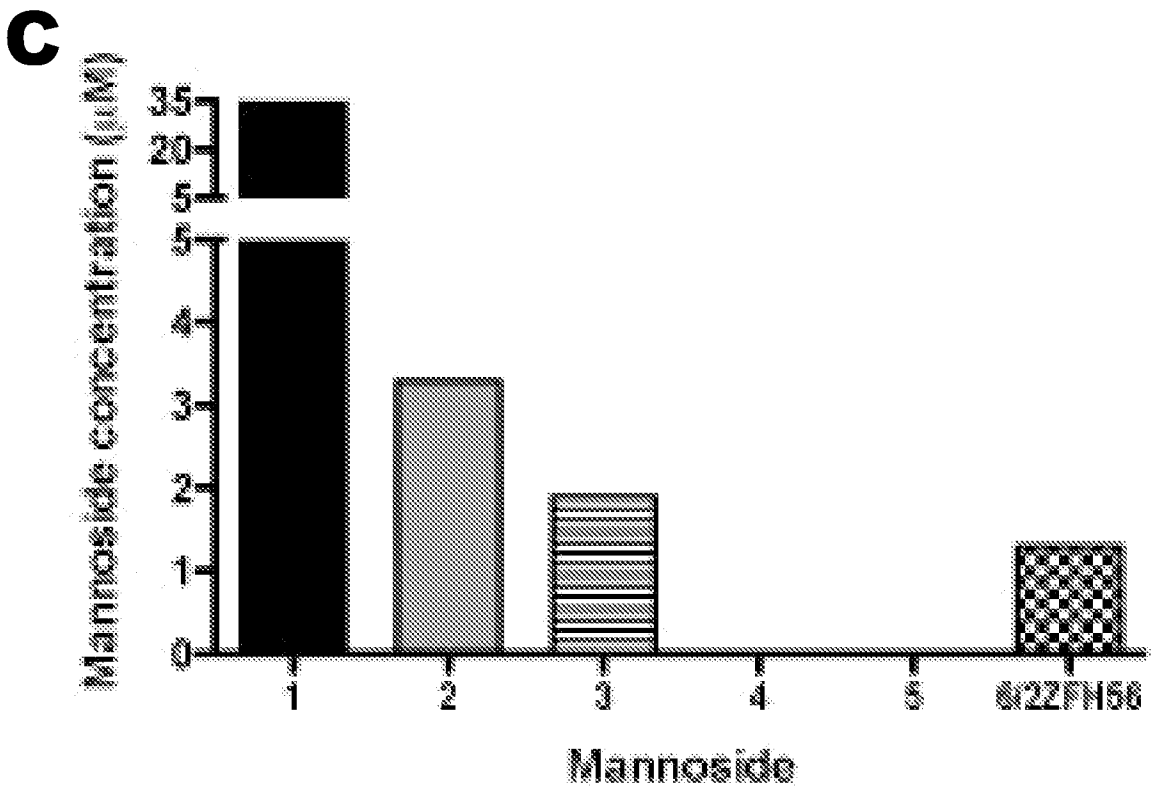
C
Mannoside concentration (μM)
35
20
5
5
4
3
2
1
0
1
2
3
4
5
6/22FH56
Mannoside

FIG. 11

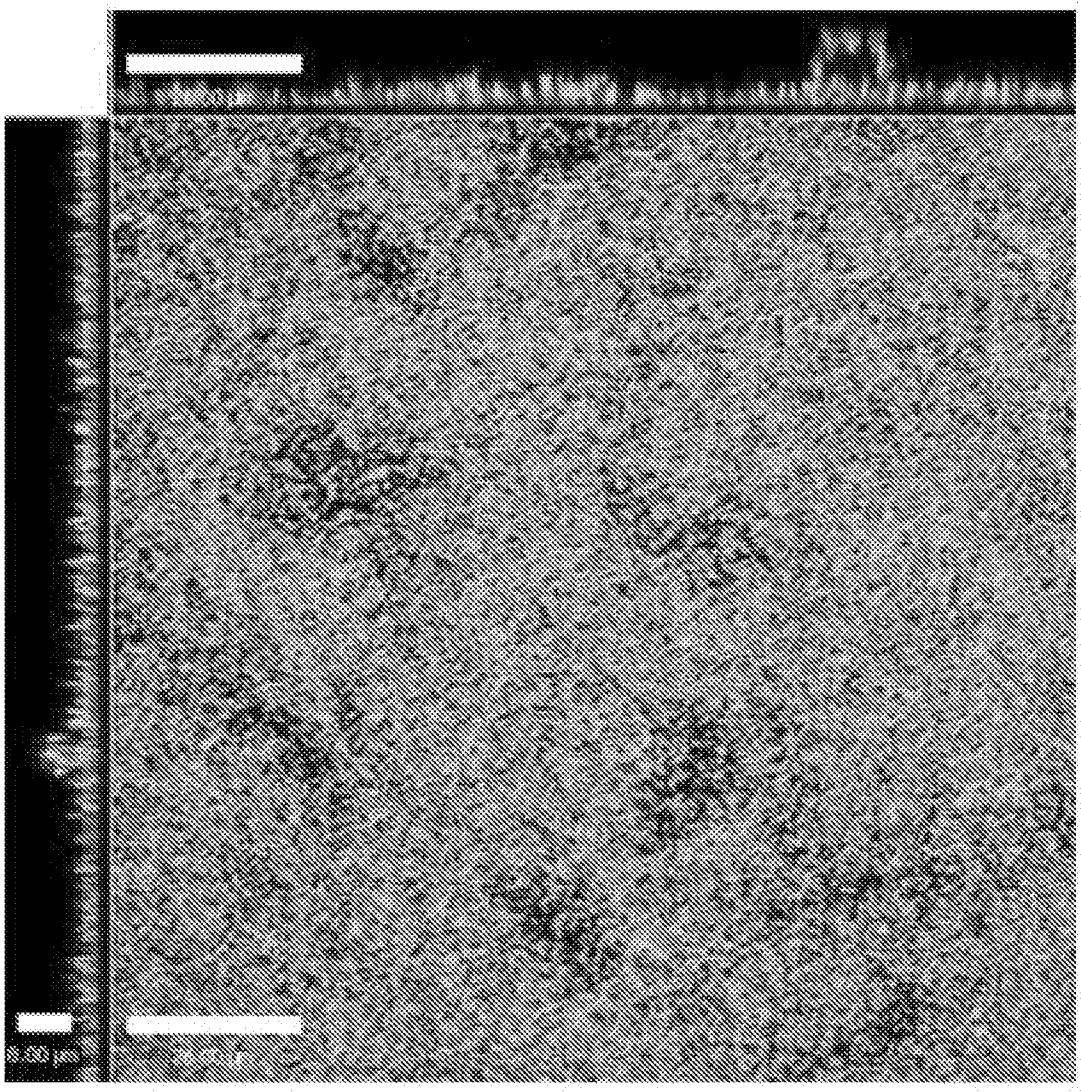

PBS

FIG. 11D

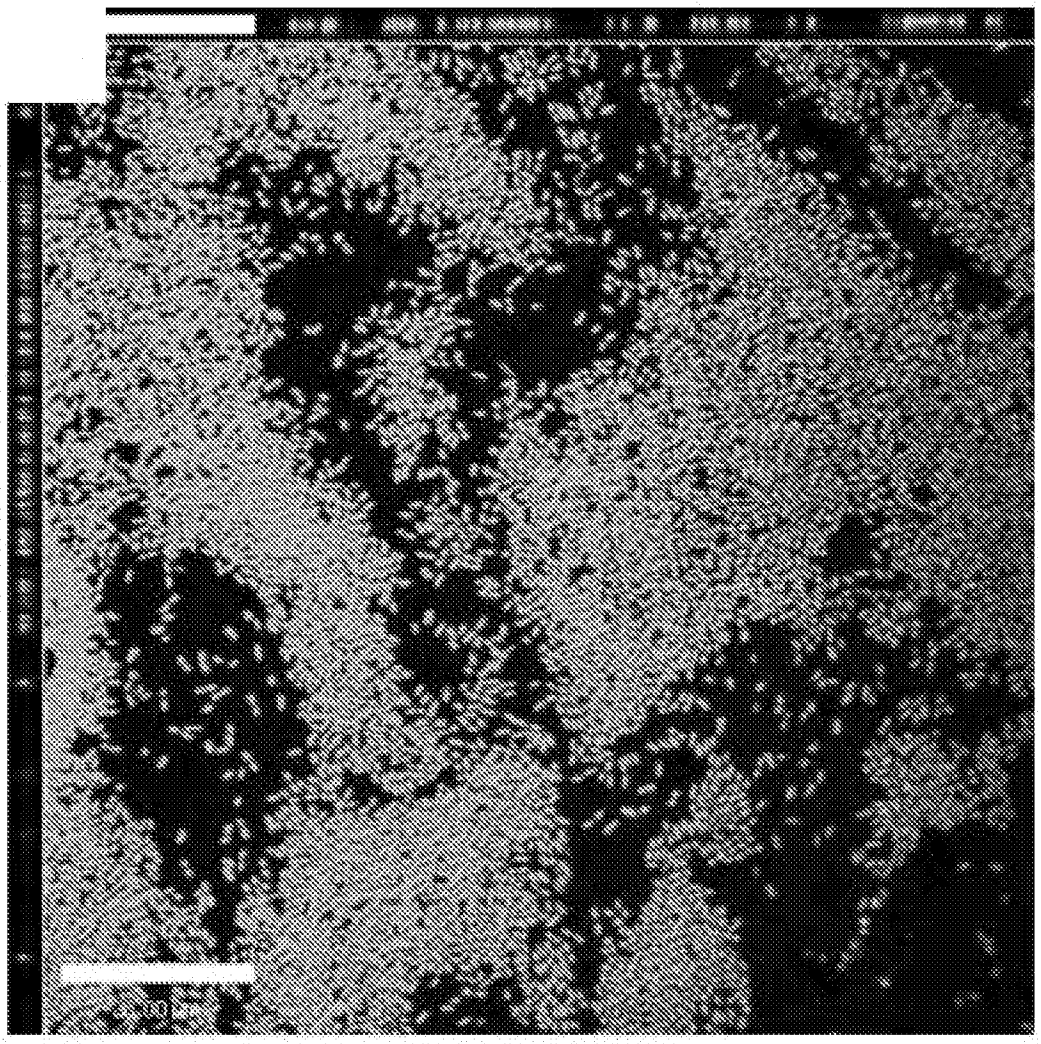

0.3 μM 6/2ZFH56

FIG. 11E

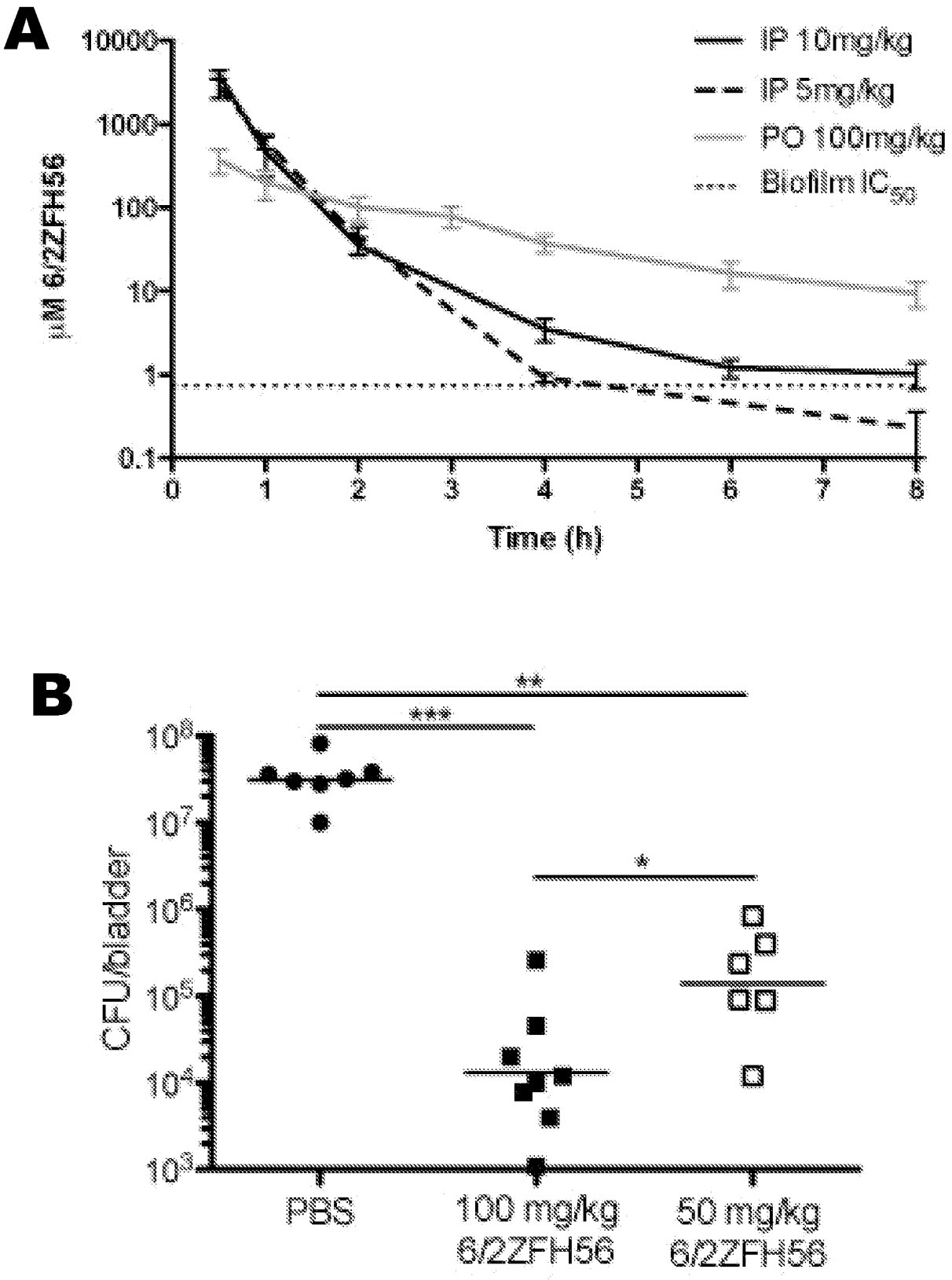
A
μM 6/2ZFH56
10000
1000
100
10
1
0.1
0
1
2
3
4
5
6
7
8
Time (h)
IP 10mg/kg
IP 5mg/kg
PO 100mg/kg
Biofilm IC50
B
CFU/bladder
10^8
10^7
10^6
10^5
10^4
10^3
**
***
*
PBS
100 mg/kg 6/2ZFH56
50 mg/kg 6/2ZFH56

FIG. 12

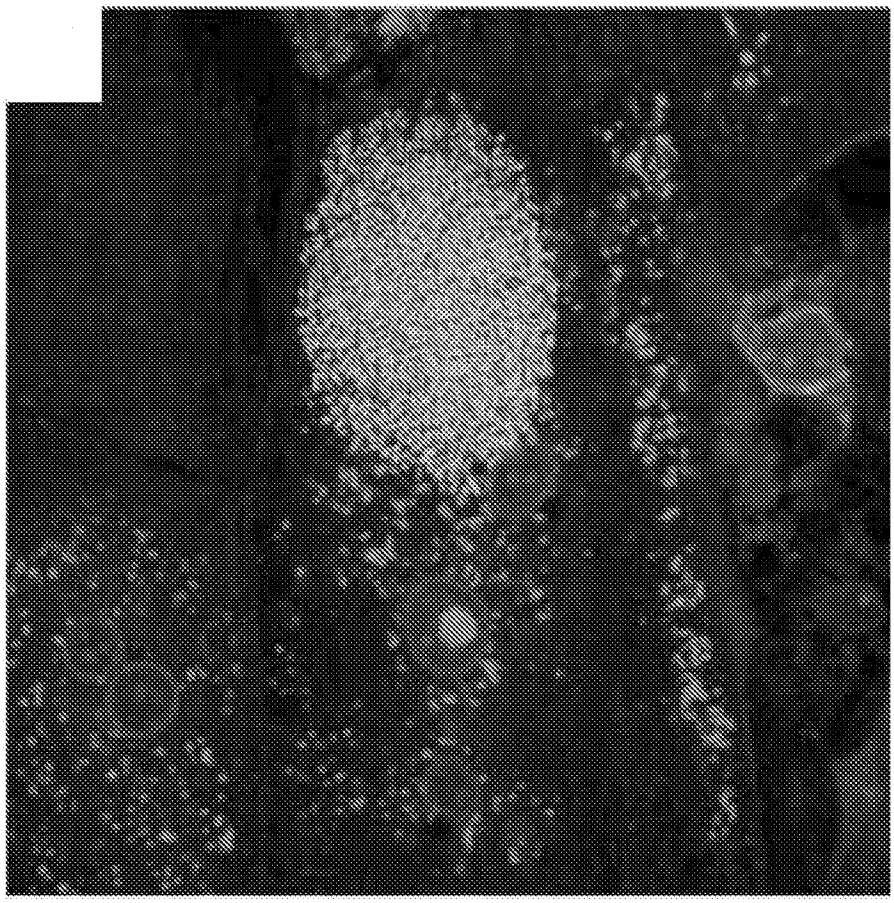

PBS

FIG. 12C

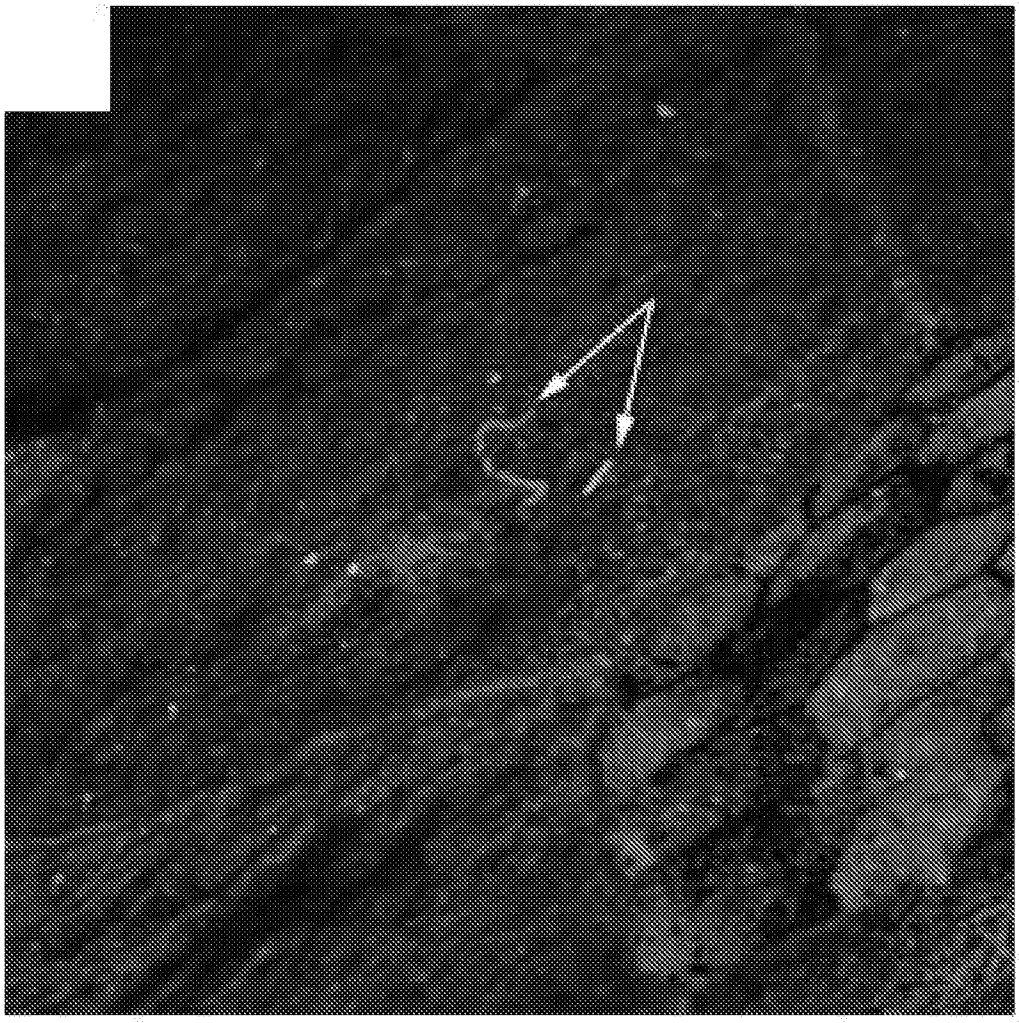

FIG. 12D

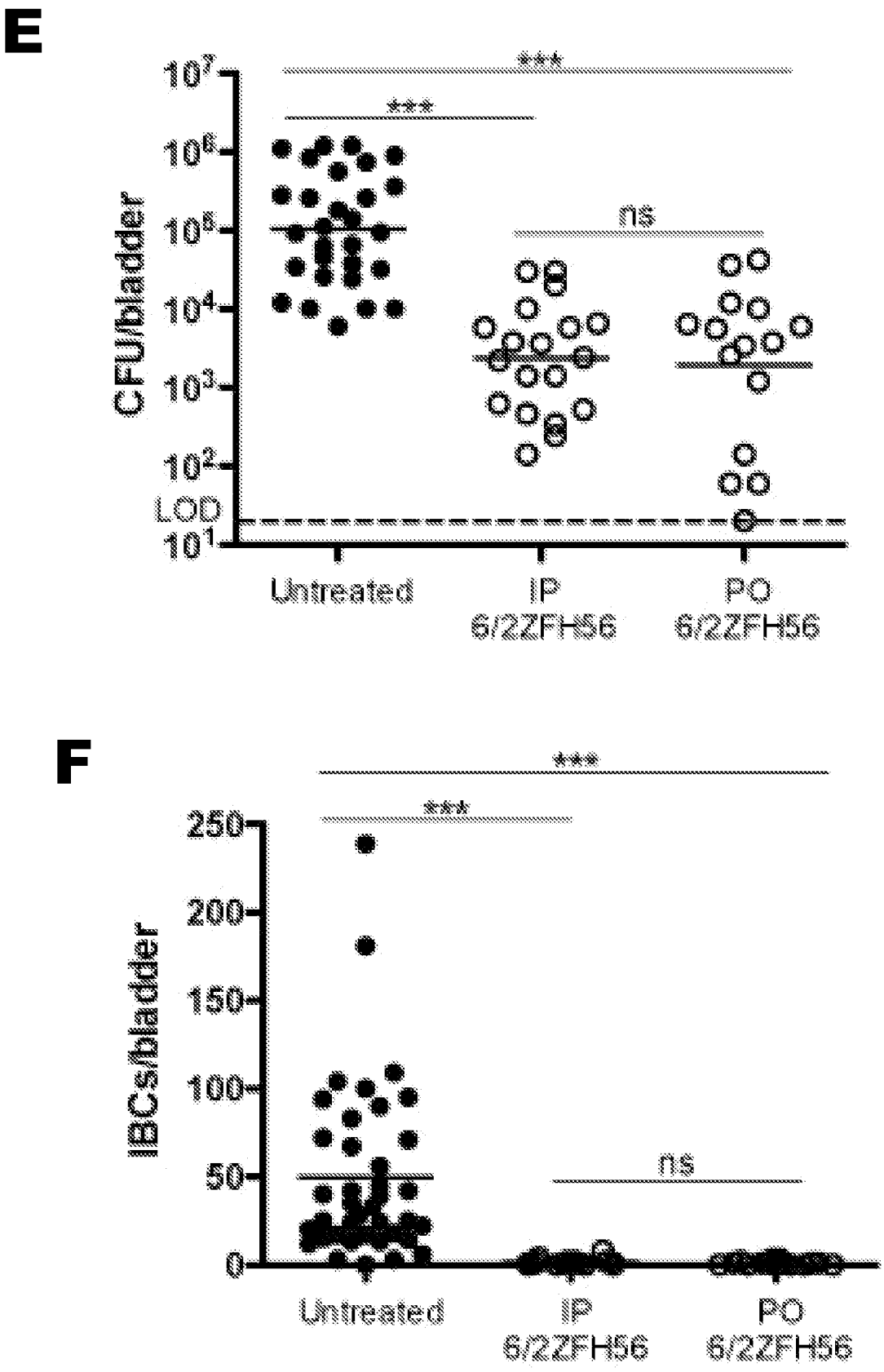
E
***
***
ns
CFU/bladder
10^7
10^6
10^5
10^4
10^3
10^2
LOD
10^1
Untreated
IP 6/2ZFH56
PO 6/2ZFH56
F
***
***
ns
IBCs/bladder
250
200
150
100
50
0
Untreated
IP 6/2ZFH56
PO 6/2ZFH56

FIG. 12

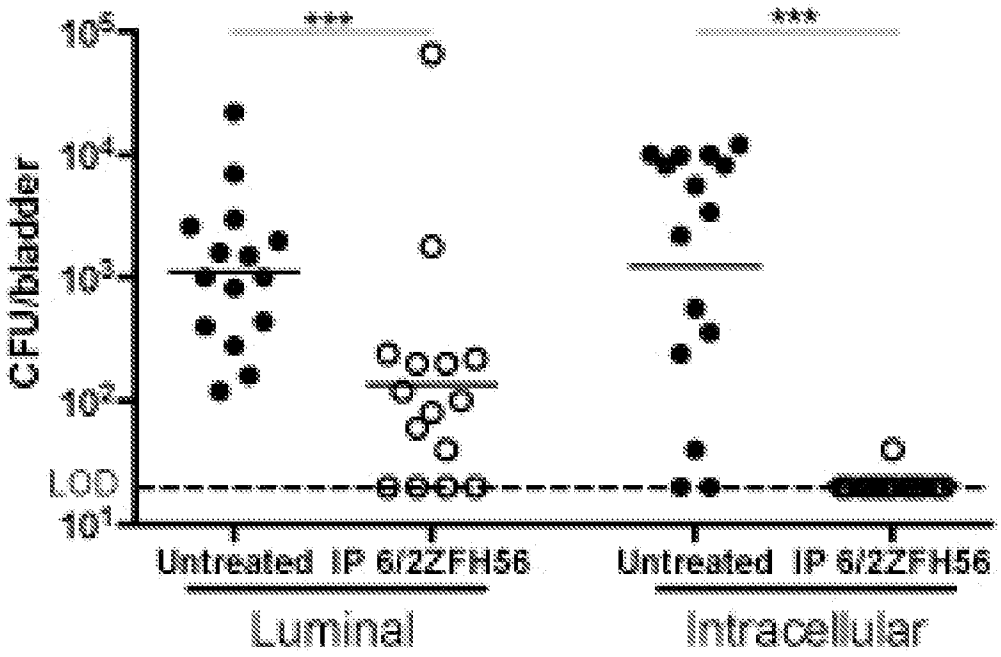
***
***
CFU/bladder
LOD
Untreated
IP 6/2ZFH56
Untreated
IP 6/2ZFH56
Luminal
Intracellular

FIG. 12G

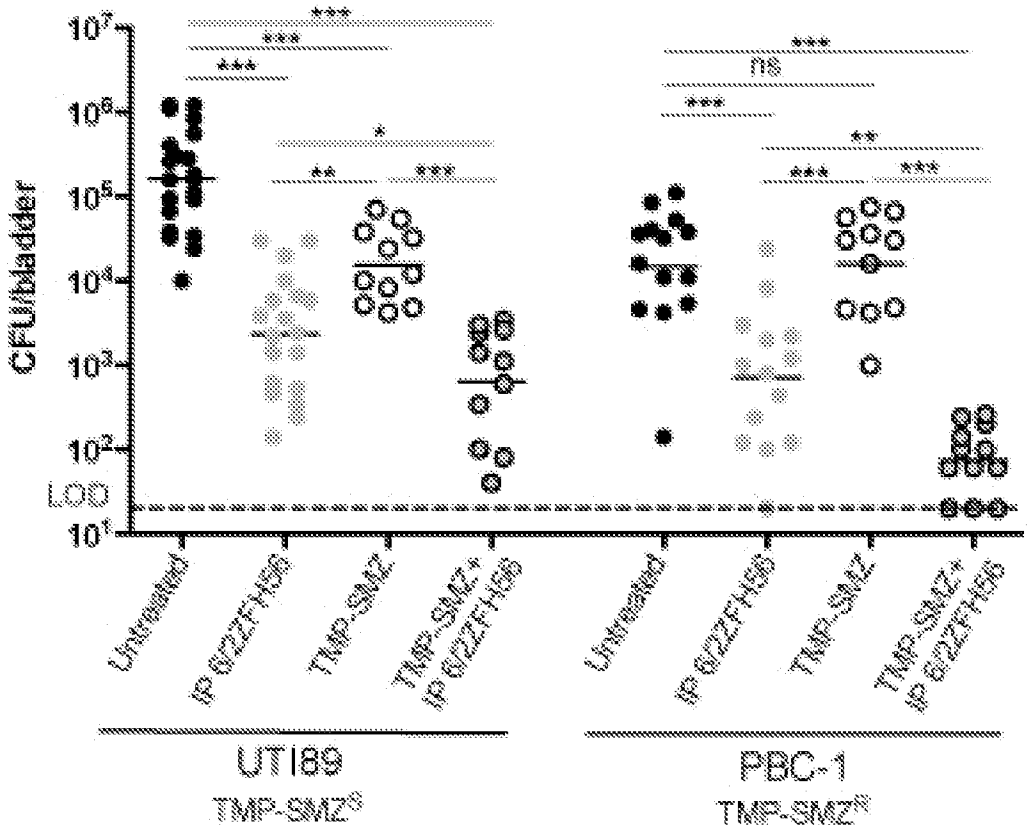
CFU/bladder
LOD
Untreated
IP 6/ZFH56
TMP-SMZ
TMP-SMZ + IP 6/ZFH56
UTI89
TMP-SMZ^S
PBC-1
TMP-SMZ^R
ns

FIG. 13

A

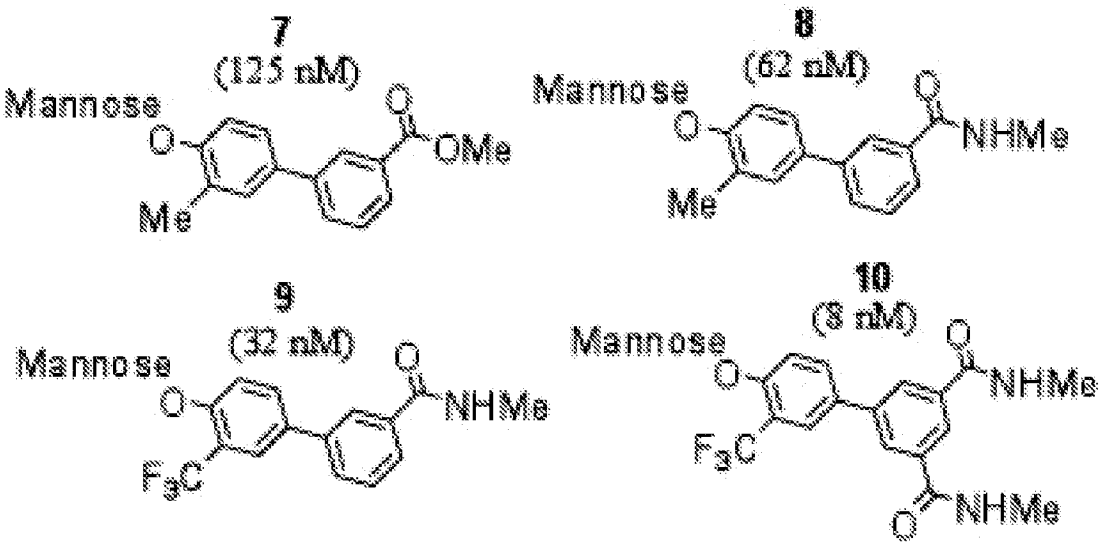
7
(125 nM)
Mannose
O
OMe
Me
8
(62 nM)
Mannose
O
NHMe
Me
9
(32 nM)
Mannose
O
NHMe
F3C
10
(8 nM)
Mannose
O
NHMe
F3C
NHMe
O

B

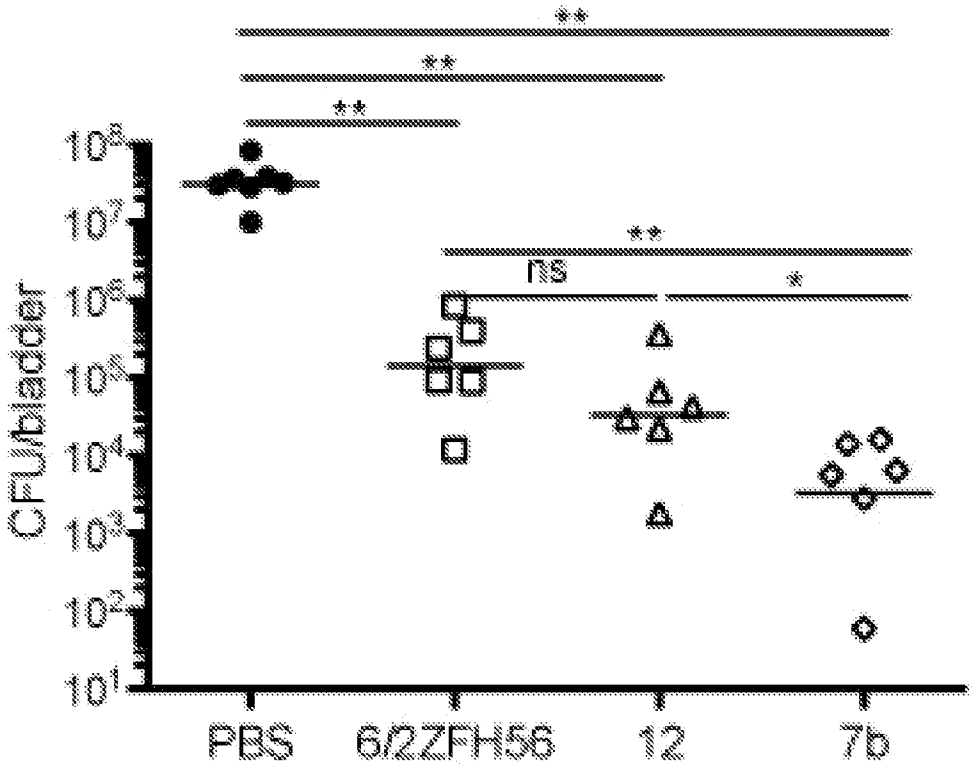
**
**
**
**
ns
*
CFU/bladder
10^8
10^7
10^6
10^5
10^4
10^3
10^2
10^1
PBS
6/2ZFH56
12
7b

FIG. 14

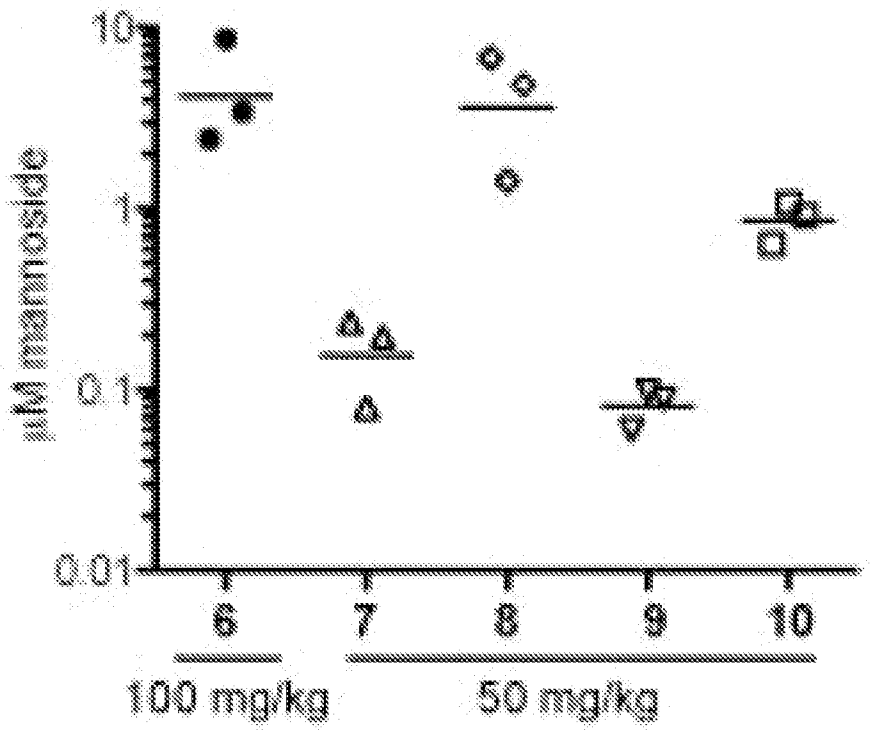

FIG. 14C

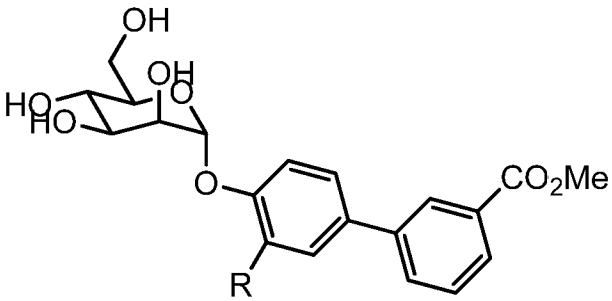

4a-e; R = F, Cl, Me, CF_3, OMe

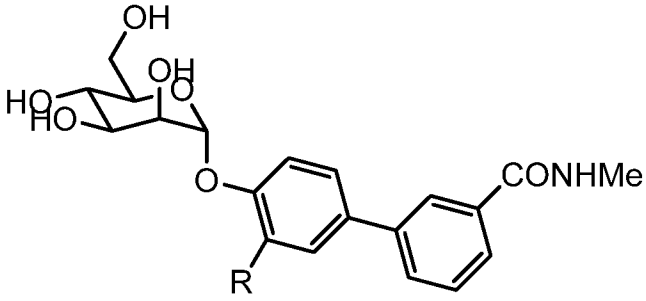

5a-c; R = Cl, Me, CF_3

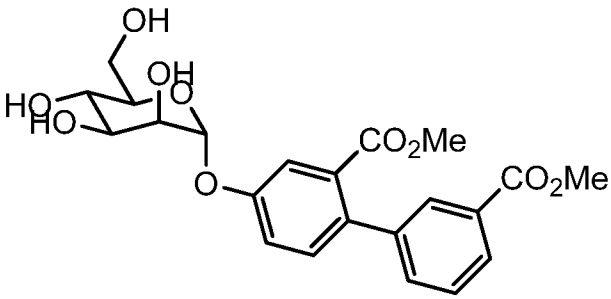

6

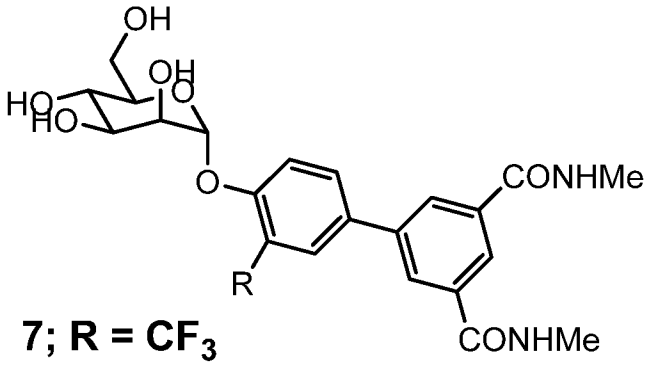

7; R = CF_3
8; R = Me

FIG. 15

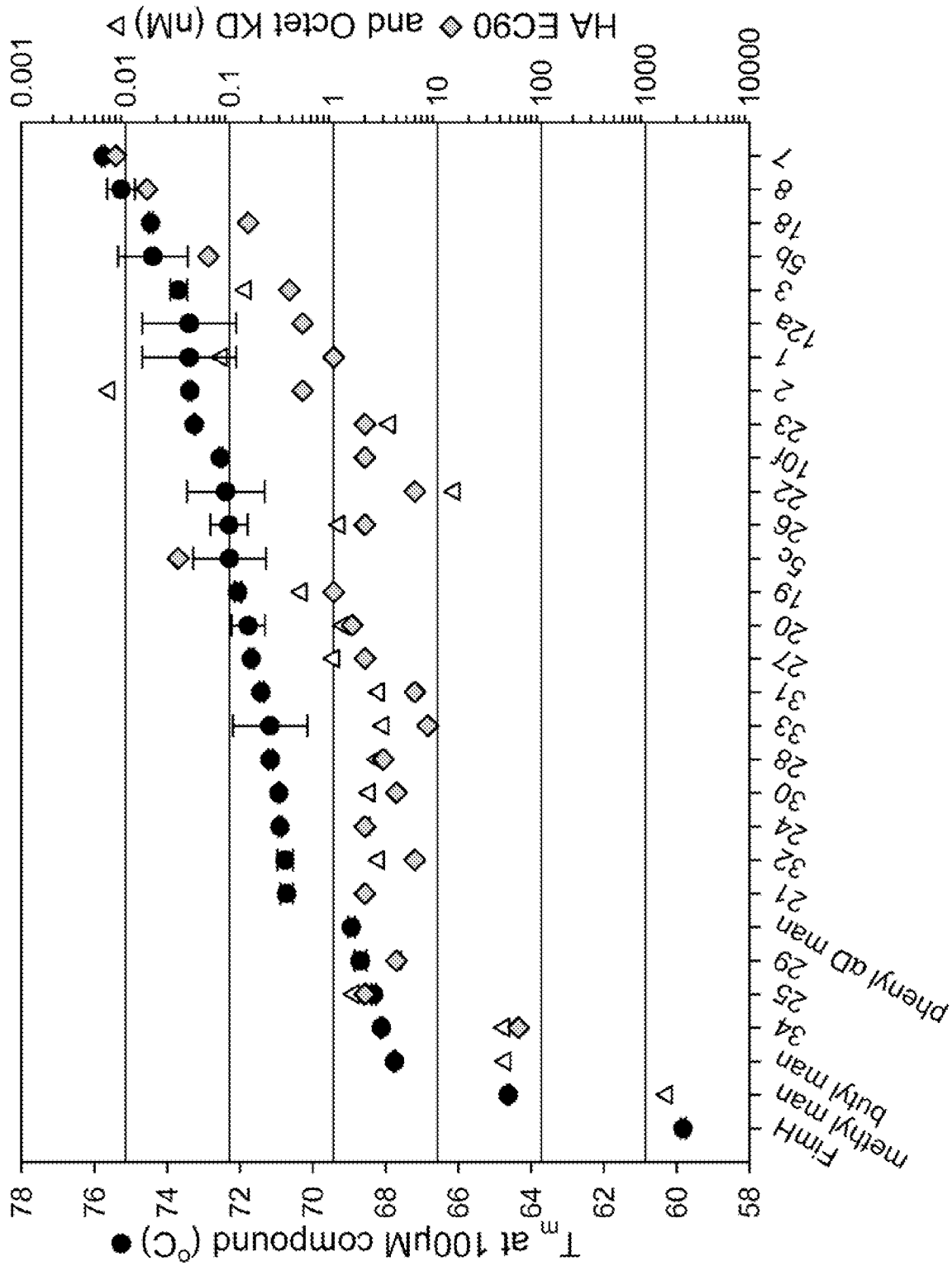
HA EC90 ◆ and Octet KD (nM) ▷
0.001
0.01
0.1
1
10
100
1000
10000
T_m at 100μM compound (°C) ●
78
76
74
72
70
68
66
64
62
60
58
FImH
methyl man
butyl man
phenyl αD man
7
8
18
5b
3
12a
1
2
23
10f
22
26
5c
19
20
27
31
33
28
30
24
32
21
29
25
34

FIG. 16

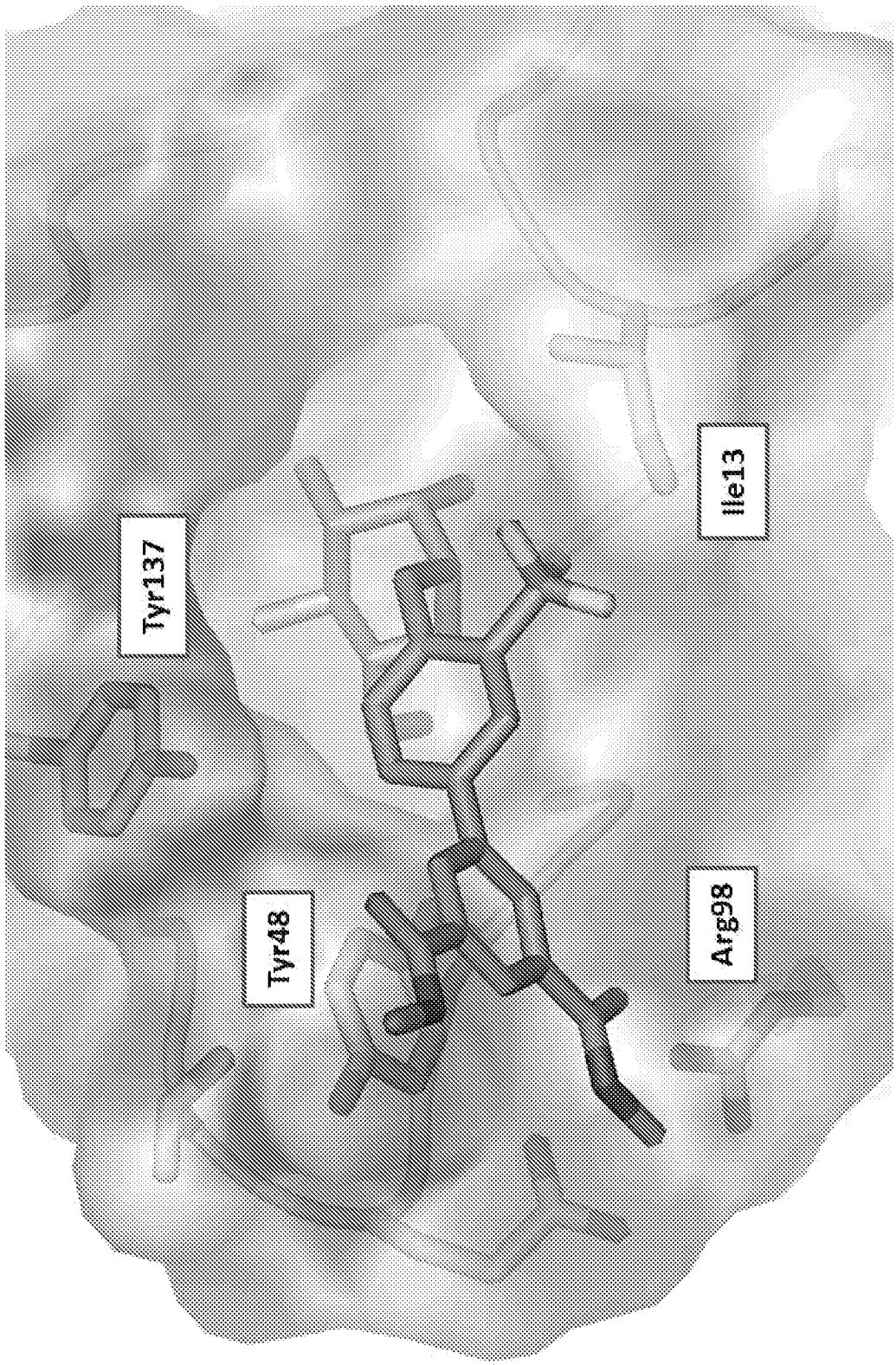

FIG. 17

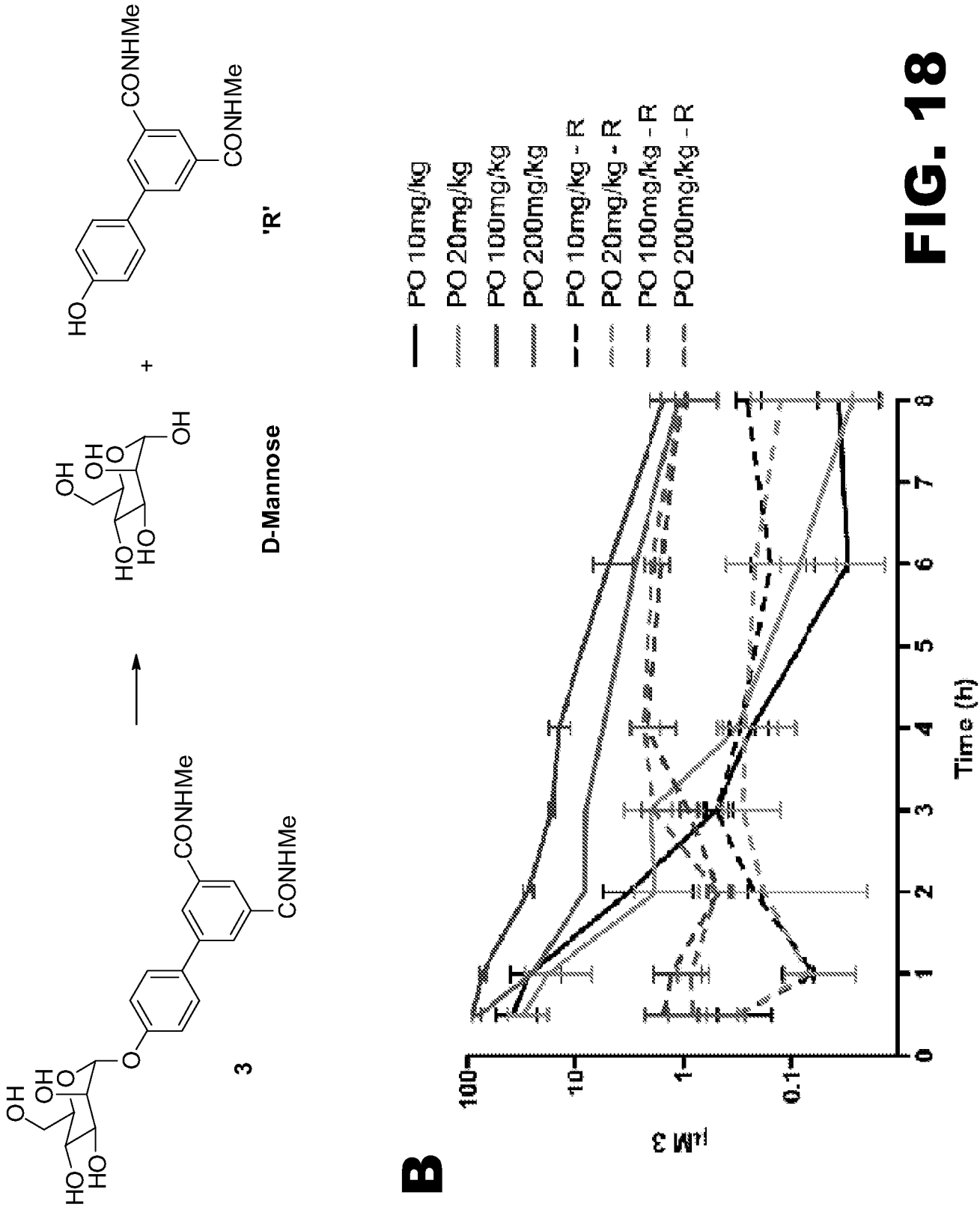
A
CONHMe
CONHMe
HO
'R'
+
OH
OH
O
OH
HO
HO
D-Mannose
3
B
PO 10mg/kg
PO 20mg/kg
PO 100mg/kg
PO 200mg/kg
PO 10mg/kg - R
PO 20mg/kg - R
PO 100mg/kg - R
PO 200mg/kg - R
100
10
1
0.1
0
1
2
3
4
5
6
7
8
Time (h)

FIG. 18

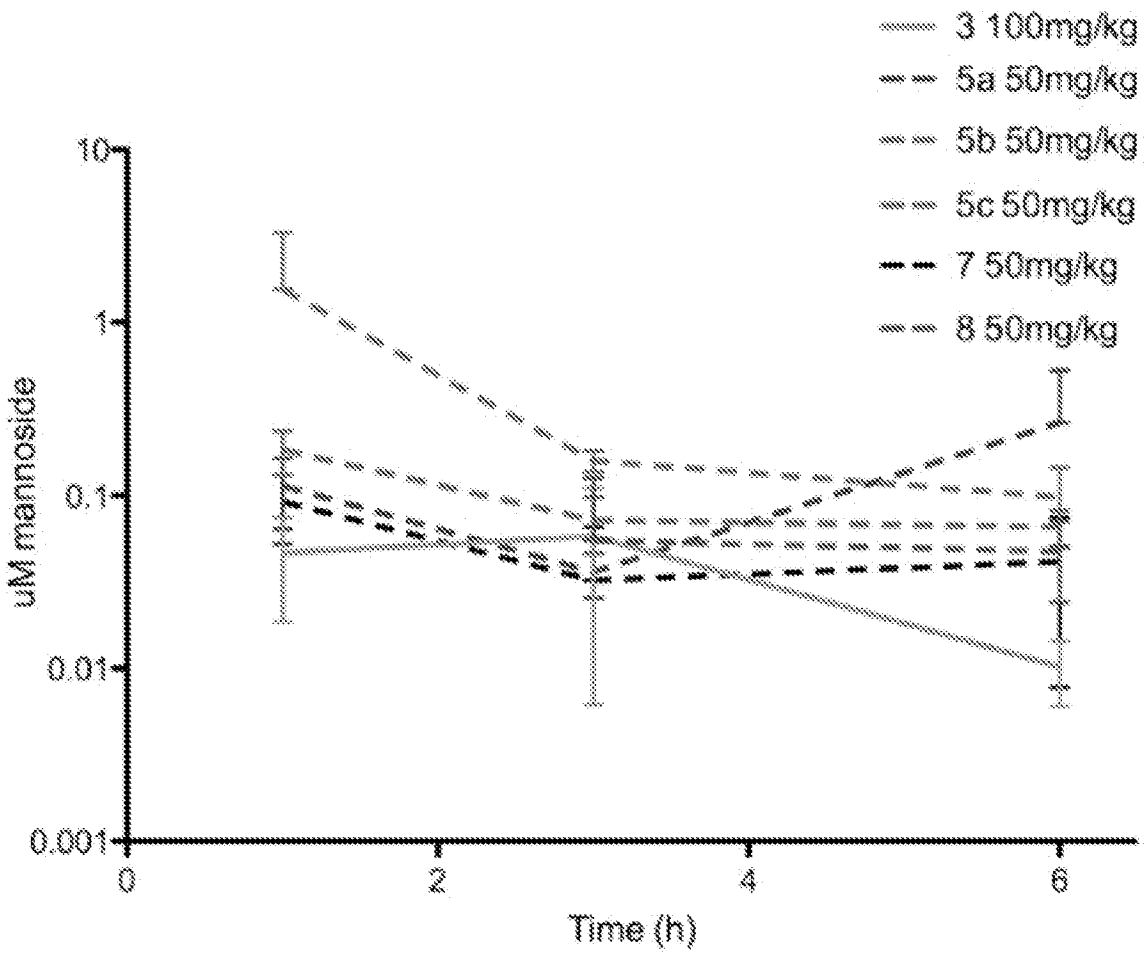
3 100mg/kg
5a 50mg/kg
5b 50mg/kg
5c 50mg/kg
7 50mg/kg
8 50mg/kg
uM mannoside
10
1
0.1
0.01
0.001
0
2
4
6
Time (h)

FIG. 19A

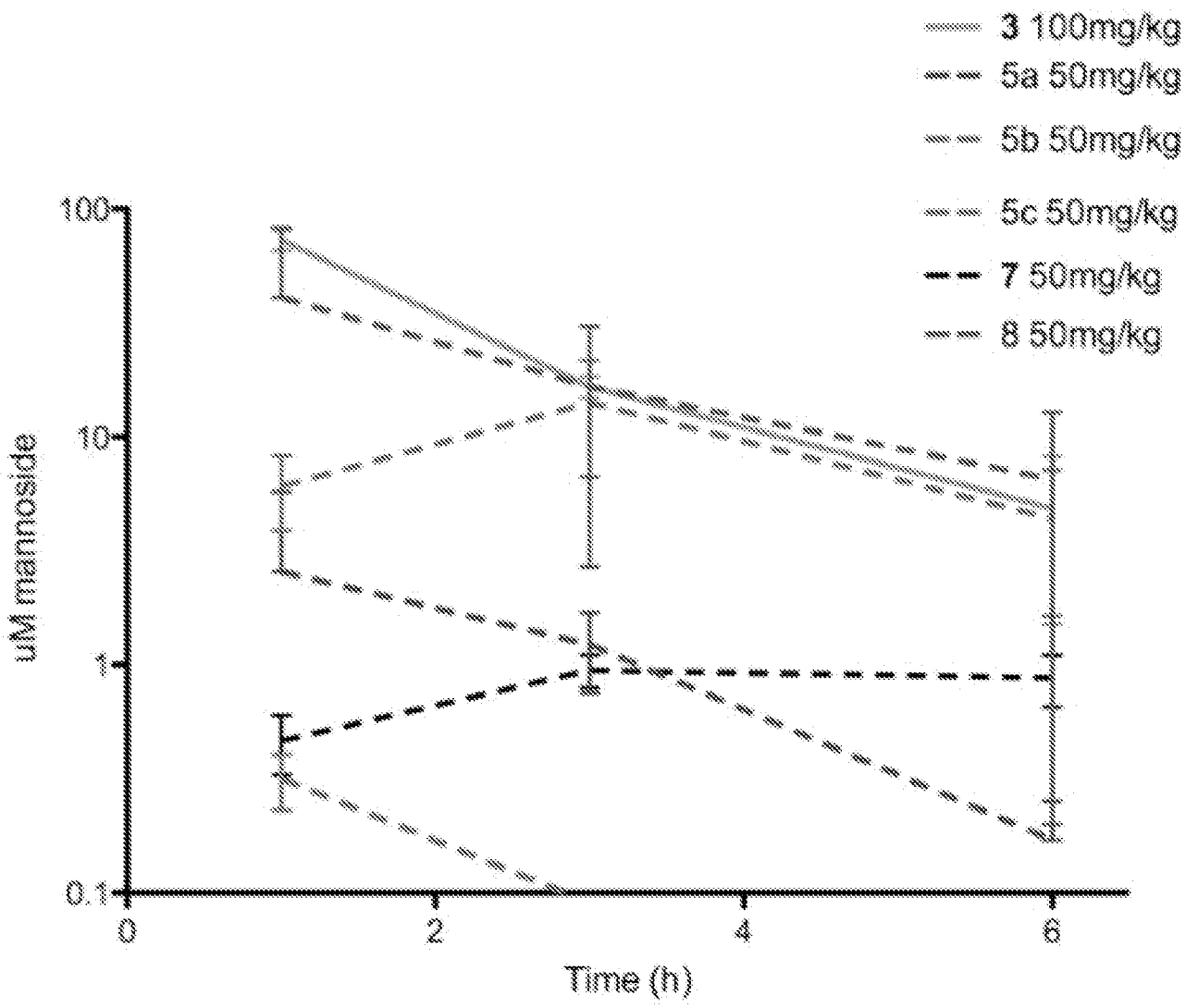
3 100mg/kg
5a 50mg/kg
5b 50mg/kg
5c 50mg/kg
7 50mg/kg
8 50mg/kg
100
10
1
0.1
uM mannoside
0
2
4
6
Time (h)

FIG. 19B

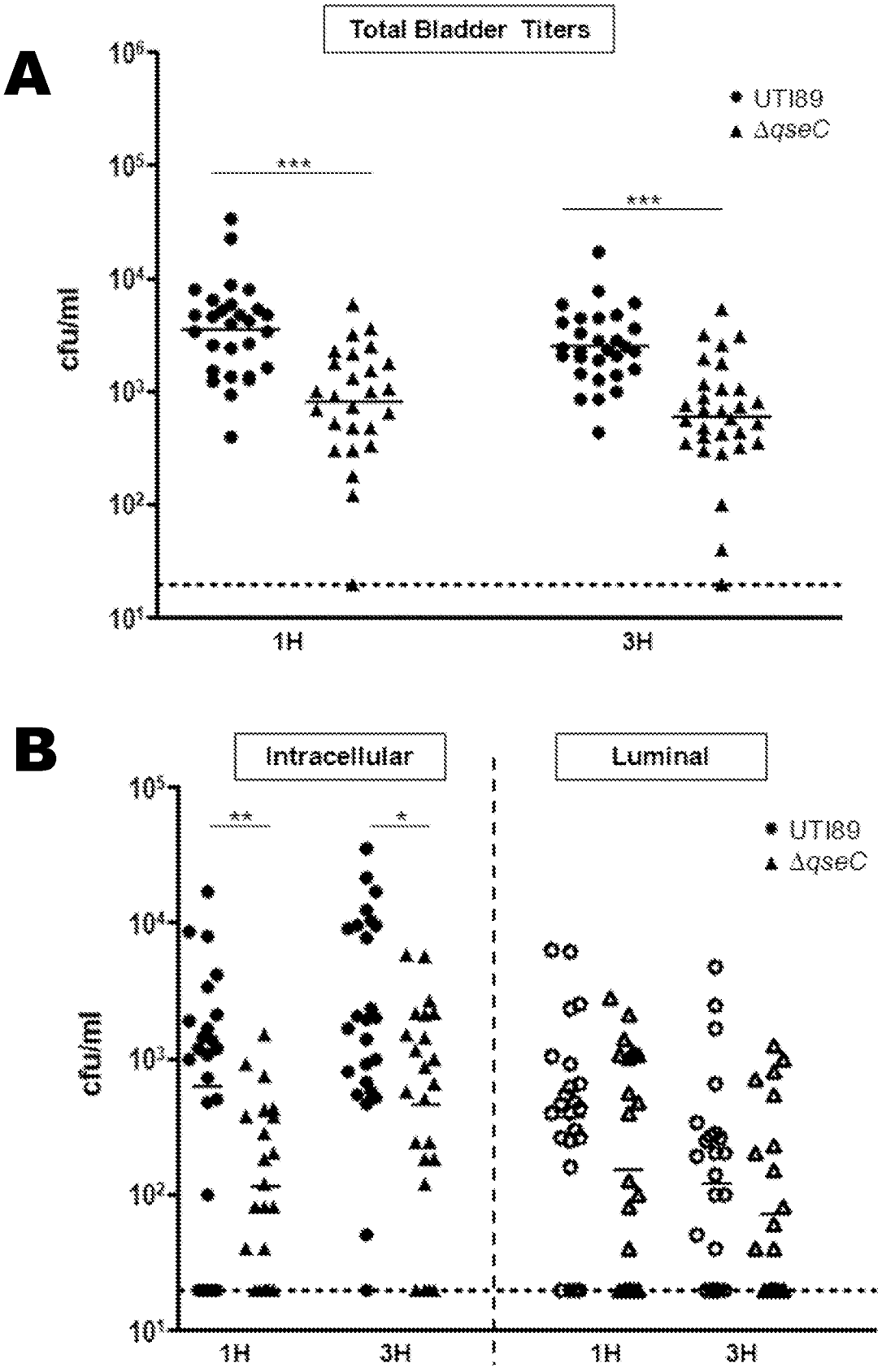
A
Total Bladder Titers
UTI89
ΔqseC
cfu/ml
***
***
1H
3H
B
Intracellular
Luminal
UTI89
ΔqseC
cfu/ml
**
*
1H
3H
1H
3H

FIG. 20

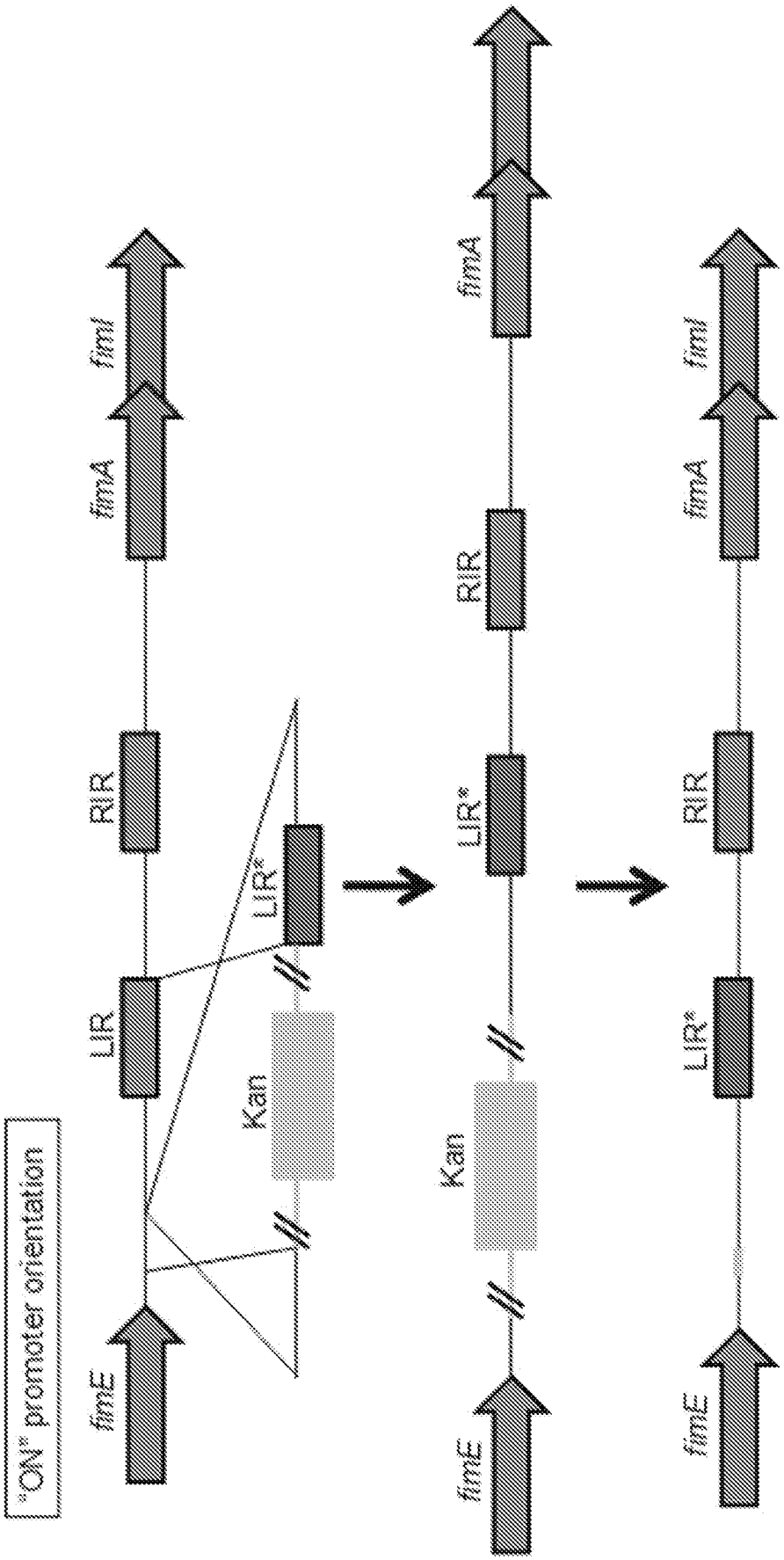
"ON" promoter orientation
fimE
LIR
Kan
LIR*
RIR
fimA
fimI
fimE
LIR*
Kan
RIR
fimA
fimE
LIR*
RIR
fimA
fimI

FIG. 21A

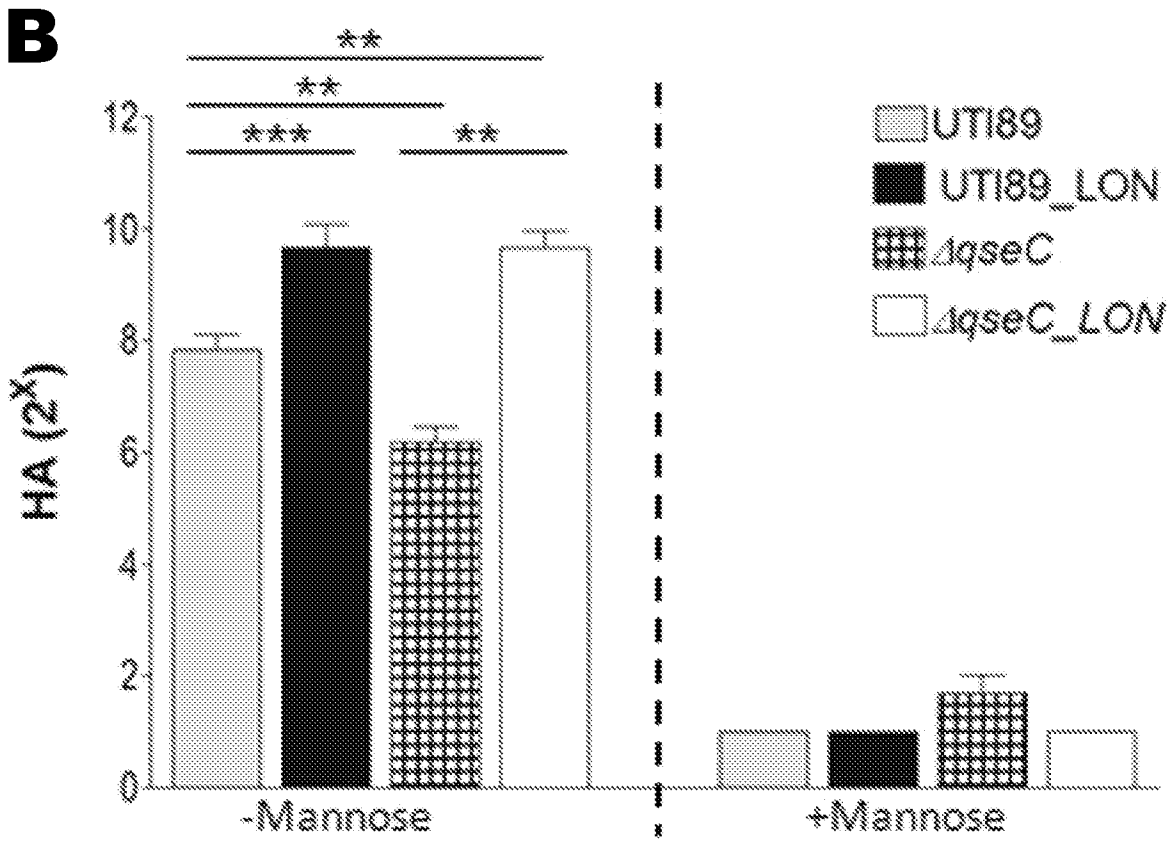
B
**
**
***
**
12
10
8
6
4
2
0
HA (2^X)
UTI89
UTI89_LON
ΔqseC
ΔqseC_LON
-Mannose
+Mannose

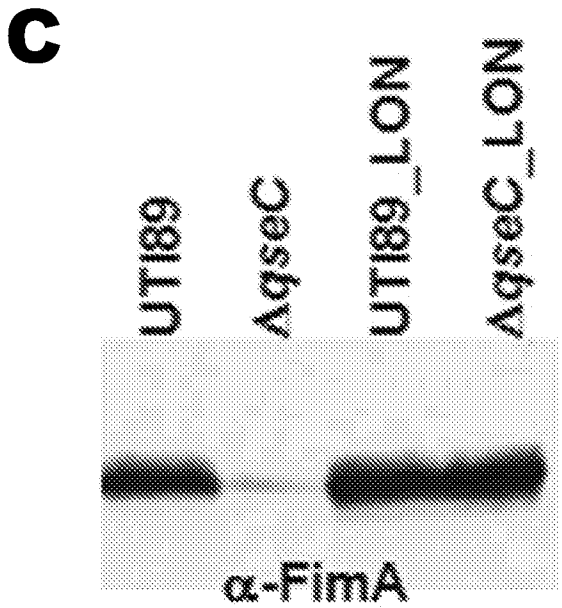
C
UTI89
ΔqseC
UTI89_LON
ΔqseC_LON
α-FimA

FIG. 21

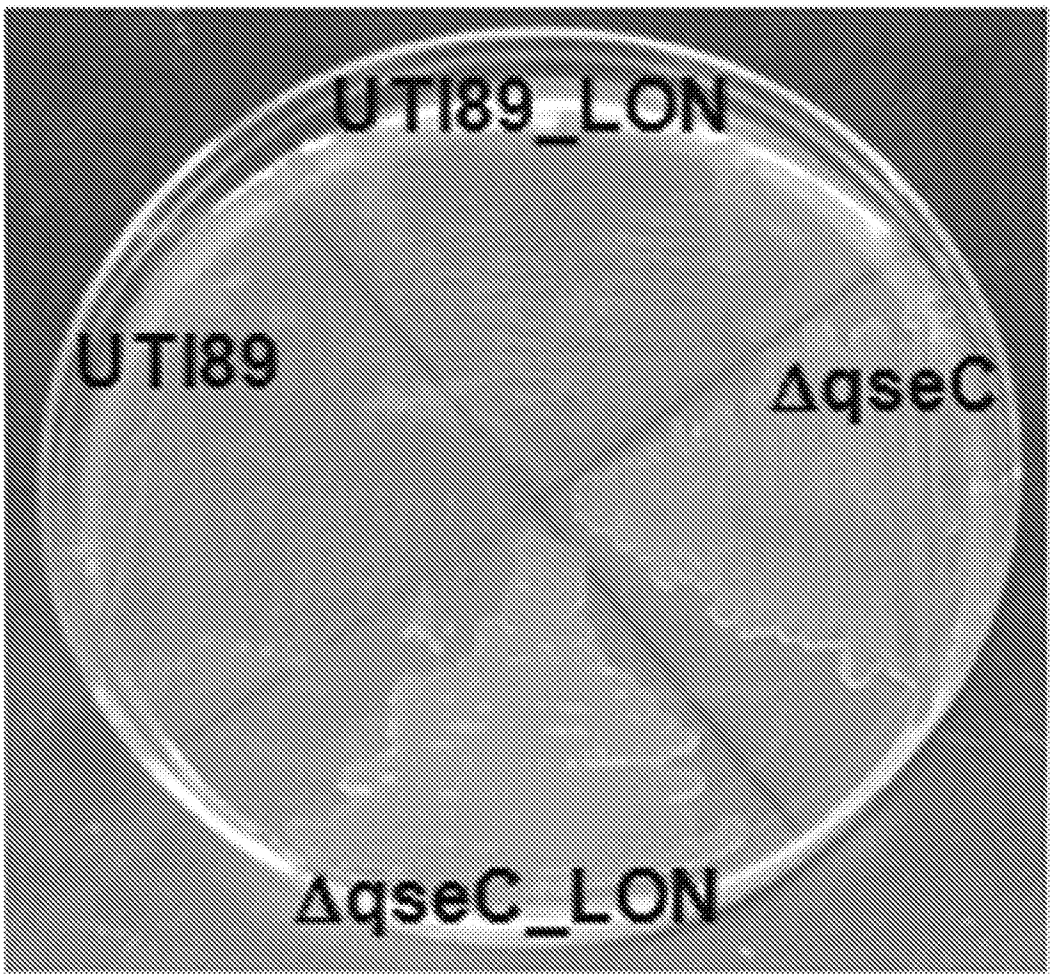

FIG. 21D

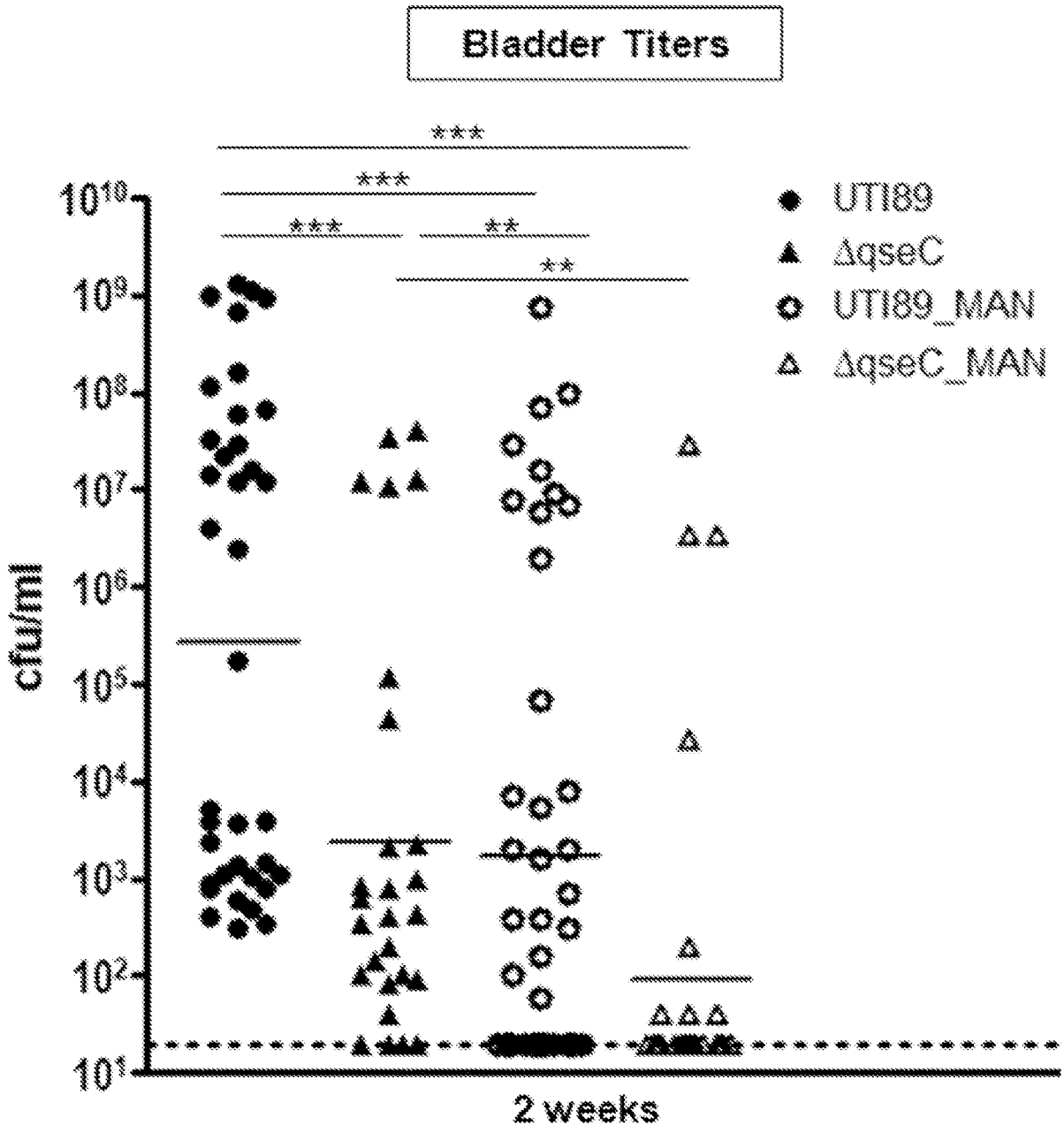
Bladder Titers
***
***
***
**
**
UTI89
ΔqseC
UTI89_MAN
ΔqseC_MAN
cfu/ml
10^10
10^9
10^8
10^7
10^6
10^5
10^4
10^3
10^2
10^1
2 weeks

FIG. 22

INTERNATIONAL SEARCH REPORT

International application No.
PCT/US 12/24169

A. CLASSIFICATION OF SUBJECT MATTER
IPC(8) - A01N 43/04; A61K 31/70 (2012.01)
USPC - 514/23
According to International Patent Classification (IPC) or to both national classification and IPC

B. FIELDS SEARCHED

Minimum documentation searched (classification system followed by classification symbols)
USPC - 514/23

Documentation searched other than minimum documentation to the extent that such documents are included in the fields searched
USPC - 514/27 (see search terms below)

Electronic data base consulted during the international search (name of data base and, where practicable, search terms used)
USPTO-WEST - PGPB,USPT,USOC,EPAB,JPAB keywords: treating, infection, gram-negative bacterium, Escherichia coli, urinary tract infection, FimH-mediated adhesion, oral administration, aryl O-mannosides, FimH, D-mannohexopyranoside, x-ray crystallography, mannose-binding pocket, docking, computer modeling, food supplement, medical device, coating. INT

C. DOCUMENTS CONSIDERED TO BE RELEVANT

Category*	Citation of document, with indication, where appropriate, of the relevant passages	Relevant to claim No.
Y	US 2008/0171706 A1 (BERGLUND et al.) 17 July 2008 (17.07.2008) para [0009]-[0035], [0040]-[0043], [0054]-[0058]	1-7
Y	WO 95/14028 A2 (HULTGREN et al.) 26 May 1995 (26.05.1995) pg 43, ln 1 - pg 46, ln 25; pg 47, ln 1 - pg 48, ln 13; pg 49, ln 17; pg 71, ln 25-33	1-7
Y	WO 01/10386 A2 (HULTGREN et al.) 15 February 2001 (15.02.2001) pg 8 - pg 9; pg 20; pg 55 - pg 58; pg 64; pg 72 - pg 74, see Ex 3	1-7
Y	US 2008/0268006 A1 (MOLIN et al.) 30 October 2008 (30.10.2008) para [0008]-[0010], [0020]-[0021], [0023], [0025]-[0026]	6
Y	US 7,790,183 B2 (DAROUICHE et al.) 07 September 2010 (07.09.2010) col 5, ln 51-59	7

☐ Further documents are listed in the continuation of Box C. ☐

* Special categories of cited documents:
"A" document defining the general state of the art which is not considered to be of particular relevance
"E" earlier application or patent but published on or after the international filing date
"L" document which may throw doubts on priority claim(s) or which is cited to establish the publication date of another citation or other special reason (as specified)
"O" document referring to an oral disclosure, use, exhibition or other means
"P" document published prior to the international filing date but later than the priority date claimed
"T" later document published after the international filing date or priority date and not in conflict with the application but cited to understand the principle or theory underlying the invention
"X" document of particular relevance; the claimed invention cannot be considered novel or cannot be considered to involve an inventive step when the document is taken alone
"Y" document of particular relevance; the claimed invention cannot be considered to involve an inventive step when the document is combined with one or more other such documents, such combination being obvious to a person skilled in the art
"&" document member of the same patent family

Date of the actual completion of the international search	Date of mailing of the international search report
07 May 2012 (07.05.2012)	29 MAY 2012

Name and mailing address of the ISA/US	Authorized officer:
Mail Stop PCT, Attn: ISA/US, Commissioner for Patents P.O. Box 1450, Alexandria, Virginia 22313-1450 Facsimile No. 571-273-3201	Lee W. Young PCT Helpdesk: 571-272-4300 PCT OSP: 571-272-7774

Form PCT/ISA/210 (second sheet) (July 2009)